

USARTL-TR -78-37B

LEVEL

12

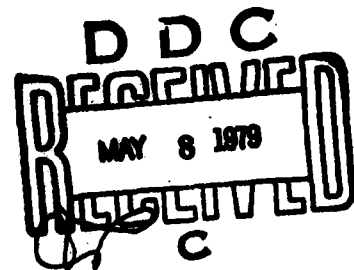


SR

**AQUILA REMOTELY PILOTED VEHICLE SYSTEM TECHNOLOGY
DEMONSTRATOR (RPV-STD) PROGRAM
Volume II - System Evolution and Engineering Testing**

AD A 068346

Grover L. Alexander
LOCKHEED MISSILES & SPACE COMPANY, INC.
Sunnyvale, Calif. 94086



W

April 1979

Final Report for Period December 1974 - December 1977

Approved for public release;
distribution unlimited.

Prepared for

U. S. ARMY AVIATION RESEARCH AND DEVELOPMENT COMMAND
P.O. Box 209
St. Louis, Mo. 63166

DDC FILE COPY

APPLIED TECHNOLOGY LABORATORY
U. S. ARMY RESEARCH AND TECHNOLOGY LABORATORIES (AVRADCOM)
Fort Eustis, Va. 23604

79 05 08 010

APPLIED TECHNOLOGY LABORATORY POSITION STATEMENT

This report provides the results of the program of design, fabrication, integration and test of the AQUILA (XMQM-105) RPV System Technology Demonstrator preparatory to delivery of this system to the US Army for engineering design test and force development test and experimentation. System performance presented herein supports the conclusion that an RPV system can provide capabilities for battlefield reconnaissance, target acquisition, and target designation. However, the reader is advised that system tests reported herein were developmental in nature and the results are limited. Complete performance of the AQUILA demonstrator system can be obtained only through an appreciation of the results in this report and the results of the Army's engineering design and force development tests. Engineering design tests were conducted by the US Army Electronic Proving Ground with results published in *Final Report/Engineering Design Test - Government (EDT-G) of Remotely Piloted Vehicle - System Technology Demonstrator*, TECOM Project No. 6-AI-53E-RPV-005, June 1978.* Force Development tests were conducted by the US Army Field Artillery Board and published in *Force Development Testing and Experimentation of Remotely Piloted Vehicle System/Final Report*, TRADOC Project No. 6-AI-53E-RPV-003, 6 January 1978.**

Mr. Gary N. Smith of the Aeronautical Systems Division served as the Contracting Officer's Technical Representative for the RPV System Technology Demonstrator Program.

Report Control

*CDR, US Army Aviation Research and Development Command, ATTN: DRDAV-RP,
P. O. Box 209, St. Louis, Missouri

**CDR, US Army Combined Arms Center, ATTN: ATCA-TSM-R, Fort Sill, Oklahoma
73503

DISCLAIMERS

The findings in this report are not to be construed as an official Department of the Army position unless so designated by other authorized documents.

When Government drawings, specifications, or other data are used for any purpose other than in connection with a definitely related Government procurement operation, the United States Government thereby incurs no responsibility nor any obligation whatsoever; and the fact that the Government may have formulated, furnished, or in any way supplied the said drawings, specifications, or other data is not to be regarded by implication or otherwise as in any manner licensing the holder or any other person or corporation, or conveying any rights or permission, to manufacture, use, or sell any patented invention that may in any way be related thereto.

Trade names cited in this report do not constitute an official endorsement or approval of the use of such commercial hardware or software.

DISPOSITION INSTRUCTIONS

Destroy this report when no longer needed. Do not return it to the originator.

Unclassified

SECURITY CLASSIFICATION OF THIS PAGE (When Data Entered)

REPORT DOCUMENTATION PAGE		READ INSTRUCTIONS BEFORE COMPLETING FORM	
1. REPORT NUMBER USARTI/TR-78-37B	2. GOVT ACCESSION NO. TR-78-37B	3. RECIPIENT'S CATALOG NUMBER	
4. TITLE (and Subtitle) AQUILA REMOTELY PILOTED VEHICLE SYSTEM TECHNOLOGY DEMONSTRATION (RPV-STO) PROGRAM, Volume II, System Evolution and Engineering Testing		5. TYPE OF REPORT & PERIOD COVERED Final Technical Report Dec 1974 - Dec 1977	6. PERFORMING ORG. REPORT NUMBER LMSC-D458287
7. AUTHOR(s) Grover L. Alexander		8. CONTRACT OR GRANT NUMBER(s) DAAJ02-75-C-1115	
9. PERFORMING ORGANIZATION NAME AND ADDRESS Lockheed Missiles & Space Company, Inc. Sunnyvale, California 94086		10. PROGRAM ELEMENT, PROJECT, TASK AREA & REPORT NUMBER D3 001 E 1763725DK81	11. D3
11. CONTROLLING OFFICE NAME AND ADDRESS U.S. Army Aviation Research & Development Command PO Box 209, RPV Development Mgt Ofc, DRDAV-RP St. Louis, Missouri 63166		12. NUMBER OF PAGES 324	
14. MONITORING AGENCY NAME & ADDRESS (if different from Controlling Office) Applied Technology Laboratory, U.S. Army Research and Technology Laboratories (AVRADCOM) Fort Eustis, Virginia 23604		15. SECURITY CLASS. (of this report) Unclassified	
16. DISTRIBUTION STATEMENT (of this Report) Approved for public release; distribution unlimited.		18a. DECLASSIFICATION/DOWNGRADING SCHEDULE	
17. DISTRIBUTION STATEMENT (of the abstract entered in Block 20, if different from Report) Final rept. Dec 74 - Dec 77			
18. SUPPLEMENTARY NOTES Volume II of a three-volume report LMSC/D458287-VOL-2			
19. KEY WORDS (Continue on reverse side if necessary and identify by block number) Remotely piloted vehicle system; mini-RPV subsystem; RPV launch and recovery; composite aircraft structures; electro-optical surveillance sensors, mini-RPV engines; battlefield surveillance; mini-RPV field operation; target location, recognition, designation			
20. ABSTRACT (Continue on reverse side if necessary and identify by block number) The Aquila system was developed using off-the-shelf hardware and best commercial practices where practical to minimize cost while retaining performance commensurate with 'HI-REL' hardware design. Evolution of proven RPV concepts, i.e., autopilot, sensor, and pneumatic launcher; development of new elements, airframe structure, servomotor, and electronic interface units; adaptation of such hardware as the data link elements; and use of existing commercial units, i.e., recorders, computer, and monitor hardware, produced an effective system that was refined through flight testing and made available to trained army crews.			

FORM 1 APR 78 1473 EDITION OF 1 NOV 65 IS OBSOLETE

Unclassified
SECURITY CLASSIFICATION OF THIS PAGE (When Data Entered)

220 220

alt

SUMMARY

The objective of the RPV-STD program was to provide the Army with hands-on experience with modern RPV system capabilities in the field environment so that the potential value of such systems could be assessed and system requirements clarified. To provide this experience with effective hardware, without the cost and time associated with an engineering development program, a short-span engineering program was conducted in which emphasis was placed on the integration and adaptation of existing and proven hardware elements. These elements were drawn from previous RPV programs, military aircraft, general aviation, missile, and satellite programs. Commercial grade components were used, wherever appropriate, to minimize costs.

The Aquila RPV configuration was based on a previously flown RPV with an extensive flight history. The structural design required a completely new development using lightweight Kevlar to minimize RPV weight. Flight control components were drawn primarily from those previously demonstrated in aircraft and missile programs; however, the flight control electronics (using a previously proven concept) was developed specifically for the Aquila application. The electrical flight control servomechanisms, while based on an existing aircraft electrical actuator unit, required considerable development before they provided acceptable control characteristics and reliability. The power plant was evolved from an existing go-cart engine with modifications for mounting, propeller drive, alternator drive, and throttle control. Cooling duct hardware was also modified to reduce weight. A special alternator, based on a previously proven design, was procured to provide electrical power. The various payload sensors were integrated into a common electro-optical gimbal unit for interchangeability. In addition, an existing aerial photo camera (with modified frame rate control) was

used. All components were acceptance tested, and system tests were conducted to ensure subsystem compatibility and function. Two wind tunnel tests were conducted to evaluate and characterize the RPV configuration. Step-by-step check-out procedures were developed for system verification and postflight preparation.

The ground support system evolved primarily through integration and adaptation of existing components. The Ground Control Station (GCS) was constructed using a standard Army shelter. The control console was constructed using commercial grade monitors, plotters, and instruments. Commercial grade digital and video recorders were used for flight data recording. The computer used to checkout and control the system and to navigate the RPV was also of commercial quality. An electronic interface unit was developed to integrate the GCS elements via proper tie-in and signal processing. Existing data-link elements were adapted to the Aquila system. The launcher evolved directly from a pneumatic launcher development in a previous RPV program. Launch loads were limited to 6 g. The retrieval system required considerable development, as it was unique to the Aquila program. The initial technique of using a trailing hook on the RPV to arrest horizontal motion was abandoned in favor of a more reliable ground-based vertical barrier. Horizontal straps were evolved from a previous RPV recovery system to arrest the vertical fall of the RPV after absorption of the horizontal momentum.

Ground tests were used to validate subsystem designs and hardware modifications, and to develop preflight checkout procedures. Because of the short time between program initiation and initiation of flight testing (11 months), system reliability was found to be insufficient to meet program objectives. After 5 months of field operations, and the loss of six RPVs, flight testing was delayed for 4 months while a program of testing and modification was conducted to improve reliability. Flight testing was then resumed and successfully completed.

The Aquila system evolution approach made use of existing, proven hardware, and commercial-grade hardware to speed system availability at a fraction of the

cost of full engineering development. However, to provide an acceptable level of operational reliability, more extensive development and testing was required than was indicated in the initial program definition. The extended program did provide the required level of reliability, and the 149 test flights (including 65 contractor flights and the 84 FDT&E and EDT flights) provided an extensive experience and data base for Army evaluation.

ACCESSION for	
NTIS	White Section <input checked="" type="checkbox"/>
DDC	Buff Section <input type="checkbox"/>
UNANNOUNCED	<input type="checkbox"/>
JUSTIFICATION	
BY	
DISTRIBUTION/AVAILABILITY CODES	
CLASS	
A	

TABLE OF CONTENTS

Section		Page
	SUMMARY	3
	LIST OF ILLUSTRATIONS	10
	LIST OF TABLES	15
I	INTRODUCTION	17
II	TECHNICAL PROGRAM DESCRIPTION	18
	2.1 Design	19
	2.2 Fabrication/Assembly/Test	22
	2.3 Crows Landing Flight Tests	23
	2.4 Fort Huachuca Flight Test - Initial Phase A	23
	2.5 System Reliability Improvement Program	24
	2.6 Fort Huachuca Flight Tests - Final Phase A	24
	2.7 B Modification Implementation	26
	2.8 Phase B Flight Testing	28
	2.9 Contractor Validation Achievements	28
	2.10 Army System Demonstration	29
III	AIRBORNE SYSTEM (RPV)	30
	3.1 RPV Evolution	30
	3.1.1 Background/Situation	30
	3.1.2 RPV Requirements	31
	3.1.3 RPV Evolution Approach	32
	3.1.4 RPV Evolution - General Arrangement	34
	3.1.5 RPV Evolution - Inboard Profile	46
	3.1.6 RPV Evolution - Mass Properties	50
	3.1.7 RPV Evolution - Performance	54

Section	Page
3.2 Airframe	55
3.2.1 Airframe Evolution - Background/ Situation	57
3.2.2 Airframe Structure Requirements	58
3.2.3 Airframe Structure Approach	59
3.2.4 Airframe Structure Evolution	59
3.3 Power Plant/Electrical Subsystem	75
3.3.1 Background	76
3.3.2 Requirements	79
3.3.3 Approach	79
3.3.4 Power Plant/Electrical Subsystem Evolution	80
3.3.5 Propulsion Performance and Functional Testing	97
3.3.6 Electrical Subsystem	107
3.3.7 Fuel System Evolution	108
3.4 Flight Control System	112
3.4.1 Background	112
3.4.2 Approach	113
3.4.3 Requirements	115
3.4.4 Flight Control and Navigation - Analytical Evolution	116
3.4.5 Flight Control and Navigation-Hardware Evolution	165
3.5 Sensors	176
3.5.1 Background	177
3.5.2 Requirements	177
3.5.3 Approach	183
3.5.4 Sensor Evolution	183
IV DATA-LINK SYSTEM EVOLUTION	194
4.1 Background	194
4.2 Requirements	195
4.3 Data-Link System Approach	195

Section

4.4	Data-Link System Requirements Evolution	195
4.5	Airborne Data-Link Component Evolution	198
4.5.1	Antennas	198
4.5.2	Command Receiver	201
4.5.3	Video Transmitter	202
4.5.4	Encoder-Decoder	202
4.6	GCS Data Link Elements Evolution	203
4.6.1	Tracking Antenna	203
4.6.2	Command Transmitter	204
4.6.3	Video-TM Receiver	206
4.6.4	Encoder-Decoder	206
4.7	System Evolution	206
V	GROUND SUPPORT SYSTEM	209
5.1	GSS Evolution	209
5.1.1	Background-Situation	209
5.1.2	GSS Requirements	210
5.1.3	GSS Evolution Approach	211
5.1.4	GSS Evolution	213
5.2	Ground Control Station (GCS) Evolution	217
5.2.1	Background	219
5.2.2	Approach	219
5.2.3	Requirements	220
5.2.4	Ground Control Station (GCS) Evolution ...	220
5.2.5	Digital Tape Recorder	237
5.2.6	Air Conditioner-Heater	237
5.2.7	Paper Tape Reader	238
5.2.8	Video Recorders	238
5.2.9	Miscellaneous	239
5.3	Launcher System Evolution	241
5.3.1	Background	241
5.3.2	Approach	242

Section	Page
5.3.3 System Requirements	243
5.3.4 Evolution	244
5.4 Retrieval System Evolution	255
5.4.1 Background	255
5.4.2 Approach	257
5.4.3 System Requirements	260
5.4.4 Evolution of Parallel Strap System	262
5.4.5 Evolution of Vertical Barrier System	281
VI SITE SETUP AND SYSTEM OPERATION	314
6.1 Site Selection and Geometry	315
6.1.1 Launch and Recovery Constraints	315
6.1.2 RPV Control Requirements	317
6.1.3 Additional Site Considerations	317
6.2 System Operation	317
6.2.1 GCS Initialization	318
6.2.2 Waypoint Programming	319
6.2.3 Prelaunch RPV Checkout	320
6.2.4 Inflight RPV Command-Status	320
6.2.5 Recovery	321
6.2.6 Procedures	321
VII CONCLUSIONS	323
REFERENCES	324

LIST OF ILLUSTRATIONS

Figure		Page
1	Initial Program Milestone Schedule Summary	20
2	As-Conducted Aquila Technical Program Schedule	21
3	Sky Eye General Arrangement	35
4	RPV-STD General Arrangement	37
5	RPV-STD Initial Wind-Tunnel Test Model and Installation in Lockheed 8- by 12-ft Subsonic Wind Tunnel	39
6	RPV-STD Model in Second Wind Tunnel Test Series in Lockheed 8- by 12-ft Subsonic Wind Tunnel	40
7	Aquila Drag Polar Evolution With Design Maturity	41
8	Aquila Propeller Thrust Coefficient Estimates - Variation With Design Maturity	42
9	RPV Configuration With Deployed Recovery Hook	44
10	RPV General Arrangement During Field Testing	45
11	Initial RPV-STD Inboard Profile	47
12	RPV-STD Inboard Profile at the Time of the Preliminary Design Review	49
13	Aquila Aircraft Weight History	53
14	Aircraft Wing Construction	60
15	Aircraft Fuselage Construction	61
16	Basic Structural Arrangement	66
17	Aquila Power Plant	77
18	Factory Delivered MC-101MC Engine	81
19	Engine Mounts, Port Side - B Model Engine	83
20	Carburetor Options: From Left - McCulloch/Walbro SDC-23, Tilletson HL-250, and Walbro SDC-43	85
21	Single Carburetor Aquila Engine	86
22	Throttle Cable Linkage - B Model Engine	90

Figure		Page
23	Carburetor Cam Throttle Control - B Model Engine	91
24	Aquila Propeller Installation	95
25	Altitude Chamber Test Stand	99
26	Engine Horsepower - Single Carburetor	100
27	Full-Throttle Specific Fuel Consumption	101
28	Engine Horsepower - Dual Carburetors	104
29	Partial Load Specific Fuel Consumption	105
30	Alternator Output Voltage - Variation With RPM	109
31	Pitch Response to Vertical Step Gust	120
32	Pitch Response to Turn Command	121
33	Aquila Flight 44 Simulated Phugoid Damper Signal	122
34	Aquila Limit Cycle Oscillations for Throttle Hysteresis, Deadband	125
35	Aquila Limit Cycle Trace for Throttle Hysteresis Deadband	126
36	Aquila RPV Response to Heading Command ($H_C = 45$ Deg)	129
37	Aquila RPV Response to Heading Command ($H_C = 90$ Deg)	130
38	Aquila RPV Response to Heading Command ($H_C = 225$ Deg)	131
39	Aquila RPV Response to Heading Command ($H_C = 270$ Deg)	132
40	Aquila RPV Response to Heading Command ($V = 100$ KEAS, $H_C = 45$ Deg)	133
41	Aquila RPV Response to Heading Command ($V = 100$ KEAS, $H_C = 90$ Deg)	134
42	Aquila RPV Response to Heading Command ($V = 100$ KEAS, $H_C = 225$ Deg)	135
43	Aquila RPV Response to Heading Command ($V = 100$ KEAS, $H_C = 270$ Deg)	136
44	Aquila Open Loop Response to Roll (δ_R) Impulse	138
45	Aquila Open Loop Response to Pitch (δ_E) Impulse	139
46	Aquila Open-Loop Response to Throttle (δ_{TH}) Impulse . . .	140
47	Aquila Response to $\dot{H}_C = 3$ -Deg/Sec Heading Loop Operational Manual Elevon and Throttle - R, ϕ , δ_R	141
48	Aquila Response to $\dot{H}_C = 3$ -Deg/Sec Heading Loop Operational Manual Elevon and Throttle - β , h	142

Figure		Page
49	Aquila Response to Pitch (δ_E) Impulse, Manual Elevon and Throttle Short Period Damper Engaged	143
50	Aquila Response to Phugoid Damper Engagement, Manual Elevon and Throttle Short Period Damper Engaged	145
51	Aquila Response to $\dot{H}_C = 3$ Deg/Sec Phugoid and Short Period Dampers Engaged and Trimmed, Manual Elevon and Throttle	146
52	Aquila Response to Engagement of A/S Loop, Phugoid and Short Period Dampers Engaged, Manual Throttle	147
53	Aquila Response to $\dot{H}_C = 3$ Deg/Sec, Phugoid and Short Period Dampers Engaged Manual Throttle, A/S Loop Engaged	148
54	Aquila Response to Full Throttle, Phugoid and Short Period Dampers Engaged, A/S Loop Engaged	150
55	Aquila Response to 1/4 Throttle, Phugoid and Short Period Dampers Engaged, A/S Loop Engaged	151
56	Aquila Response to Engagement of Altitude Loop	152
57	Loiter Guidance - Effect of Variation in K_L	156
58	Aquila Approach Simulation	162
59	Aquila RPV Vertical Errors During Final Approach Due To 15-Knot Step Headwind Beginning at Varying Distances Before Recovery	164
60	Aquila RPV Lateral Errors During Final Approach Due To 15-Knot Step Sidewind Beginning at Varying Distances Before Recovery	164
61	Aquila Launch Dynamics Angle-of-Attack Transients	166
62	Aquila Altitude Profile - Automatic Launch	167
63	Development Baseline Configurations, Phases I Through V	184
64	Aquila Payload Sensors	186
65	Original Antenna Location	200
66	Antenna Location Mod A	200
67	Summary of the GCS Antenna Changes	205
68	Initial Aquila Site Layout	214
69	Aquila Site Layout - Preliminary Design Review	215
70	Aquila Site Layout With Truck-Mounted GCS and Launcher	216

Figure		Page
71	Final Aquila Site Layout	218
72	Initial Ground Station Shelter Configuration	221
73	Ground Control Station - Final Equipment Layout	222
74	Initial Ground Control Console Equipment Layout	224
75	Ground Control Console Soft Mockup	225
76	Final Ground Control Console Component Location	227
77	Sensor Control Panel - GCS	229
78	Radio Control Unit and Autopilot Mode Test Box	240
79	Launcher Assembly	246
80	Evolution of RPV Launcher Shuttle Design	247
81	RPV Launch Velocity Versus Weight, Pressure	253
82	RPV Acceleration Versus Velocity	254
83	Photographs of Sky Eye Flight Retrieval Site	258
84	Photographs of Sky Eye Flight Retrieval	259
85	Sketch of Aquila RPV in Final Approach to Parallel Strap Retrieval System	263
86	Aquila RPV in Final Approach Before Retrieval	265
87	Aquila RPV Decelerating After Hook Engagement, Before Landing in Net	265
88	Aquila Inert Test Vehicle (ITV) in Process of Retrieval During Simulated Flight Test	266
89	Acceleration Data From 9-4-75 Static Drop Tests	270
90	Acceleration Data from 9-19-75 Static Drop Tests	271
91	Axial Deceleration Data (ITV)	277
92	Typical Hook Engagement of Arresting-Line Array	278
93	Engagement Hook Assembly	279
94	Sketch of Aquila, Showing Deployed Hook Assembly Before Arresting Line Engagement	280
95	Vertical Barrier System Concept	282
96	Operational Concept of Vertical Barrier System	283
97	Inert Test Vehicle Mounted on Pneumatic Launcher for Retrieval Test	288
98	RPV Airframe Test Vehicle in Battery Position Before Launch into Vertical Barrier Retrieval System	290

Figure		Page
99	Retrieval of Inert Test Vehicle	293
100	Three-Axis Force Traces of Loads Experienced by RPV Structural Test Vehicle During Launch and Retrieval	298
101	Forces, Revolutions, and Time Traces of Hydraulic Energy Absorbers During RPV Retrieval	300
102	Maximum Axial Deceleration Loads Imposed on RPV by Vertical Barrier	302
103	Longitudinal Force Trace as Affected by Application of Elastic Line Load to RPV	303
104	Maximum Vertical Deceleration Loads Imposed on RPV by Horizontal Landing Net	305
105	Viscosity of Hydraulic Fluid Used in Energy Absorbers ..	306
106	Aquila RPV Being Decelerated by Engagement With Vertical Barrier	308
107	Aquila RPV at Nearly Full Arrest by Vertical Barrier . . .	309
108	Aquila RPV at Rest in Horizontal Landing Net After Successful Retrieval	310
109	Maximum Velocity of Headwind Against Which Vertical Barrier Will Remain Erected (Hold-Back Brake Release Load of 160 lb on Each Energy Absorber)	312

LIST OF TABLES

Table		Page
1	Typical Weight Savings	51
2	Historical Variation of Sensor and Fuel Weights	52
3	History of RPV-STD Component Weights	53
4	RPV Performance Evolution	56
5	Margin of Safety Summary Table	69
6	Engine Candidate Comparison	78
7	Alternator Comparison	107
8	Initial Phase I, Real-Time TV Surveillance Sensor Specifications	178
9	Initial Phase II, Photographic Reconnaissance Sensors Specification	179
10	Initial Phase III, Target Acquisition Sensor Specifications	180
11	Initial Phase IV, Target Location and Artillery Adjustment Sensor Specifications	181
12	Initial Phase V, Target Designation Sensor Specifications	182
13	Link Analysis - Original Data Link	197
14	Link Analysis - "A" Change	197
15	Link Analysis - "B" Change Final Configuration	198
16	Launcher Test Summary	252
17	Comparative Characteristics of Various Retrieval Systems	256
18	Results of Static (ITV Drop) Tests of 9-4-75	268
19	Results of Static (ITV Drop) Tests of 9-19-75	269
20	Results of Dynamic (ITV Engagement) Tests	273
21	Test Data Summary (Development Tests Conducted at Facilities in Wilmington, DE)	291
22	Test Data Summary (Development Tests Conducted at Facilities in Fort Huachuca, AZ)	292

Section I
INTRODUCTION

This volume, Volume II of three, describes the evolution of the system hardware elements. Section II of this volume describes the technical evolution program. Sections III, IV, and V describe the evolution of the RPV, the data link, and the ground support system elements, respectively. Section VI describes the site setup and the system geometry. Section VII states the conclusions relative to RPV system development.

Section II
TECHNICAL PROGRAM DESCRIPTION

The Aquila Remotely Piloted Vehicle System Technology Demonstrator (RPV-STD) Program originally consisted of a 25-month program. The program was structured on three key technical features:

- Use of proven hardware:
 - Launcher. Derivative of a previous subcontractor design
 - Airframe. Derivative of a previous subcontractor design with 60 successful flights
 - Engine. Successful demonstrations on Army, NASA, and Air Force RPV programs
 - Data link. Proven design hardware modified for installation
 - Servos, accelerometers, and rate gyros. Off-the-shelf proven hardware
- Use of proven technique:
 - Autopilot. Mechanization technique proven on Lockheed and Air Force RPV programs
 - Sensors. Techniques validated in Government laboratory tests
 - Retrieval system. Adaptation of design used for larger aircraft
 - GCS. Derivation of the technique used for Air Force RPV program
- Positive margin of system performance:
 - RPV. Weight margin to accommodate additional payload and/or full capacity; structural margin to minimize damage and permit repair and reflly capability
 - Launcher. Weight margin to accommodate increases in RPV weight
 - Retrieval system. Oversized to accommodate unknowns in retrieval accuracy
 - GCS. Additional computer core capacity for potential increased demands on software

Based on these precepts, the program assumed an optimistic, success-oriented nature. The original schedule, as proposed in Figure 1, reflects those characteristics as follows:

- Early design commitment. Preliminary Design Review (PDR) in 6 weeks; build-to-baseline definition in 4 months, test-to-baseline in 6 months.
- Compact schedule. First flight scheduled 2 months after build-to-baseline defined; initial system acceptance 2 months after completion of initial flight; completion of all hardware deliveries 17 months after contract award
- Minimal contingency planning. Overlapping of design validation and system validation flight testing without adequate allowance for analysis, resolution, and verification of resolution to flight anomalies.

This approach was taken to provide urgently needed data to the Army for program decisions. The approach produced hardware early, provided for early recognition of deficiencies and their correction, and provided early operational data.

2.1 DESIGN

The final evolution of the Aquila Technical Program is described in Figure 2. This figure presents a program schedule showing the relationship between the key program phases and milestones. The following paragraphs discuss the phases and milestones, and reference to this figure will be beneficial to the reader's understanding.

The Aquila program contract was awarded on 20 December 1974. The Preliminary Design Review (PDR) was held on 5-6 March 1975. This review confirmed the technical approach and hardware selections as originally proposed with one major exception. A cost, schedule, and technical risk comparative study was

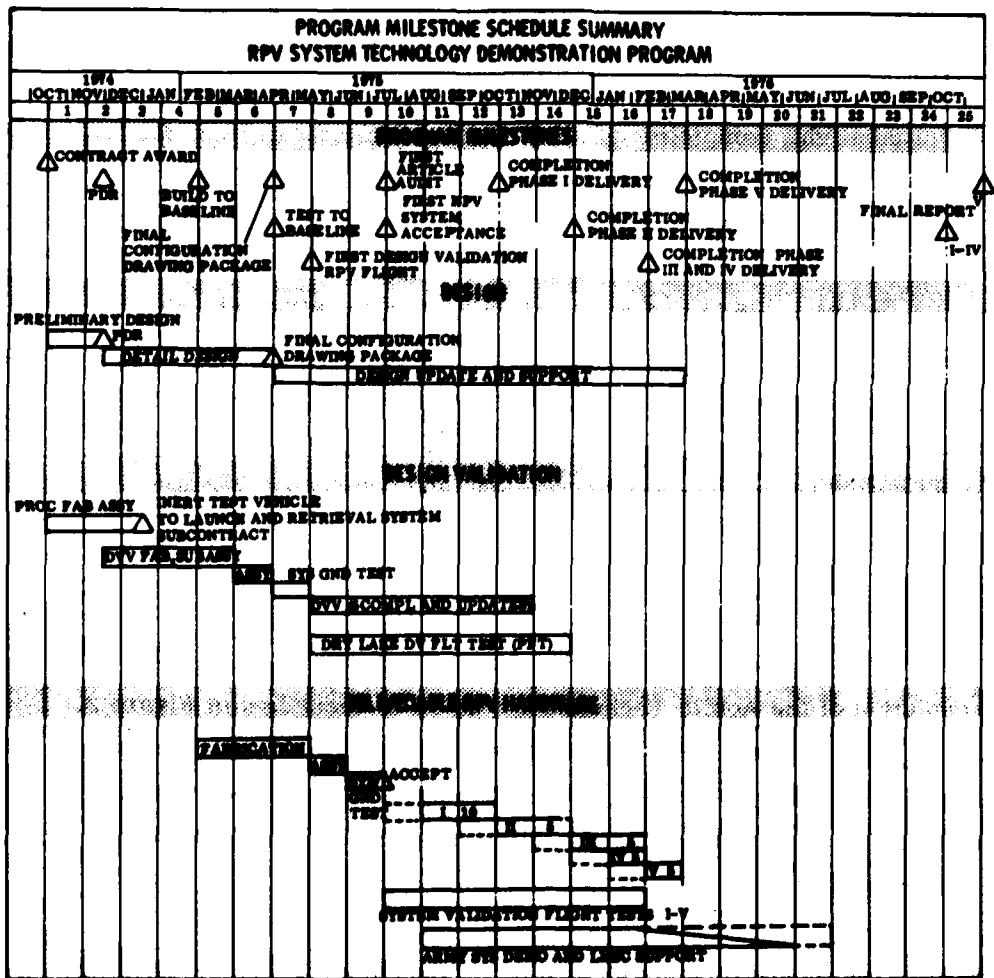


Figure 1. Initial Program Milestone Schedule Summary

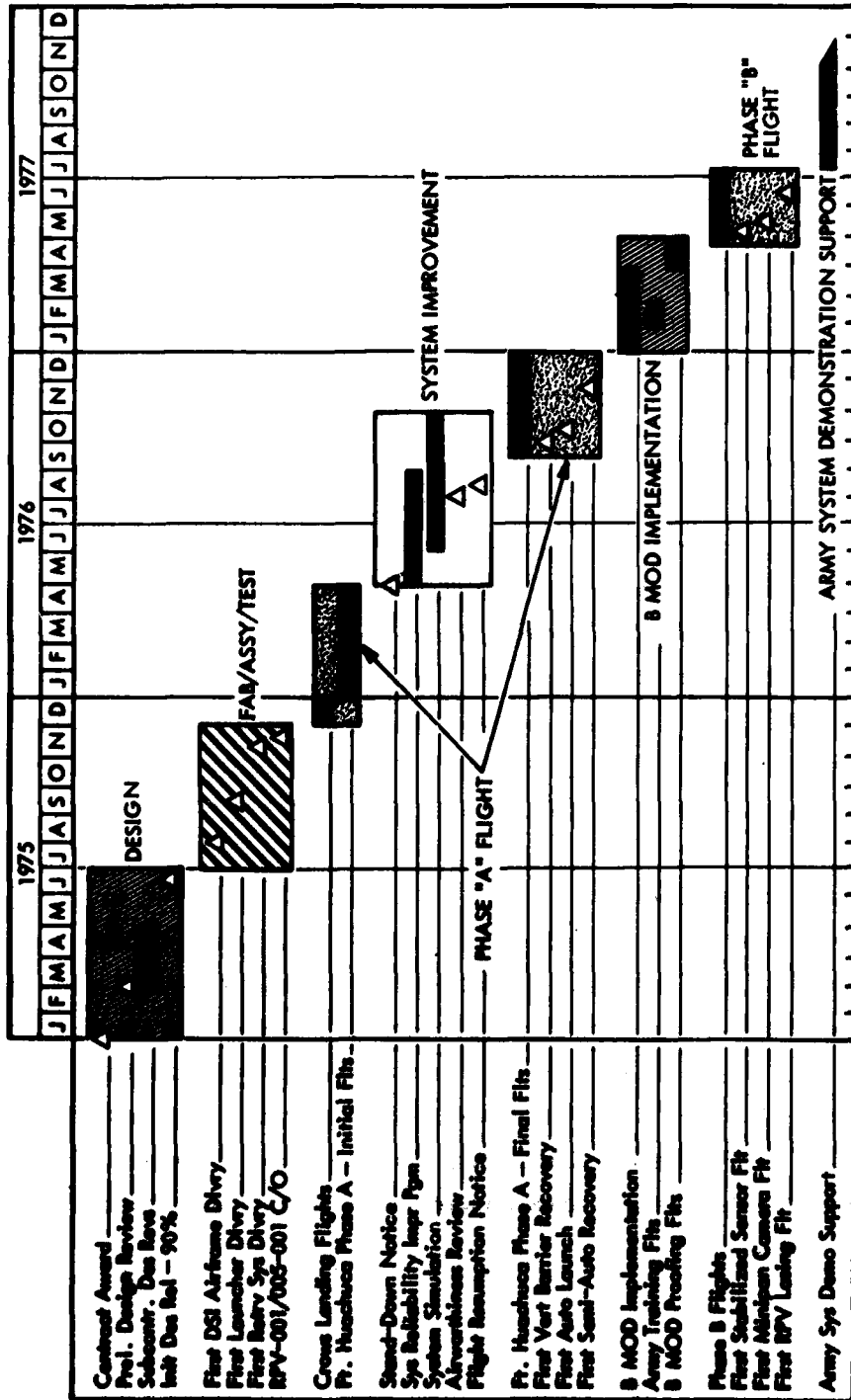


Figure 2. As-Conducted Aquila Technical Program Schedule

performed between the originally proposed Westinghouse Blue Spot sensor and the Honeywell Poise sensor. The results of this study were reviewed at the PDR and the decision was made to change the baseline to the Poise sensor.

Changes recommended in the PDR were incorporated during March and April 1975 as the detailed design phase progressed. Design reviews were held at each of the subcontractors during April and May to finalize design and to confirm interfaces. The result of all these efforts was the achievement of the 90-percent design release point in mid-June 1975.

2.2 FABRICATION/ASSEMBLY/TEST

Fabrication and assembly of Lockheed-provided hardware began in May 1975. The first Developmental Sciences Inc. (DSI) airframe (RPV-001) was received on 28 July 1975 and required additional efforts to correct interface discrepancies and to effect weight reduction changes for subsequent airframes. RPV-001 with subsystem hardware installed was released to Test Engineering on 27 August 1975. On the same date GCS-001 was also released to Test. Ground checkout of both elements commenced on 28 August 1975.

The first All American Engineering (AAE) launcher was delivered on 19 September 1975. Launcher mounting on the M-36 truck, installation of a new skag release mechanism, and interface validation with the engine started were completed and the tested launcher system was shipped to Fort Huachuca in late November 1975. The first retrieval system was received at Fort Huachuca directly from AAE. RPV-001 was completed and system ready on 30 November 1975. GCS-001 and RPV-001, with landing gear installed, completed their final checkouts and were on site at Crows Landing Naval Auxiliary Landing Field on 16 November 1975.

2.3 CROWS LANDING FLIGHT TESTS

Taxi tests with RPV-001 at Crows Landing were completed as precursors to the takeoff and landing of RPV-001 on 1 December 1975. In all, six successful flights were carried out through 12 December without loss of RPV and for a total flight time of 90 min. The objectives that were accomplished on these flights included determination of the following:

- RPV airworthiness
- Autopilot capability
- RVP/GCS integrated performance

2.4 FORT HUACHUCA FLIGHT TEST - INITIAL PHASE A

GCS-002 launcher and retrieval systems were checked out and readied at Fort Huachuca. The landing gear was removed from RPV-001 and minor refurbishment accomplished before shipment. At Fort Huachuca a complete system checkout was accomplished in time to support Flight 7, the initial Fort Huachuca flight test, on 22 January 1976.

Between that date and 28 March 1976, there were six additional flights at Fort Huachuca, Flights 8 through 13. During these seven flights, the following flight test objectives were accomplished:

- Acquisition of data base to support automatic launch decision
- Verification of waypoint navigation
- Continued accrual of RPV performance data
- Continued demonstration of RPV/GCS integrated performance
- Limited parallel strap retrieval system evaluation

On six of the seven flights the RPV was lost; four of the six crashes were attributed to system design deficiencies, two to human factors/procedural errors.

The fact that the causes of these crashes were irregular and neither repeated nor associated with the same hardware component led to the conclusion that the level of system and design maturity and level of flight confidence testing were inadequate to support a successful field flight test program.

On 4 May 1976, Fort Huachuca flight testing ceased, immediately followed by the issuance of a series of instructions which resulted in implementation of the Aquila System Reliability Improvement Program.

2.5 SYSTEM RELIABILITY IMPROVEMENT PROGRAM

The purposes of this program were to review, evaluate, and test the suspect elements of the system, to determine the areas of inadequacy and low reliability, to devise acceptable system improvement changes, and to perform simulations and system confidence testing to validate the acceptability of the improvements. For 4 months, May through August 1976, all efforts were directed to implement this program - e.g., risk reviews, system reviews, independent Army team reviews, flight anomaly reviews, parachute backup recovery system implementation, increased system flight confidence testing, hardware and software improvement modification, additional system simulations, procedural revisions, and strengthening of test operations capability. At the completion of these efforts, an Airworthiness Review was held at Lockheed on 3-4 August 1976. On the basis of information presented in this review, which verified that all flight critical changes and recommendations had been incorporated, the decision was made to resume flight testing at Fort Huachuca.

2.6 FORT HUACHUCA FLIGHT TESTS - FINAL PHASE A

Testing operations resumed at Fort Huachuca on 25 August 1976, with the first flight occurring 13 September 1976. The original flight test planning was revised to (1) preclude sensor testing until RPV and GCS systems were validated, (2) reflect the logical derivation of flight-test requirements that evolved from

the System Reliability Improvement Program, and (3) provide conservative planning by scheduling contingency flights. This revised planning resulted in 14 flights whose basic objectives were to validate the following:

- Automatic launch
- Waypoint navigation
- Search and loiter patterns
- RPV flight performance
- Semi-automatic recovery
- RPV/GCS interface
- Software verification
- Procedures evaluation
- Army crew training

Sixteen flights (Flights 14 through 29) were actually required to complete this phase of the program. All objectives were achieved except for the moving box search pattern and the dead reckoning mode of waypoint navigation. These objectives were delayed due to lack of validated software or minor flight control hardware deficiencies. The first seven flights, which occurred between 13 September and 2 November 1976 (Flights 14 through 20), were conducted from the RPAODS site; the remaining nine flights, which occurred between 15 November and 21 December 1976 (Flights 21 through 29), were from a more open site at Sycamore Canyon. The move to Sycamore Canyon was made to allow flight operations out to a range of 20 km.

The system was configured with incorporation of all changes agreed on during the Airworthiness Review of 3-4 August 1976. The radio control (RC) recovery mode was retained for use in support of the validation of automatic launch and retrieval and as a backup flight mode when the RPV was in visual contact.

During the 4 months, 16 flights were flown with loss of only 2 RPVs; i. e., one due to a low approach during RC (Flight 14) and the other a procedural-hardware malfunction during transfer of control between RC pilot and RPV

operator (Flight 19). There was one aborted flight due to errant data-link performance (Flight 25) without loss of RPV. Following Flight 14 on 13 September 1976, the decision was made to replace the parallel strap retrieval system with the trailer-mounted vertical ribbon barrier retrieval system. This change was brought about because of problems with arresting array rigging, overall complexity of operations, frequent replacement of components and adverse impact of the trailing hook assembly on RPV performance. After Flight 14 the only RPV loss was associated with the procedural-hardware malfunction on Flight 19.

2.7 B MODIFICATION IMPLEMENTATION

At the conclusion of the Phase A Aquila flight test activity, there were still system improvements that had not been implemented. Those improvements not implemented were (1) noncritical flight system improvement changes, which were bypassed to concentrate on higher priority improvements for tests at Fort Huachuca, (2) nonflight initial system improvements identified during final Phase A flight testing at Fort Huachuca, and (3) system modifications required to support the sensor-mission validation (Phase B) flight testing.

During the period from January through March 1977, the system improvements or B modifications incorporated included the following:

- RPV-GCS electrical and mechanical changes to accommodate sensor installation and functional performance
- Dual-carburetor-system improvements to increase engine performance and improve accessibility
- GCS tracking antenna improvements to increase performance and resolve roll instability problem
- RPV-GCS electrical and mechanical changes associated with deletion of backup parachute system
- RPV mechanical and electrical design improvements associated with installation of new accelerometers and servo motors to increase RPV reliability

- Software changes to improve system performance in areas of search patterns, final approach pattern abort options, dead reckoning, roll stabilization, targeting computations, and sensor capabilities

During this period Army crew training continued. Eight training flights for the U.S. Army Electronic Proving Ground (USAEPG) crew were scheduled and eight successfully flown. The first, Flight 30, was flown on 19 January 1977 and the last, Flight 37, was flown on 23 February 1977. Primary objective of these flights was USAEPG crew training, but some secondary objectives were accomplished as follows:

- Roll instability evaluation
- Dead reckoning evaluation
- Retrieval system rerigging demonstration (time < 5 min)
- Cross-wind retrieval demonstration (18 km/h)
- RPV performance evaluation

By the middle of March 1977, the evolution of several significant B modifications had matured to the point where flight verification was required. Phase B RPVs were a month away from delivery; therefore, two Phase A RPVs were modified to accept the select B mods.

Four flights were scheduled and all four were successful; the first, Flight 38, was flown on 1 April 1977 and the last, Flight 41, was flown on 22 April 1977. The following system performance evaluations were accomplished:

- New accelerometer
- Relocated RPV command antenna
- GCS with B mods
- Engine with B mod dual carburetor installation
- New propeller
- Roll stability resolution mod

- Heading hold/dead reckoning mod
- Data link (C³ and video) at 20 km and 1,000 ft/2,000 ft AGL
- RPV position accuracy
- Final approach software

2.8 PHASE B FLIGHT TESTING

The phase B flight test activity followed in the successful footsteps of the B mod flight testing. The initial flight, Flight 42, was flown on 28 April 1977 and the last, Flight 65, was flown on 10 July 1977. During this period, 24 flights were flown with only one, Flight 48, resulting in the loss of the RPV. The cause of RPV loss was a human factors error. During the process of changing retrieval nets due to a wind shift and while the sensor operator was aligning the ground camera, the RPV operator's video was dimmed to force the student to concentrate on instruments. During this period of no RPV video presentation, the RPV struck a hill south of the GCS. Subsequent investigation revealed a calibration problem in the GCS altitude circuits, which resulted in erroneous altitude commands in manual mode; this fact contributed to the problem but could have been avoided with proper RPV video monitoring.

The 24 flights are reported in Volume III of this report.

2.9 CONTRACTOR VALIDATION ACHIEVEMENTS

At completion of the Aquila contractor validation testing, the following system characteristics and objectives had been demonstrated:

- Automatic launch
- Semiautomatic recovery
- Unstabilized sensor performance
- Stabilized sensor performance
- Panoramic camera (35-mm performance)

- Fully automatic waypoint guidance
- Endurance of 3+ hours
- Range of 20+ km
- Area surveillance
- Target detection and recognition
- Sensor lock-on and centroid tracking
- Laser target designation

2.10 ARMY SYSTEM DEMONSTRATION

The Army began system demonstration flight testing at Fort Huachuca using Lockheed-trained Army crews from U.S. Army Field Artillery Board (USAFAB), Fort Sill, Oklahoma, and U.S. Army Electronics Proving Ground (USAEPG), Fort Huachuca, Arizona. The first flight occurred on 20 July 1977, and by the last flight on 18 November 1977 the Army had completed a total of 84 flights in their test program. During this period an average of one flight per day was achieved and, on occasion, two flights per day were achieved with less than one hour turnaround time. In total, 149 flights of Aquila were made during the System Technology Demonstrator program.

Section III
AIRBORNE SYSTEM (RPV)

The Aquila airborne system (RPV) consists of:

- Airframe
- Power Plant/Electrical Subsystem
- Flight Controls
- Sensors
- Data Link (airborne elements)

The RPV and its elements, as delivered to and tested by the Army, are described fully in Volume I of this report, "Aquila System Description and Capabilities." This section describes the engineering analysis design, development and testing involved in the evolution of the RPV and its subsystems.

3.1 RPV EVOLUTION

The integrated airborne system evolved from the variety of technologies, components, and techniques drawn from previous and on-going RPV, aircraft, and sensor programs. The Aquila program requirements were examined in light of these existing capabilities, and the design and evolution approach was defined and accomplished. This process of evolution for the Aquila RPV is defined in the following paragraphs.

3.1.1 Background/Situation

A variety of contractor- and Government-funded RPV and sensor programs had been completed with various degrees of success at the time of initiation of the Aquila RPV procurement. Several RPV programs, including Aequare (ARPA/USAF), RPAODS (U.S. Army), Prairie I, II (ARPA) and Savoir (U.S. Army)

had demonstrated the ability of a mini-RPV and general requirements for carrying modern targeting sensors. However, these early systems required close engineering attention to operate and maintain, proved marginal or inadequate relative to flight performance, and were deficient in terms of field operations characteristics for Army "hands-on" operations.

Direct LMSC experience with the Lockheed "Tuboomer," the ARPA/USAF Aequare, and other Lockheed RPV designs and other contractor experiences supported the conclusion that an effective mini-RPV design could be built and produced in sufficient numbers and with sufficient design maturity to support a comprehensive Army field evaluation of RPV capabilities. Evaluating the history of mini-RPV programs, the Army derived a realistic set of specifications for an RPV system technology demonstration program. Specifications for the RPV of this system are indicated in the following paragraph.

3.1.2 RPV Specifications

The contract specifications for the Aquila RPV as an integrated flight vehicle are summarized as:

- Performance

- Cruise airspeed (band) - 75-120 KEAS
- Maximum cruise altitude - 12,000 ft MSL
- Time to climb 0-10,000 ft MSL - 15 min
- Takeoff/land conditions - 4,000 ft MSL 95°F
- Typical operational altitude - 2,000 ft AGL
- Winds (maximum for operation) - 20 knots, gusting to 35 knots
- Endurance - 1.5 hr (minimum)
- Operating radius - 15-20 km from GCS

● Mass Properties

- Gross weight - 120 lb maximum
- Maximum payload capability - 30 lb

● Design

- Structural design load factor - 6 g
- Interchangeability of payloads - Phase I through Phase V
- Sorties per day - 4 (maximum)
- Total sorties per aircraft - 15 (maximum)
- Approach - Simple/low cost
- Skill level of personnel - minimum
- Detectability/observability - minimum
- Design level - limited production

Further experience in the RPAODS test series led the Army to require the use of a flight-proven air vehicle design. The LMSC approach to meeting these requirements is indicated in the following paragraphs.

3.1.3 RPV Evolution Approach

Following a review of available RPV technology and related program experience, LMSC made the following selections as baseline elements upon which to base the evolution of the RPV-STD air vehicle to meet the Army requirements:

General Arrangement	DSI Sky Eye RPV
Power Plant	McCulloch MC 101 engine/DuFresne Alternator
Flight Control Autopilot	LMSC RPV Autopilot
Sensor	GE Blue Spot

During the proposal effort, LMSC identified the basic adaptations necessary to incorporate these and other elements into an effective RPV design. These adaptations include:

- **General Arrangement.** Modify the Sky Eye contours to fit the RPV-STD requirements and to reduce observability, derive an internal arrangement to support access, installation, checkout and cooling, and to balance the RPV for stable flight. Wind tunnel test the configuration to verify stability, controllability, and performance characteristics.
- **Power Plant.** Convert the MC 101 engine to an aircraft power plant with adaptations for the propeller, suitable carburetion, fuel system, engine rpm control, cooling, and shock mounting. Procure a DuFresne alternator and couple it through a flexible drive to the engine. Characterize the resulting power plant in altitude chamber tests, and establish assembly specifications and test procedures.
- **Flight Control Autopilot.** Adapt the second generation LMSC autopilot concept to the RPV-STD, adding way point, dead reckoning and specific discrete signals. Package the autopilot for the unique RPV application. Test the autopilot components and functions, and evolve checkout procedures.
- **Sensor.** Adapt the GE Blue Spot sensor to the RPV-STD mission requirements and procure a family of sensors - unstabilized TV, stabilized TV with scene tracker, laser ranger, and laser designator - in the Blue Spot form factor for interchangeable installation in the RPV.

Accommodations built into the RPV for interfaces with the launcher, retrieval system, and ground handling equipment were kept to a minimum with most of the compromises assigned to the ground-based elements.

Using this basic approach, the evolution of the RPV began at LMSC in the summer of 1974. That evolution is discussed below.

3.1.4 RPV Evolution – General Arrangement

In preparation for the RPV-STD program, several designs were evaluated by LMSC. In keeping with the Army requirement to use a flight-proven RPV, the Sky Eye (Figure 3) with over 60 successful radio-controlled flights was selected as the starting point for the Aquila airframe and Developmental Sciences, Inc., the Sky Eye developer, was selected as the airframe subcontractor. After selection of the basic airframe design arrangement, the design was examined against the specific requirements of the proposed program to identify design improvements. The resulting configuration is shown in Figure 4. Some of the major changes from the Sky Eye were:

- Landing gear removal and adaptation for catapult launch and hook recovery
- Reduced propeller shroud size for reduced observability
- Blended wing-body for reduced observability and increased performance
- Minor wing twist and dihedral change to account for body geometry changes
- Eliminated a float type carburetor for the engine
- Increased structural capability

A wind-tunnel test of a half-scale model of the resulting configuration was performed in August 1974 at Lockheed's low speed 8- by 12-ft tunnel in Burbank, California. Figure 5 shows the RPV in its test arrangement. The purposes of this test were to:

- Obtain static stability derivatives and control coefficients to allow formation of the autopilot design.
- Obtain data for basic aircraft performance characteristics.
- Determine engine power effects on performance characteristics.
- Study a limited amount of flow field characteristics.

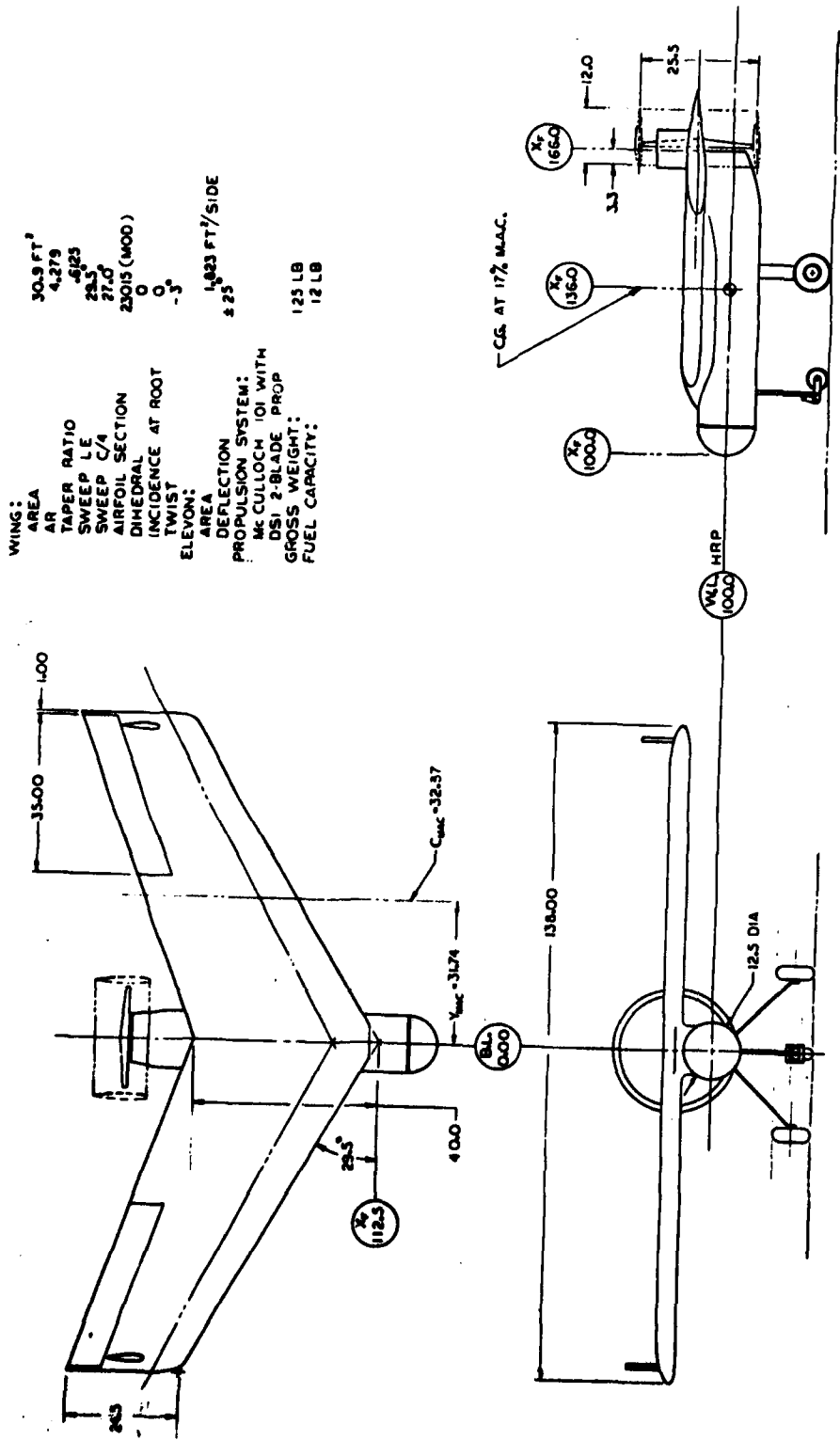


Figure 3. Sky Eye General Arrangement

WING AREA
 4.18
 395
 25.4
 40.08 m
 21.00 m
 23.00 (WING)
 +4.5
 0

WING AREA
 1.7714/1.06
 2.87

PROPULSION SYSTEM:
 INCALLOCK 10-1A1 WITH
 DSI 3 SLABE PROP

GROSS WEIGHT 600 lb
 FUEL CAPACITY 15 lb

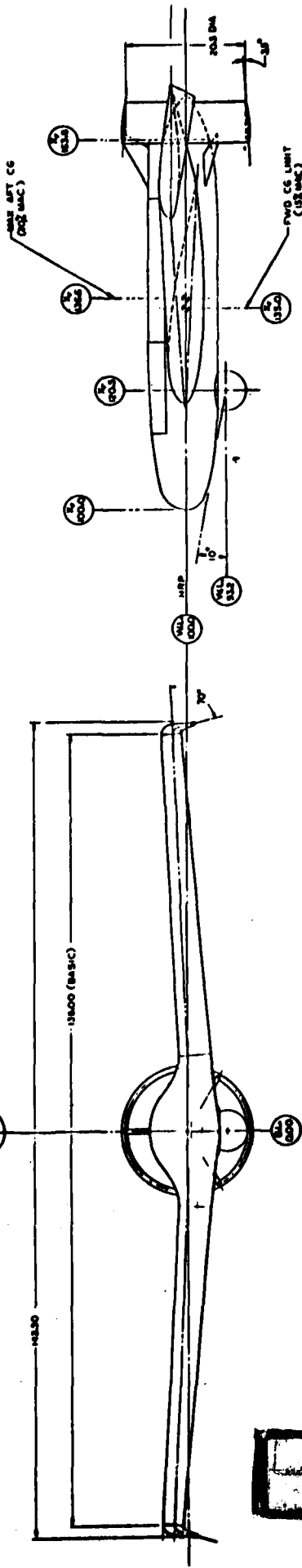
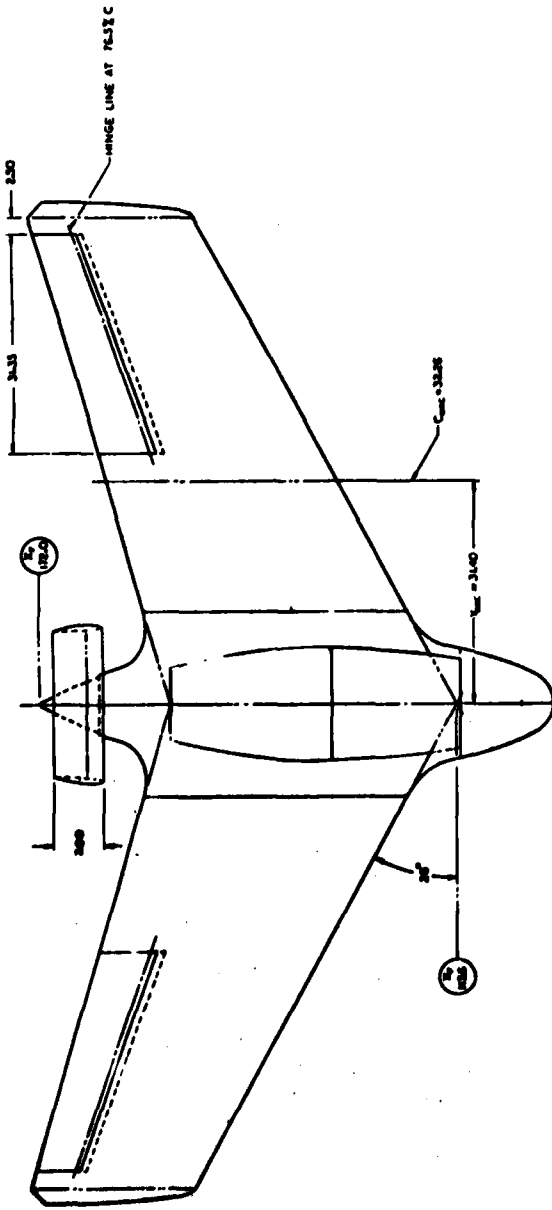


Figure 4. RPV General Arrangement



Figure 5. RPV-STD Initial Wind-Tunnel Test Model and Installation in the 8- by 12-ft Subsonic Wind Tunnel

Following initiation of the program in December 1974, a second windtunnel test was performed in February 1975, with the model modified to reflect the evolving configuration. Some of the objectives of the second wind-tunnel test were to obtain stability and performance data including the following:

- Inclusion of a payload protector and recovery hook
- Definition of the effects of a modified duct
- Definition of the effects of the Bagley/Beasley wing tips
- Definition of the effects of a drag brake
- Calibration of the onboard air data system
- Definition of the effect of increased elevon deflection angles
- Definition of the effects of an upright engine installation
- Definition of the effects of a larger sensor dome

Figure 6 shows the revised model in the 8- by 12-ft wind tunnel.

As a result of the wind-tunnel testing, it was determined that for the selected range of center-of-gravity locations (21% MAC \pm 1%) the RPV would be stable



a. RPV-STD Model With Recovery Hook, Payload Protector, Drag Brake, and Upright Engine Fairing



b. RPV-STD Model With Large Payload Dome and Film Camera Geometry

Figure 6. RPV-STD Model in Second Wind Tunnel Test Series in the 8- by 12-ft Subsonic Wind Tunnel

and controllable in all three stability axes. Drag and propeller thrust efficiency data, as they varied throughout the program, are shown in Figures 7 and 8. The low level of drag indicated in the first wind tunnel test series (Figure 7) supported performance levels equivalent to or greater than those goals cited in the contract statement of work. As the RPV design evolved and was better defined, the estimated drag of the system increased. This increase in drag evolved from a multitude of design changes and from manufacturing techniques that were undefined during the initial evaluation. Factors that increased the drag during the RPV development include:

- Recovery hook drag higher due to required configuration
- Gaps and slots in doors and joints larger than anticipated

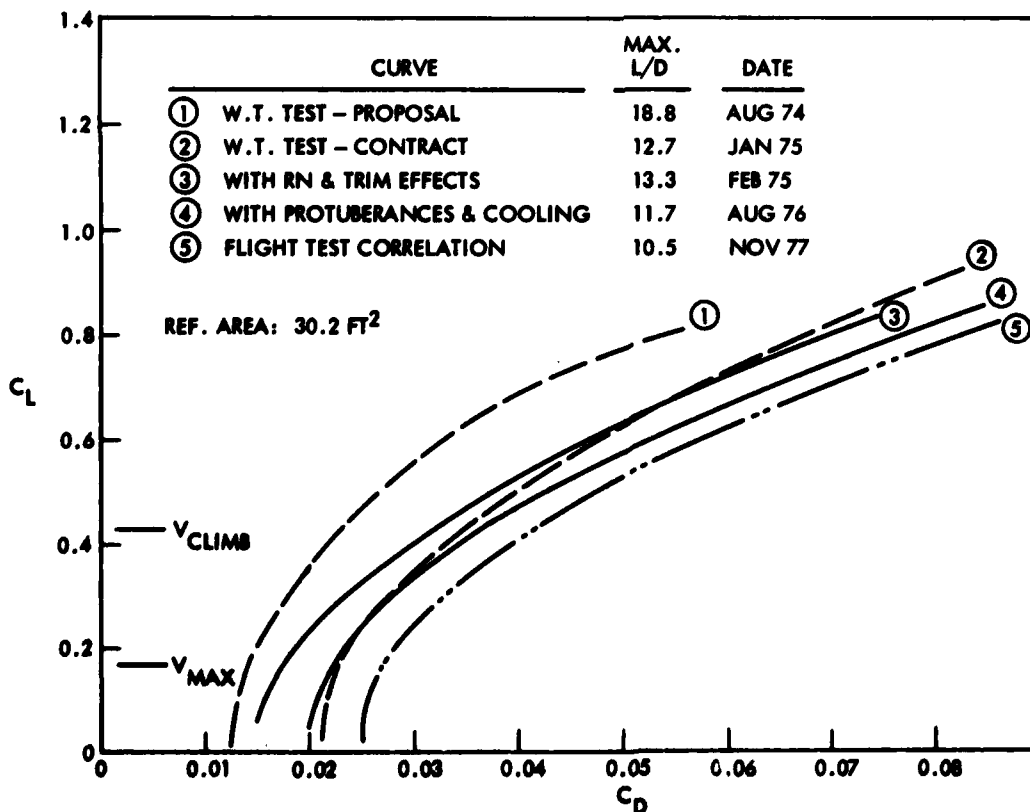


Figure 7. Aquila Drag Polar Evolution With Design Maturity

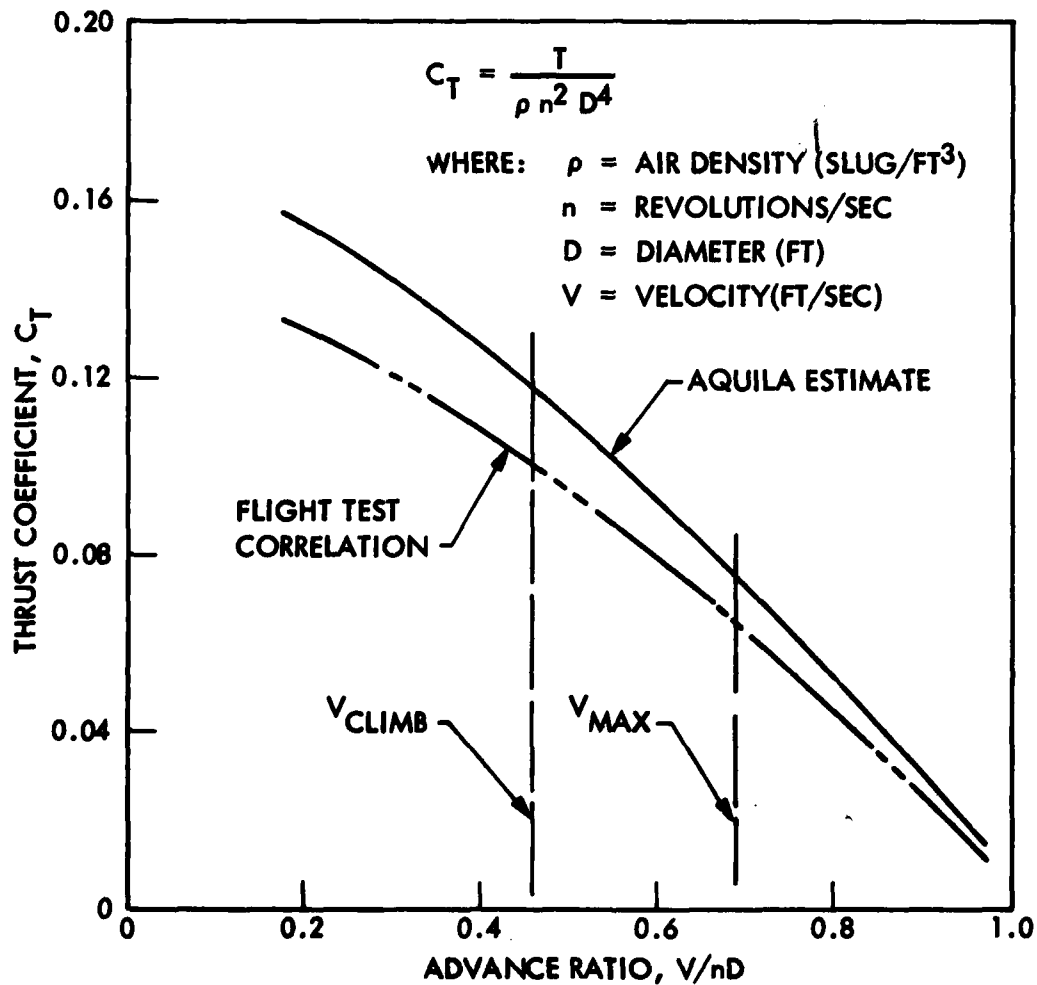


Figure 8. Aquila Propeller Thrust Coefficient Estimates - Variation With Design Maturity

- Payload protector not faired in stowed position as originally intended
- More cooling air (cooling drag) required than anticipated
- Skin roughness greater than anticipated (minimum resin to reduce weight)
- Protruding wing tip fasteners required
- Rf antenna drag higher than anticipated (internal installation originally planned)

- Trim deflection (and drag) higher than predicted
- Push pad (launcher interface) load distribution channels produced added drag.

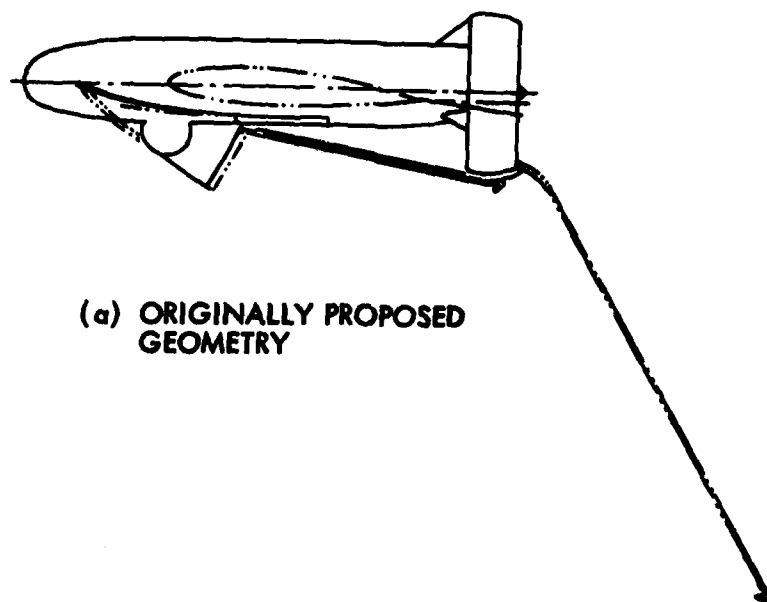
Similarly the propeller efficiency in the pusher arrangement appears to be significantly lower than originally assumed.

The final drag polar and propeller efficiencies (Figures 7 and 8) are estimated, both in level and distribution, from flight test data. Since the flight performance of the Aquila RPV-STD proved to be adequate to perform the field evaluation, expensive and time-consuming drag reduction efforts to restore performance to predicted levels were not conducted. Various propellers were tested, however, to improve low-speed climb performance at the expense of the maximum speed.

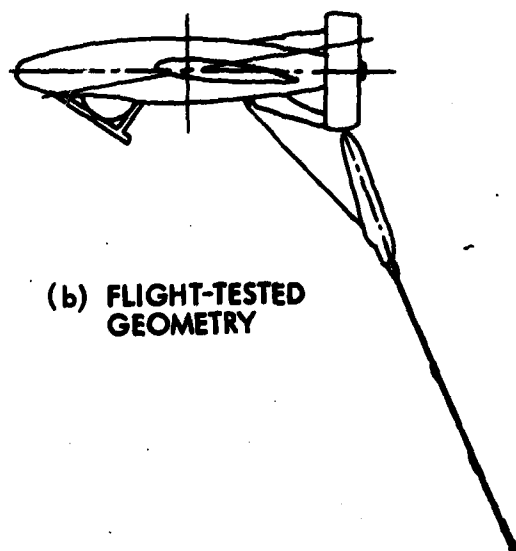
LMSC-L028081 (Reference 1) summarizes the wind tunnel test data and aerodynamic analysis of the Aquila RPV. Throughout preliminary design, the general arrangement remained relatively fixed. At the preliminary design review, the only observable changes from the originally proposed configuration were the addition of the large dome (to reflect the change to the "Poise" family of sensors), "inversion" of the propeller shroud support arrangement to improve engine access, support of duct loads during emergency skid landings, and provision of a solid support for the recovery hook assembly. Mylar prints of the mold lines of the configuration were developed at this time by LMSC and provided to the airframe subcontractor for mold development (see Volume I for mold line description).

Figure 9 shows the recovery hook assembly as proposed and as flown. The recovery hook assembly (described in the recovery system section of this report) was ultimately placed within a fairing in front of the lower propeller shroud support. In this stowed position there was no significant effect on aerodynamic stability or performance. In the deployed position, however, the fairing extended well below the RPV, and with the hook pole assembly, produced significant drag and nose-down pitching moments. This effect contributed

(1) Lockheed Missiles & Space Co., Inc., Aquila RPV System Test Report, CDRL A00D, Aerodynamics, LMSC-L028081, Sunnyvale, Calif., May 1977



(a) ORIGINALLY PROPOSED
GEOMETRY



(b) FLIGHT-TESTED
GEOMETRY

Figure 9. RPV Configuration With Deployed Recovery Hook

directly to the loss of RPV 002 in test flight 9 at Fort Huachuca. These effects also complicated the job of the RC pilot in recovering the RPV with the recovery hook arrangement. These difficulties plus design and logistic problems ultimately led to the deletion of the hook assembly and adoption of the vertical barrier recovery system.

The general arrangement, frozen shortly after the preliminary design review in April 1975, remained relatively fixed from that time until initiation of field testing. During field testing, the deletion of the spinner and the hook recovery system and some minor antenna relocations finalized the configuration.

Figure 10 shows the RPV mounted on the launcher during field tests at Fort Huachuca. The unfaired, stowed payload protector, the large payload dome, the cooling air ducts (nose and wing), the launch push pads and load distribution channels, the deletion of the recovery hook assembly, and the deletion of the spinner can all be observed in this figure.



Figure 10. RPV General Arrangement During Field Testing

3.1.5 RPV Evolution - Inboard Profile

The inboard profile of the Aquila RPV-STD evolved parallel with the general arrangement. Overall height and length dimensions of the fuselage were selected for compatibility with the major subsystems, e.g., payloads, engine, fuel tank, and autopilot. The resulting aerodynamic fairings produced a general arrangement which provided generous volume for the internal placement of subsystems. Subsystem placement was driven by considerations of balance for stability, access for checkout and installation, mounting provisions, and favorable flow of cooling air.

The initially proposed inboard profile is shown in Figure 11. This arrangement reflects the original consideration of the Blue Spot family of payloads. The originally inverted engine (Sky Eye) arrangement was abandoned for improved access to spark plug and carburetor installations, for improved fuselage fairing, and to prevent fuel and oil from gravitating to the spark plug and causing fouling during rich starts. The fuel tank was placed to minimize center-of-gravity shift during flight. The flight control electronics package was shaped to lay over the payload installation. Flight Control sensors, electrical system, and data link elements were housed in the nose. Access to the internal elements was planned through two large doors on the upper surface, a removable nose fairing and a removable engine cowl.

Changing to the Poise family of payloads early in the contract led to a significant rearrangement of internal components as shown in Figure 12. The larger volume sensor unit required a modified installation for the 35-mm film camera, forcing it to the next bay aft. The payload electronics package was moved forward to the nose bay. The autopilot was repackaged and moved aft. Also, the data link encoder decoder was repackaged to fit within the autopilot enclosure to save weight by deleting the encoder enclosure. The command receiver and power supply (conditioner) were placed under the flight control electronics

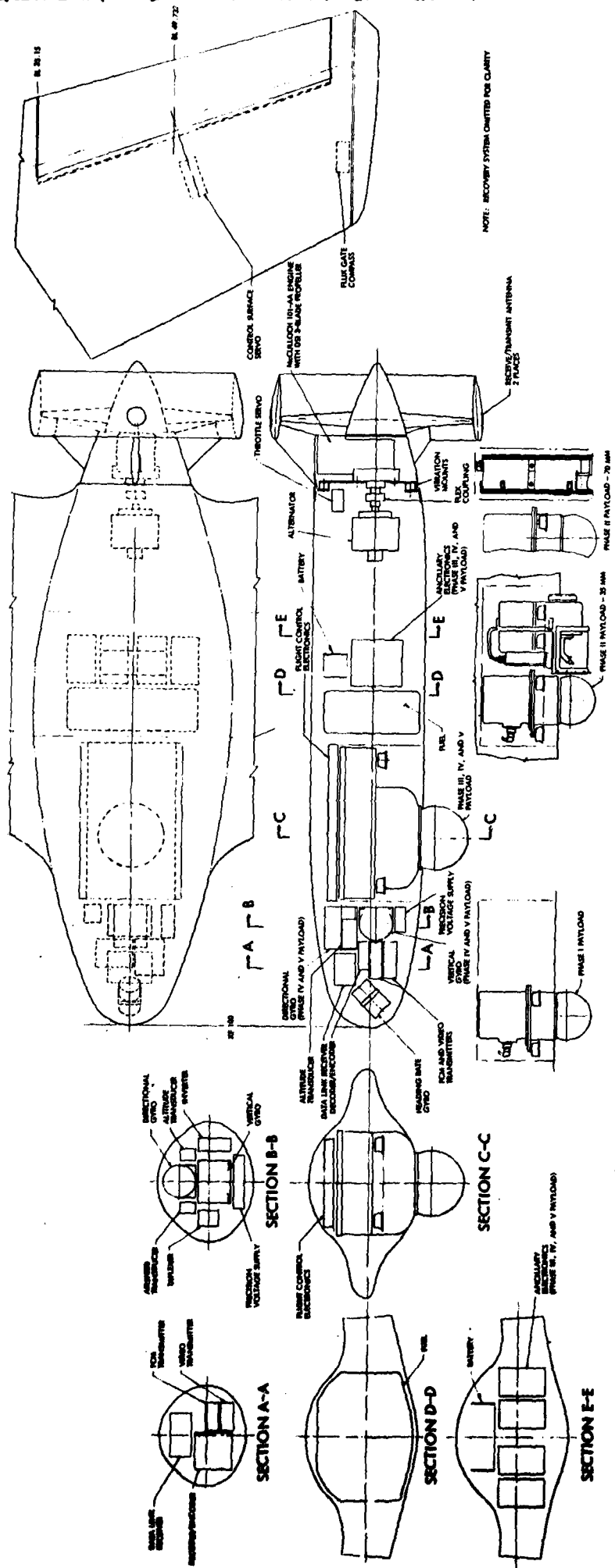


Figure 11. Initial RPV-STD Inboard Profile

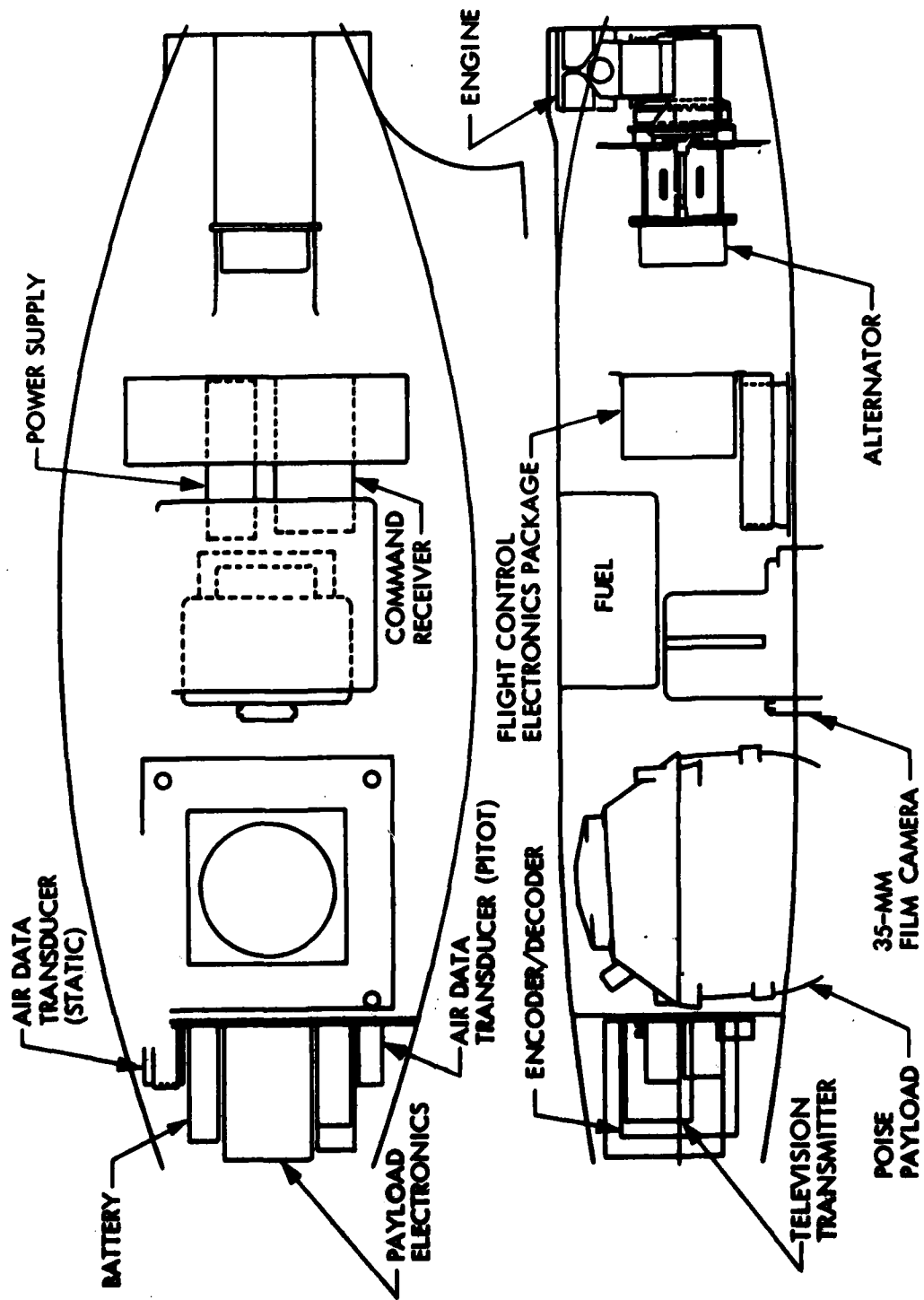


Figure 12. RPV-STD Inboard Profile at the Time of the Preliminary Design Review

package on the same bulkhead. The gas tank compartment was flattened and moved to the top of the compartment to clear the film camera. The position on the center of gravity was maintained. This arrangement evolved to the final configuration, which is described fully in Volume I of this report. This internal arrangement, like the general arrangement, became basically frozen shortly after the preliminary design review. Throughout the evolution of the internal arrangement, consideration was given to maintaining adequate cooling air flow for the heat-generating components. Access doors were sealed to ensure that the air flow from inlets in the nose and wing stub flowed through the body and into the engine cooling fan. As part of the reliability improvement program in 1976, the effectiveness of the cooling air was evaluated. Temperature surveys were made and, as a result of these surveys, a larger heat sink was added to the voltage regulator, a larger air passage was provided behind the wing scoop for the avionics compartment, and ventilation ports were added to the flight control electronics package enclosure. While no flight failures had resulted from overheating, these changes were made to provide more cooling margin.

3.1.6 RPV Evolution - Mass Properties

The goal established by the Army for maximum all-up RPV weight was 120 lb. The primary reason for this goal was the desire for ease of handling by two people. Initial estimates indicated that the maximum RPV wet weight for the Phase IV and Phase V payloads and with 7 lb of fuel would be 119.73 lb. This left no room for weight growth, and provided an early indication of difficulty in maintaining maximum RPV weight within 120 lb. Consequently, at the outset a rigorous weight control program was established. Elements of that program included:

- Assignment of weight bogeys to subsystem groups
- Buying more expensive subsystems where they provided weight savings

- Reviewing designs to reduce weight
- Applying lighter weight materials where applicable

Program scope and resources led to compromises in the weight program requiring a variety of guidelines and constant reevaluation of those guidelines as the program progressed. Assignment of bogeys and rigorous design review are difficult to assess in terms of weight saved. Purchase of lighter, more expensive subsystems, and materiel substitutions are more easily evaluated. Representative weight savings from these approaches are shown in Table 1. This table shows that, without a concentrated weight control program, the RPV weight could have easily grown to exceed the current weight of 146 lb by 22.45 lb.

TABLE 1. TYPICAL WEIGHT SAVINGS

Lighter More Expensive Subsystems

<u>Item</u>	<u>Weight Saved (lb)</u>
Voltage Regulator	1.0
Battery	1.0
Power Supply	1.0
Rate Gyros	1.6
Air Data Sensors	<u>0.8</u>
Subtotal	5.4

Material Substitutions

<u>Item</u>	<u>Material Change</u>	<u>Weight Saved (lb)</u>
Airframe	Kevlar for fiberglass	12.5
FCED Enclosure	Graphite for aluminum	1.8
Encoder/Decoder	Graphite (FCED) for aluminum	1.75
Engine Cooling Shroud	Fiberglass for steel	<u>1.0</u>
Subtotal		<u>17.05</u>
Total		<u>22.45</u>

The sensor and fuel weights also changed significantly during the program, contributing to the RPV weight increase. Table 2 shows the weight variation of these elements during the program.

TABLE 2. HISTORICAL VARIATION OF SENSOR AND FUEL WEIGHTS

Item	Weight Allocation at Contract Go-Ahead (lb)	Final Weight (lb)	Weight Increase (lb)
Fuel	7 ^(a)	15 ^(b)	+8
Sensor (ϕ IV/V)	33	39.95 ^(c)	+6.95

(a) 1.5-hour duration

(b) Increased duration to 3 hours

(c) Includes 2.1 lb of ballast for RPV balance

Figure 13 shows a weight history of the Aquila air vehicle less the payload and fuel. Preliminary estimates of the component weights resulted in an airframe weight of about 74 lb. In November 1975, the first vehicle weight was recorded at about 101 lb. The weight of the next five vehicles steadily decreased to a value of about 90 lb, where they stabilized. The primary reason for this decrease is the improvement in the airframe manufacturing process. Table 3 provides a tabulation of the component weights at the time of the proposal, during LMSC field tests, and at the time of delivery to the Army.

The basic airframe structure of the Aquila was estimated to weigh about 33 lb; in reality the final weight is about 39 lb, or 6 lb heavier. This is due primarily to the number of access panels and bracketry required as the design matured.

The electrical group ultimately weighed about 6 lb heavier than predicted. This was due primarily to the addition of a relay assembly and a slightly heavier alternator than predicted and to underestimating the wiring harness weight.

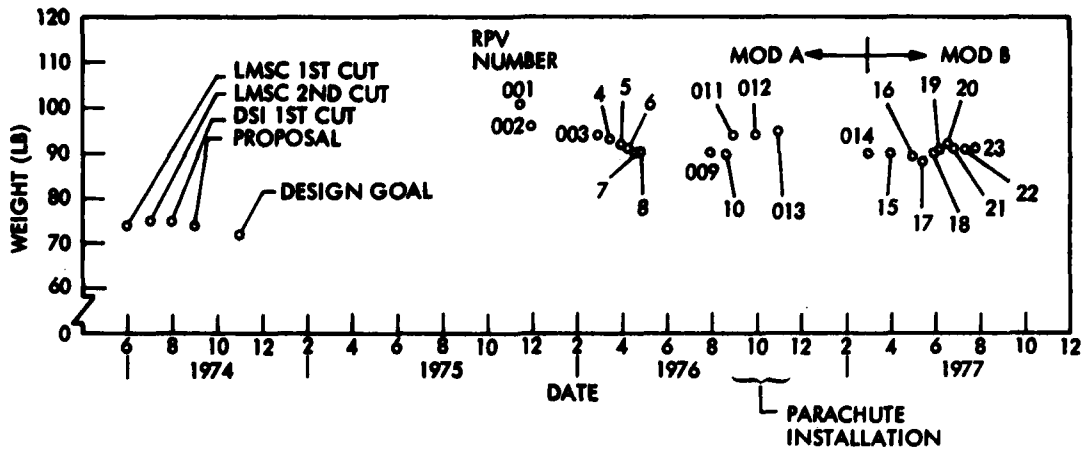


Figure 13. Aquila Aircraft Weight History

TABLE 3. HISTORY OF RPV-STD COMPONENT WEIGHTS (LB)

Reference	Proposal	LMSC Field Test A Modification	Delivered to Army B Modification
Wing Group	}	13.18	13.32
Fuselage Group		20.36	20.66
Retrieval Group		5.48	3.46
Propulsion Group	12.94	16.26	15.98
Electrical Group	11.1	16.90	18.17
Flight Control Group	10.18	10.88	10.95
Data Link Group	<u>6.72</u>	<u>6.52</u>	<u>7.53</u>
TOTAL	73.73	89.58	90.07

The propulsion group weight is about 3 lb heavier than predicted. This is due primarily to the design maturity of the installation with the addition of the second carburetor, final design of the propeller mount, etc.

The mass properties of the Aquila were analyzed through the use of a computer program. The inputs to this program are the individual component weights and

spacial positions within the airframe and the radius of gyration. The output of the program consists of categorized weights, center of gravity, and moments of inertia. The stability and control analysis of the vehicle showed that the center of gravity of the all-up weight should be at the 21-percent MAC point with a tolerance of ± 1 percent (± 0.32 in.). To accomplish this and have interchangeable components for all vehicles, ballast kits were made up for each phase payload. The weights in these kits were determined by weighing the actual vehicle. Each vehicle has two types of ballast: one is payload dependent and the other is basic airframe dependent and permanently installed.

The estimated mass properties of the initial vehicles were recorded in summary weight status reports. The weights of later RPVs were recorded in actual weighing of the vehicles. After RPV weights stabilized, they were then recorded only during the acceptance test procedure and the results were placed in each vehicle log book.

A detailed description of the mass properties of the RPV, as delivered to and tested by the Army, is given in Volume I of this report.

3.1.7 RPV Evolution - Performance

Performance goals for the RPV-STD were established by the Army in light of experience with previous RPV programs in which poor performance seriously hampered the demonstration of RPV capabilities. Consequently, the goals set initially for RPV performance contained considerable margin to ensure effective field demonstrations.

Initial estimates of RPV flight performance indicated essentially full compliance with the Army goals. These estimates subsequently proved optimistic as weight and drag increased and installed thrust efficiency apparently decreased from original estimates.

Since the RPV was known to possess significant performance margin, the approach to evolving the RPV performance involved judiciously yielding performance capability in favor of schedule and cost considerations. However, performance levels were closely scrutinized, and reviewed continually with the Army to ensure that the performance did not fall below critical levels.

Table 4 shows the evolution of the RPV performance throughout the program. The Army's desire for a cruise speed above 75 knots is fully satisfied by the flight speed indication of 86 knots. The degradation in speed as the program progressed is apparent. Cruise altitude did not vary greatly, and the specification was met. Initial time to climb predictions proved optimistic and predicted values increased rapidly with drag and weight increases. The final result, however, was acceptable for the field test missions. The specified conditions for takeoff and landing were ultimately exceeded with those operations occurring at density altitudes of 8,000 ft. Throughout the analyses of RPV response to winds and gusts, the 20-knot wind gusting to 35 knots criteria were met. The 20-knot wind condition was approached during field tests, but gusts were not monitored. The typical operating altitude was indicated to pace sensor characteristics. During the field tests (particularly for the laser operations) an altitude of 2,200 ft was typical. RPV endurance goals were met, but required an increase in fuel load from 7 to 15 lb, as weight and drag increased.

Detailed discussions of the major subsystems of the RPV are included in the following paragraphs.

3.2 AIRFRAME

The principal components of the RPV-STD airframe during its evolution were

- **Wings**
 - **Panels**
 - **Tips**
 - **Elevons**

TABLE 4. RPV PERFORMANCE EVOLUTION

Parameter	Army Specification	Proposal	Prel. Design Review	Flight Readiness Review	Flight Test Correlation
Cruise Speed (Band) (KEAS) (sl)	75 to 120	75 to 120	39 to 110	49 to 103	49 to 86
Cruise Altitude (ft) (With 300 FPM Climb Capability)	12,000	> 12,000	18,000	11,000	12,000
Time to Climb From Sea Level to 10,000 ft MSL (min)	≤ 15	7.3	12	19(a)	19(a)
Atmospheric Temperature at Altitude for Takeoff and Landing (ft/°F)	4,000/95	4,000/95	4,000/95	4,000/95	4,560/99
Maximum Winds for Operation (Steady/Gusting to) (Knots)	20/35	20/35	20/35	20/35	20/35
Typical Operating Altitude (ft AGL)	2,000	2,000	2,000	2,000	2,200
Endurance (Hours)	1.5 (Min.) 3.0 (Desired)	3.9 (Max.)	3+ (Max.)	3+ (Max.)	{ 2.62 - Typical profile 3.38 - Max. endurance conditions

(a) For 120-lb RPV. Flight GW of Aquila = 132.22 to 146.46 lb.

- **Fuselage**
 - Brackets
 - Payload protector
 - Recovery hook
 - Fuel compartment/bladder
- **Propeller Shroud**
 - Shroud
 - Shroud supports

The airframe geometry was determined in conjunction with the general arrangement and inboard profile, and guided by load-path considerations. Materials were selected initially for low cost and lightweight rugged fabrication. Weight growth led to the eventual selection of lighter weight material and construction techniques. The short schedule and iterative nature of the airframe evolution required dependence on conservative design practices in lieu of proof testing to ensure structural adequacy. Details of the airframe evolution are presented in the following paragraphs.

3.2.1 Airframe Evolution - Background/Situation

Prior to initiation of the Aquila contractual program, a multitude of mini-RPVs had been built and flown. Construction techniques for these airframes varied from those used for model airplanes to composite and metallic techniques used in advanced aircraft. Molded fiberglass was found to be the most popular technique with its great flexibility in application. With this background, and considering the number of aircraft (30), the airframe construction technique for the Aquila program originally proposed by the airframe subcontractor included the wet lay-up of layered fiberglass in female molds, vacuum bagged. The Sky Eye wing construction, foam core with fiberglass skin, was also proposed as the initial wing structure concept. These selections were made in consideration of the successful history of the Sky Eye RPV, low cost, and some recognized small weight penalty. Model airplane techniques were considered, but

were judged inadequate for the loads, handling and field environment anticipated. The more exotic fabrication techniques and materials were also examined and found to offer advantages, but with additional cost and fabrication complexity. Given the Army requirement for a flight-proven airframe, the successful history of the Sky Eye, together with the flexibility offered with the wet lay-up of fiberglass provided a strong basis for the selection of that airframe technique for the Aquila RPV.

The early structural arrangements considered for the Aquila RPV provided the first indications that significant departures from the Sky Eye concept would be required. The early layouts indicated that access requirements eliminated the efficient monocoque (or semi-monocoque) structural arrangement unless heavy structural panels were used. Further, wing carry-through structure interfered with effective internal component arrangement in the fuselage unless integrated with fuselage bulkheads. These factors provided the point of departure for the Aquila airframe development.

3.2.2 Airframe Structure Requirements

Army requirements specified for or related to the airframe structure included:

- Simple, low-cost, rugged design
- Minimum time and skill for assembly/disassembly
- Minimal detectability
- Ground transportability
- Lifetime of 15 one hour flights
- Structural design load factor of 6 g
- Interchangeability of payloads

From initial analyses, and further Army reviews, additional requirements were levied, these included:

- Interchangeability of aircraft components
- Ultimate load factor = 1.25 times design load

- Payload protector: serves as an emergency landing skid (6 g vertical and axial, 2.5 g lateral)
- Paint
- Break-away wing tips

These requirements were derived to produce a rugged airframe, and simple RPV operations, and to set the basis for the airframe design approach.

3.2.3 Airframe Structure Approach

The approach to the Aquila airframe structure included the following elements:

- Subcontract the airframe structural design and construction to the Sky Eye manufacturer.
- Specify requirements and closely monitor progress to determine need for advanced aerospace techniques.
- Stress conservative design in lieu of extensive development testing.
- Procure airframe with early interface definitions to meet tight flight schedule. Change as required.
- Require subcontractor performance of acceptance test procedure prior to delivery.
- Assemble RPV following verification of airframe characteristics.

3.2.4 Airframe Structure Evolution

The initially proposed airframe structure concept is shown in Figures 14 and 15. The outer wing panel of the aircraft consisted basically of a styrofoam core of 1 lb/ft³ density, to which were bonded (with a PM 108A bond) preformed 0.020-in.-thick upper and lower surface epoxy fiberglass skins (Figure 14). These skins were then closed out at the leading and trailing edges to complete

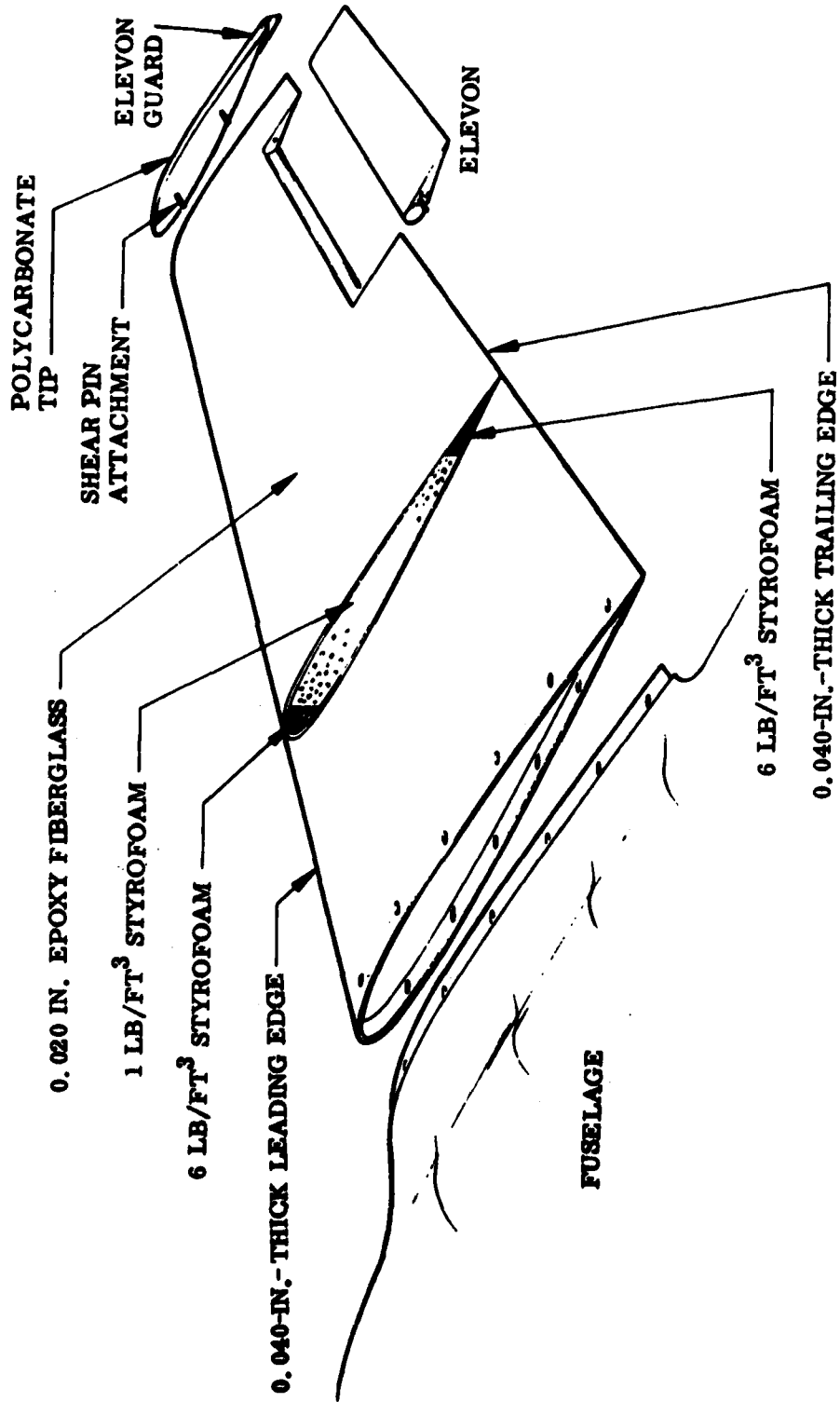


Figure 14. Aircraft Wing Construction

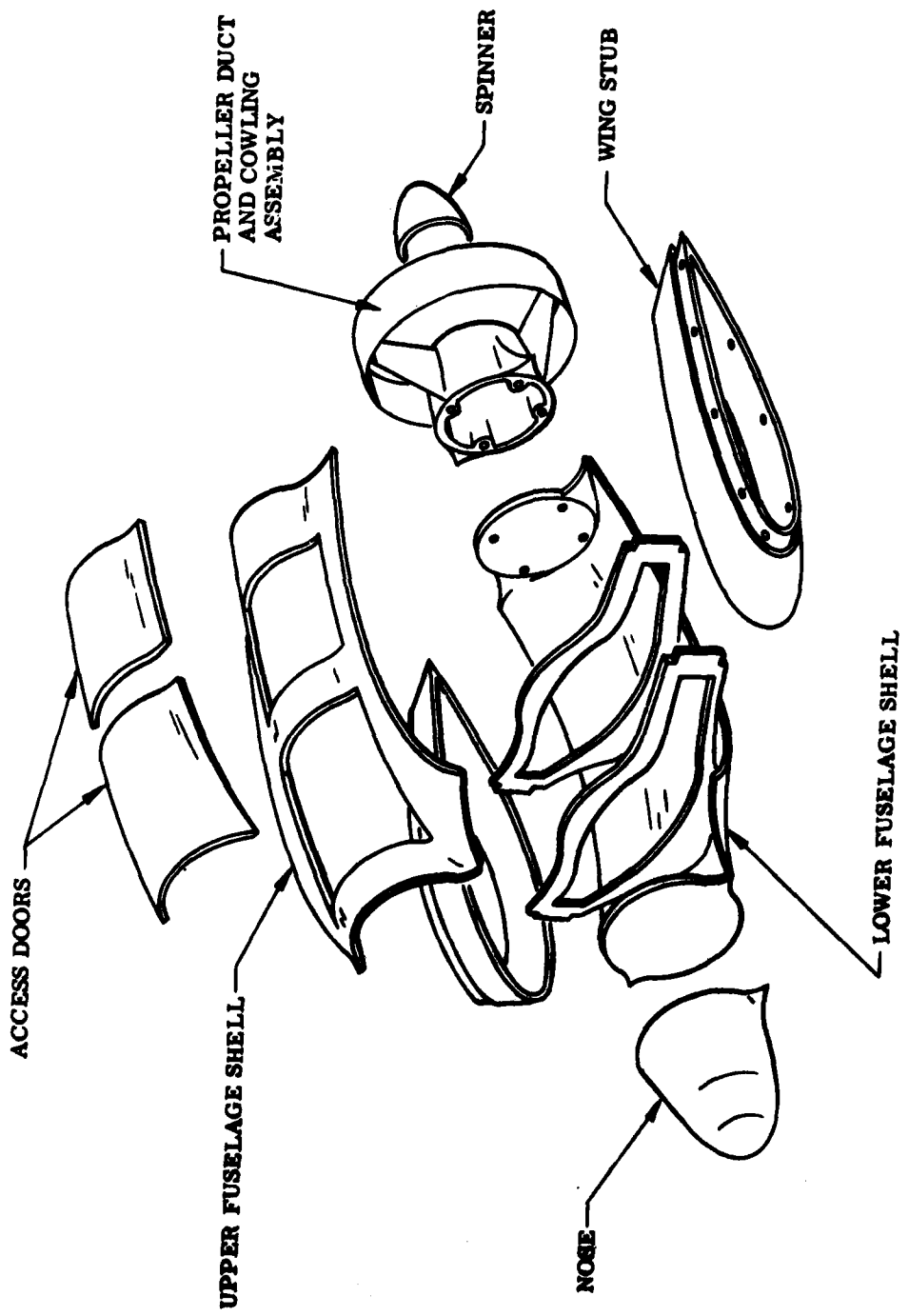


Figure 15. Aircraft Fuselage Construction

the structural skin. The styrofoam core was hot-wire-cut from factory-supplied MIL SPEC slabs. Styrofoam was selected over urethane because of its availability and low density. Urethane forms (with the required quality assurance) were available only in densities of 2 lb/ft³, and this imposed an unacceptable weight penalty unless the core was lightened by hollowing out the inside. The latter alternative raised questions of dimensional stability and reduced resistance to handling damage, and would have resulted in greater manufacturing complexity. The leading and trailing edges were filled with 6 lb/ft³ density styrofoam in order to enhance the resistance to damage of these particularly vulnerable portions. The trailing edge skin thickness was increased to 0.040 in. to reduce handling damage. The wing skins were reinforced locally at the root for fastening to the stub wing.

The upper and lower skins were made of hand-laid fiberglass cloth and epoxy, preformed to the airfoil contour in a vacuum-bagged female mold to ensure that dimensional tolerances were maintained during the bond curing process.

The elevon-protecting wing tips (Figure 14) were fastened to the outer-wing panels by frangible shear connections to help protect the outer wing panels against damage by a sharp load applied to the elevon guards.

The wing tips were vacuum-formed from a fuel-resistant polycarbonate plastic to facilitate their easy and inexpensive replacement. Closing ribs at both ends of the wing panel sealed the foam core from exposure to moisture and fuel. An elevator spar was provided to support the elevon and elevon servos.

The fuselage shell was fabricated in two halves (top and bottom) from 0.032-in.-thick epoxy fiberglass vacuum-bagged in female molds at room temperature. The general arrangement of structural members is shown in Figure 15.

The fuselage structure was intended to be pure monocoque in that no longitudinal stringers were provided (except for intercostals that frame the access

doors). The fuselage was fabricated in four basic parts: upper and lower fuselage shells and right-hand and left-hand wing panel attach stubs. Alignment of the fuselage shells during assembly was ensured by use of the female layup molds, joined by locator pins, to hold the fuselage shells while the wing panel attach stubs were bonded. The attach stubs, when bonded, formed doubler hard points for attachment of the wing panels. The upper fuselage shell provided wing bending and shear load carry-through, and the lower shell contained integral mounting provisions for the aircraft subsystems and payload. Large access doors were provided on the top of the fuselage to permit easy access to the payload and other electronic components. The payload components were installed from the top of the fuselage through the forward access panel (Figure 15). All doors closed flush with the fuselage surface and were retained by dzus fasteners.

The outer wing panels slid over the stub wing and were fastened to it by means of a line of flat-head machine screws anchored into nut plates permanently installed in the stub-wing. Six screws on the top and six on the bottom completed the installation. The molded-in recess in the end of the stub ensured an uninterrupted spanwise surface.

The engine was semirigidly mounted to the firewall through hard rubber mounts. The cowling, which was formed of fiberglass in the same manner as the fuselage halves described previously, was mounted to the firewall. The duct was attached directly to the cowling by three streamlined fiberglass supports. This whole unit (cowling, duct, engine) was mounted on the aft fuselage frame through very soft engine mounts.

The duct was a styrofoam core with two-piece (inner and outer) epoxy skins (0.025-in. thick). The spinner was also formed of fiberglass.

The tail-less, pusher configuration provided high potential for survival inasmuch as easily damaged elements were deleted or redesigned. A normally

vulnerable portion of an RPV is the tail, because in a conventional configuration, the tail has control surfaces, servos, etc., that make repair in the field both difficult and complicated. The proposed simple, rugged duct minimized these difficulties.

Additional steps were taken to further minimize repairs. For example, specially designed and easily replaceable wing tips served as guards for the elevons. The outer panels had hardened leading edges in addition to the reinforced trailing edges. The wing panels were designed to be easily replaced by spares (if damage was extensive) or quickly repaired in the field (if damage was relatively small) using a simple repair kit supplied with each vehicle. The outer panel-to-fuselage interface was designed so that upon very hard impact in any direction on the outer panel, structural damage to the outer panel and even break-off of this panel would occur well before critical loads were applied to the center section.

The proposed structure was designed to withstand ± 6 g vertical and ± 6 g axial design loads (applied through the launch and recovery hardpoints), and ± 7.5 g vertical and ± 7.5 g axial ultimate loads.

During launch, 6 g were anticipated for the proposed aircraft, and 6 g axial and 3 g vertical were anticipated during recovery. The fully loaded craft could be lifted by its wingtips and a 2 g load applied while supported in this manner. It could likewise be lifted by the duct and nose with 2 g loading.

Shortly after the program initiation, this structural concept began to show specific deficiencies. First, wing carry-through loads caused excessive deflection predictions if reacted only in the fuselage shell. This condition was further complicated by the large access door cutouts. It became apparent that carry-through loads would require more substantial structure, such as bulkheads with edge caps. Second, the wire-out foam core for the wing could not be sufficiently precise to prevent the need for excessive amounts of epoxy to

prevent bond voids between the core and the skin, providing the necessary epoxy resulted in large weight increases. A more precise core shaping technique was required. Third, and perhaps most significant, the predicted RPV structural weight became excessive, requiring consideration of lighter materials and structural design. To meet this last requirement, direct technical consultation was provided to the airframe subcontractor and supported the decision to select Kevlar as the principal structural material. Fourth, soft mounting of the duct to move in conjunction with the engine produced heavy, complex mounting hardware. Corrections of these deficiencies were presented in the March 1975 Design Review.

A sketch of the airframe structure presented at the Design Review is shown in Figure 16. The airframe structure concept shown in this sketch is constructed primarily of Kevlar (PRD-49). The wing panels are field-assembled to the fuselage at WS 13.0. The attachment design includes 10 screw fasteners each on the top and bottom surfaces to collect load from the sparless wing. Wing load carry-through is provided by two primary bulkheads at FS 128 and FS 146.25. Other bulkheads at FS 13 and FS 158 provide for equipment and engine mounting. The propeller shroud is rigidly supported by three struts that carry forward to the fuselage structure independent of the engine installation. The fuselage shell is 0.030-in., 3-ply Kevlar semimonocoque construction, supported by the bulkheads and closing ribs at WS 13.

The sparless wing is fabricated by bonding skins to a full-support foam core. The styrene foam core is 6 lb/ft^3 in the leading edge area and 1 lb/ft^3 elsewhere; it is cored for weight reduction and machined for precision fit in preparation for bonding of the skins. The upper and lower skins are laid up in female molds. The thickness is 0.016-in. one-ply over the span, increasing in the 6-in. outboard of the field attachment to 0.030-in. three-ply. The skin molds also serve as holding fixtures for the operation of bonding the core to the skin.

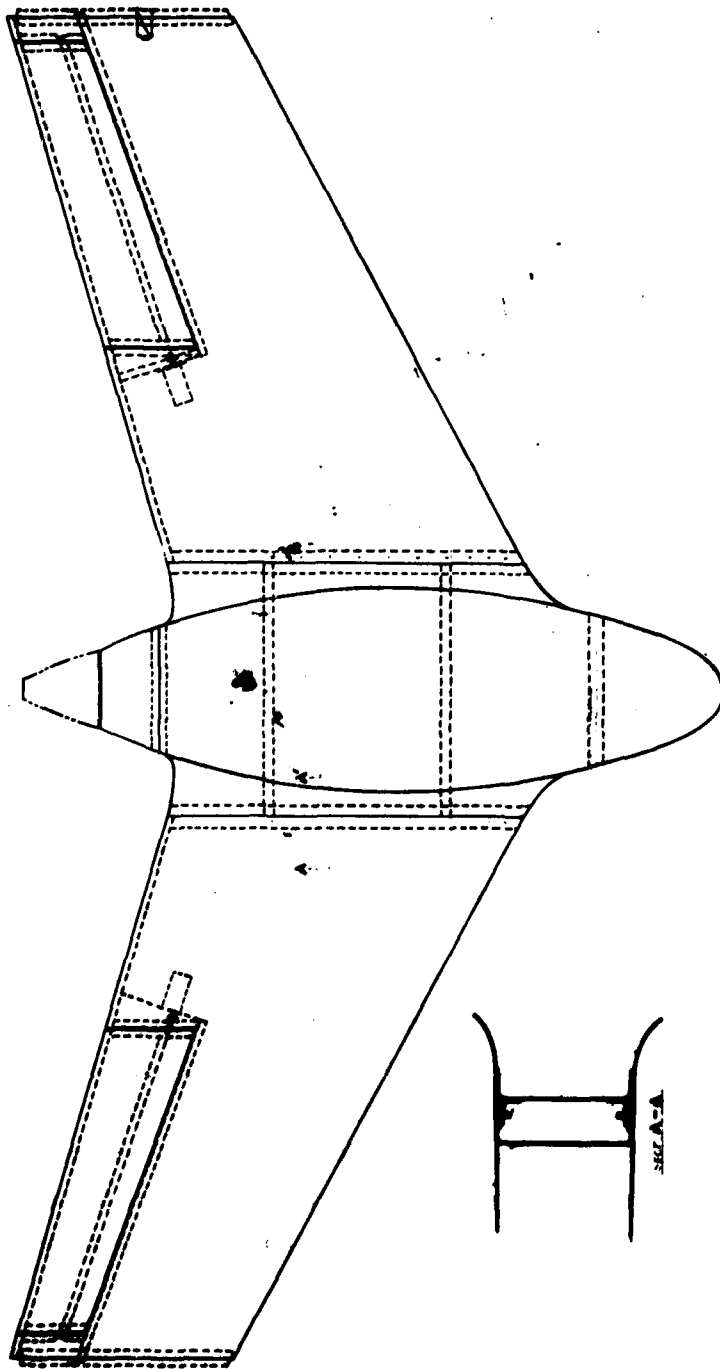


Figure 16. Basic Structural Arrangement

The airframe structure evolved rapidly after the design review to the final arrangement described in detail in Volume I. The major changes occurred in the wing structure and attachment, and in fuselage bulkheads.

After further analysis and sample tests, the use of a foam core for the wing was abandoned. This action was taken primarily because sample cored wing sections showed excessive warp and set when exposed to a combination of day and night cycles. A second reason lay in the excessive cost of machining and fabricating with the foam. After dropping the foam core concept, a two-spar design with honeycomb skin for stiffness and shape retention was selected. In addition, wing attachment was changed to take advantage of the spar geometry, reducing the number of attachment screws from 20 to 8 per wing. This became the final wing structure concept. Other structural changes, primarily in the fuselage, were directed at weight reduction. The most significant of these included the use of Nomex honeycomb in the fuselage bulkheads.

It is apparent that the structural concept evolved from a simple concept with a simple material to an advanced concept using advanced materials and assembly concepts. This evolution was caused primarily by weight considerations.

This rapid change in airframe structural arrangement and the wide variation in early structural assemblies presented a difficult challenge to the verification of structural design integrity. This problem was further compounded by the highly redundant nature of the structural geometry and the unavailability of structural elements for destructive testing. (All early airframes were dedicated to flight testing due to scheduling considerations.) Consequently, it was required that structural integrity be verified primarily through conservative design and supported by stress analysis. The subcontractor's structural integrity analysis provided the necessary stress analyses. In this report, redundant structural elements were approximated by conservative determinant models and analyzed by simplified techniques. The resulting stress levels were

reviewed to ensure the existence of a sufficient safety factor. Table 5 summarizes the findings of the structural integrity report (Reference 2). The margins of safety shown, almost without exception, safely exceeded the 0.25 required. In those few exceptional cases (i. e., alternator bracket flange, internal skeg bracket flange) corrective structural design was initiated.

Selective nondestructive testing was conducted on critical items including the propeller shroud (lift and side force design loads), the payload protector (three-axis design loads), the engine mounts (deflection test to ensure propeller/shroud clearance during recovery), and hook recovery line/fittings (pull tests to design loads).

The pull test on the hook recovery lines and their anchors attached to bulkhead 147 was accomplished on each airframe configured with the hook recovery system. The other tests were one-time proof tests. This limited testing plus bonding tests conducted by the airframe subcontractor constitute the total Aquila structural testing. However, this testing plus the large safety factors obtained through conservative analysis were considered adequate to ensure the structural integrity of the airframe. As the program progressed, analyses continued to ensure structural adequacy when modifications were made. In addition, functional tests were performed under simulated air loads for payload protector and recovery hook deployment. During the reliability improvement phase of the program, shock load tests and deployment tests were performed on the interim parachute recovery system.

As a further check on structural integrity, handling loads were analyzed. It was found that up to 80 percent design load was imposed in the wing attach fittings during the assembly and checkout processes. This factor proved very useful in locating poorly bonded wing fittings and reinforcement strips. The flight test program verified the airframe structure in that no structural failure occurred in normal flight or field operations.

²Developmental Sciences, Inc., Aquila Structural Integrity Reports, by Howard E. Krachman, LMSC subcontract GS10B7130 A, DSI Job 2846-SR, 30 Oct 1975

TABLE 5. MARGIN-OF-SAFETY SUMMARY TABLE

Member or Part	Construction Material	Type	Maximum Stress (psi)	Ultimate Stress (psi)	L. Buckling Allowable (psi)	Margin of Safety
<u>Wing</u>	Honeycomb sandwich	Compression	8,880	12,000		0.35
		Core shear	12	36		2.00
Eleven Panels	Honeycomb sandwich	Compression	2,534	12,000		3.74
		Torsional shear	524	20,000		
Eleven Connection of Wing Tip	Kevlar	Bearing	4,070	20,000		3.91
Eleven Connection at Root	Kevlar	Bearing	4,400	20,000		3.54
Spar at 25 percent	Kevlar	Compression	17,868	25,700		0.443
Spar at 70 percent	Kevlar	Compression	14,578	25,700		0.763
<u>Wing Fuselage Construction</u>						
Booms	70-75 Aluminum	Shear	1,462	2,200		0.50
		Flexure	137,512	180,000		0.309

Margin of Safety = Ultimate Allowable/Design - 1

TABLE 5. (Cont.)

Member or Part	Construction Material	Type	Maximum Stress (psi)	Ultimate Stress (psi)	L. Buckling Allowable (psi)	Margin of Safety
<u>Wing Fuselage Connection (Cont.)</u>						
Aluminum Plates Provided for Bearing	70-75 Aluminum	Bearing	56,440	88,000		0.56
Brad Between Kevlar and Aluminum	Hastings 1208	Shear	361	2,000		4.54
Root Rib Flange	Kevlar	Flexure compression	19,376	25,700		0.327
Aluminum on Fuselage Side of Connection	70-75 Aluminum	Flexure due to eccentricity	61,000	78,000		0.279
<u>Payload Protector</u>						
Main Frame	60-65 Aluminum	Flexure compression	23,295	35,000		0.50
Lower Strut	60-65 Aluminum	Compression	2,048	35,000		16.0
Connection of Struts	60-65 Aluminum	Bearing	7,600	48,000		5.35

TABLE 5. (Cont.)

Member or Part	Construction Material	Type	Maximum Stress (psi)	Ultimate Stress (psi)	L. Buckling Allowable (psi)	Margin of Safety
<u>Propulsion Assembly</u>						
Bottom Panel	Sandwich	Compression	6,480	12,000		0.852
Stiffener Between Bulkheads	E-Glass	Compression	8,325	25,000		2.00
Lower Strut	Kevlar	Vertical load	300	391		0.30
		Horizontal load	200	260		0.30
Lower Strut Connection	20-24 Aluminum	Bearing	60,421	88,000		0.464
Strut Bolts	Steel	Shear	44,320	180,000		3.06
	Steel	Tension	88,755	180,000		1.028
Flange of Closing Rib of Strut	Kevlar	Flexure	20,240	25,700		0.279
Fuselage Bolts	Steel	Tension	98,000	180,000		0.836
Fuselage	Kevlar	Bearing	12,000	20,000		0.66
<u>Alternator Connection</u>						
Bolts Between Alternator and Bracket	Steel	Tension	470			
		Shear	270			
Bracket Flange (see Text)	Kevlar	Flexure	23,577			0.09

TABLE 5. (Cont.)

Member or Part	Construction Material	Type	Maximum Stress (psi)	Ultimate Stress (psi)	L. Buckling Allowable (psi)	Margin of Safety
<u>Alternator Connection (Cont.)</u>						
Bracket	Kevlar	Flexure	574		3,018.8	4.25
Shear in Baseycomb	Nomex 1.8 lb/ft ³	Shear	26.6	36		0.35
<u>Engine Mount</u>						
Bulkhead Core	Nomex	Shear	23.5	36		0.53
<u>Arresting Mechanism</u>						
Tube	Fiberglass	Tension	5,305			
Hinge	Aluminum	Bearing	8,000			
Glue	Hastings 1208	Shear	133	2,000		14.0
Cables	Nylon	Tension	360	1,200		2.33
Bulkhead	Sandwich	Flexure	15,440	20,000		0.295
<u>Payload Mount</u>						
Sandwich	Kevlar-Nomex	Compression	13,974	20,000		0.43
<u>Battery Mount</u>						
	E-glass	Flexure	17,333	25,700		0.674
	E-glass	Shear	2,766	20,000		6.23

TABLE 5. (Cont.)

Member or Part	Construction Material	Type	Maximum Stress (psi)	Ultimate Stress (psi)	L. Buckling Allowable (psi)	Margin of Safety
Fuselage						
Bulkhead XF-130	Kevlar Cap	Compression	11,983	25,700		1.145
	Kevlar-Nomex Sandwich	Shear	2,365	20,000		7.45
Bulkhead XF-147	Kevlar Cap	Compression	8,664	25,700		1.967
Payload Protector	Kevlar-Nomex Sandwich	Compression	17,832	25,700		0.44
Intercostal	Kevlar	Compression	14,773	25,700		0.239
	Kevlar	Shear	913		1,785	0.95
Close-out Rib	Kevlar	Compression	3,800		9,050	1.38
	Kevlar	Shear	1,459		2,172	0.489
	Kevlar	Differential bonding				0.25
Skog	60-61 Aluminum	Flexure	20,201	42,000		1.1
External Skog Fitting						
Bracket Flange	60-61 Aluminum	Flexure	15,900	42,000		1.64
Bolts	Steel	Tension	1,526	2,200		0.44

TABLE 5. (Cont.)

Member of Part	Construction Material	Type	Maximum Stress (psi)	Ultimate Stress (psi)	L. Buckling Allowable (psi)	Margin of Safety
Fuselage (Cont.)						
Internal Skog Fitting						
Bulkhead Flange	Kevlar	Flexure	18,624	25,700		0.38
Bracket Flange	60-61 Aluminum	Flexure	37,248	42,000		0.13

As stated earlier, the airframe design was frozen early to permit the airframe subcontractor to meet the rigorous airframe delivery schedule. It was recognized that this approach would precipitate required modifications prior to complete RPV assembly. Twenty-four such changes were required, including major redesign of the payload and recovery hook deployment mechanisms, subsequent deletion of the hook assembly, addition of launch push-pads at the wing trailing edge, stiffening of the wing skin around the cooling scoop, enlarging the cooling air passage, and mounting bracket modifications.

Initial plans to paint the vehicles light grey to reduce observability during flight were modified to provide the customer-preferred olive drab. After several iterations, a prime coat of Deft, Inc. 02419 applied in accordance with MIL-P-23377, and a top coat of Deft, Inc. 03GN40 (O. D. color) polyurethane applied in accordance with MIL-C-83286 AF were selected for the finishing technique.

3.3 POWER PLANT/ELECTRICAL SUBSYSTEM

The Aquila power plant (Reference 3) and electrical subsystem consists of the following elements:

- Engine
- Fuel system
- Carburetor
- Propeller/propeller hardware
- Engine mounts
- Throttle controls
- Alternator
- Alternator mounting bracket
- Flexible alternator drive shaft
- Voltage regulator
- Electrical relay assembly
- Battery

(3) Lockheed Missiles & Space Company, Inc., Aquila RPV System Test Report, CDRL AOOD, Engine System Development, LMSC-L028081, Part 11
Sunnyvale, Calif., 22 Dec 1977

The power plant was located in the rear of the RPV with a pusher propeller arrangement. Figure 17 shows the power plant buildup in three stages. The hardware shown is characteristic of an early stage of evolution.

3.3.1 Background

The variety of RPV programs preceding the Aquila procurement had clearly established that no qualified aircraft power plant existed for mini-RPV applications. All previous RPV designs had required adaptation of an engine normally used in ground applications, or large model aircraft engines with special fuel requirements. Lockheed participation in the ARPA Aequare and Army Savoir RPV Programs had resulted in a set of proven techniques for converting the McCulloch MC101A/MC-101MC series of engines to acceptable RPV power plants. Other RPVs, including the Sky-Eye, the USAF Academy Telecraft, and the Fairchild Sail-Wing RPV, had also used the MC101A and similar MC-101MC series of engines with success. In the Lockheed RPV programs, techniques had been developed for remote starting after cold soak at 10,000-foot altitude conditions. In addition, engine operations had been characterized in altitude chamber tests at altitude conditions from sea level to 20,000 ft. In short, at the beginning of the Aquila program a considerable body of experience existed with the MC-101A and MC-101MC engines in RPV applications. Before its selection, however, a survey was made to see if a more suitable engine existed. Table 6 summarizes the survey. It is apparent from this table that with cost, weight, availability, and performance characterization as selection criteria, there was no other reasonable choice.

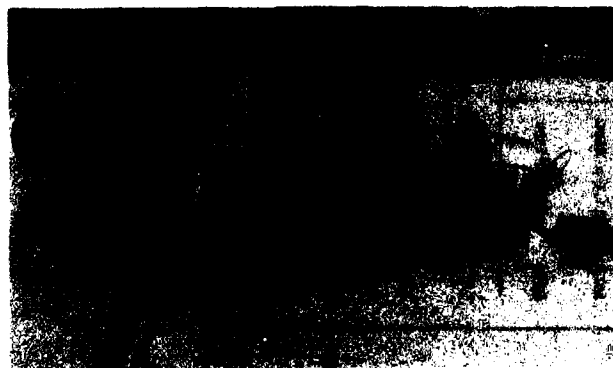
A wide range of selectivity existed in finding an alternator baseline. Available direct drive units, including aircraft and automotive units, were found to be excessively heavy and were discarded as candidates. Small, lightweight units required gearing up in rpm with gears and belts. These were discarded because of the short development time available to derive reliable drive systems. The experience with the Aequare alternator and mounting arrangement pointed to an adaptation of that system as a logical choice for the Aquila RPV.



(a) Preassembled



(b) Partially Assembled



(c) Ready for Installation

Figure 17. Aquila Power Plant

TABLE 6. ENGINE CANDIDATE COMPARISON

Manufacturer	Model	hp at 2700 (Std Sea Level)	BHP in/Sp-Ar (Std Sea Level)	Dry Weight (lb)	Fuel	Altitude, Operation (ft)	Unit Cost (\$ approx)	In Production	Reliable	Maintainability	Starting Ease	Life	No. of Cylinders	Engine Cycle (Strokes)	
McCulloch	101A	11.0 at 2500	6.28	12.2	Gas-oil mix	to 20,000	150	Yes	Yes	Easy	Easy	Long	1	2	
Kalco	2074	12.0 at 1600	2.35	7.0	Gas-oil mix	5000	1700	New	New	Easy	Easy	De-known	2	2	
Buhl		Integrated with chain saw head; not well defined			Gas-oil mix	?	200	Yes		Not well characterized				1	2
Hamelin					"	?	200	Yes					1	2	
JLO	L-220	15.5 at 2000	-	20.0	"	-	88	Yes	-	-	-	-	1	2	
Currier-Wright	WCL-16.5	20 at 2000	6.72	54.0	"	-	350	Yes	Yes	Easy	Easy	Long	Washed	2	
Birch	102R	20.5 at 1700	-	50.0	"	-	N/A	Yes	-	-	-	-	1	2	
Birch	F20A	20.0 at 2000	-	55.4	"	-	N/A	Yes	-	-	-	-	4	2	

3.3.2 Requirements

Specific engine requirements were not cited in the Aquila procurement documentation except by inference. After design study and evaluation, a list of requirements included the following:

- Brake horsepower ≥ 11 hp
- Low specific fuel consumption
- Low dry weight
- Demonstrated operation at altitude
- Common fuel
- Easy starting
- Low cost
- In current production
- Reliable operation
- Easy maintainability
- Long life (15+ flights)
- 500 W electrical power
- Regulated 28.4 ± 0.2 Vdc with ≤ 5 -percent ripple
- Full power (500 W) output above 4,000 rpm
- Alternator survival at 11,500 rpm for 1 min

3.3.3 Approach

The approach to the Aquila power plant evolution basically involved the following:

- Adapt the McCulloch MC101 engine for propeller drive, alternator drive, and Aquila RPV installation.
- Verify performance, fuel consumption, and altitude operation in altitude chamber tests.
- Procure a DuFresne alternator and regulator to the Aquila specification.

- Design the power plant installation based on Aequare and Sky Eye RPV flight experience.
- Evolve assembly and test procedures to ensure reliable operation.

Initial plans called for the airframe subcontractor to procure, modify, and install the engine, propeller, and alternator prior to delivery. As requirements evolved to lighten the weight, change the carburetion, and modify the engine controls and mounting, this task was moved to the contractor's facility.

3.3.4 Power Plant/Electrical Subsystem Evolution

The evolution of the McCulloch MC-101 engine into the Aquila power plant is summarized in the following paragraphs. The final power plant configuration is described in Volume I of this report.

Figure 18 shows an MC-101MC engine as delivered from the factory. Conversion of the MC-101MC engine to the Aquila engine includes the following steps:

- Removal of unnecessary parts such as the recoil hand starter to provide a lighter weight configuration
- Installation of a thermistor to monitor the engine temperature
- Inspection and modification of the engine (This includes safety wiring all critical parts to prevent them from loosening due to vibration.)
- Addition of the engine mounting bracket
- Replacing the metallic cooling shroud with a lighter weight fiberglass substitute
- Installation of a resistor type spark plug to eliminate EMI problems
- Changing the carburetion system to give better fuel consumption and throttle control characteristics, as well as a smaller profile for installation

A discussion of the evolution of this procedure follows.



Figure 18. Factory Delivered MC-101MC Engine

Engine Mounting. Throughout the fabrication of the original single carburetor and A model dual carburetor Aquila engines, the engine was attached to the airframe at bulkhead 155 by bolting four sections of extruded aluminum channel to the engine block casting at points originally used to mount the engine cooling fan shroud. These channel sections protruded radially about the crankshaft axis. Each was drilled to accept the mounting stud of a Lord Model J-4624-27 shock isolation mount. The bulkhead pickup was by four aluminum U-shaped channels with flanges that bolted through inserts (for stiffening) in the honeycomb-filled bulkhead.

The channel section brackets attached to the engine provided adequate support to meet operational loads but did not provide for precise location of the engine, nor for the precise positioning of the propeller within the propeller duct. Other than the clamping force of the one attachment bolt per bracket, there was nothing to prevent rotation of the bracket. Also, as a mounting bolt loosened, or if the casting interface was not true, the brackets would not be parallel.

The B model engine incorporates a single horseshoe-shaped bracket with four tabs extending radially outward which replace the four channel brackets previously used. Attachment to the engine is through the same bolt locations used before. This revised mounting method (see Figure 19) has nearly eliminated the need for shims to align the engine (with its small weight penalty). As an additional benefit, engine alignment is not affected by engine operating time.

Engine Cooling. The standard McCulloch cooling fan, which is cast integrally with the flywheel, is used instead of free stream air engine cooling. This fan provides supplemental cooling air to vehicle electronic components when the vehicle is run statically or at low flight velocities. Cooling air enters the vehicle at a nose opening and a wing root duct, and from these points it is circulated through the forward bays to remove waste heat. After passing through the 137 bulkhead the air enters the alternator compartment where heat



Figure 19. Engine Mounts, Port Side - B Model Engine

that is generated by the alternator, voltage regulator, and throttle servo is extracted. The exit path from the alternator compartment is through the alternator mounting bracket and then bulkhead 155. The inlet to the engine cooling fan faces the 4-in. -diameter exit passage of bulkhead 155. The cooling fan forces air through the engine cooling fins and out through an aperture which faces aft and is located above the level of the propeller spinner.

The shroud that mounts on the engine and directs air flow from the cooling fan around the cylinder fins is a Lockheed-produced item. The original McCulloch part was a two-piece metal design. Initially, a two-piece graphite epoxy unit was the replacement, and a weight savings of approximately 1 lb resulted. Eventually a redesign brought about a cost reduction for this shroud. Fiberglass replaced graphite epoxy as the material for construction, and a permanent bond was used to reduce the number of pieces to one per engine. The weight savings was essentially retained.

Carburetion. The original Aquila carburetion system was composed of commercial McCulloch parts, although not those with which the MC101 was delivered.

The standard MC101 carburetor, a Walbro Corp. Model BDC-22 is intended for go-cart racing applications of the engine, where high power is the central consideration, and the duty cycle comprises full throttle and idle throttle. Smooth running and low fuel consumption as well as weight and size are minor considerations. Because these characteristics differ with basic Aquila engine design philosophy, it was decided that the carburetion system should be changed to meet aircraft requirements more effectively. The three carburetors considered are shown in Figure 20. Early tests with a Walbro SDC-43 "cube" chain saw carburetor demonstrated several advantages this carburetor would provide. A McCulloch manifold and reed set made to adapt the SDC-43 carburetor to the Model MC 49E engine were interchangeable with the MC101 engine. This installation, shown in Figure 21, was small enough that it

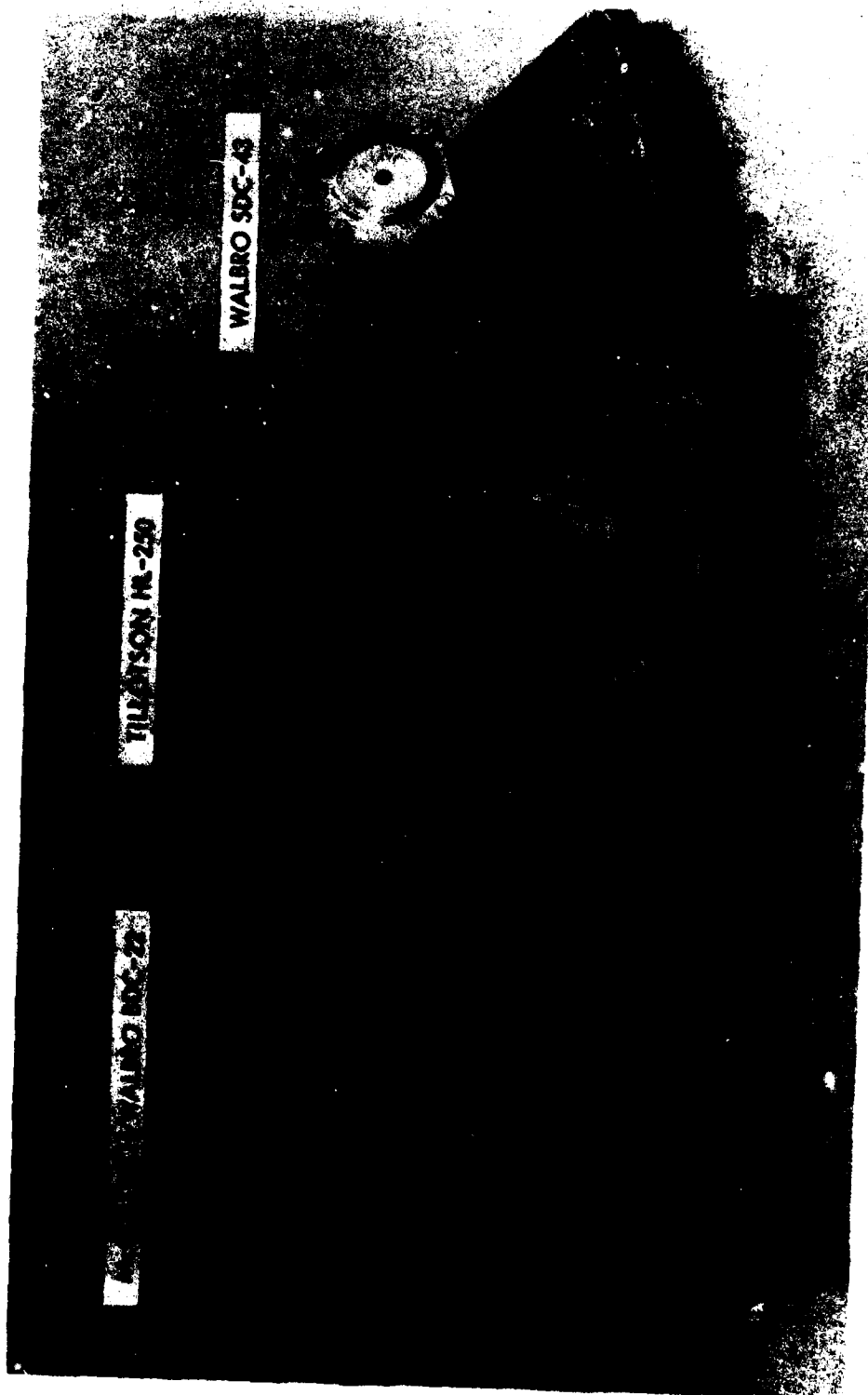


Figure 20. Carburetor Options: From Left - McCulloch/Walbro BDC-22, Tillotson HL-250, and Walbro SDC-43

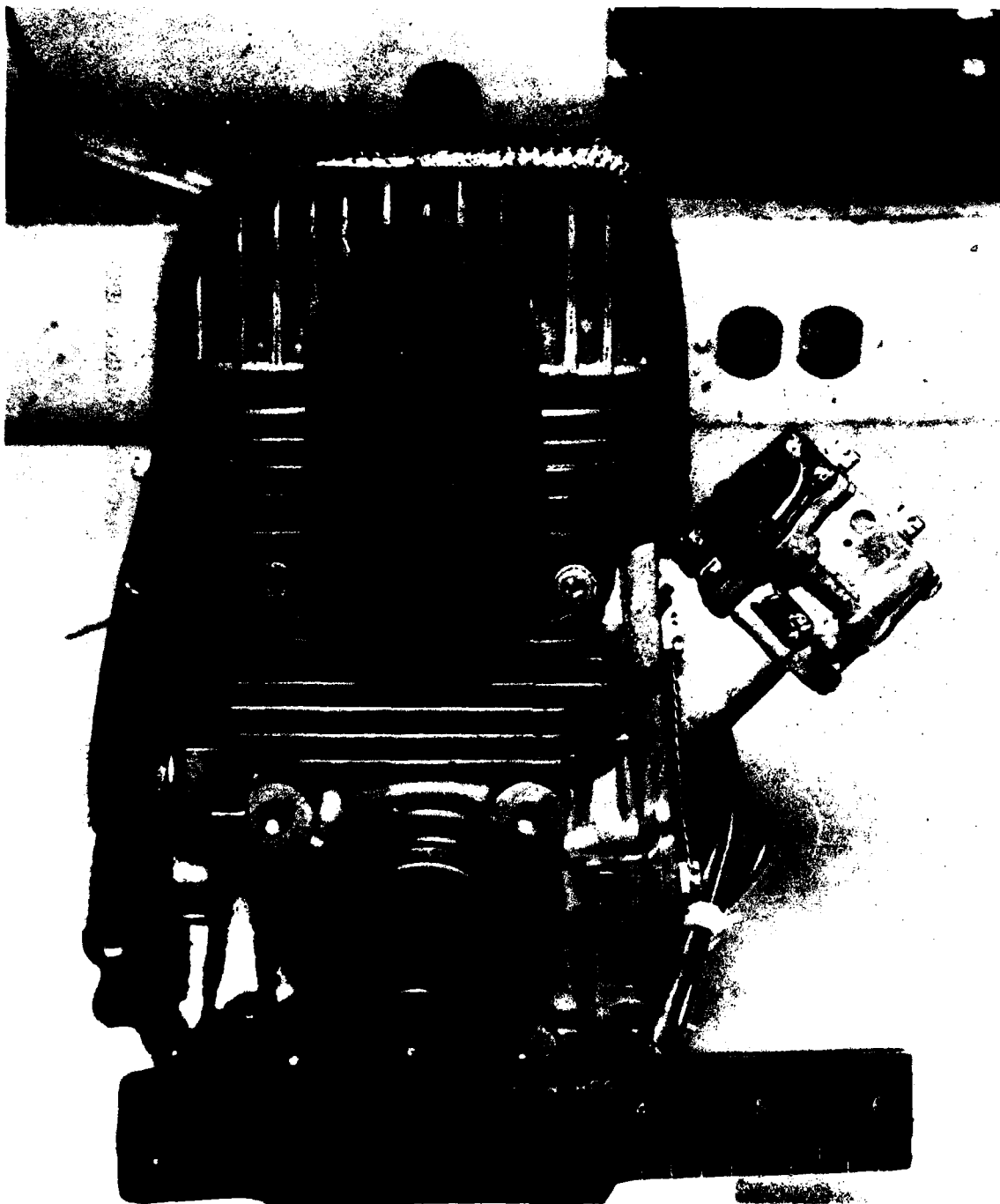


Figure 91 Single Carburetor Aquila Engine

could be totally contained within the fuselage. Weight was very low for the system. Engine throttle response was greatly improved and fuel consumption was very low. The main fuel jet was fixed by an orifice that would reduce field adjustments. The one disadvantage was a reduction of maximum power (by approximately 1) to 10 hp at 7,300 rpm. Since performance predictions indicated that 10 hp was sufficient to meet requirements, it was decided to proceed.

The system was installed on vehicles up to No. 007. Operation with this configuration went smoothly as it was relatively simple to adjust and worked well with the flight controls rpm loop command circuit. It did have the drawback of insufficient power, unfortunately magnified by drag and propeller inefficiencies, which were higher than predicted. As a result, performance values were lower than predicted.

A decision to improve vehicle performance by increasing engine power was made, but it was considered important to retain as many of the attributes of the first configuration as possible. The dual carburetor, progressive control linkage system was the design that resulted.

The theory of operation for the dual carburetor design was that the secondary carburetor, another Walbro SDC-43, would only be engaged when full power was demanded of the engine. Operation at lower power settings would be accomplished using one active Walbro carburetor. Excellent control characteristics and fuel consumption would be retained but maximum power would be increased.

The equipment required to make this change consisted of another Walbro carburetor and McCulloch manifold. An adapter plate was milled from aluminum plate that allowed the attachment of the second carburetor and manifold at the bottom of the engine. A four-bar linkage with a slider section provided linkage to the lower, secondary carburetor. The arm lengths and slider travel

caused the secondary carburetor to engage at approximately 60 percent of throttle travel. The wide open throttle position was reached simultaneously by both carburetors.

The additional carburetor increased power to 11.7 at 8,300 rpm. Propeller speeds during static running were raised to a nominal 8,000 rpm as opposed to the previous 7,200 rpm. This rpm change caused propeller spinners and spinner mounting plates to fatigue fracture on a regular basis. Since wind tunnel tests had shown very little drag reduction resulting from the spinner installation, it was removed to reduce weight and eliminate the fatigue failure problem.

The dual carburetor A model increased power available, maintained low fuel consumption, and had good throttle control; however, it was difficult to set up the fuel mixture ratios and linkage. It was necessary to carefully balance mixture ratios and throttle openings in order to maintain smooth idle, to provide rapid acceleration and low fuel consumption at cruise power, and to obtain maximum power. Once initial adjustments were made at the Fort Huachuca test base it was usually possible to run the engine many hours prior to a need for readjustment.

One mechanical failure problem that initially plagued the dual carburetor system was breakage of carburetor butterfly shafts. At first, the standard Walbro brass shafts were retained, but as failures occurred due to the increased loads imposed by the control linkages which bore directly on these shafts, the shafts were remanufactured of stainless steel to the original design. This change reduced the frequency of breakages but did not totally eliminate such occurrences. The shafts were eventually redesigned to eliminate stress risers, and the material was changed to 4130 steel. This completely eliminated shaft breakages. A long-term wear problem remained in that the high bearing loads elongated the throttle shaft bearings, which are the unbushed holes drilled in the aluminum carburetor castings.

A third Aquila carburetor configuration is the B model system in use on all RPVs from aircraft No. 014 on. The intent of this design was to eliminate problem areas of the A model system. A new induction manifold and reed block is used which is manufactured for the McCulloch racing engines. The reason for its use is that it is designed to allow a tandem dual carburetor installation, one carburetor above the other. An adapter plate is required to interface with the Walbro "cube" type carburetor. A revised linkage (Figures 22 and 23) accompanied this design change which simplified carburetion adjustments. Carburetor models were changed from the SDC-43 to SDC-58. The SDC-58 is essentially equal to the SDC-43 but has a relocated low-speed fuel-to-air adjustment screw that allows improved access for adjustments. Power and fuel consumption changes were not the object for the A to B model change and power was not changed; however, fuel consumption at partial throttle settings was reduced.

Exhaust System. The exhaust system is comprised of a short stack which is formed from a length of mild steel seamless tubing, 1.375-in. inside diameter. A mandrel is used to shape the upstream end to the outline of the engine exhaust port. A steel flange is welded to the stack to provide an interface to the engine mating bolt pattern. At first, the gas flow is directed aft but then it turns upward at a 45-degree angle before exiting the exhaust pipe.

The propeller hub is extended away from the engine in such a way that a 3-in. clearance exists between the aft facing engine exhaust port and the forward edge of the plane of propeller rotation. This clearance provides sufficient space to employ an unrestricted exhaust pipe and to allow substitution of a muffler system if required.

The exhaust system employed is designed to perform two basic functions: direct exhaust gases out of the fuselage and provide minimal restriction to exhaust gas flow. This indeed is the case, since removal of the exhaust causes no significant change in peak propeller speed. Tuned exhaust systems were



Figure 22. Throttle Cable Linkage - B Model Engine

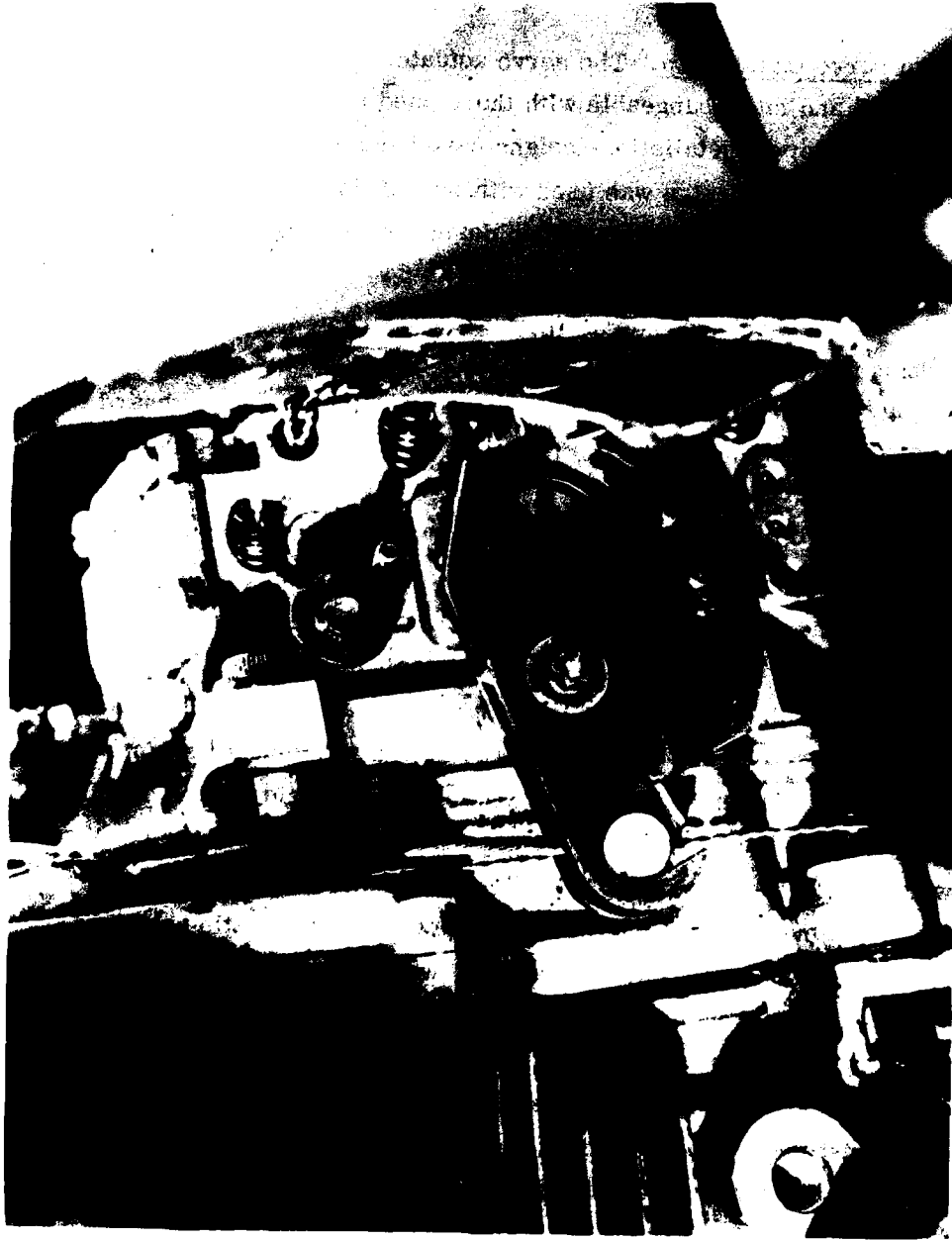


Figure 23. Carburetor Cam Throttle Control - B Model Engine

avoided because of problems associated with use of such devices. A tuned exhaust system can raise power output, but at the expense of good engine control and the necessity of packaging a bulky, heat-emitting device.

Throttle Control Servo Installation. The servo actuator used to control the throttle position is identical and interchangeable with those used for vehicle elevon control. Basically, two servo installation designs have been used throughout the Aquila program. The first design was used with the original single carburetor and the dual carburetor A model. The second design is used in conjunction with the B model dual carburetor system.

The earliest design employed a single Walbro SDC-43 carburetor on the McCulloch MC-49E manifold and the carburetor was located on the starboard side of the engine with the throttle butterfly shaft aligned with the longitudinal axis of the vehicle. The servo actuator was mounted, using an adapter block, to the forward side of bulkhead 155. The servo actuator output shaft was co-linear with the carburetor butterfly valve shaft. A tubular steel extension shaft with a flanged end was attached to the actuator output shaft flange using four screws. The carburetor end of the extension shaft was externally threaded to accept a 1/4-28 thread. To complete the attachment, a Lovejoy AO-35 flexible coupling was used. One end was modified in such a way that it was internally threaded to match the extension shaft. The carburetor side of the coupling and the butterfly valve shaft were drilled to use a roll pin for engagement. A rubber spider was fitted between the coupling halves to provide transmission of torque while allowing relative angular movement between the throttle shaft and servo actuator extension shaft. Fore and aft play were provided by leaving an air gap between coupler halves and the rubber spider. This air gap was adjusted by rotating the servo side coupler on its threads to either advance or move away from the carburetor. Once this adjustment was made, a jam nut was tightened against the coupler to lock it in position. The same adjustment was used to position the servo shaft relative to the throttle shaft for rotational orientation.

Single carburetor operation went smoothly with the original servo installation; however, difficulties arose when the same system was used to operate the A model dual carburetor. The increased loads caused by friction, higher mass and spring tension of the dual carburetor linkage caused large and unpredictable deflections in the rubber spider coupler. Spiders of increased durometer rating (hardness) were tried, which did improve the characteristics of the throttle response; however, increased amounts of engine-induced vibration were transmitted to the servo actuator, posing a threat to actuator life. The B model dual carburetor redesign provided an opportunity to eliminate the vibration found in the former throttle linkage. In its stead, the servo actuator drives a cam linkage through a cable.

The servo actuator is repositioned so that the output shaft is perpendicular to the longitudinal axis of the aircraft. Attached to the servo output flange is a lever arm which engages a steel cable at a pivoting joint. The cable penetrates bulkhead 155 into the engine compartment. A nylon sheath positions and protects the cable within the engine compartment (Figure 22). A threaded fitting at bulkhead 155 positions the cable sheath relative to the cable providing adjustments to throttle position. A barrel fitting is attached to a control cable at the cam end, which slides into a recess in the cam. A roll pin is then inserted into the cam to prevent accidental disengagement. A mounting shaft is threaded into the edge of the adapter plate used to mate the carburetors and induction manifold. This shaft is the pivot point for the cam. The cam, shown in Figure 23, is a machined steel plate that has separate bearing surfaces for the followers of the two carburetors. The primary carburetor has a steel pin follower that is driven by a slot in the cam. This provides constant retention of the follower. A torsion spring on the primary throttle shaft is used to eliminate backlash of the follower in the slot. The slot constantly varies in radius relative to the cam pivot point except at the maximum throttle position where a constant radius exists. Since the slot has excess length at the idle position, the cam is without a hard stop that could overload the servo actuator.

The secondary carburetor cam follower is driven by an outside edge of the cam. It has a torsion spring which is necessary to provide a force to keep the follower in contact with the cam surface and to keep the secondary butterfly valve closed when not in contact with the cam. The cam does not open the secondary carburetor until it has traversed through approximately two-thirds of its travel. The two carburetors reach the wide open position simultaneously. The throttle is adjusted so that the engine idles between 3,500 and 3,800 rpm when the servo is not under the autopilot rpm loop control. The autopilot rpm loop, when operating as in flight, will hold idle rpm to $4,000 \pm 200$. This system allows the autopilot to keep idle speeds lower in a descent than if a fixed stop were used to set an idle position. A sheathed steel cable which slides in a nylon outer sheath is used to pull the cam to the idle position. A torsion spring wound on the cam pivot shaft drives the cam to the wide open throttle position. If the cable were to break, or if power were disconnected to the servo actuator, then the throttle linkage would move to the wide open position.

Propeller. The Aquila propeller, shown in Figure 24, is of laminated birch construction. It is a simple two-bladed design with a 19.5-in. diameter. The blade activity factor is 150 with a blade angle of 20 deg at the 75-percent chord. This propeller is manufactured by Propeller Engineering Duplication of San Clemente, California. Initial flight testing of Aquila vehicles was carried out using a propeller of similar design manufactured by the Sensenich Corporation of Lancaster, Pennsylvania. The activity factor and diameter of both designs are equal but the Sensenich used a higher blade pitch angle, 21.5 deg at 75-percent chord. This change to the lower blade pitch angle was to allow the engine to operate at higher speeds to increase power available for climb at lower airspeeds.

Engine Assembly and Acceptance Testing. All Aquila engines have been assembled and tested in accordance with specifications which describe tests and modifications to be performed by shop personnel. Engines assembled prior to the B model dual carburetor configuration underwent an internal

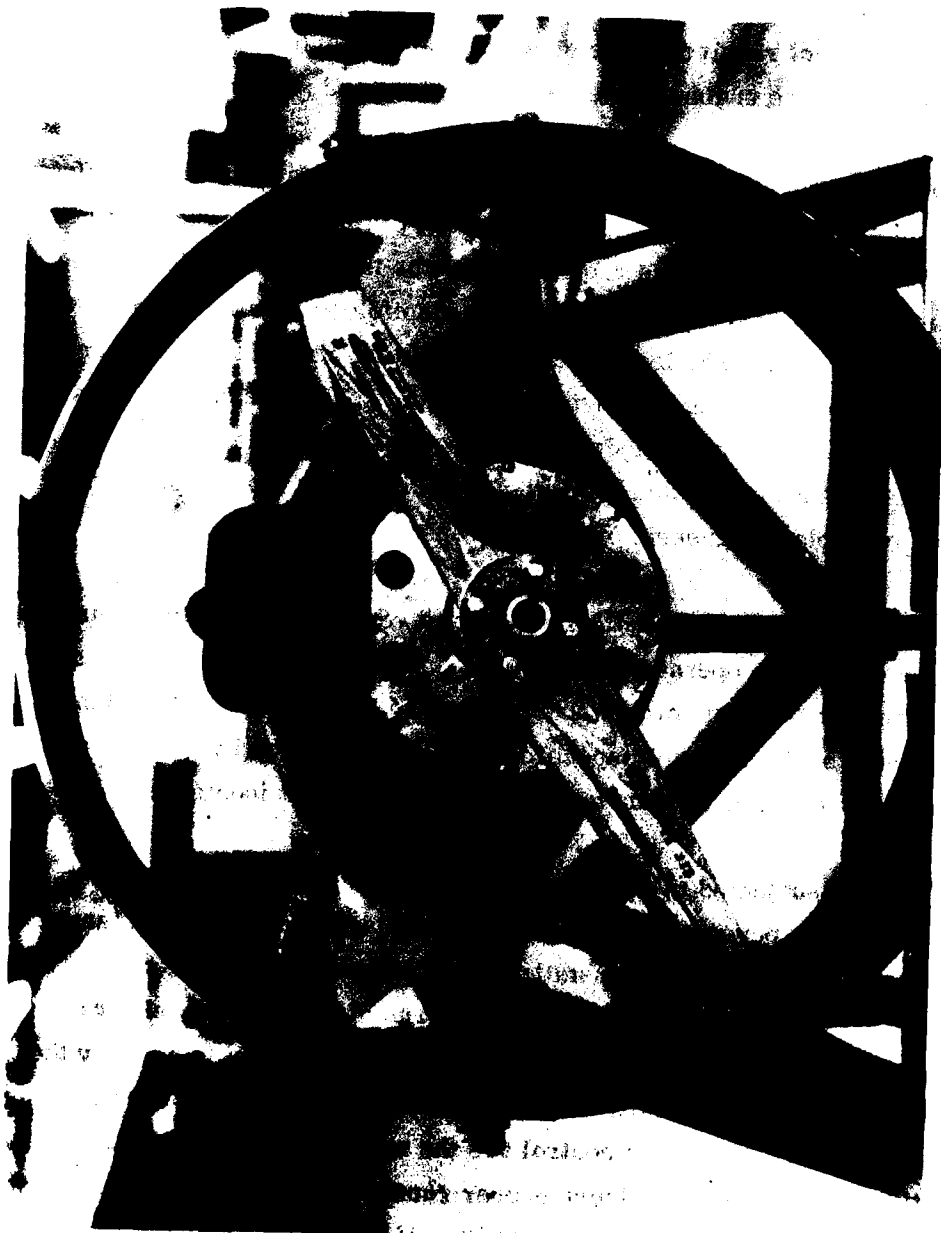


Figure 24. Aquila Propeller Installation

inspection. The engine was sufficiently disassembled to allow measurement of piston to cylinder bore clearances, measurement of piston ring clearances, and inspection for foreign objectives or incorrect assembly. Experience showed that this effort was not required since clearance adjustments required were of a minor nature, and since engines were delivered clean and properly assembled.

Assembly of all engines required checks and tests which are currently in effect. Each engine ignition is checked for proper ignition timing and corrected if necessary. Each engine is modified as required to fit the thermistor, exhaust stack and engine mounting bracket. Aquila induction manifolds are fitted prior to an air pressure leak check. The leak check entails fitting air tight plates over orifices and then pressurizing the engine to 12 lb/in.² The pressure loss is observed for a required time period; if it exceeds a specified level, then the technician must use a liquid solution to find leaks and bring those found within specification by replacing gaskets or sealants as required.

Fastener torques are specified and correct use is verified by Quality Assurance personnel throughout the operation. Safety wire is installed at specified locations to ensure that fastener torques are maintained. Following completion of the requirements of the assembly specification and acceptance by Quality Assurance personnel, the engine is transferred to the facility test location.

The engine is next subjected to an Acceptance Test Procedure that is witnessed by Quality Assurance personnel. The engine assembly is installed in a test stand which simulates an actual vehicle installation. Carburetion is set to deliver a slightly fuel-rich mixture and then the engine is run at varying but relatively low power settings for approximately one hour. If compression tests show the piston rings to be sealing normally the testing is continued. Maximum rpm, fuel consumption, and ease of throttle control are the main items of interest. Fuel mixture settings are varied to achieve proper running; however, the engine must pass all tests with the same settings to qualify. If the engine passes all tests, acceptance is noted, and then the engine is installed in a flight vehicle or stored.

3.3.5 Propulsion Performance and Functional Testing

The Aquila propulsion system has been the subject of a wide variety of tests. The objective of this testing has been to evolve an engine configuration that performs its functions in a reliable, satisfactory, and efficient manner.

Knowledge gained from previous experience with RPV engines was combined to produce the initial Aquila flight configuration. Since that time, testing has continued throughout the program to match engine capabilities to current vehicle requirements.

Carburetion and Control. During March and April 1975, static ground tests were conducted to characterize the power potential, fuel consumption, weight, bulk, and adaptability to closed loop control of candidate carburetion systems to be employed with the McCulloch MC-101MC engine.

During these tests the MC-101MC engine displayed superior control characteristics when coupled to the Walbro Corp. SDC-43 carburetor. Weight, bulk, and fuel consumption characteristics of this system were superior to any of the other three systems tested. However, with this configuration the maximum power was the lowest (approximately 10 hp).

Altitude Tests. During May 1975, ground tests were run at altitude to determine altitude effects upon the fuel consumption, power, and control characteristics of the Walbro carburetor-equipped MC-101MC and the next most acceptable option, a Tillotson HL series carburetor.

Altitude range was limited to 8,000 ft or less for this test since remote sites in mountains local to LMSC were used. The results demonstrated that the relative differences between the carburetion systems were stable over the altitude range of the test.

Fort Belvoir Altitude Tests. In July 1975 altitude chamber tests were conducted at the Fort Belvoir altitude chamber, to characterize the performance of the engine configuration over the range of altitude expected in flight tests. Figure 25 shows the test arrangement.

Figures 26 and 27 graph horsepower output and fuel consumption as a function of altitude. It is interesting to note the low specific fuel consumption data recorded.

Installation Testing. During the period of August through September 1975, the completed engine installation, including throttle servo actuator, exhaust system and enclosed engine were tested. The objective of this testing was to ensure that no mechanical or thermal problems existed in the complete installation.

The installation demonstrated *satisfactory operation as tested*. Ambient air was supplied for induction and cooling requirements. No abnormal power losses were observed. Engine cylinder head temperature remained at 390° F or below regardless of the duty cycle. Engine control by the throttle servo was very good.

Alternate Fuel Tests. In October 1975, a test was conducted to determine the feasibility of increasing the power output of the McCulloch MC-101MC by changing fuel mixtures while retaining the Walbro SDC-43 carburetor. By changing from a gasoline-based mixture to an alcohol base, it was possible to increase power to over 11 hp. It was found that modifications were required to the carburetor that caused its control response characteristics to deteriorate. Fuel consumption was increased by a factor slightly less than two. MIL spec aircraft fuel was selected over high test automotive fuel due to the lower rate of bubble formation observed with the aircraft fuel in altitude chamber tests. Use of regular automotive or MO gas was discontinued due to the potential for detonation with those fuels.



Figure 25. Altitude Chamber Test Stand

- NOTES: 1. AQUILA ENGINE, SINGLE CARBURETOR
2. ALTITUDE CHAMBER DATA - JULY 1975

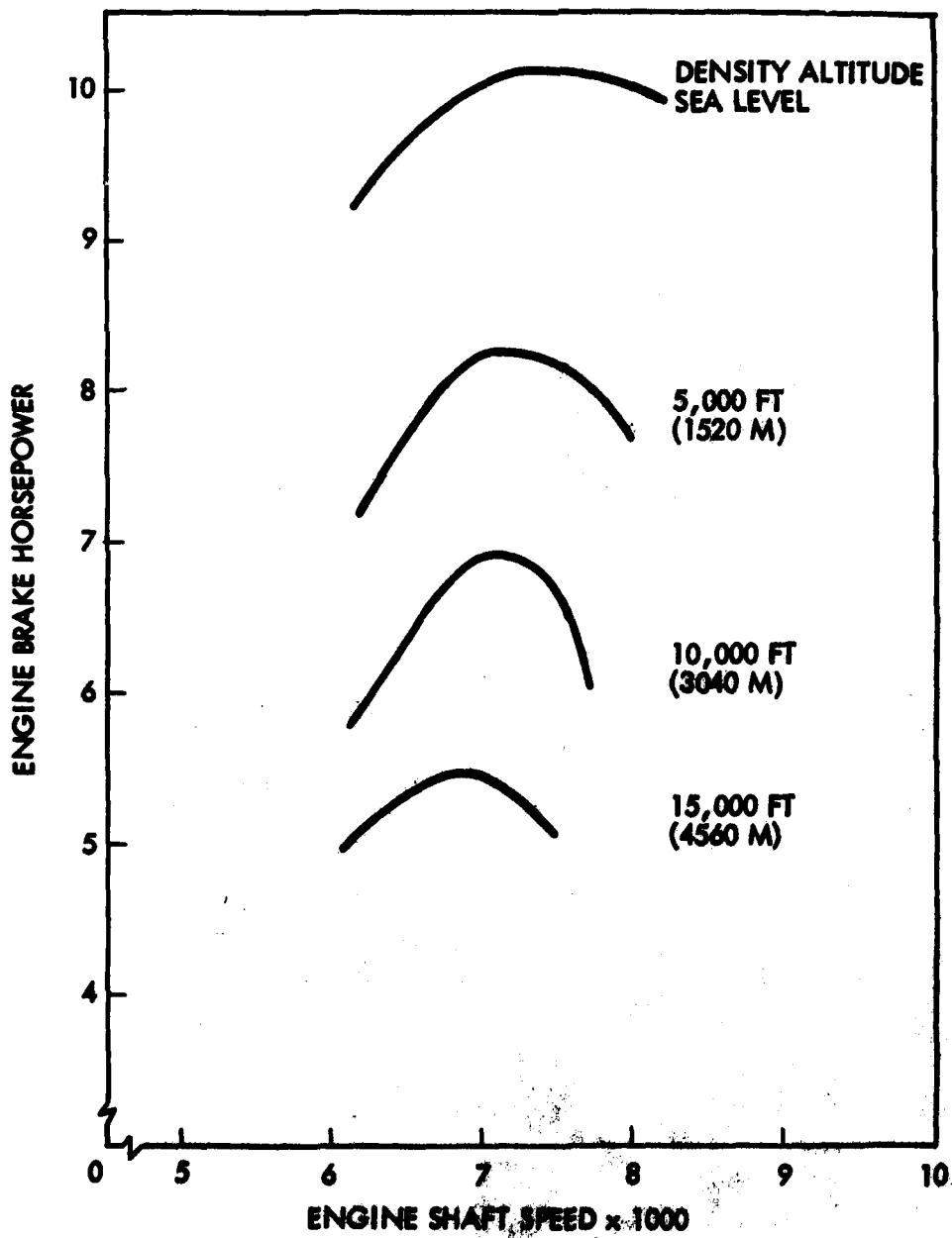


Figure 26. Engine Horsepower - Single Carburetor

- NOTES: 1. AQUILA ENGINE, SINGLE CARBURETOR
2. ALTITUDE CHAMBER DATA - JULY 1975

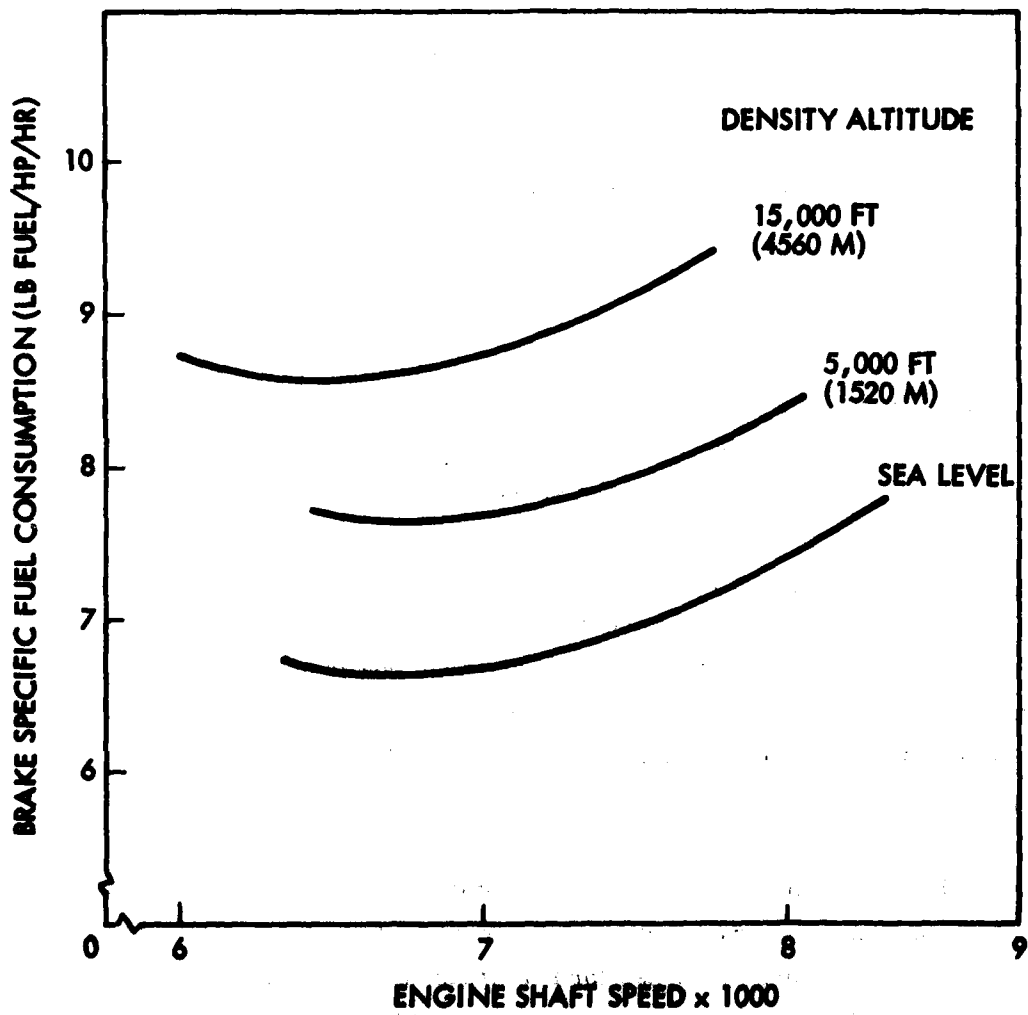


Figure 27. Full-Throttle Specific Fuel Consumption

Starting Tests. In November 1975, a series of static ground tests was conducted to determine a starting sequence that could be inserted into the computer operated launch procedure.

Cool mornings were the times chosen to conduct tests. Various throttle positions were tried to determine the optimum setting. Forty percent of wide-open throttle was found to produce the best results and required no choking or priming.

Thermistor Calibration. In November 1975, thermistor calibrations were accomplished. The location chosen for the thermistor that indicates engine temperature during flight is offset downward from the engine cylinder head. A correlation between true cylinder head temperatures at the thermistor location was required.

By installing a flight item thermistor and comparing the readings obtained to a thermocouple at the spark plug base, a temperature difference of 40° F was found in the 300 to 400° F range, with the spark plug TC the hottest.

Dual Carburetor Development. During the period of March through May 1976, a series of static ground tests was accomplished to test ways of adding a second carburetor to the MC-101MC engine to increase peak power output. A progressive linkage was to be employed to allow one carburetor operation at low power levels so that fuel consumption would remain low and throttle response acceptable.

Four manifold configurations were tested during this period. The majority of tests were propeller stand runs; however, a dynamometer was employed to calibrate the results. The design chosen for use produced the greatest power, 11.7 hp, and eliminated the need for casting a new manifold. A second carburetor and manifold unit, as previously used, was attached to the bottom of the engine with a simple plate adapter. A four-bar linkage was designed with a sliding section that provided the progressive feature required. Fuel consumption was increased over the single carburetor engine.

The testing included many runs to determine optimum fuel jet sizes and linkage geometry.

Altitude Chamber. During June and July 1976, a series of altitude chamber tests was conducted. The objective of this series, which was again conducted at the Fort Belvoir altitude chamber, was to characterize the performance of the dual carburetor engine configuration at altitudes representative of actual flight conditions. Figures 28 and 29 graph horsepower output and fuel consumption as a function of altitude.

Developmental Testing - B Model Dual Carburetor Configuration. During January and February 1977, the deployment of the dual carburetor engine for flight testing incurred some problems. The engine was difficult to adjust properly, although it would maintain adjustment once set. The linkage caused no serious in-flight problems but tended to wear out rapidly. A test program was required to find a revised configuration which eliminated these problems.

A replacement induction manifold was found which allowed the carburetors to be mounted adjacent to one another. The four bar linkage was then replaced by a cam driven by a cable from the servo actuator. The cam used two separate ramps to provide progressive opening of the carburetors. Tests involved the varying of cam ramp shapes and fuel jet sizes in order to operate the engine as desired.

Field Tests. During April 1977, prior to full deployment of the B model dual carburetor engine configuration for field use, a prototype system was sent to the Fort Huachuca test base to ensure proper operation of the system at that altitude (4,500 ft).

Engine runs indicated that a problem did exist in that the ability to accelerate rapidly was sensitive to altitude changes. A revised arrangement of fuel metering jets was found that eliminated engine stall when the throttle was rapidly moved with the engine idling.

- NOTES: 1. AQUILA ENGINE (MC-101MC),
DUAL CARBURETORS
2. PROPELLER LOAD - ALTITUDE
CHAMBER DATA - JULY 1976

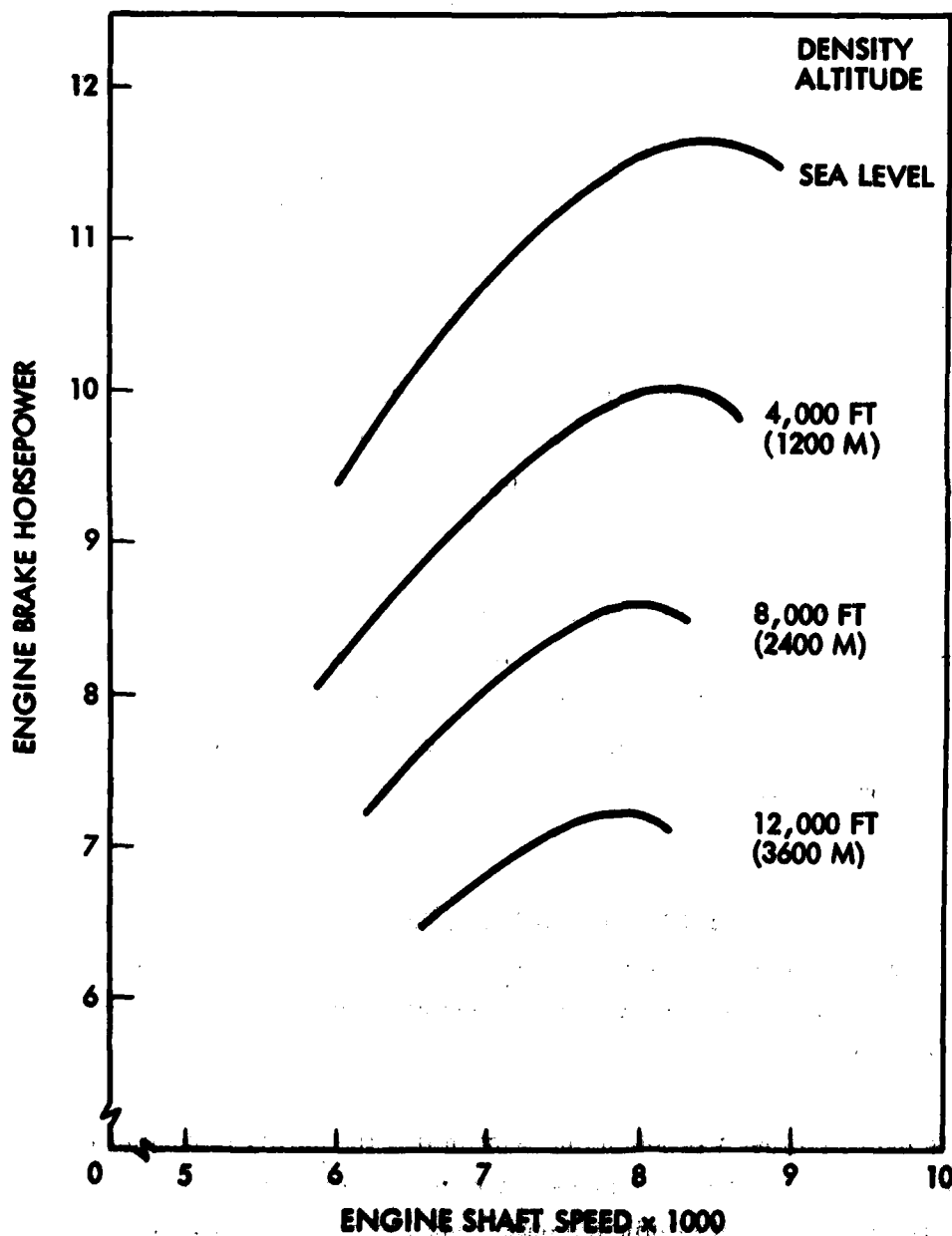


Figure 28. Engine Horsepower - Dual Carburetors

- NOTES: 1. AQUILA ENGINE (MC-101MC), DUAL CARBURETORS
 2. PROPELLER LOAD-ALTITUDE CHAMBER DATA

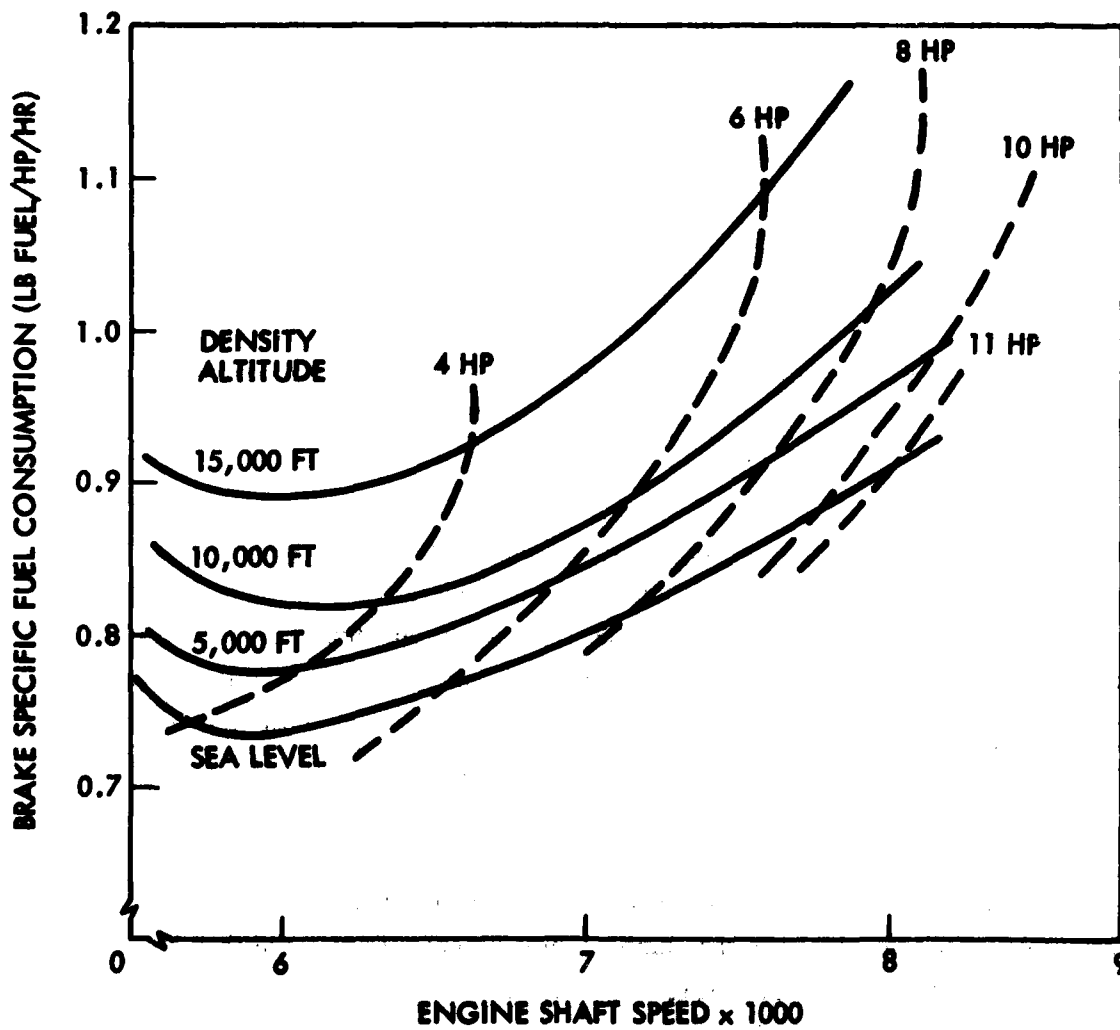


Figure 29. Partial Load Specific Fuel Consumption

Altitude Tests. In May 1977, because of the altitude sensitivity shown by the B model engine, an altitude test was conducted at the Lockheed "STARS" altitude chamber located in Sunnyvale. The purpose of this test was to determine the acceptability of the B model engine at high altitudes.

Runs were made at several altitude levels up to 16,000 ft. A strip chart record of rpm and throttle position was made for all runs. A throttle control system that could open the throttle at predetermined rates was employed for consistency. Five separate fuel metering arrangements were tested. The arrangement arrived at during the April field tests at Fort Huachuca was the best system tried and was adopted for the flight vehicles.

Fuel Line. During the course of the May altitude tests bubbles were observed forming in the fuel line downstream of the quick-disconnect coupling when operated at altitudes in excess of 8,000 ft. In June 1977, tests were conducted to determine the cause of bubble formation and to arrive at a modification to eliminate the cause.

An electric pump, accumulator, and valve arrangement was constructed that recreated the flow and pressure conditions of the altitude chamber. This device showed that bubble formation was resulting from air outgassing from the fuel as it made a transition from the small diameter outlet of the coupling to the relatively large volume of the fuel line. A change of fuel-line size with sleeve joints produced a more constant area path for fuel flow, which eliminated the possibility of severe bubble formation.

Installation Losses. A modification made to the B model vehicles was the inclusion of a temperature transducer in the engine compartment. Data could then be made available defining the elevation of engine compartment temperatures over ambient. Once these values were known, a test was run to determine the extent of power loss during field tests due to the elevation of induction air temperatures.

Test data taken in June 1977 demonstrated that losses up to 10 percent of peak power were being sustained during flight tests or at launch conditions on hot days.

3.3.6 Electrical Subsystem

Alternator. The alternator is a three-phase rotating field alternator requiring external field excitation supplied by the Aquila battery. The unit is derived from that used in the U.S. Air Force Aequare program, providing additional output power with the attendant penalty of increased weight: as used on Aquila, it provides up to 600 W at a regulated voltage of 28.2 Vdc (max.) when driven at 4,000 rpm or faster.

The power sizing for the proposed RPV-STD was estimated to require 500 W of power. As more detailed vehicle requirements became known, the power requirement was increased to 600 W. Table 7 compares weight and power output.

TABLE 7. ALTERNATOR COMPARISON

	Aequare (USAF)	RPV-STD Proposed	Aquila (U.S. Army)
Power Output (W)	300	500	600 (4000 rpm)
Weight (lb)	5.4 (actual)	6.4 (est.)	7.8 (max.)
Finish	Aluminum, no finish	N/A	Gold, anodized

Regulator. The regulator is a compact 3.5-oz proportional regulator controlling the field excitation to maintain the output at 28.2 to 28.4 Vdc. In the original design for the charging system the vendor proposed a switching regulator which required no heat sinking. This design was not available for the Aquila due to design failures experienced in the switching transistors at high temperatures.

Consequently, a proven proportional regulator was substituted. The proportional unit required approximately 9 in.² of finned aluminum heat sink stock and is mounted to the Aquila bulkhead at FS 147.

Alternator Drive Coupling. Previous experience gained with the Aequare program had demonstrated that an alternator should be mounted directly to the airframe and not to the MC-101 engine. The remote drive developed for Aequare was considered to be the best alternator drive available. A flexible, wound steel wire shaft is fitted with a swaged sleeve at the alternator end and pinned to the alternator armature shaft. An aluminum adapter is bolted to the engine flywheel that is broached with a 0.25-in.-square hole. The flexible shaft is squared at this end and inserts into the adapter at the flywheel centerline. This arrangement allows engine movement in all axes while torque is continuously transmitted to the alternator.

The alternator is attached to the forward side of bulkhead 155 by a bracket which is a Kevlar cylinder with flanges at both ends. The flanges provide locations for screw fasteners that attach the alternator to the bracket and the bracket to bulkhead 155. The cylinder is not solid, and several air passages are cut lengthwise to allow cooling and induction air flow to the engine compartment.

Power output as derived from vendor test data is given in Figure 30 as a function of rpm.

3.3.7 Fuel System Evolution

Two basic requirements were established in the beginning for the fuel system: first, the tank would be a bladder; second, it would be removed from the airframe to be refueled. A bladder provided two important advantages: it would be more resistant to shock damage than a normal rigid tank, and, by expelling all air from the bladder during the fueling process, it would be impossible for the engine to ingest air from the tank in unusual maneuver attitudes.

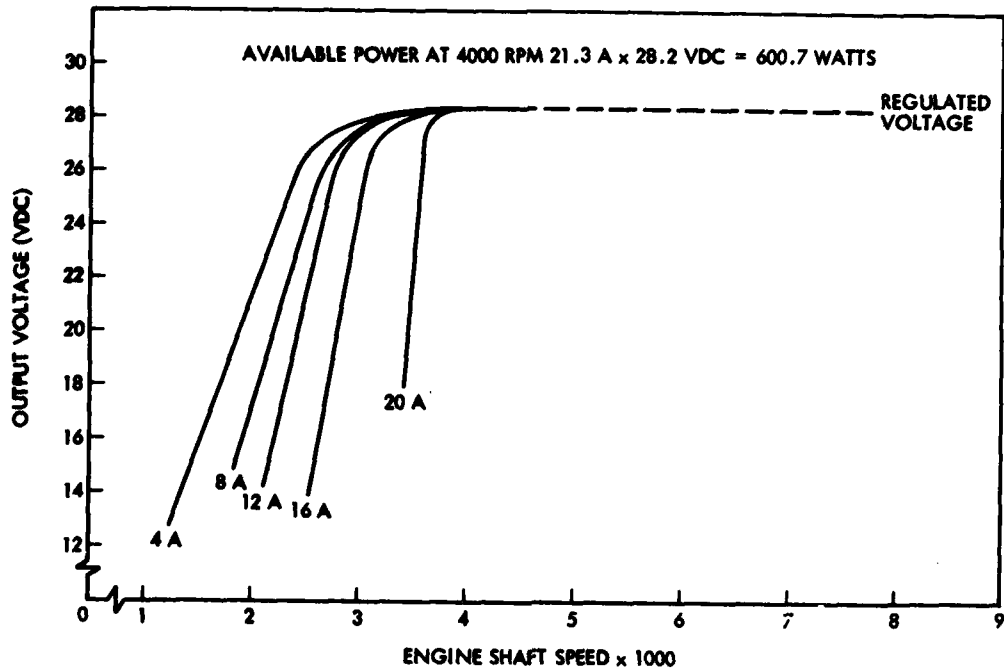


Figure 30. Alternator Output Voltage - Variation With RPM

The requirement for removal from the airframe to fuel the tank and the need to have a rigid-walled container for a bladder led to the installation of a Kevlar box under the central fuselage access hatch. Thus, the bladder container or cage could be easily removed by removing the access cover.

In addition, a convenient method of disconnecting the fuel line was required, so a conventional quick disconnect coupling was added to the system. The male portion of the coupling was fitted to bulkhead 137 located in the wing root area. Lifting the fuel tank provided access to the coupling. In practice, the quick-disconnect coupling was difficult to operate since it was not possible to use two hands for the operation. The design was modified in such a way that an aluminum bracket extended below the fuel bladder cage, to which the male portion of the coupling was fixed. By lifting the access cover and then resting it on the fuselage side, the quick-disconnect coupling was easily operated.

The plastic bladder was pierced at one location only for the fuel-line fitting. Tygon, a clear plastic fuel line, was used and was secured at fittings by pulling the Tygon over the fitting nipple and then wrapping it with two loops of 0.032-in. -diameter safety wire. The fuel line was originally a 0.25-in. -internal-diameter formulation B-44-4X.

During testing at the "Stars" altitude chamber in May of 1977, bubbles were observed forming at the downstream side of the quick-disconnect coupling at density altitudes in excess of 8,000 ft. This resulted in erratic engine behavior when large bubble accumulations entered the carburetion system. Further testing demonstrated that the coupling was not leaking air but that air was outgassing during the transition from the 0.125-in. internal diameter of the coupler to the 0.25-in. internal diameter of the fuel line. The bubbles observed were assumed to be composed basically of air since an accumulation of air within the fuel line would be reduced in volume in inverse proportion to atmospheric pressure changes, but would not go back into solution with the gasoline, as it would be expected to do, at sea level pressures.

Following this discovery, a design change was tested and then installed on all B model RPVs. A replacement fuel line with a 0.125-in. internal diameter was substituted for all applications downstream of the quick-disconnect coupling, and a sleeve was used at all fittings to minimize changes in internal cross sectional areas.

The result of the design change was a major reduction in bubble formation: bubble accumulations would break away suddenly upon a rapid change in fuel flow and move to the carburetion system. The replacement fuel line used was Tygon formulation R-3603 to provide increased resistance to hardening due to exposure to gasoline.

Tests run to demonstrate the ability of the engine mounted carburetor/fuel pump to empty the fuel tank bladder were completely successful. The tank was

totally flattened as the fuel pump vacuum drew all the fuel contained to the engine. There was no observed tendency for the upper tank wall to collapse across the tank outlet and shut off the fuel supply to the engine. Although these observations were encouraging, there remained the possibility that an unusual loading or flight dynamic condition could cause the fuel tank outlet to be closed prior to total fuel exhaustion. Following January of 1977, all B model fuel tanks incorporated a rigid fuel line extension, internal to the fuel tank that was capped on its end but slotted lengthwise to allow fuel flow if the tank walls collapsed upon it.

A method of indicating a low fuel level condition was required for the vehicle. A search was made for a fuel flow meter that would provide an integration of fuel used, which in turn could be compared with a known fuel load and consequently indicate the amount of fuel remaining. The lightweight fuel flow meters studied lacked sufficient accuracy at the low flow levels to provide measurement. The method developed provided a hinged lever arm that followed the fuel bladder as its height diminished with fuel used. A micro switch was tripped by the lever at a predetermined point to indicate 2 lb of fuel remaining.

Following January of 1977, two changes were made to the fuel low indicator for B model vehicles. A shim was added that changed the indicating level to 3 lb remaining as opposed to the former 2 lb. Also, a disconnect electrical connector was added for the micro switch circuit to ease fueling operations.

After April of 1977, a modification was made to the fuel line at the point of exit from the fuel tank. Formerly, the Tygon tube exited the fuel bladder and was then forced into a tight radius turn to reach the quick-disconnect coupling. B model vehicles were equipped with a 90-deg elbow that eliminated the tight radius turn and the possibility of an accidental closure of the fuel line. In addition, the special fitting was provided inside the tank to prevent the flexible tank wall from sealing the exit orifice. Another change incorporated on the

B model vehicle was the addition of stencilled instructions on the fuel bladder to specify the fuel mixture to be used.

Flight experience with the final fuel system has indicated no known instances of improper fuel delivery due to trapped air in the fuel tank. The fuel tank does not tend to burst in a crash landing.

3.4 FLIGHT CONTROL SYSTEM

The principal elements of the Aquila flight control system are:

- **Flight controls electronic package (FCEP)**
 - Pitch autopilot
 - Heading autopilot
 - Altitude autopilot
- **Sensors**
 - Altitude transducer
 - Air speed transducer
 - Rate gyro package (heading and pitch)
 - Accelerometer
 - Magnetometer
- **Controls**
 - Elevon servo actuators
 - Engine servo actuator

A description of the field tested system is given in Volume I of this report. The analytical and hardware evolution of the system is discussed below.

3.4.1 Background

Prior to the Aquila program, the flight control systems for RPVs had ranged from simple radio control (RC) with direct control of the aerodynamic control

surfaces, to complete digital autopilot design. The requirement, therefore, was to select the proper approach for the special Aquila requirements. Experience had flight proven a simple analog/digital concept in the Tuboomer RPV and in the Aequare program. The concept had been assembled on regular PC cards that provided design and checkout flexibility while providing reliable electronic operation. The concept combined aerospace and general aviation techniques into a proven autopilot electronic system. It was a logical decision, therefore, to select this system and approach for the Aquila RPV.

A wide range of sensors suitable for RPV application existed from aircraft and missile developments. The task at hand, therefore, was to select or specify, procure, and (if required) adapt the sensor for the Aquila application.

Flight control servo-actuators presented quite another problem. No flight qualified servo-actuators existed in the load range anticipated. The Tuboomer had used automotive headlight actuator motors with an LMSC-developed servo electronics system. Aequare employed radio control servo units, which were unacceptable for the Aquila application.

The Aquila autopilot design approach was determined against this background.

3.4.2 Approach

The approach to the Aquila autopilot and flight controls evolution included the following elements.

Hardware Approach. The hardware approach is as follows:

- FCEP
 - Develop a third generation of the proven Tuboomer/Aequare system
 - Use PC card construction for flexibility

- Use space system proven card retention techniques
- Design circuits and select components for low (electrical) stress
- Use special enclosure design and fabrication to reduce weight
- Combine the data link encoder/decoder into the FCEP to reduce enclosure and cable weight
- Sensors
 - Use high quality pressure transducers for accuracy (use data in RPV location)
 - Adapt missile components for gyros and accelerometer – specify adaptations and procure
 - Use a three-axis magnetometer – high quality – for heading indications
- Controls. Specify and procure a new servo-actuator.

Analytical Approach. The analytical approach to the autopilot and flight controls development included the following:

- Use progressively updated computer models for analysis
- Provide conservative damping rates for all loops
- Close all RPV stability loops on board to avoid loss of control due to pilot error
- Use simulation to validate recovery flight path stability and control
- Analytically verify acceptable stability and control in all flight modes

Testing Approach. The approach to testing and validating the autopilot and flight controls involved the following:

- Ground tests
 - Electronically test each assembled PC card against approved acceptance test procedures
 - Electronically test the assembled FCEP against an approved acceptance test procedure
 - Acceptance test and/or calibrate all sensor components

- Acceptance test all servo actuators
- Conduct complete RPV systems test prior to shipment for field tests
- Flight tests
 - Provide radio control capability for initial flights
 - Provide switching system to build up the autopilot and separately test different loops in order to isolate design weaknesses

3.4.3 Requirements

The basic requirements for the autopilot and navigation capabilities were for performance consistent with the required operational levels. Specific requirements included the following:

- Augmented stability
- Link-loss maneuver to recover link
- Pre-programmable flight path control with operator override/correction
 - Repetitive search patterns
 - Loiter orbit
 - Landing approach
 - Ascend/level off
- Automatic and manual flight path control
- Autopilot modes
 - Heading command/hold
 - Altitude

A further basic requirement was the simultaneous development of the RPV stability loops (closed on board the RPV) and the flight path stability loops (closed through the GCS computer) to ensure flight path and RPV control and stability in all flight modes. The analytical evolution and RPV hardware evolution are described in the following paragraphs.

3.4.4 Flight Control and Navigation - Analytical Evolution

Guidance loops for the RPV-STD were designed with good stability margins as a basic requirement. Guidance equations for the various modes were either linear or could be linearized for small perturbations about a nominal path. Although no strict requirements were imposed, guidance gains were normally set to provide at least 50 percent of critical damping for motion about the nominal path. Guidance loop bandwidths were made as high as possible without significantly affecting airframe or autopilot stability characteristics. After design to linearized requirements, large-amplitude stability was verified by simulations.

Since no contractual requirements were specified for the airframe stability characteristics other than that they be adequate to meet program objectives, no arbitrary stability requirements were imposed. Whereas it was recognized that each airframe or autopilot mode must have positive damping to avoid catastrophic flight, the more significant aspect of stability was felt to be that associated with gust response. Recovery was considered to be the most critical phase of the RPV-STD mission; therefore, a low-amplitude, well-damped gust response transient was necessary if the aircraft were to follow the desired approach path with a minimum of disturbance. This motivation shaped the design of the autopilot and suggested the incorporation of a normal accelerometer to provide a quick response signal to the elevon to alleviate vertical gust loads. Stability against lateral gusts was improved by tilting the roll-yaw gyro for roll rate dominance while retaining only enough yaw rate to ensure an adequate heading rate reference. With this gyro orientation, stability augmentation of the Dutch roll mode was difficult since only elevons were available for lateral control. Furthermore, since no vertical aerodynamic surface was available for yaw damping, the airframe Dutch roll mode was only lightly damped. However, since the Dutch roll amplitudes expected to occur in flight did not appear to be large enough to degrade target location accuracy or jeopardize any other aspect of the RPV-STD mission, this low damping was considered no cause for concern, and no design modifications were attempted.

3.4.4.1 Flight Control/Navigation System Loop Evolution. The RPV/STD flight control/navigation system underwent significant changes from its inception to the final design. The basis for these changes lay primarily in the results of analyses and simulations previously derived from LMSC independent development programs, which provided the technology necessary to understand many unique aspects of the RPV-STD program.

The basic concept of the RPV-STD onboard flight control system experienced little change during the design and development phase of the program. Mechanization details, however, underwent significant change. The original autopilot was designed to incorporate three electrically independent closed loop systems to provide:

- Airspeed control
- Altitude control
- Heading control

The final design retained this basic control concept, although the autopilot categorization was revised to the following semi-independent closed loop autopilots:

- Pitch autopilot
- Altitude autopilot
- Heading autopilot

Block diagrams of the three fully evolved autopilots are shown in Volume I of this report. Each autopilot is uniquely characterized by its control element: in-phase elevon motion is the control element in the pitch autopilot; engine rpm is the control element in the altitude autopilot; differential elevon motion is the control element in the heading autopilot. In contrast with the original design concept, however, the flight variable controlled may vary with the guidance mode. Activation of switches according to guidance mode is shown in Volume I. Discussion of the three autopilot loops is presented in the following sections.

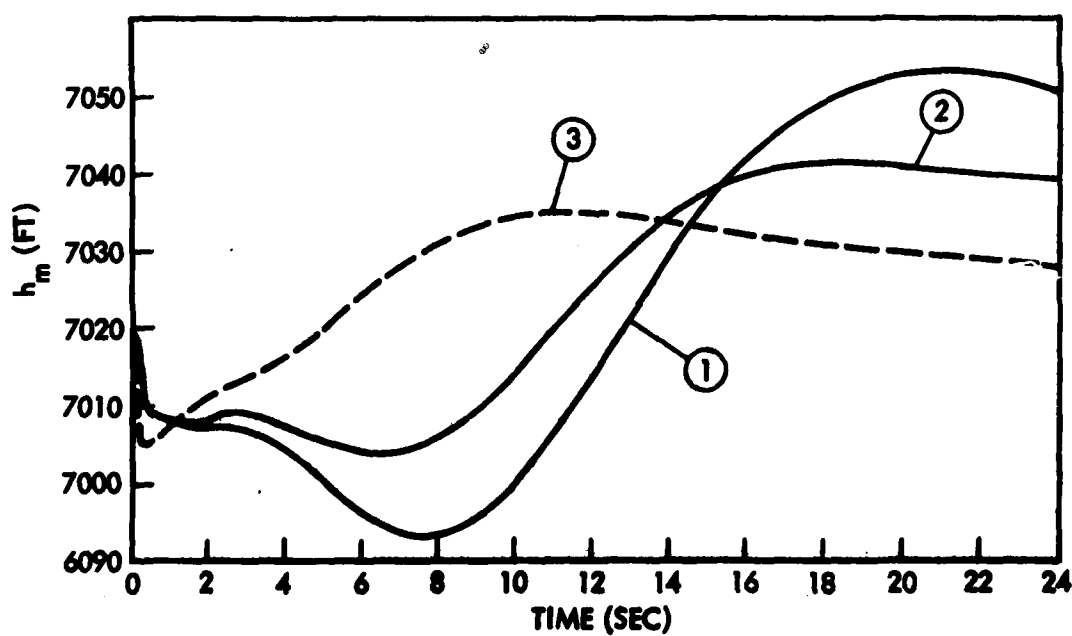
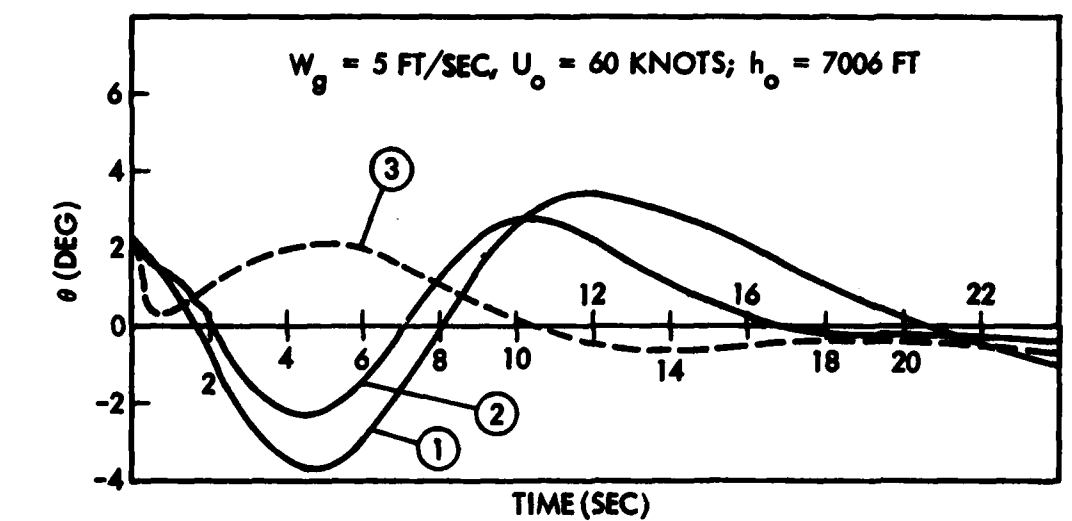
Pitch Autopilot. In all guidance modes except the final approach, the pitch autopilot controls airspeed; during final approach, the pitch autopilot controls the vertical displacement from the ideal approach path, which coincides with the boresight of the approach TV camera. In the originally conceived version of the flight control system, in-phase elevon motion was to be used to control airspeed during all guidance modes. However, early in the program it was realized that the tight control requirements imposed by the recovery process necessitated a control system with as fast a reaction time as possible for controlling flight path deviations, whereas vehicle airspeed control during approach was not so critical. Therefore it was decided to interchange the control roles of the elevon and engine during final approach; that is, the elevon would control path deviations, and the engine would control speed. This complicated the clean division that had originally existed between the speed and altitude control loops, but a switching logic was developed that minimized the requirements for additional flight control electronics to accommodate the dual control roles imposed by this approach. Six-degree-of-freedom simulations of the recovery dynamics verified the great improvement brought about by this change and more than justified its cost.

The original RPV-STD flight control concept had no provision for a pitch rate gyro or normal accelerometer. Because of the requirement for more damping in the short period mode, it was decided that a rate gyro should be incorporated to measure pitch rate, the output being fed through a gain to the elevons to provide short-period damping. The normal accelerometer was added to provide a fast control loop for vertical control during final approach. It served a secondary purpose by providing a signal for damping phugoid motion.

In the original flight control concept of the RPV-STD, phugoid damping was achieved by a derived rate signal obtained by passing the output of the airspeed transducer through a lead filter. Dynamic simulations disclosed the existence of violent short-period instabilities due to errors induced in the pitot-static system by angle-of-attack variations. Furthermore, the amplification of noise from the airspeed transducer by passing the signal through a rate filter was of

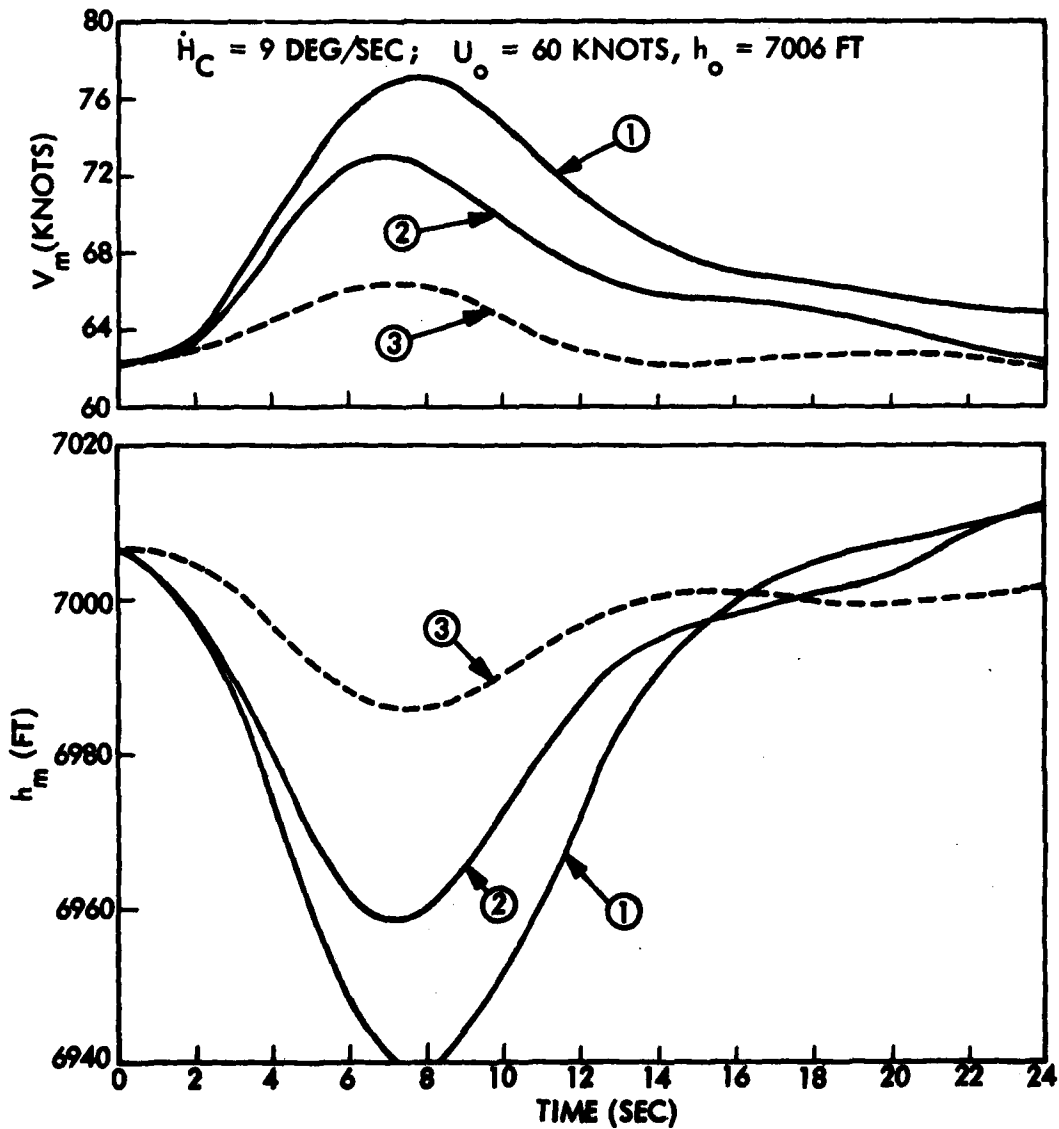
considerable concern. With the existence of a pitch rate gyro and a normal accelerometer, however, effective phugoid damping signals could be shaped by "pseudo-integration" of either signal, i. e. , passing the signal through a first-order lag circuit with a time constant considerably greater than the time constant of the phugoid mode. Studies were performed to determine the relative merits of the two methods. It was found that the filtered accelerometer signal was superior to the filtered rate gyro signal in every respect. Both signals provided adequate phugoid damping; however, the accelerometer signal caused smaller pitch excursion and altitude variation during a gust and exhibited a milder coupling effect during a turn. Based on these results, the accelerometer signal was chosen for the phugoid damper input. Because of the high dc gain of the phugoid damper, a dc washout circuit was also incorporated into the filter. Figures 31 and 32 show the results of 6 degree of freedom (DOF) simulations to determine the pitch responses to gusts and turns, respectively, in order to obtain performance comparisons of the two phugoid damping concepts.

Initial flight tests showed sporadic accelerometer errors that seriously affected the aircraft performance. Inspection of the flight records revealed considerable wandering of the phugoid damper signal with frequent saturation (limits were set at ± 10 deg). The accelerometer errors were attributed primarily to deterioration of the output signal potentiometer induced by in-flight vibrations. It was decided to replace the accelerometer with a force balance servo unit, which was smaller and inherently more accurate. Flight performance was much improved with the new accelerometer. However, occasional bursts of phugoid type motion were observed, which signal simulation eventually showed to coincide with periods of damper saturation, as illustrated by the signal time history shown in Figure 33. This curve was generated by passing actual flight accelerometer data through a simulated phugoid damper filter. This was necessary since the output of this filter was not monitored during flight. It is clear that the high amplitude oscillations started at the same time signal saturation occurred. As a result of this operation, the phugoid damper authority limits were raised from ± 10 to ± 15 deg. Simultaneously, the pitch



- ① θ' DAMPING; $K_{\theta'} = 1.3 \text{ DEG/DEG/SEC}; \tau_W = 10 \text{ SEC}$
- ② θ' DAMPING; $K_{\theta'} = 0.8 \text{ DEG/DEG/SEC}; \tau_W = 10 \text{ SEC}$
- ③ \dot{h}' DAMPING; $K_{\dot{h}'} = 0.006 \text{ RAD/FT/SEC}; \tau_W = 10 \text{ SEC}$

Figure 31. Pitch Response to Vertical Step Gust



- ① θ' DAMPING; $K_{\theta'} = 1.3 \text{ DEG/DEG/SEC}; \tau_W = 10 \text{ SEC}$
- ② θ' DAMPING; $K_{\theta'} = 0.8 \text{ DEG/DEG/SEC}; \tau_W = 10 \text{ SEC}$
- ③ \dot{h}' DAMPING; $K_{\dot{h}'} = 0.006 \text{ RAD/FT/SEC}; \tau_W = 10 \text{ SEC}$

Figure 32. Pitch Response to Turn Command

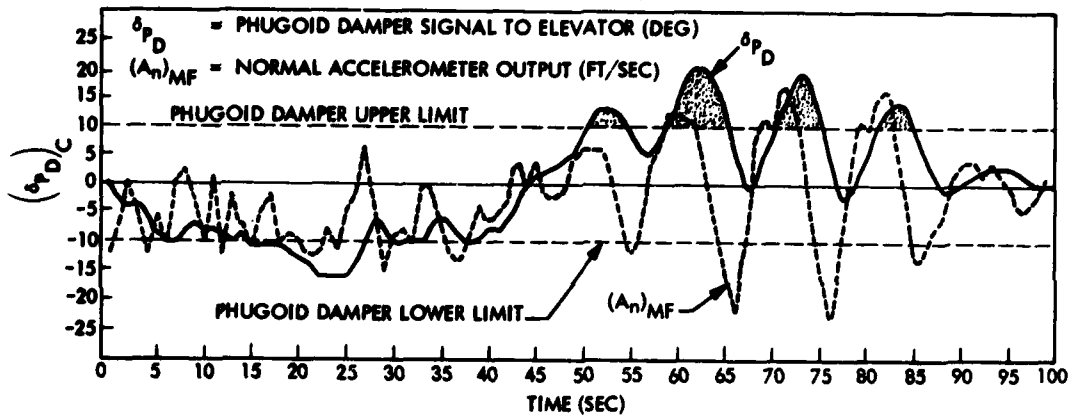


Figure 33. Aquila Flight 44 Simulated Phugoid Damper Signal

outer loop trim authority and the pitch outer loop authority limits were increased from ± 10 to ± 15 deg to permit these signals to adjust the elevator trim commands to allow for spurious phugoid damper outputs.

In accordance with the decision to use the elevon to control vertical path displacement during final approach, a filter was designed, with the accelerometer signal as input, to produce a \dot{Z} signal for comparison with the telemetered command \dot{Z}_C . Since the resulting filter was similar in form to the phugoid damper filter, common circuitry was used so that during final approach the output of the phugoid damper signal was switched to an additional lead filter and the output used to compare against \dot{Z}_C . The 15-sec time constant in the pseudo-integrator and dc washout portions of the phugoid damper, however, proved to be an unsatisfactory approach, since the transient introduced in this filter at the initiation of the final approach mode created offset recovery errors whose magnitudes had not diminished to acceptably small values when the aircraft reached the recovery net. Therefore, the \dot{Z} filter time constants were changed from 15 to 5 sec, and separate circuitry from the phugoid damper was required for this portion of the \dot{Z} filter.

Other features incorporated into the pitch autopilot during the developmental phase of the program were:

- A 4-sec lag altitude command filter to reduce peak transient loads due to step changes in the altitude command
- An elevon gain scheduler to reduce the gains at high velocities and associated high dynamic pressures
- A -6-deg elevon bias command to provide capability for higher negative elevon settings in accordance with observed airframe trim requirements

Altitude Autopilot. The final design of the RPV-STD altitude autopilot is basically equivalent to the original conception with only a few modifications. As originally conceived, the commanded altitude is compared to the output of an altitude transducer, and the error is fed through a gain and limiter to generate a climb rate command. The altitude measurement is passed through a differentiating filter and the resulting \dot{h} estimate is compared to the commanded climb rate. The climb rate error is then passed through a proportional-plus-integral gain to generate an engine rpm command. An rpm sensor provides the feedback in the rpm servo loop, which is closed around an inner throttle servo loop.

The decision to use the elevon to control vertical path deviation during final approach required transfer of the speed control task to the engine. Thus, during the final approach mode, altitude error and the feedback altitude rate are switched out and replaced by speed error. Thus, the title autopilot becomes somewhat of a misnomer, since during final approach the controlled flight variable is airspeed.

Early flight tests revealed that fluctuations in the altitude rate signal were being introduced by angle-of-attack changes. It was concluded that angle-of-attack feedback was being introduced in the altitude rate loop through the altitude pressure port located in the nose section. It was found that the value of

the time constant τ_D in the altitude rate loop could be increased significantly while maintaining adequate gain and phase margins in the loop. This would permit more effective filtering of frequencies in the short period range. The final design value of τ_D was 4 sec, which proved to be adequate to filter out the undesired frequencies.

Observed quantization effects due to coulomb friction or deadband in the actuator servos led to analyses and simulations to determine what effects such phenomena might have on the RPV performance. One consideration was the effect of throttle servo deadband on aircraft performance. Figures 34 and 35 show the results of a 6-DOF simulation of the vehicle dynamics with a 2.5-percent throttle servo deadband. Since the full throttle range corresponds to an 80-deg servo displacement, the assumed deadband was equivalent to a total servo free play of 4 deg. The variations in speed, altitude, and engine rpm associated with the limit cycle oscillations caused by the deadband were observed to be quite small and were not expected to cause any significant adverse effect on the RPV performance.

Abort provisions in the initial design of the RPV-STD altitude autopilot included a step input directly to the throttle at the initiation of the abort command. This had the tendency to kill the engine. Therefore, a change was made to input the throttle command at the summing junction ahead of the integrator inside the rpm servo loop. This resulted in a command signal to the throttle that was ramped at 25 percent per second, thereby reducing the probability of killing the engine.

A 1-sec lag filter was incorporated to reduce the transients associated with a step input.

Heading Autopilot. The original heading autopilot consisted of an inner heading rate loop closed through a rate gyro with an outer heading loop closed through a magnetometer. The inner loop is always closed, but the outer loop is closed only during the dead reckoning mode.

THROTTLE HYSTERESIS
DEADBAND = ± 2.5 PERCENT
 $V_{TRIM} = 60$ KEAS

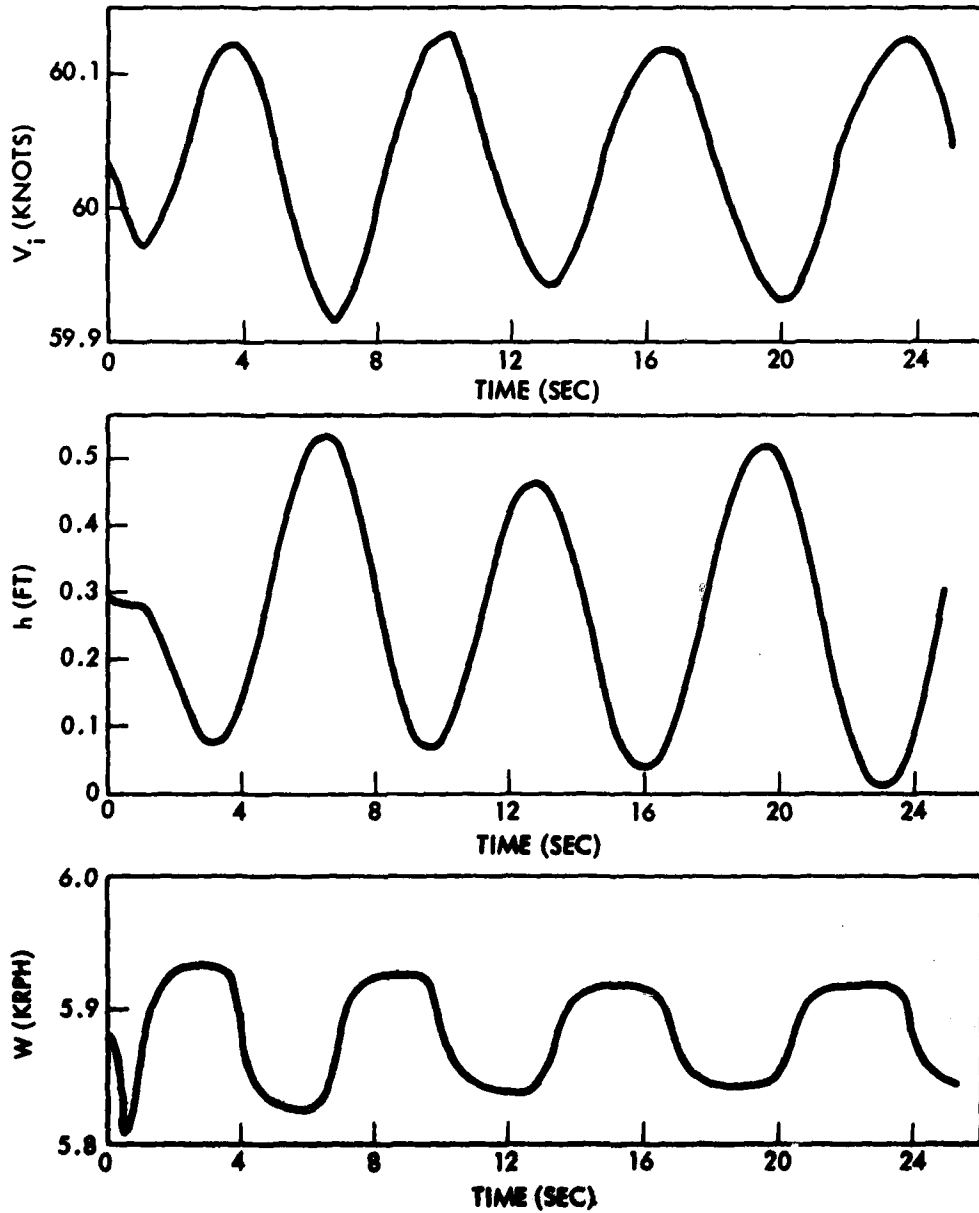


Figure 34. Aquila Limit Cycle Oscillations for Throttle Hysteresis, Deadband

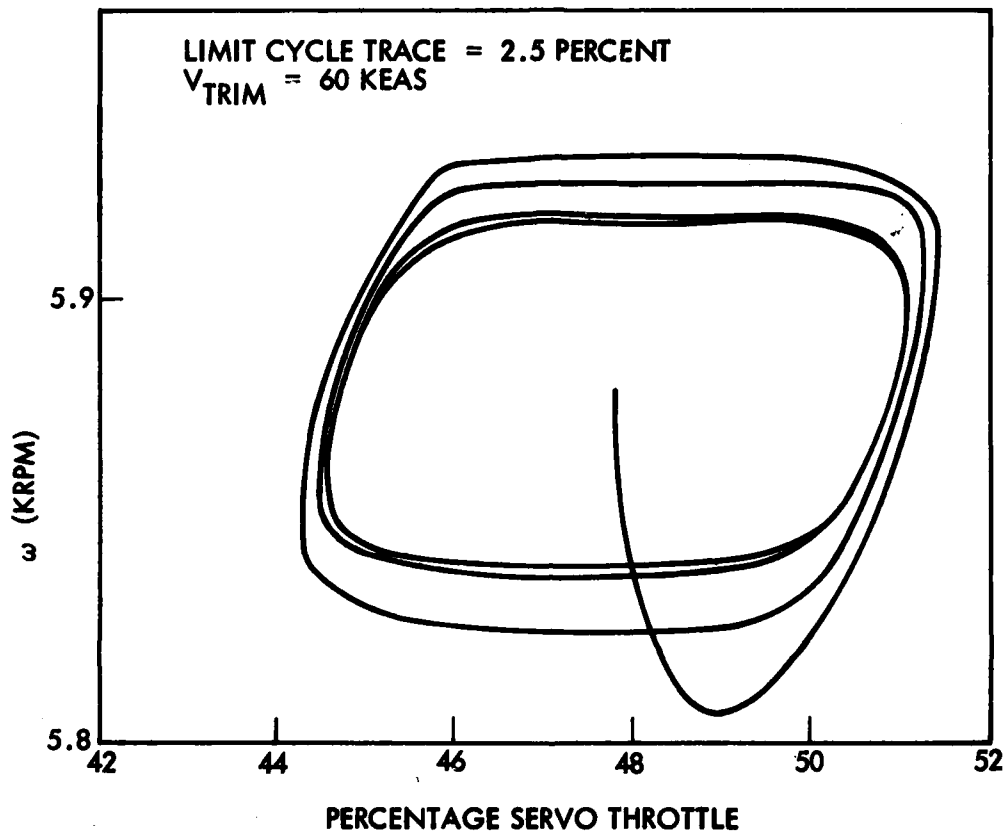


Figure 35. Aquila Limit Cycle Trace for Throttle Hysteresis Deadband

The inner (heading rate) loop is closed through a rate gyro tilted so as to pick up components of both roll and yaw rate. Originally, the gyro signal was compared directly with the heading rate command to generate a heading rate error, which was passed through proportional and integral gains to produce a differential servo command to roll the aircraft into the direction commanded. Subsequent design studies revealed that a feedback filter increased the loop bandwidth significantly. Gyro tilt angles which resulted in predominantly roll rate indication with adequate yaw rate to produce a heading rate reference were found to be most desirable from a lateral gust stability viewpoint. The tilt angle selected was 20 deg downward from the longitudinal axis of the RPV.

This heading rate loop was formulated early in the program and remained unchanged during most of the demonstration flights. However, high-frequency servo/airframe instabilities were observed prior to launch, which hampered prelaunch checkout activities. A first-order lag circuit with a 0.016-sec (10 Hz) time constant was inserted in the loop immediately after the rate gyro. This eliminated the prelaunch vibrations while not significantly decreasing the loop phase margin.

The outer loop of the heading autopilot is active only when the dead reckoning mode is being employed. In this mode, the heading autopilot receives its commands in the form of sine and cosine of the desired heading, stored onboard the aircraft in a circulating register to permit transfer to successive legs of a dead reckoning pattern. These commands are mixed with the X- and Y-magnetometer outputs according to the sine difference formula to produce an error signal, which (for level flight) is the sine of the heading error. Multiplication of this error signal by a proportional gain produces a heading rate command which then completes the outer loop.

The original outer loop design incorporated sampling logic such that the error signal would be computed and sampled only when the roll-yaw rate gyro output was low enough that a near-wings-level flight condition was indicated, thereby ensuring that the Y-axis magnetometer output would not be corrupted by the dip angle component of the magnetic field vector. After each sampling, an open loop heading rate profile would be commanded, after which the wings level condition would again exist, and a new heading error could be computed and sampled and a new heading rate profile generated.

It was determined, however, that the sampling system just described was not necessary and that the heading autopilot could be made to work with a continually closed outer loop if the outer-loop gain were maintained at a sufficiently low level. That is, the error signal computation would ignore the roll condition of the aircraft (as indicated by the output level of the roll-yaw rate gyro)

and perform the computations as if the airplane were flying straight and level. The errors introduced thereby would affect the nature of the response to a given heading command but the steady-state values would not be affected.

Simulations were performed on the LMSC 6-D digital program to determine the response to various direction commands, using an outer loop gain $[K_H = 0.1 \text{ (deg/sec)/deg}]$ which provided adequate damping in the heading mode for all directions and an airspeed of 100 KEAS. Figures 36 through 43 show the heading and roll angle response to various heading commands (H_C) for initial heading angles (H) of 0 and 180 deg. Velocities of 60 KEAS and 100 KEAS were simulated. It can be seen from the figures that a steady-state error normally exists between the commanded and the final steady-state heading. An error analysis of the heading autopilot showed that this steady-state error arose because the X-magnetometer axis was not precisely horizontal. The simulations illustrated in these figures were based on the assumption that the X-magnetometer was oriented parallel to the aircraft longitudinal axis. In the straight-and-level flight condition, therefore, the X-axis magnetometer would be tilted from the horizontal by an amount equal to the aircraft angle of attack. The corruption of this magnetometer output due to the dip of the magnetic field vector can be shown to introduce a heading error which, for small pitch error, is approximately equal to the magnitude of the pitch error angle multiplied by the tangent of the dip angle and the sine of the heading command. Since the dip angle in the vicinity of the RPV-STD flight tests is approximately 65 deg, the steady-state heading error induced by the X-axis magnetometer pitch error is approximately 2.7 times the pitch error times the sine of the commanded heading. Since the aircraft flies a speed range for which the angle of attack varies by approximately 5 deg, tilting the X-axis magnetometer for zero pitch error at the midrange angle of attack would result in a maximum pitch error of about 2.5 deg. This translates into a maximum steady-state heading error of almost 7 deg.

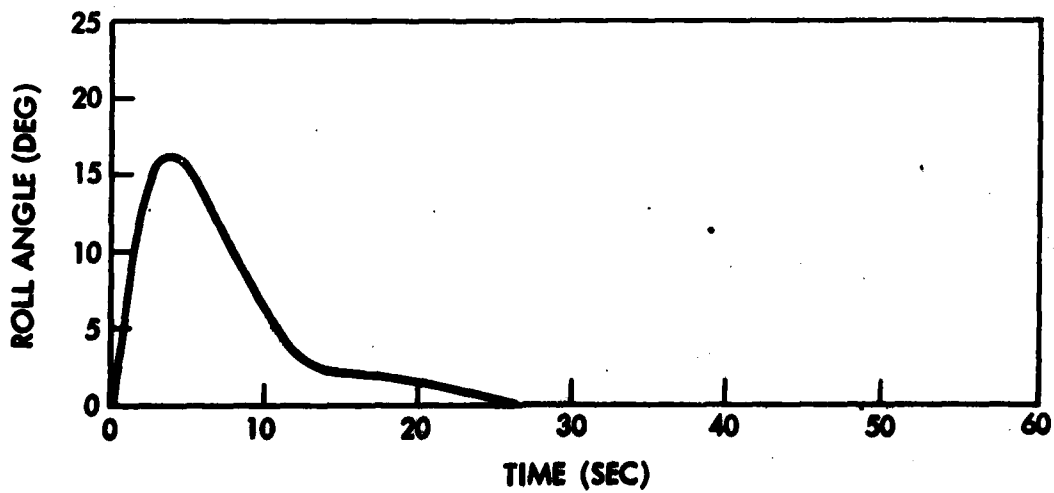
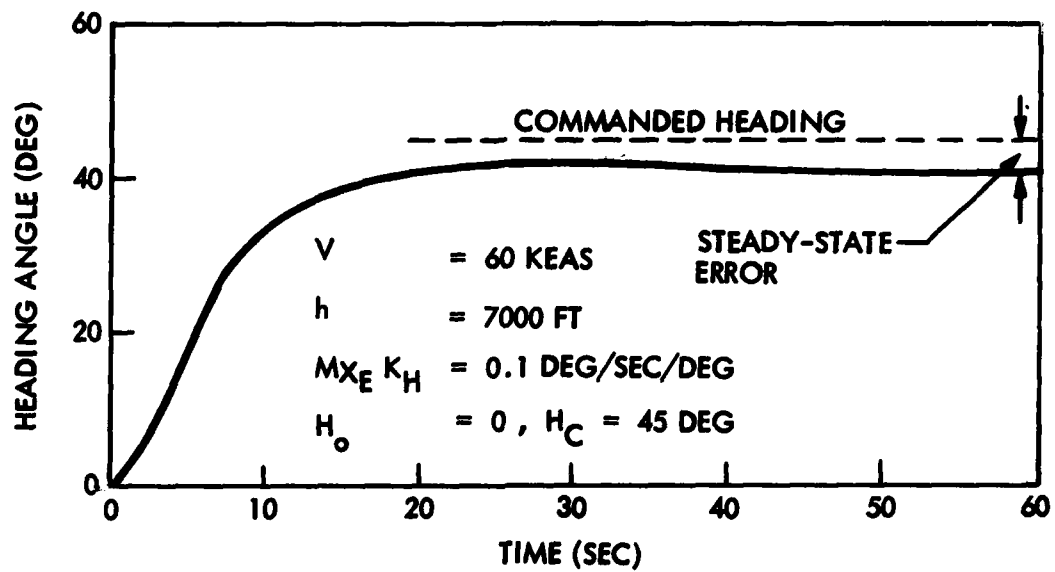


Figure 36. Aquila RPV Response to Heading Command ($H_C = 45 \text{ Deg}$)

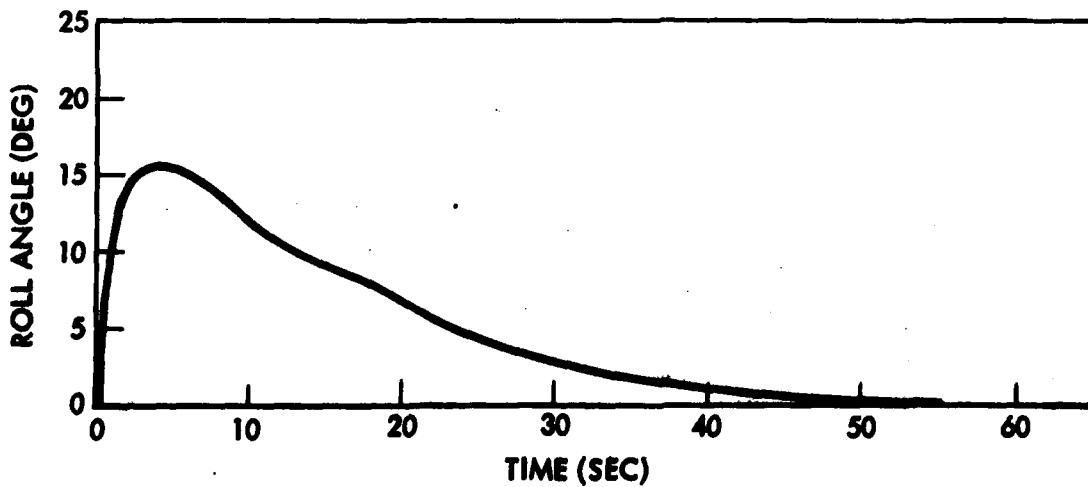
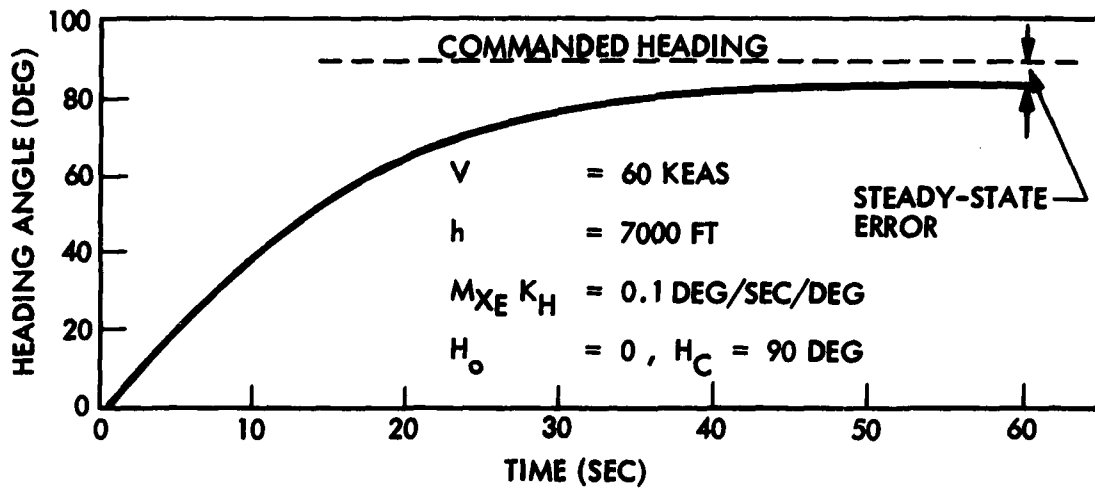


Figure 37. Aquila RPV Response to Heading Command ($H_C = 90 \text{ Deg}$)

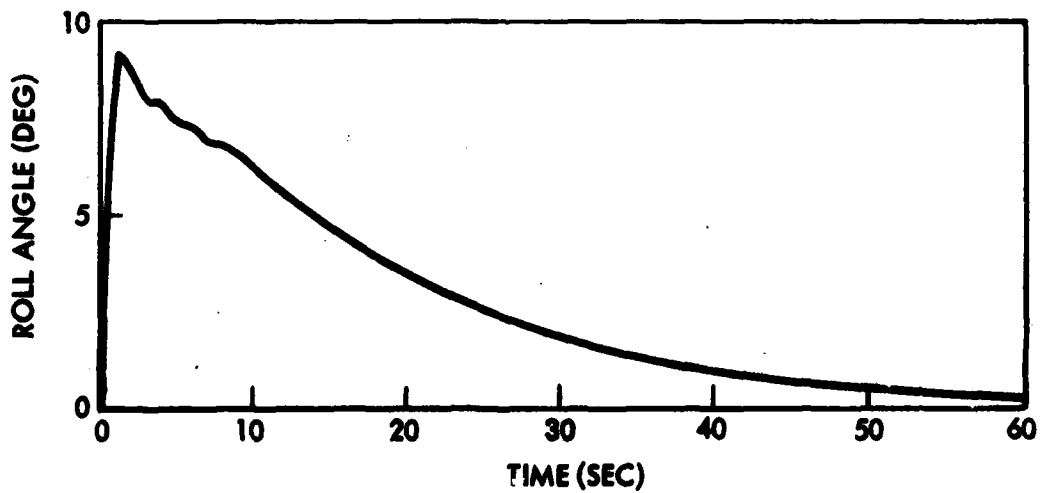
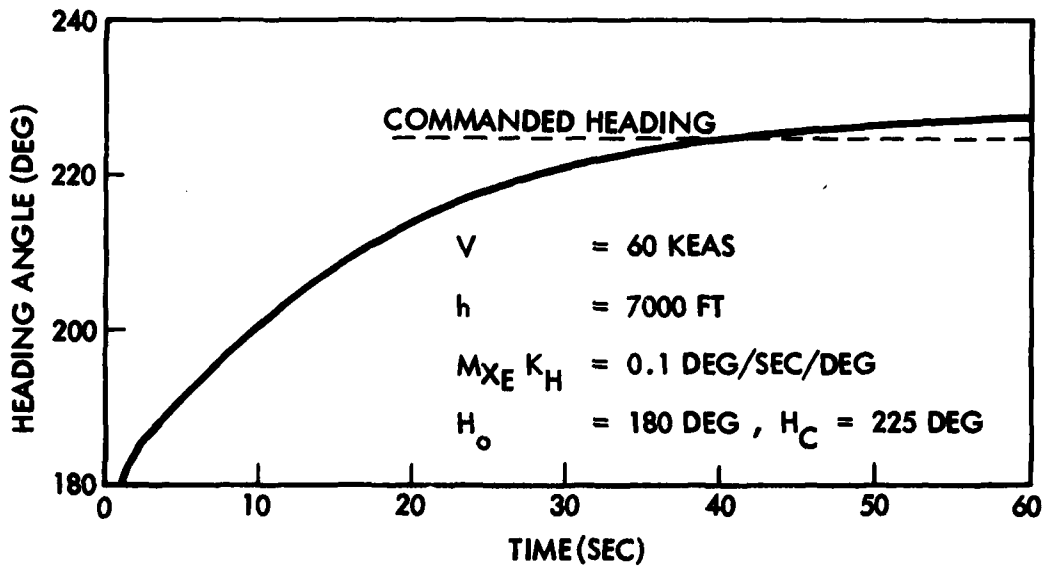


Figure 38. Aquila RPV Response to Heading Command ($H_C = 225 \text{ Deg}$)

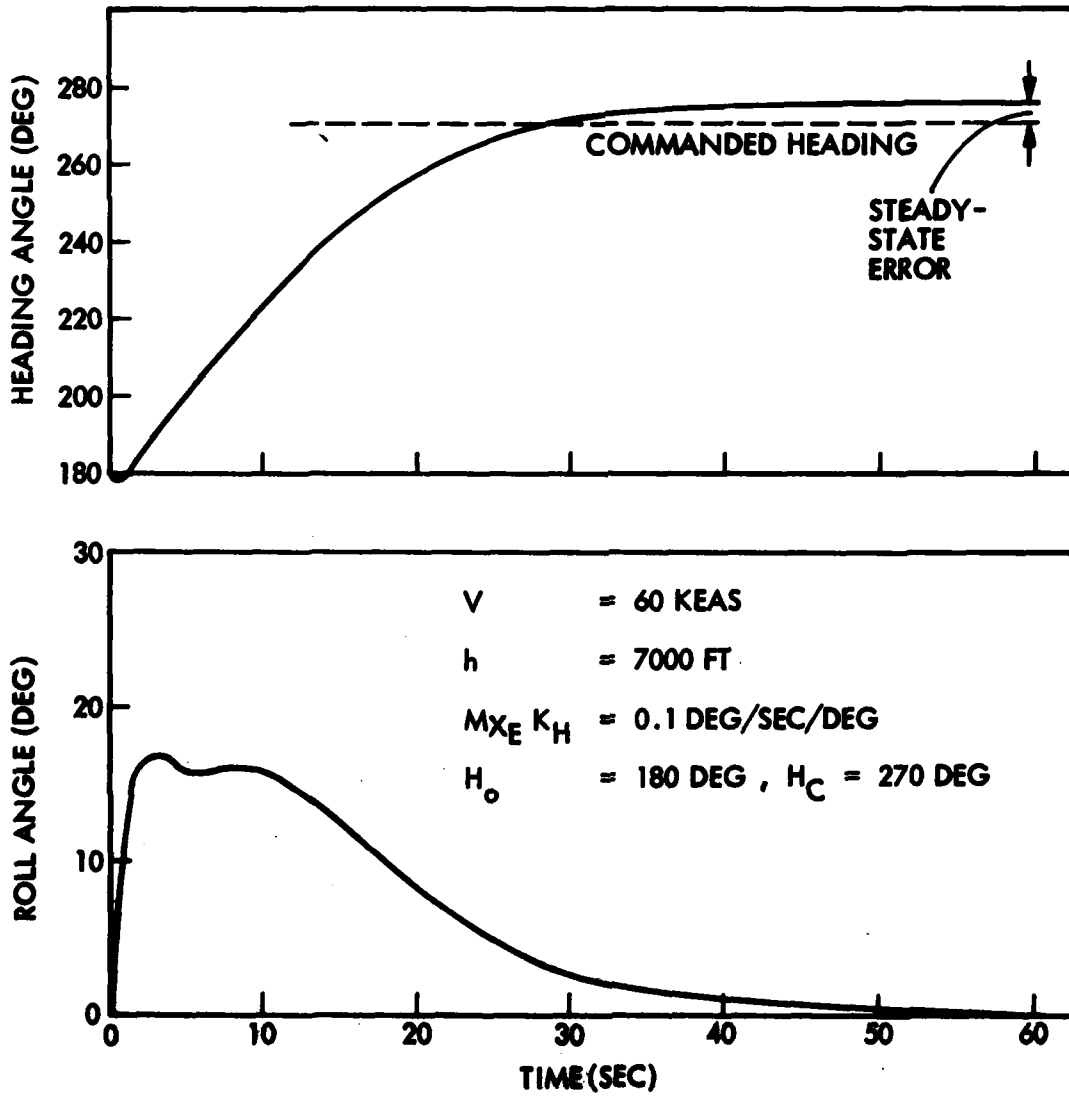


Figure 39. Aquila RPV Response to Heading Command ($H_C = 270$ Deg)

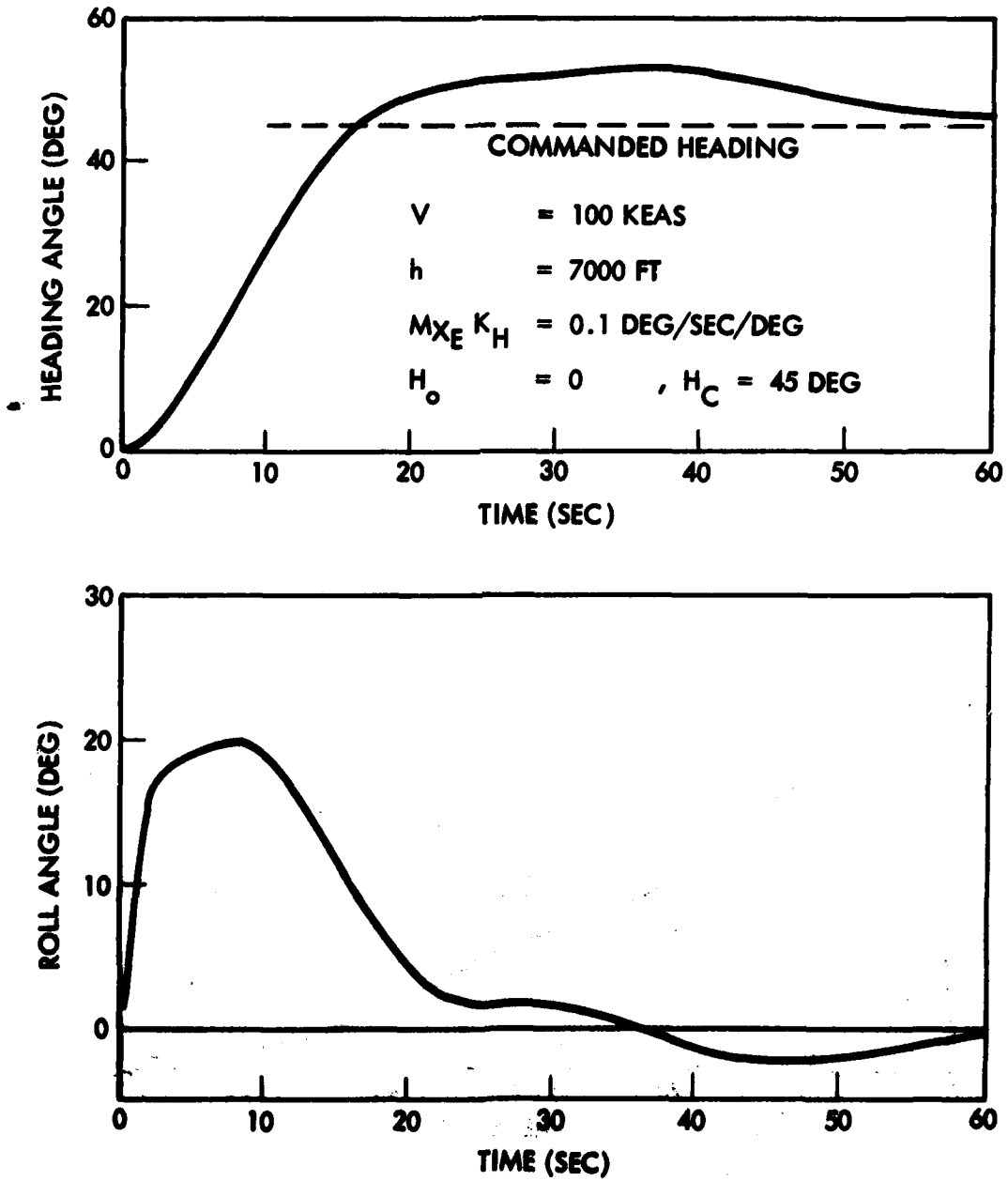
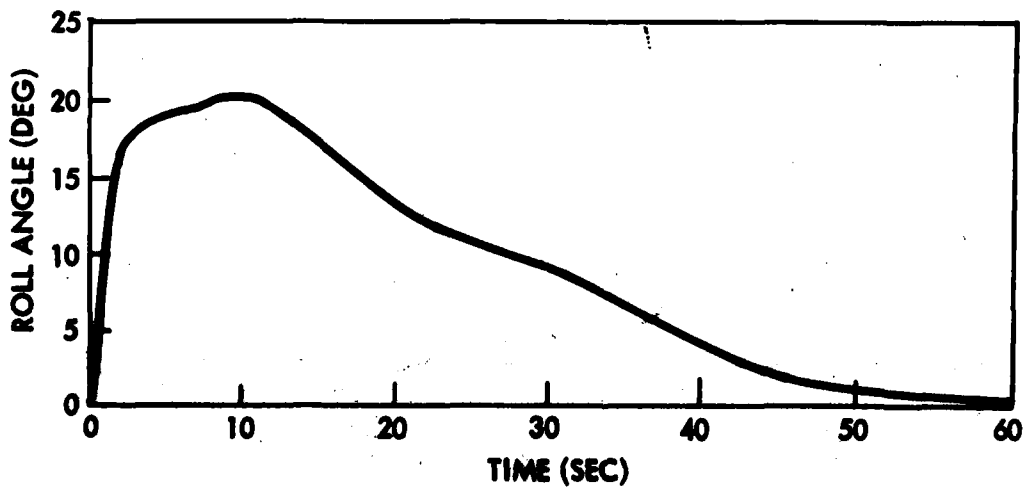
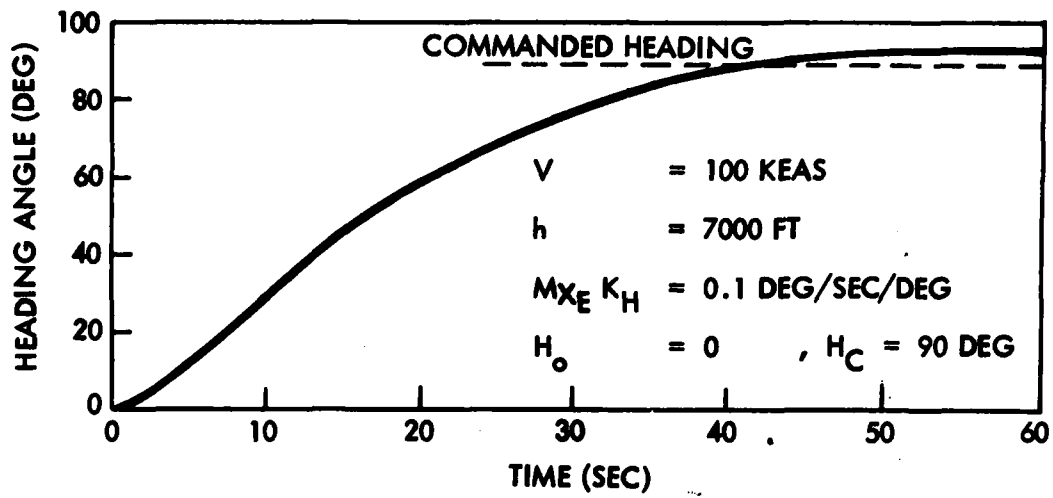


Figure 40. Aquila RPY Response to Heading Command
 ($V = 100$ KEAS, $H_C = 45$ Deg)



**Figure 41. Aquila RPV Response to Heading Command
($V = 100 \text{ KEAS}, H_C = 90 \text{ Deg}$)**

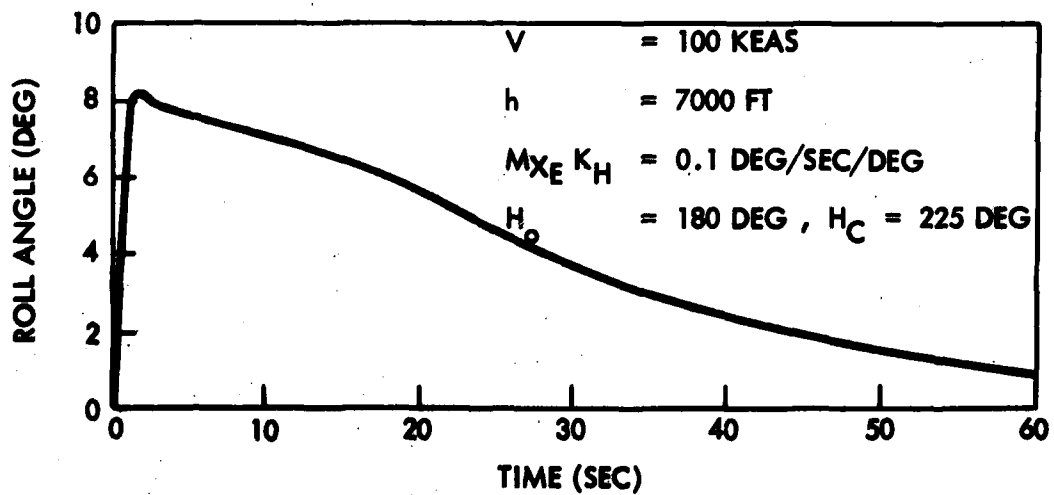
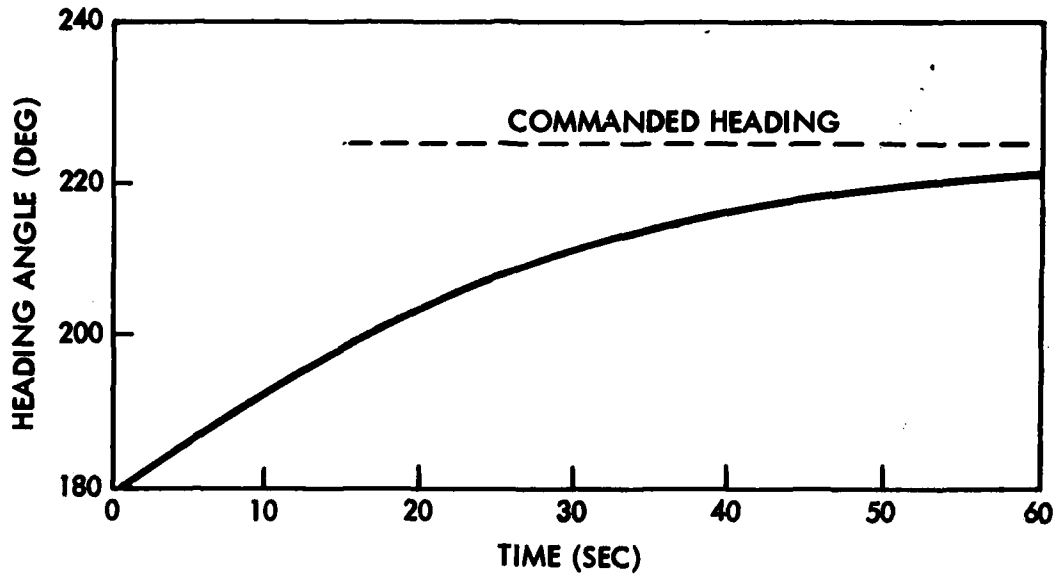


Figure 42. Aquila RPV Response to Heading Command
 ($V = 100 \text{ KEAS}, H_C = 225 \text{ Deg}$)

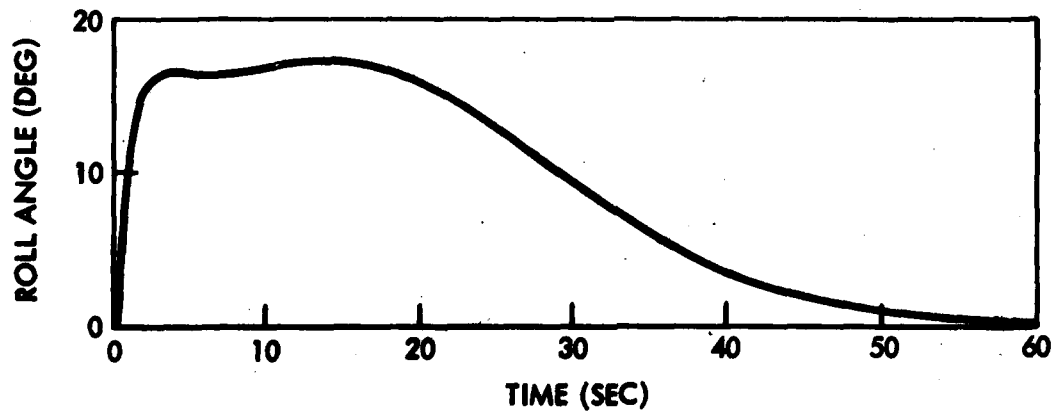
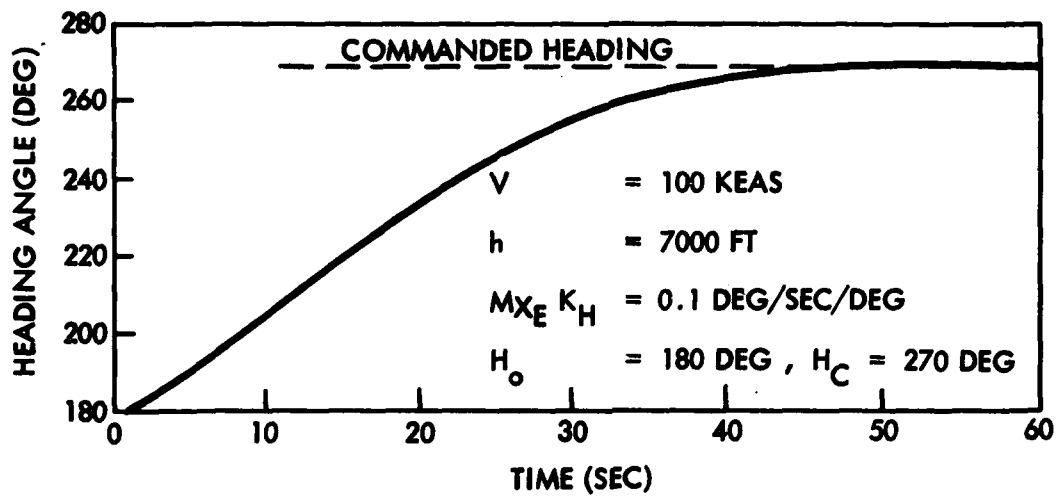


Figure 43. Aquila RPV Response to Heading Command
 ($V = 100 \text{ KEAS}$, $H_C = 270 \text{ Deg}$)

An additional error source is bias error of the roll-yaw rate gyro in the inner loop. A bias error of 0.5 deg/sec, for example, will produce a steady-state heading error of approximately 19 deg. Since this amount of heading error was considered to be intolerable, an integral gain was added to the outer loop to trim out the steady state error due to roll-yaw rate gyro bias error. The output of this contribution to the heading rate command was limited to ± 2 deg/sec to avoid large buildups and overshoots for a large turn angle command.

In the autopilot linear stability analyses, initial gains in the RPV-STD flight control system were established by performing linear closed-loop stability analyses of the airframe and associated avionics. Root locus and Bode plots of the various autopilot loops were constructed. The analyses showed the successive effects of closing the loops in the pitch and altitude autopilots. The aircraft speeds associated with the analyses were 120 KIAS and 48 KIAS, which adequately bracketed the capabilities of the RPV.

In preparation for the RPV-STD initial flight tests at Crows Landing, extensive 6-DOF simulation was performed to verify the validity of the airframe/flight control system and to ensure that the planned autopilot loop engagement sequence had no hidden pitfalls. Figures 44 and 45 show the responses of the open-loop airframe to elevon impulses in roll (δ_R) and pitch (δ_E), respectively. A lightly damped Dutch roll mode is seen in the response (S_g) of the roll-yaw rate gyro. Spiral divergence is evident from the slowly increasing roll angle (ϕ). In the longitudinal mode, a well damped short period mode is seen in response to the pitch disturbance. Figure 46 shows the response to a throttle servo impulse (δ_{TH}). The lightly damped phugoid mode is clearly evident in the altitude and velocity traces.

Figure 47 shows the differential elevon, roll angle, and yaw rate (body fixed) responses to a heading rate command 3 deg/sec after closing the inner loop of the heading autopilot. Pitch elevon and throttle servos are assumed fixed during this maneuver. Figure 48 shows the altitude and sideslip angle variations resulting from the maneuver.

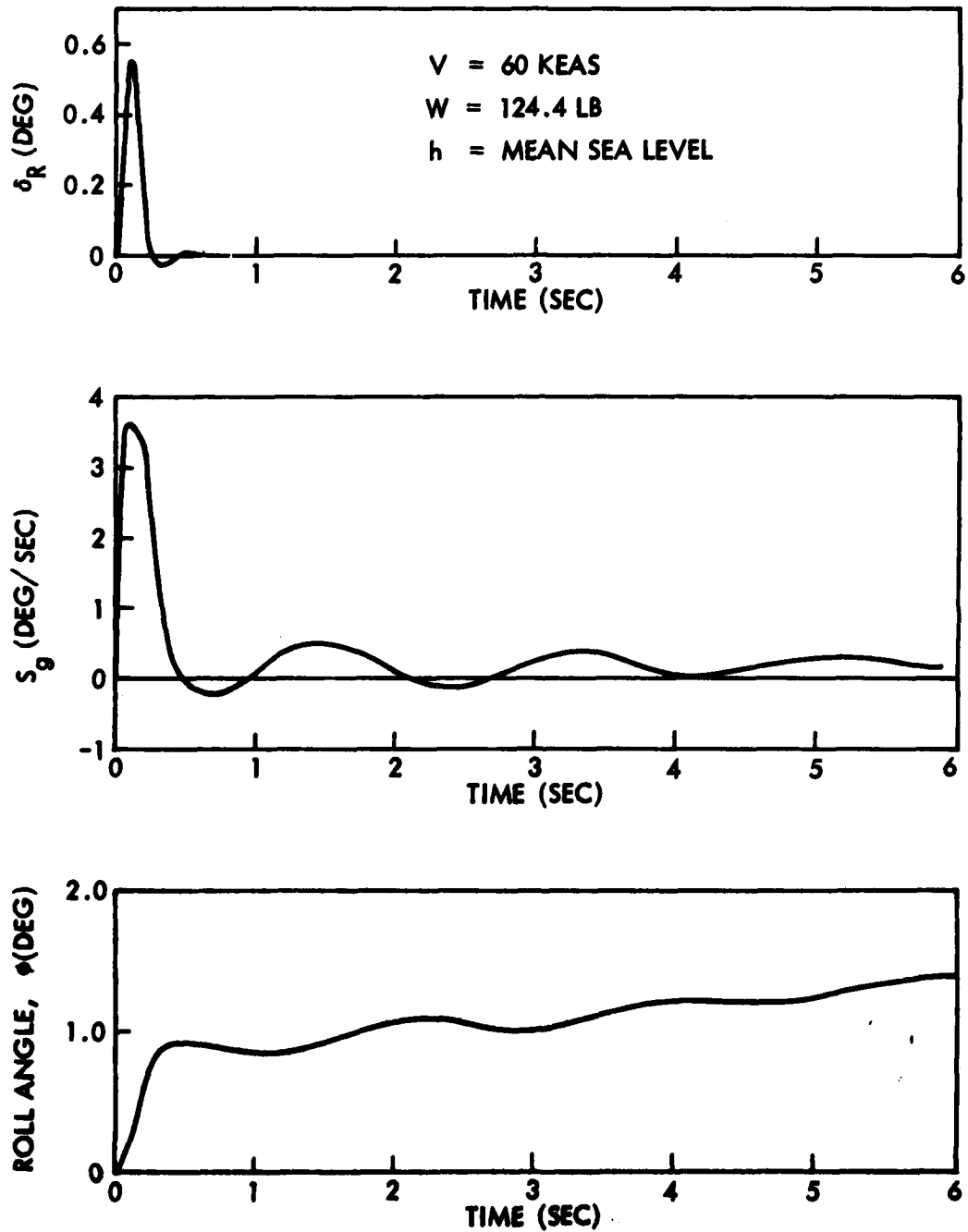


Figure 44. Aquila Open-Loop Response to Roll (δ_R) Impulse

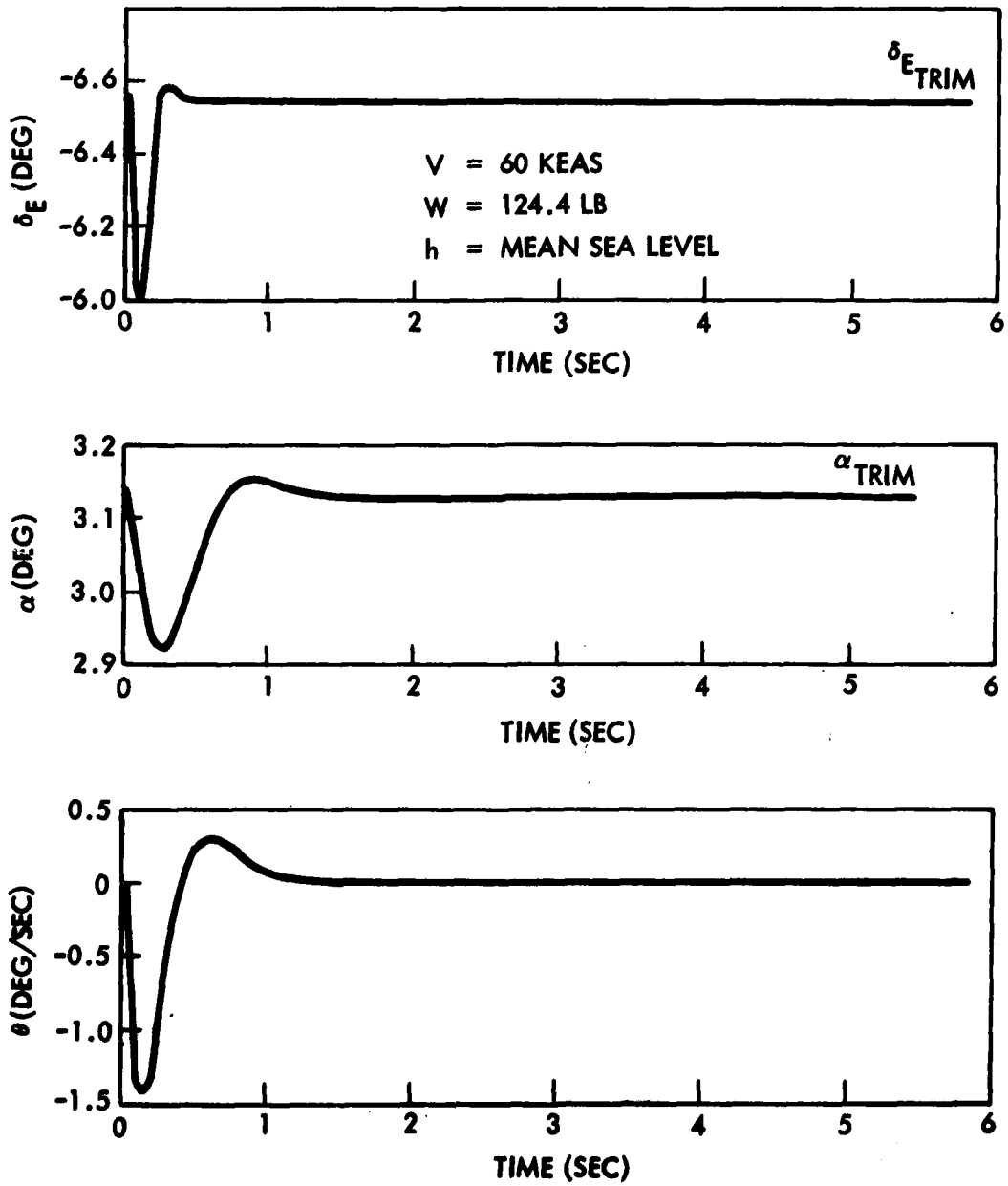


Figure 45. Aquila Open-Loop Response to Pitch (δ_E) Impulse

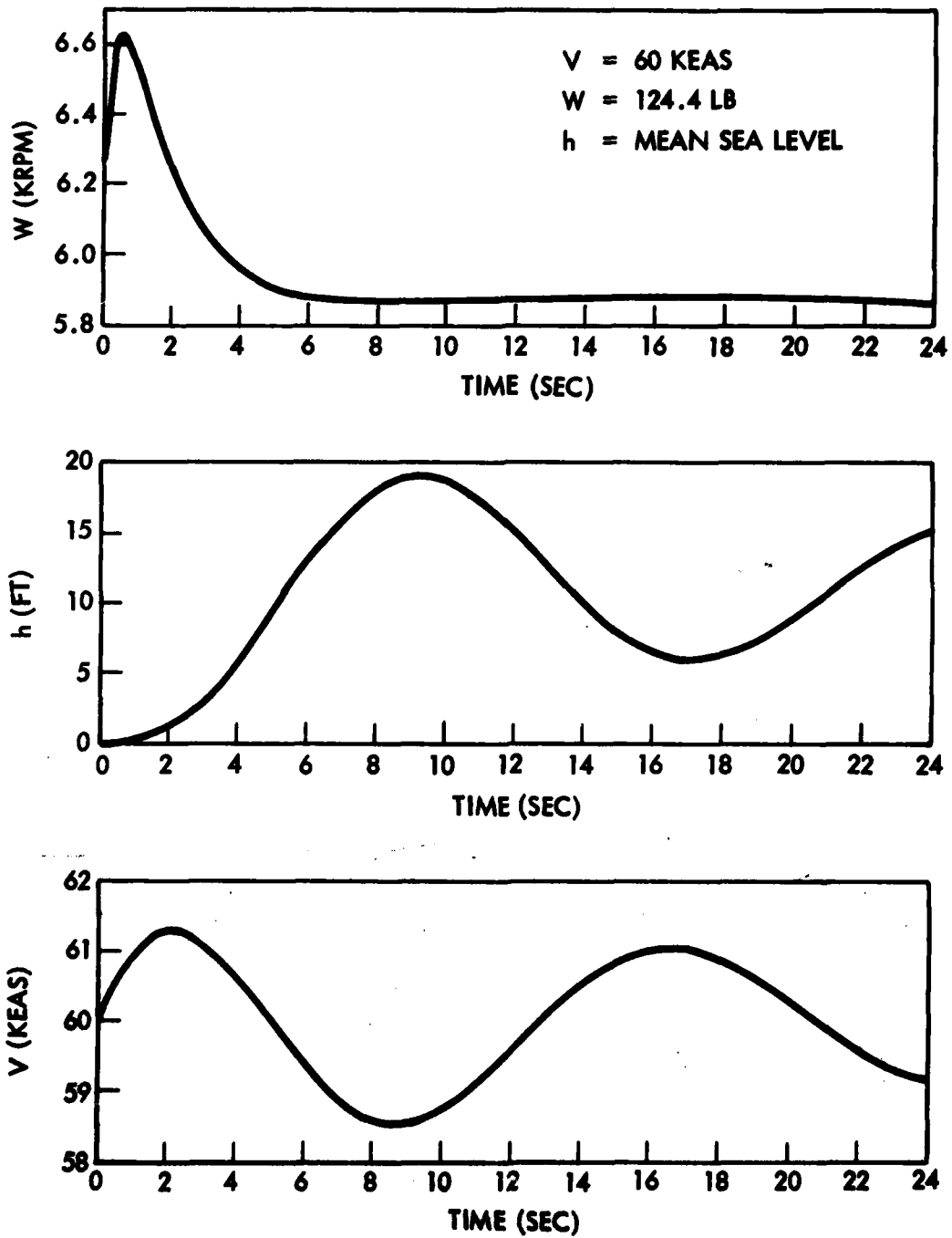


Figure 46. Aquila Open-Loop Response to Throttle (δ_{TH}) Impulse

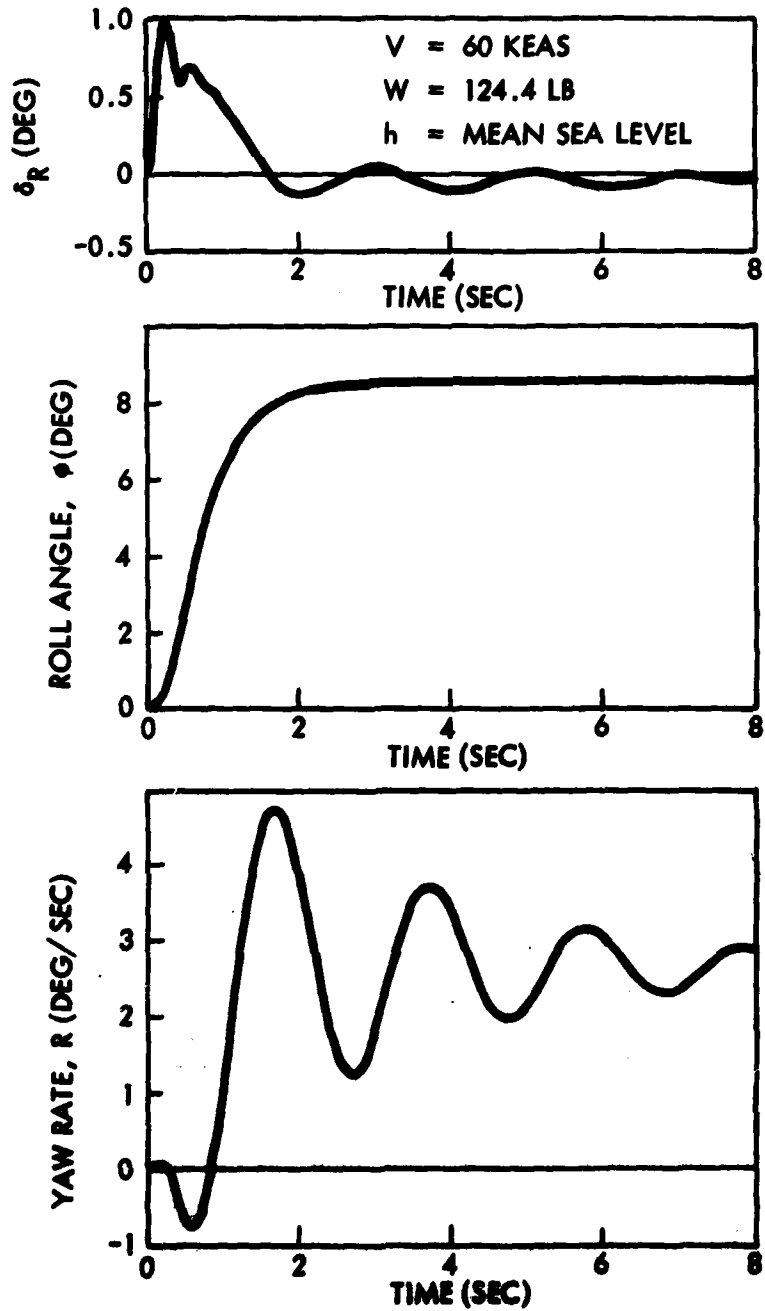


Figure 47. Aquila Response to $\dot{H}_C = 3\text{-Deg/Sec}$ Heading Loop Operational Manual Elevon and Throttle - R, ϕ , δ_R

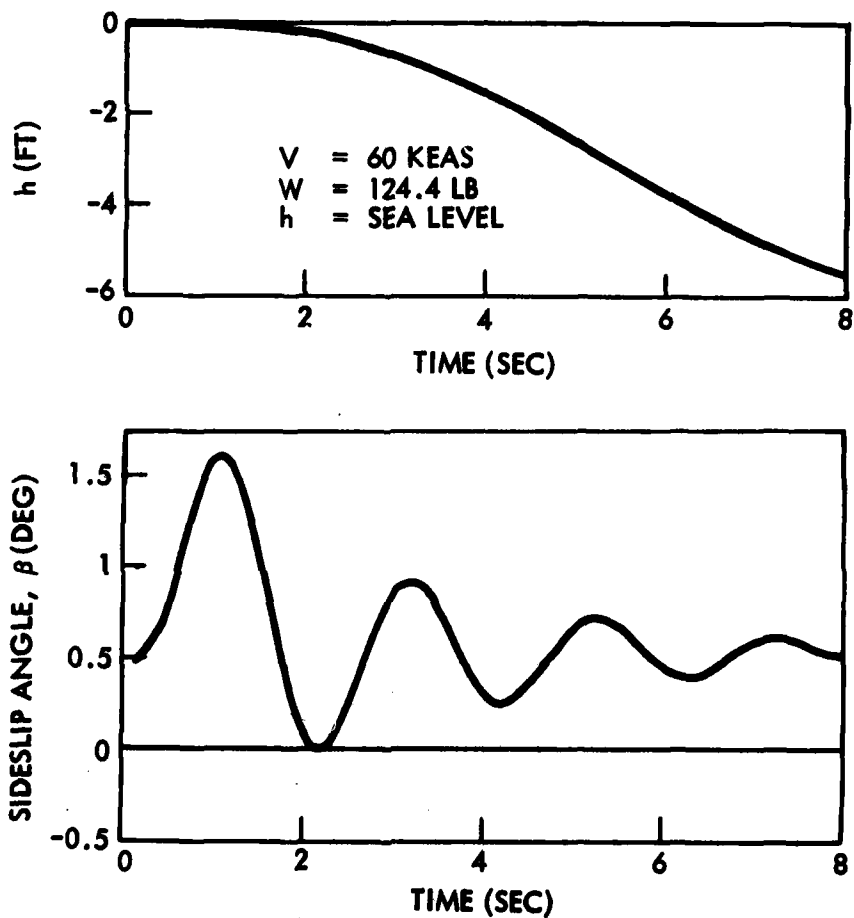


Figure 48. Aquila Response to $\dot{H}_C = 3\text{-Deg/Sec}$ Heading Loop Operational: Manual Elevon and Throttle - β , h

The next step in the autopilot engagement sequence was the closing of the short-period damper loop. Figure 49 shows the response to an initial elevon disturbance with the damper loop closed. The ensuing angle-of-attack history shows that the short-period mode damps out almost immediately after the initial excitation.

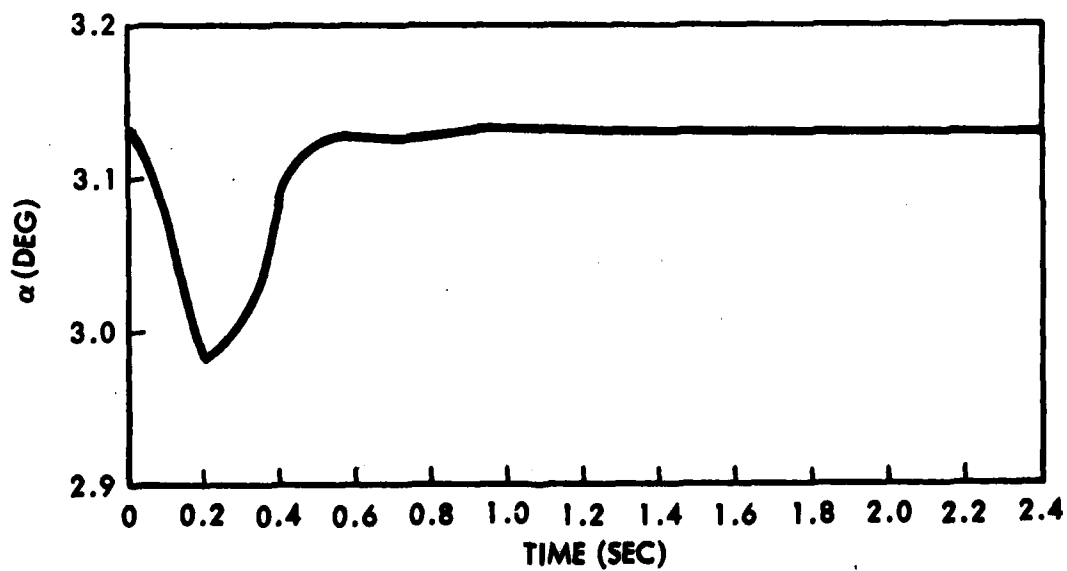
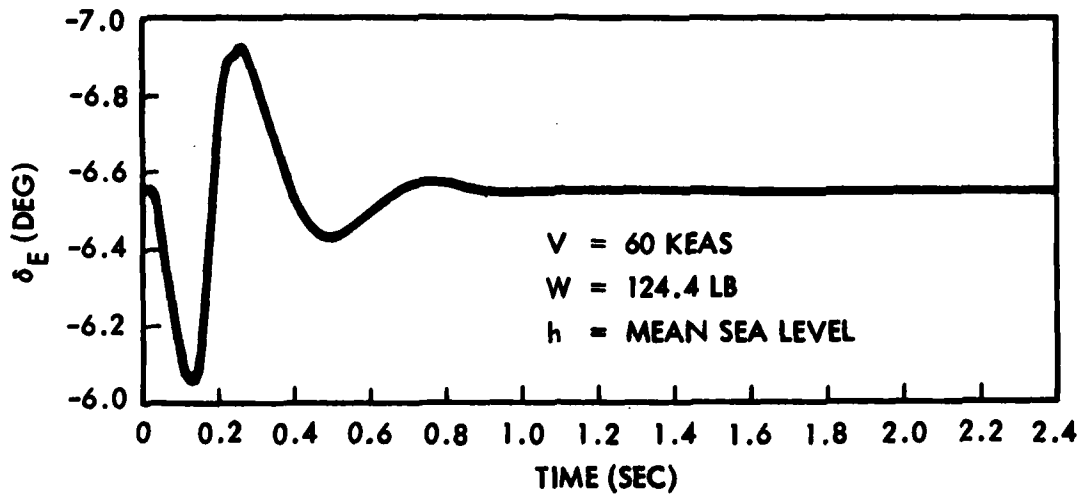


Figure 49. Aquila Response to Pitch (δ_E) Impulse, Manual Elevon and Throttle Short-Period Damper Engaged

The engagement of the phugoid damper – the next step in the sequence – was expected to excite phugoid motion in the aircraft in the process of closing the loop, since the phugoid damper had a very low bandwidth and was expected to have some output when the switch engaging this loop was closed. This output could be due to the disturbance associated with rolling out of a turn, which would induce a transient in the output of the damper, the residue of which would cause a step change in the elevon command when the switch was closed. Figure 50 shows the effect of engaging the loop for an initial phugoid damper output of 5 ft/sec. The resulting dive and recovery occurs with the throttle servo fixed and no speed error signal to the elevon.

Figure 51 shows the response to be expected to a 3-deg/sec turn command with the short period and phugoid dampers engaged. A much greater altitude loss occurs than in the case shown earlier with these damper loops open with the same turn rate command. This is because the accelerometer begins to pull more load in the turn, resulting in significant phugoid damper output and subsequently a positive (trailing edge downward) command to the elevon.

Figure 52 shows the transient to be expected from engagement of the airspeed loop, assuming an initial RPV airspeed of 60 KEAS and a commanded airspeed of 57.5 knots at the time of loop closure. Another simulation – not shown here – showed that for a 5-knot error between commanded and indicated airspeed, a change in altitude of approximately 25 ft might result.

Next, with the airspeed loop engaged, a 3-deg/sec turn was commanded. The transient responses in roll angle, airspeed, and altitude to be expected from this command are shown in Figure 53. Much smaller speed buildups and altitude losses are noted in this case, since the speed error now introduces a negative command to the elevon, counteracting the spurious command from the phugoid damper.

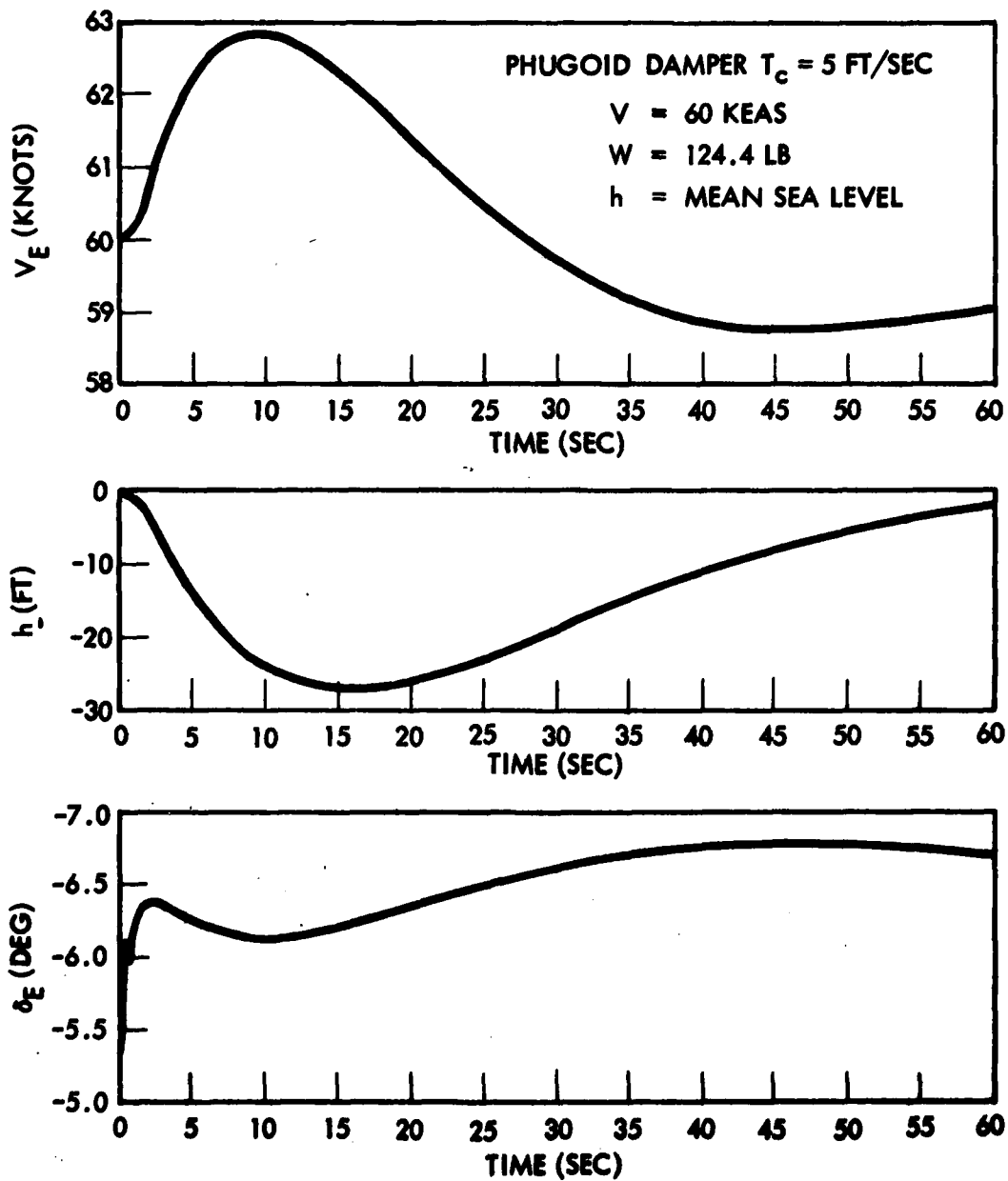


Figure 50. Aquila Response to Phugoid Damper Engagement, Manual Elevon and Throttle Short-Period Damper Engaged

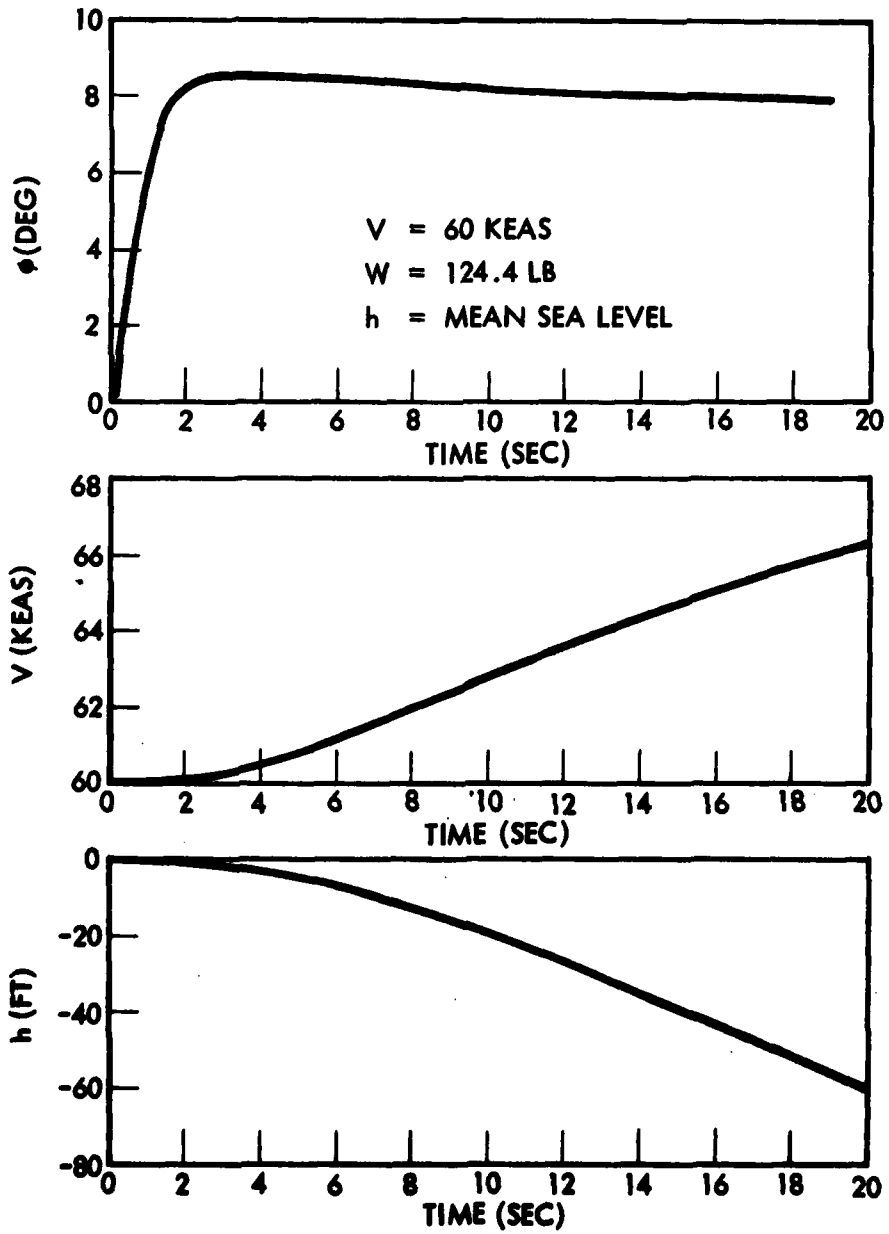


Figure 51. Aquila Response to $\dot{\alpha}_C = 3$ Deg/Sec Phugoid and Short-Period Dampers Engaged and Trimmed, Manual Elevon and Throttle

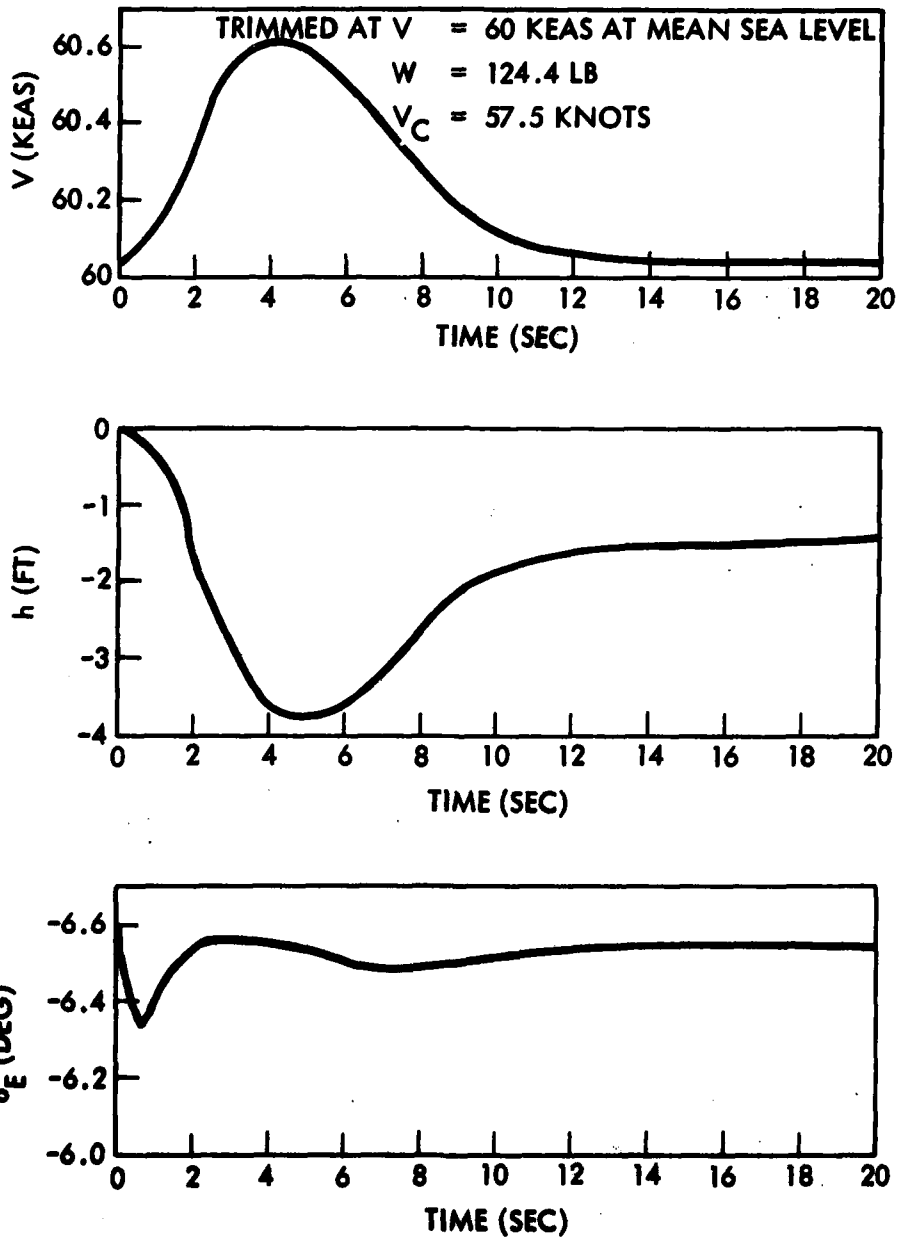


Figure 52. Aquila Response to Engagement of A/S Loop, Phugoid and Short-Period Dampers Engaged, Manual Throttle

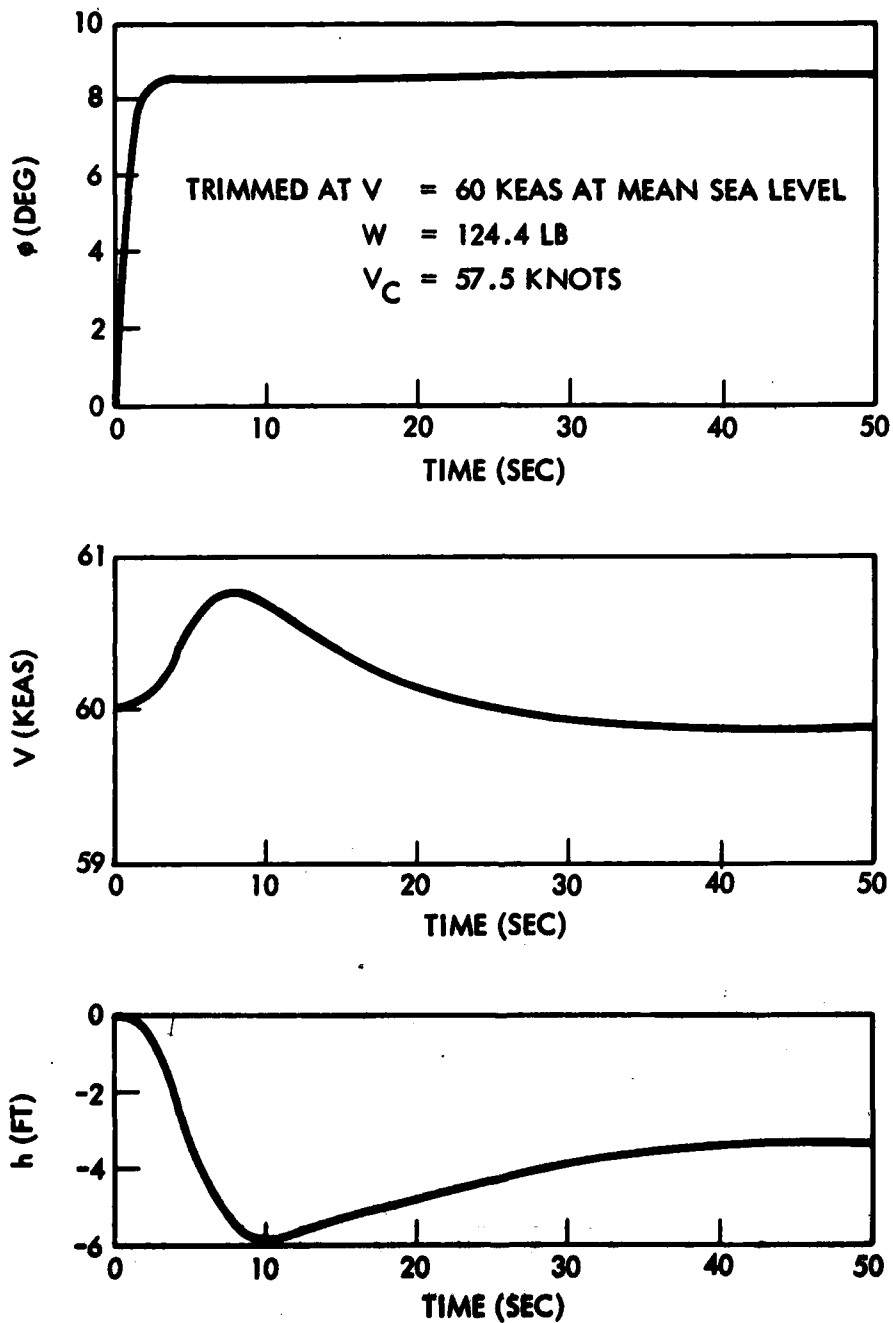


Figure 53. Aquila Response to $\dot{\theta}_C = 3$ Deg/Sec, Phugoid and Short-Period Dampers Engaged Manual Throttle, A/S Loop Engaged

Figures 54 and 55 show the responses to full and quarter throttle commands with the phugoid and short period dampers engaged and the airspeed control loop closed. As expected, tight airspeed control is maintained, while the RPV adjusts to a climb or descent rate compatible with the throttle setting.

Finally, the response of key parameters to engagement of the altitude loop is shown in Figure 56, based on an assumed altitude error of 100 ft at the instant of closure. The plots show that the vehicle climbs to the required altitude and levels out with very little fluctuation in airspeed. Engine rpm peaks quickly and gradually decays to its trimmed condition.

3.4.4.2 Guidance Mode Evolution. The RPV-STD system was designed with six guidance modes from which any required mission could be constructed.

These modes are as follows:

- Manual
- Waypoint
- Loiter
- Spiral Search
- Dead Reckoning
- Final Approach

Although these modes have retained their same basic character throughout the program, some changes have been incorporated which have resulted in needed improvement in performance. These changes are discussed in the following subsections. A seventh section is included to discuss the RPV-STD launch. Although not a separate guidance mode, this phase deserves special attention because of the increased sensitivity of performance to mission success.

Manual Mode. During the manual operating mode, the RPV is in a semi-automatic control mode. Airspeed and altitude are controlled by thumbwheels on the manual flight control panel. Heading rate is controlled by a rate command knob, which allows up to ± 6 deg/sec turn rate commands, and a manual

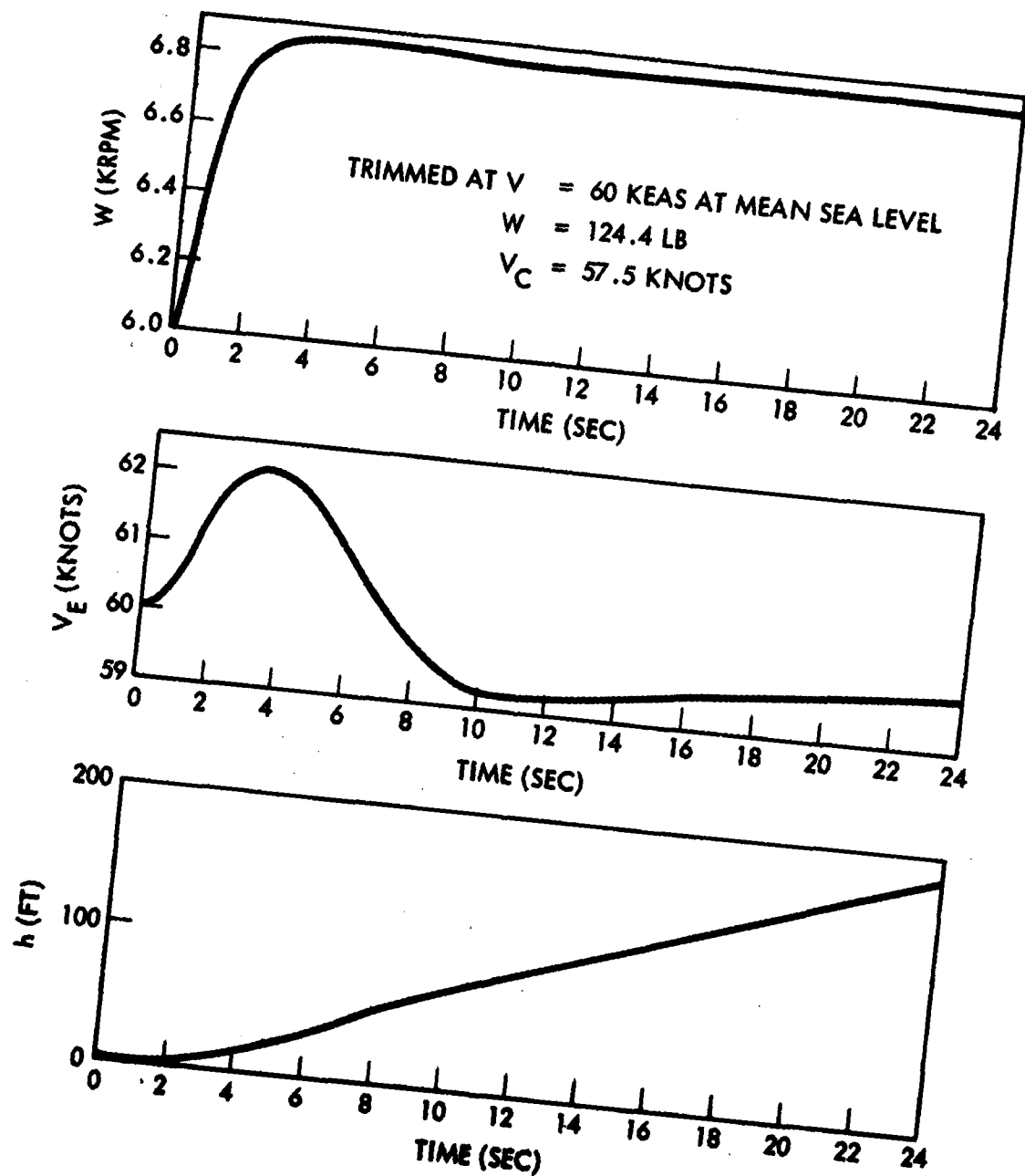


Figure 54. Aquila Response to Full Throttle, Phugoid and Short-Period Dampers Engaged, A/S Loop Engaged

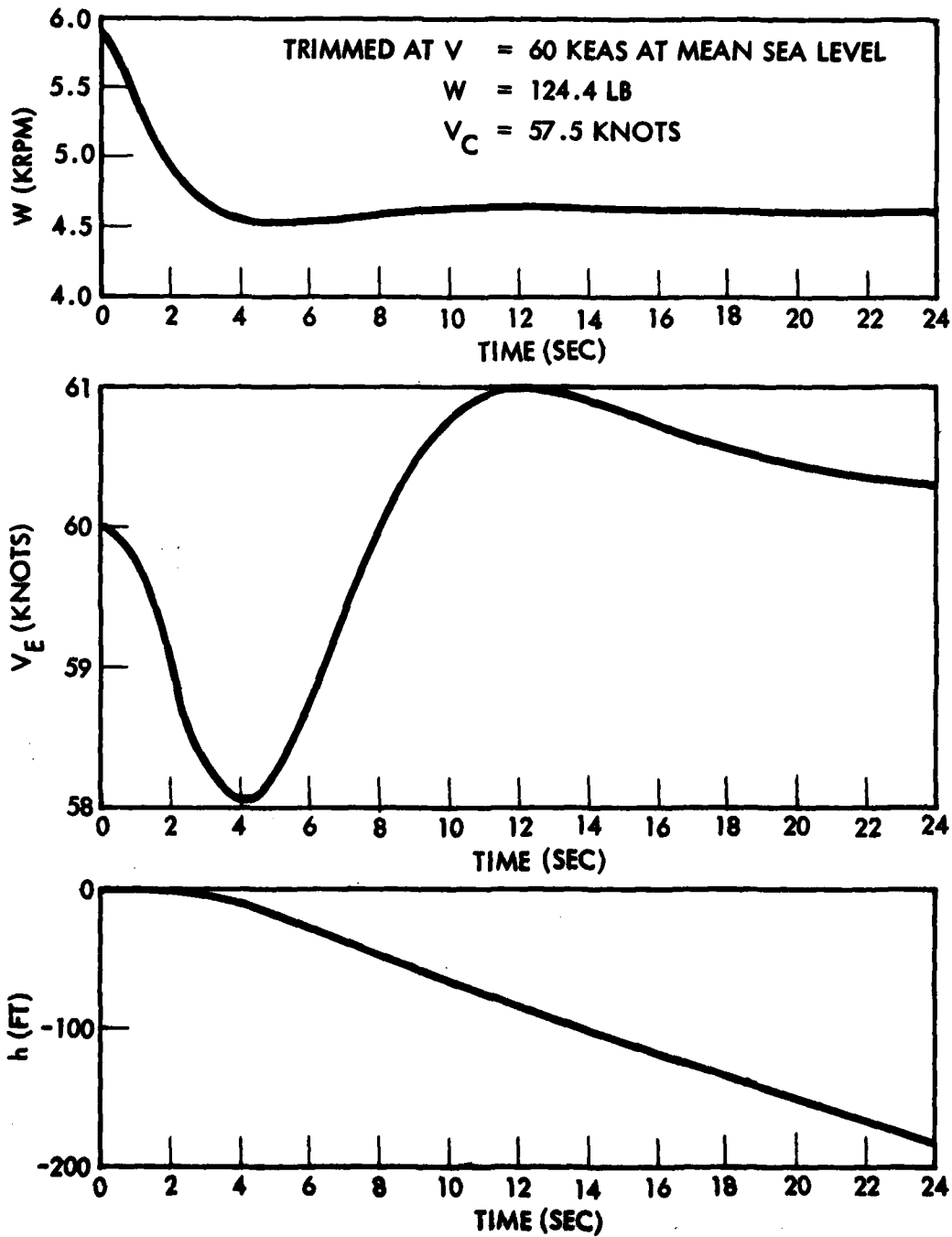


Figure 55. Aquila Response to 1/4 Throttle, Phugoid and Short-Period Dampers Engaged, A/S Loop Engaged

$\Delta h_c = 100$ FT
A/S LOOP ENGAGED
TRIMMED AT $V = 60$ KEAS AT MEAN SEA LEVEL
 $W = 124.4$ LB
 $V_c = 51.5$ KNOTS

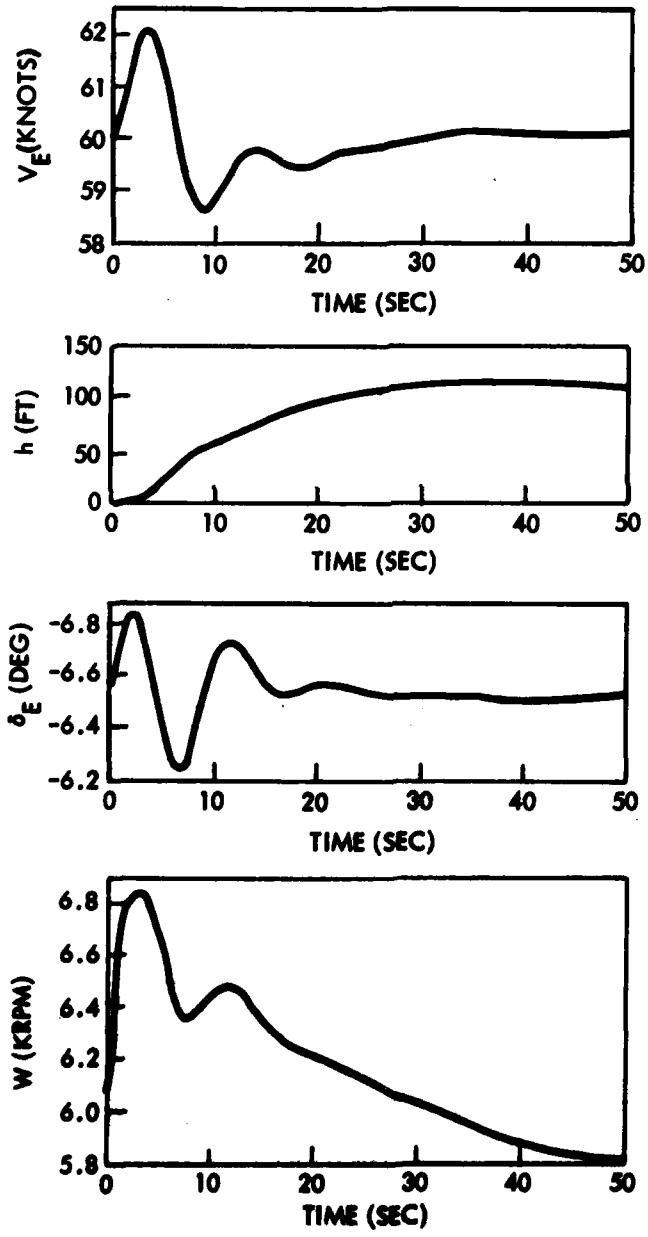


Figure 56. Aquila Response to Engagement of Altitude Loop

trim knob, which is used primarily for trimming out bias errors originating in the roll-yaw rate gyro.

Waypoints. Waypoints are locations defined by the universal transverse mercator (UTM) coordinate system. Each waypoint has a five-digit northing coordinate and a five-digit easting coordinate. In addition, each waypoint is assigned an altitude and airspeed that the aircraft will be commanded while flying from the first waypoint to the second waypoint. Altitude and airspeed control are achieved in exactly the same way as during the manual mode. However, heading rate commands are variable and computed in the GCS computer according to the following guidance law:

$$-\dot{H}_C = \left\{ \left[\left(K_D D \right)_1 \text{ LIM} + \left(K_{D_R} \dot{D} \right)_2 \text{ LIM} \right]_3 \text{ LIM} + \left[\int_{t_1}^t \left(K_{D_I} D \right)_4 \text{ LIM} dt + \dot{H}_{C_{BIAS}} \right]_5 \text{ LIM} \right\}_6 \quad (1)$$

where

- \dot{H}_C = heading rate command
- D = lateral deviation from desired ground track (straight line between WP 1 and WP 2)
- \dot{D} = time rate of change of lateral deviation
- K_D = proportional gain
- K_{D_R} = rate gain
- K_{D_I} = integral gain
- $\dot{H}_{C_{BIAS}}$ = starting value for integral term

The value of D in the guidance equation is based on RPV coordinates computed from smoothed values of RPV range and azimuth relative to the tracker.

The original waypoint guidance equation had only a proportional and a rate term. The integral term was added early in the program to eliminate standoff errors resulting from bias errors in the roll-yaw rate gyro. This term introduces an additional characteristic motion in the waypoint guidance mode, characterized by a slow exponential decay. A magnitude of gain small enough that the stability of the primary waypoint motion was only minimally affected was chosen.

Early flight tests revealed the existence of a limit cycle instability in the waypoint mode, which occurred at long ranges when the RPV flight path was nearly in line with the range vector. This instability took the form of a periodic roll oscillation at a period ranging from 2 to 4 sec. The amplitude of the oscillations was associated with peak heading rate commands of ± 6 deg/sec corresponding to the limiting values in the waypoint guidance algorithm. Analysis of the flight data showed that the observed heading rate commands could not possibly have caused flight path deviations of sufficiently large magnitude to have generated those commands. This reasoning led to the conclusion that the RPV position computations must be in error. Correlation of roll angle (from video tape playbacks) with tracker azimuth angle showed that an azimuth error was induced by aircraft roll. This error was attributed to antenna polarization effects and was later confirmed by field tests. The effect on the system dynamics is obviously enhanced at long ranges (where a given azimuth error produces a larger RPV position error) and for RPV motion along the range vector (a condition in which the azimuth error sensitivity is most pronounced).

Root locus analyses and point mass guidance simulations verified that the instability was caused by roll-tracker coupling. Efforts to alleviate this instability constituted a significant engineering effort on the RPV-STD program. The following changes were incorporated into the waypoint guidance equation to eliminate this instability:

- Reduce all waypoint guidance gains
- Smooth range and azimuth data over 0.5 sec (previously 0.8 sec)

- Change command update interval to 0.5 sec (had been 1 sec)
- Compute \dot{D} from digital algorithm to simulate
 $\dot{D} = [5(1+0.45)]/[(1+5)^2]$ [had been computed from second backward difference formula, i. e., $\dot{D}_1 = (D_1 - D_{1-2})/2$]
- Limit allowable rate of change of \dot{H}_C

All of the above changes had a beneficial effect on the stability of the system. However, the last of the listed changes was the most effective, although it was discovered that if the limit imposed were too small, it could introduce enough lag into the primary guidance mode that a "snaking" motion could occur, which would build up into a large limit cycle motion about the waypoint line. The limit finally incorporated into the guidance equation ($\dot{H}_{C\text{LIM}} = 1.2 \text{ deg/sec}^2$) was set large enough to minimize the probability of this occurrence and small enough to provide adequate reduction of the amplitude of the roll-tracker coupling oscillations.

Loiter. Any time the loiter button is activated and waypoint registers 70 and 71 are all zeros, the RPV must enter the programmed loiter pattern using the last calculated RPV position coordinates as the loiter point. Airspeed and altitude commands in the loiter mode will be the same as commanded prior to loiter activation.

The original guidance equation implemented for the loiter mode was:

$$\dot{H}_C = (K_L \cdot L + K_L' \cdot \dot{L})_{\text{LIM}} \quad (2)$$

where

- \dot{L} = radius from loiter point to RPV
- L = rate of change of L
- K_L = proportional gain
- K_L' = rate gain

The loiter mode has worked well in RPV-STD flight tests. It has at times exhibited the same roll-tracker coupling problems apparent in waypoint flight; however, the problem has not been as pronounced in loiter because of the absence of sustained flight in a direction parallel to the range vector. Point mass simulations of the RPV position following loiter mode guidance were run to evaluate the loiter mode guidance scheme (see Figure 57). Generally, the higher value of K_L was found to provide improved loiter performance in strong wind conditions, although at the expense of increased noise to the ele-
 von servos. The gain chosen was felt to provide adequate performance under windy conditions while maintaining the noise at an acceptable low level.

During the course of the RPV-STD program, an improvement in the loiter guidance equation was incorporated, represented by (signal limiters not shown)

$$\dot{H}_C = \dot{H}_{C_0} + K_L (L - L_0) + K_L \dot{L} + \int K_{L_1} (L - L_0) dt \quad (3)$$

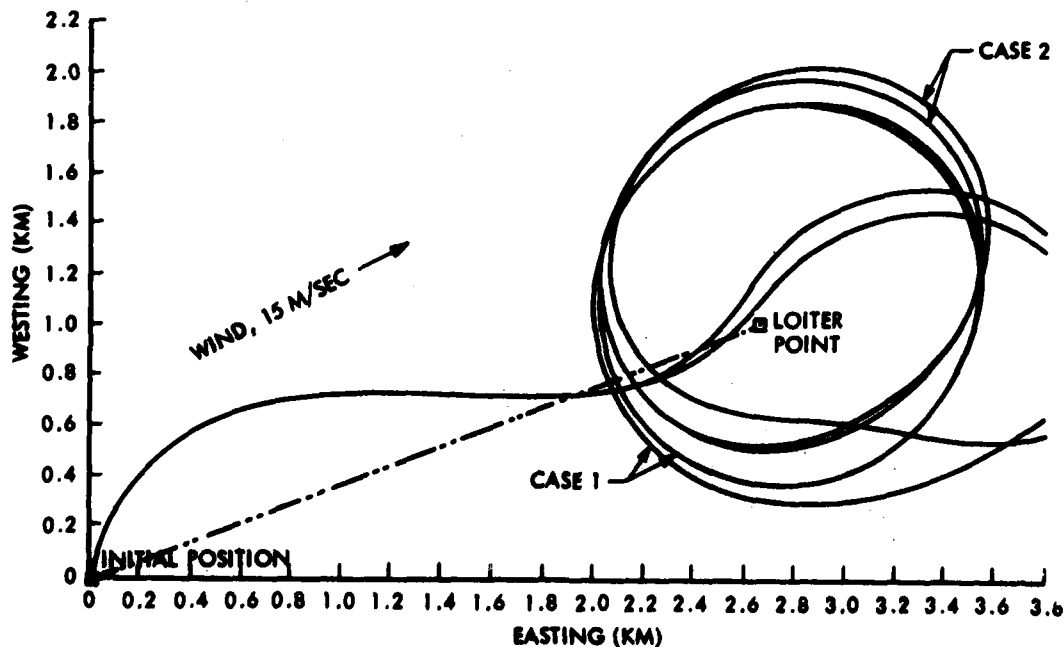


Figure 57. Loiter Guidance - Effect of Variation in K_L

where L_0 is the desired loiter radius and \dot{H}_{C_0} is determined as the value of the steady-state turn rate compatible with the selected value of L_0 and the RPV speed. This guidance law permits the selection of the loiter radius independently of the gain K_L .

Because of the similarity in the forms of the waypoint and loiter guidance equations, the guidance software was designed with many points of commonality in the computation of the heading rate commands for the two modes. Therefore, some changes in the loiter guidance equation mechanization were effected as byproducts of the changes to the waypoint guidance equations. Examples of such changes are:

- Increased update rate of guidance commands
- Digital algorithm used for rate computation
- Limit imposed on \dot{H}_C
- Gains reduced

All of these changes were discussed in the waypoint guidance section.

Spiral Search. If waypoint 60 airspeed is zero, a spiral search pattern will be flown about the present RPV position when the search command is given. The guidance equation for this mode is designed to produce a path which spirals outward from the RPV location at the time of initiation of the search mode.

The guidance equation for the spiral search mode is as follows:

$$\dot{H}_C = \left(\frac{K_L L}{T} + K_L \dot{L} \right)_{LIM} \quad (4)$$

where

- L = radial distance from point where search was initiated
- \dot{L} = rate of change of L
- T = time lapsed since search was initiated

K_L = proportional gain
 $K_{\dot{L}}$ = rate gain
 \dot{H}_{CLIM} = ± 6 deg/sec

The search mode has worked well from the beginning. No significant changes have occurred since its inception, except for certain changes incorporated in waypoint because of roll-tracker coupling problems and changes incorporated in search because of software commonality characteristics.

Dead Reckoning. The dead reckoning mode was designed to give the RPV the capability of self-guidance while out of contact with the data link. Commands to the flight control system are stored onboard the aircraft in the form of sin (magnetic heading), cos(magnetic heading), lag time, altitude, and airspeed. Three consecutive dead reckoning legs may be flown; therefore, three sets of stored data are required.

This is a basically simple guidance mode and has not undergone any significant changes during the development of the RPV-STD system. Any evolutionary development in this mode has taken place in the outer heading loop of the heading autopilot and was discussed earlier in this section.

As indicated in Section 4.4 of Volume III of this report, three dead reckoning legs were flown, and the command data link was reestablished. Analysis of the data indicated anomalies in positioning the legs and in reestablishment of the command link. Software and circuit changes to correct these anomalies were not accomplished in light of higher priority objectives. Consequently, this flight mode was not available for evaluation at the time of delivery to the Army.

Final Approach. The final approach mode is by far the most demanding of controlled airframe performance and has received a major share of attention in engineering design and development. Extensive analog and digital simulations were conducted.

The commands issued by the GCS during this mode are as follows:

$$-\dot{H}_C = \left\{ \left[\left(K_Y (d + d_b) \lambda_Y \right)_{LIM 1} + \left(K_{YR} (d + d_b) \dot{\lambda}_Y \right)_{LIM 2} \right]_{LIM 3} + \left[\int_{t_1}^t \left(K_{YI} (d + d_b) \lambda_Y \right)_{LIM 4} dt \right]_{LIM 5} + \dot{H}_{CBIAS} \right\}_{LIM 6} \quad (5)$$

$$\dot{Z}_C = \left[K_Z (d + d_b) \lambda_Z \right] \dot{Z}_{CLIM} \quad (6)$$

where

- \dot{H}_C = heading rate command
- d = range from ground video camera to RPV
- d_b = range bias (constant)
- K_Y = lateral proportional gain
- K_{YI} = lateral integral gain
- λ_Y = lateral angular deviation from vertical approach plane
- $\dot{\lambda}_Y$ = time rate of change of λ_Y
- LIM 1-6 = lateral guidance signal limiters
- \dot{Z}_C = vertical velocity command
- K_Z = vertical guidance gain
- λ_Z = vertical angular deviation from glideslope
- \dot{Z}_{CLIM} = limiting value of \dot{Z}_C

These commands are designed to keep the RPV on a 4-deg glide slope that intersects the vertical net in its approximate center. An operator-controlled cursor tracks the RPV via a ground-mounted television camera aligned with, and establishing, the glide slope. Offsets of the cursor from the center of the TV screen, λ_Z (vertical angular offset) and λ_Y (lateral angular offset, are used in the computation of the guidance commands presented above.

Control of the cursor is effected by an operator using a two-degree-of-freedom control lever that generates cursor rates $\dot{\lambda}_Y$ and $\dot{\lambda}_Z$ proportional to the lever displacement components in the two directions of freedom. The cursor offset amplitudes are obtained by integrating the cursor rates.

Early in the RPV-STD program, it was determined that the time lag of the operator in his efforts to track the RPV image with the cursor was a potential source of error. Both digital and analog computer programs were developed to simulate the recovery process. Human operator transfer functions were used in the digital program, which included the complete RPV non-linear equations of motion; simulated electronics; and analytical models of sensors, servos, and engine dynamics. The analog program used linearized perturbation equations for the RPV and engine dynamics, and simulated servos and avionics. Human operator control was incorporated by tying the simulated aircraft motion into an oscilloscope to simulate the RPV image on the TV screen and generating a cursor image driven by the operator's control action. Guidance commands were computed using analog elements with the cursor offsets and rates as inputs. The guidance commands were tied into the RPV dynamic simulation to complete the loop. These simulations were later complemented by an analog simulation (Reference 4), which allowed improvements in the RPV dynamic simulation and tied in the actual avionics and GCS software to the simulation. These simulations provided much insight, which contributed greatly to the success of the recovery operation.

The following brief summary illustrates the changes incorporated during the course of the program:

- Range biasing in the guidance equations allowed the recovery gains to be tightened as the RPV approached the recovery net.
- An integral term in the lateral guidance equation permitted washout of lateral offset error due to incomplete gyro bias trim.
- Guidance gains were adjusted for optimum recovery based on actual operator experience in simulated recoveries.

(4) Lockheed Missiles & Space Company, Inc., Aquila RPV System Test Report, CDRL AOOD, System Simulation, LMSC-L028081, Part 2, Sunnyvale, Calif., 14 Feb 1977

- Electronic cursor gains were adjusted to optimize operator performance in controlling the cursor to follow the RPV image.

A significant source of error associated with the RPV recovery system is caused by the transient induced in the accelerometer lead filter when the RPV undergoes the transition from straight-and-level flight to a 4-deg glide slope. If the output of the filter just before transition is zero, the output immediately after would be (assuming a dirac delta transition) $V_{\text{TRUE}} \sin 4^\circ$. This effective initial error in \dot{Z} (the vertical velocity normal to the glide slope) would decay gradually during the approach and would result in a gradually decreasing standoff error that is proportional to the gain in the vertical guidance equation. The exponential rate at which this standoff error changes is a function of the time constant τ_{A_3} in the filter. The formula for this standoff error (for an ideal transaction) can be shown to be approximated by

$$\epsilon_Z = \frac{V_o \sin 4^\circ}{2 K_Z} \left(1 - \frac{t}{\tau_{A_3}} \right) e^{-t/\tau_{A_3}} \quad (7)$$

The value originally set for τ_{A_3} was 15 sec, which represented a filter identical to that of the phugoid damper. This allowed a dual purpose for the filter during approach and other modes. However, since this yielded an unacceptably large standoff error at recovery, it was necessary to build a separate filter for the accelerometer signal during approach. Recovery simulations indicated that $\tau_{A_3} = 5$ sec would provide good control performance while reducing the transition standoff error to an acceptable level.

Results of a typical recovery simulation are shown in the plots of Figure 58. These curves show the vertical error from the glide slope, assuming no initial displacement error. The resulting transients are caused by overshoot as the RPV crosses the glide slope. A slight velocity buildup occurs as the RPV pitches over and starts its descent. This excess velocity decreases again as

NO DRAG BRAKE
 $\tau_{A3} = 5 \text{ SEC}$
 $K_{\lambda Z} = 0.75 \text{ (FT/SEC)/FT}$
 $\dot{z}_C = 10 \text{ FT/SEC}$

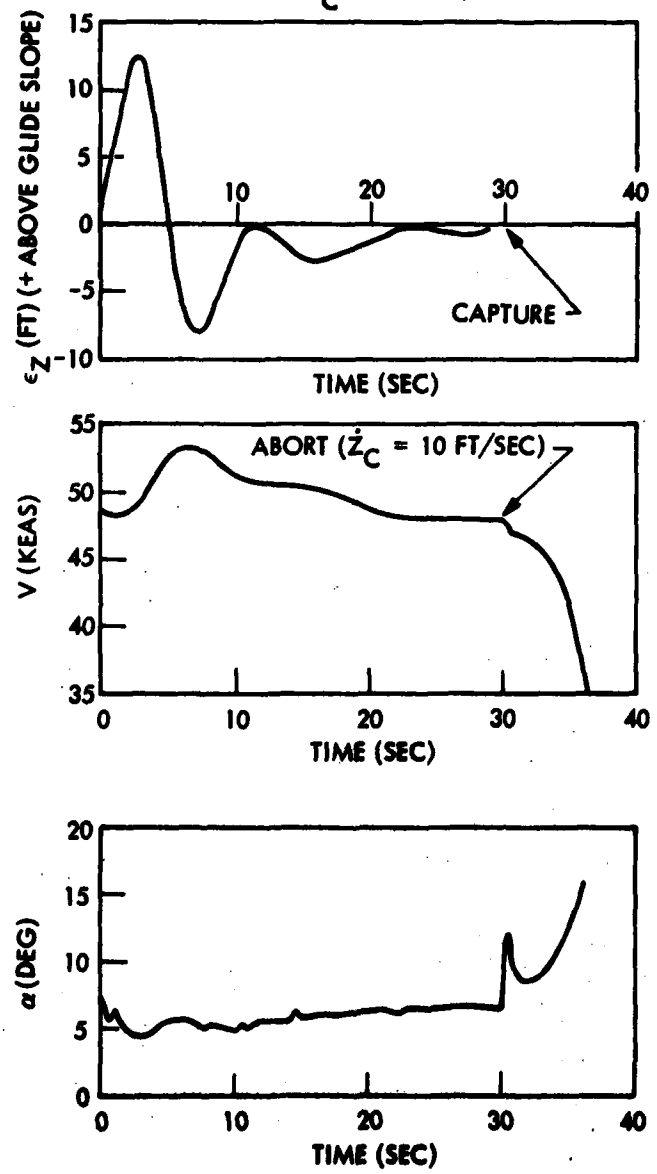


Figure 58. Aquila Approach Simulation

the engine backs off in response to the negative speed error signal. When the aircraft reaches the recovery net, the simulation shows that the airspeed has dropped back to the desired approach speed (≈ 48 KEAS). The simulation assumes an abort command of $\dot{Z}_C = 10$ ft/sec initiated just prior to recovery. The simulation disclosed the danger of such a design, since approximately 6 sec after abort initiation the airspeed has dropped back to 35 KEAS, and the aircraft is dangerously close to a stall condition. This abort concept was abandoned because of the stall danger. Present abort provisions consist of a transfer from approach guidance to Waypoint guidance. Abort in the current version must be triggered earlier in the approach phase than the original concept required.

The effects of sharp-edged gusts on miss distance are illustrated in Figures 59 and 60, which show the vertical and lateral errors caused by a 15-knot step wind initiated at varying distances before recovery. A headwind was used to excite the vertical errors, and a sidewind was assumed for the lateral errors. A vertical wind of this magnitude was considered highly unlikely at such a low altitude. The most critical time to be hit by either a head or side wind is seen from these plots to be about 100 ft before recovery. If the wind hits later than this, it has little time to create a significant disturbance; if it hits earlier, the RPV flight control system has time to adjust.

Launch. During launch, the RPV is flying with a fixed airspeed command and a heading rate command that has been biased to trim out the feedback signal resulting from roll-yaw rate gyro bias. The engine is responding to an altitude command which is high enough to cause full throttle operation.

Extensive launch simulations were performed early in the RPV-STD program, using a 6-DOF simulation, which had been developed under LMSC independent development funds. These simulations considered a large number of variations from nominal conditions including head and tail winds, side winds, altitude variations, launch speed variation, RPV weight variations, tipoff

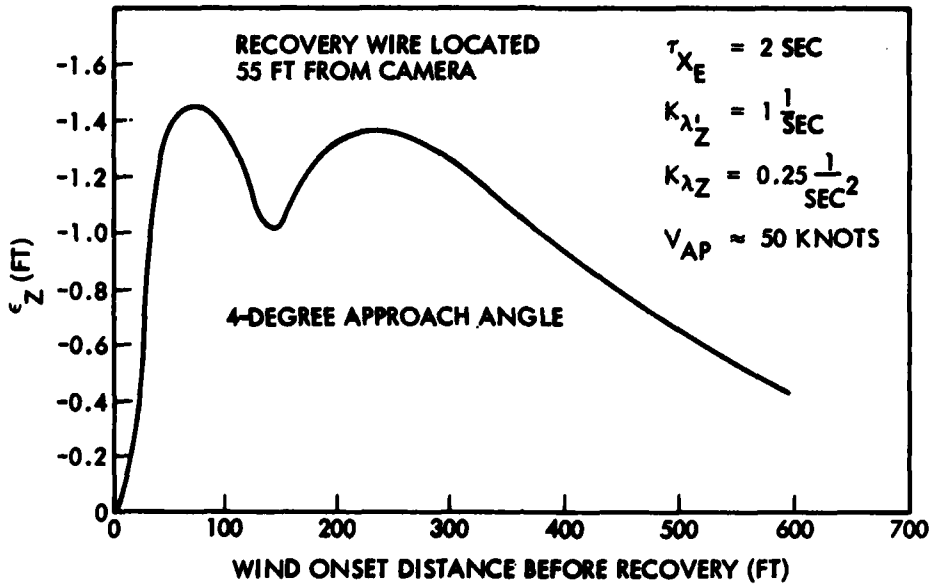


Figure 59. Aquila RPV Vertical Errors During Final Approach Due To 15-Knot Step Headwind Beginning at Varying Distances Before Recovery

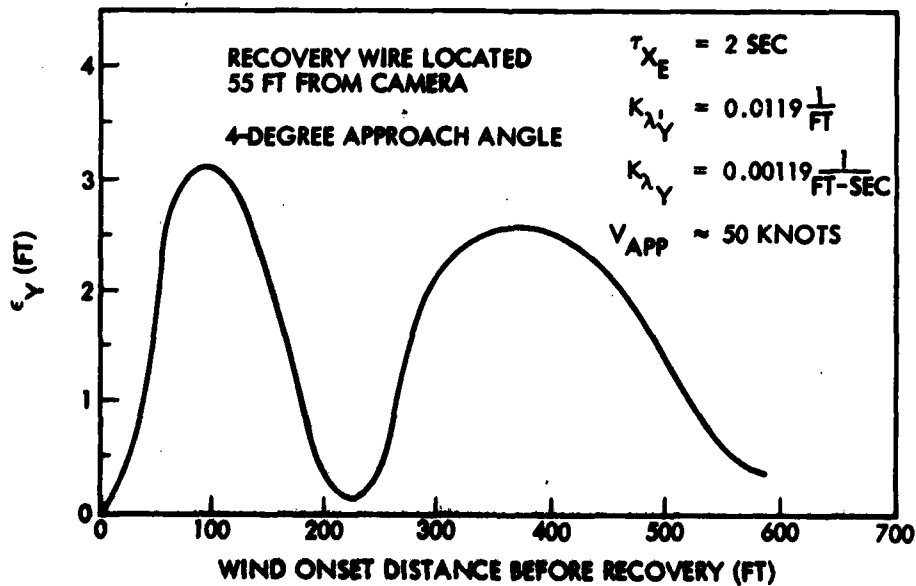


Figure 60. Aquila RPV Lateral Errors During Final Approach Due To 15-Knot Step Sidewind Beginning at Varying Distances Before Recovery

rates, angle of attack, and flight-path-angle variations. As a result of these simulations, it was found that the velocity command at launch (and about 20 sec thereafter) was the most critical parameter in a successful launch. The indicated airspeed at launch should exceed the airspeed command by several knots to ensure a sharp climb angle. It was found that angle of attack was relatively unimportant. The RPV quickly adjusts to the proper angle of attack after launch. Therefore, it was decided to design the launcher for a single angle of attack launch, thereby simplifying the launcher design.

Figures 61 and 62 show the results of some typical simulations. The first figure shows how the angle of attack quickly adjusts for initial angles of attack of 5 and 9 deg. The second figure shows how the launch velocity affects the climb profile. In each of the three curves shown, the airspeed command is 85 km/h, or 45.8 knots. For a true launch velocity of 56 KTAS, the climb is good out to 24 sec, at which time the speed command is increased to 92 km/h. After the increase, a slight dip in the profile is seen, although the climb rate is still substantial. For $V_L = 50$ KTAS, the climb profile is seriously degraded, but the launch would probably be successful. The third curve, $V_L = 44.7$ KTAS, shows a climb profile which would definitely result in a crash.

Tailwinds at launch result in lower indicated airspeeds that have the same effect as lowered airspeeds. It is therefore not recommended to launch with a tailwind. Launching into a headwind, on the other hand, has a beneficial effect. The indicated airspeed will be high, and the RPV will climb steeply in an attempt to lose speed.

3.4.5 Flight Control and Navigation-Hardware Evolution

The flight control and navigation hardware includes the flight control electronics package and the multiple transducers and servo actuators. The Aquila RPV represents the third-generation RPV flight control system designed and built by LMSC. The prototype flight control system was flown at Hamilton Air Force Base, Calif-

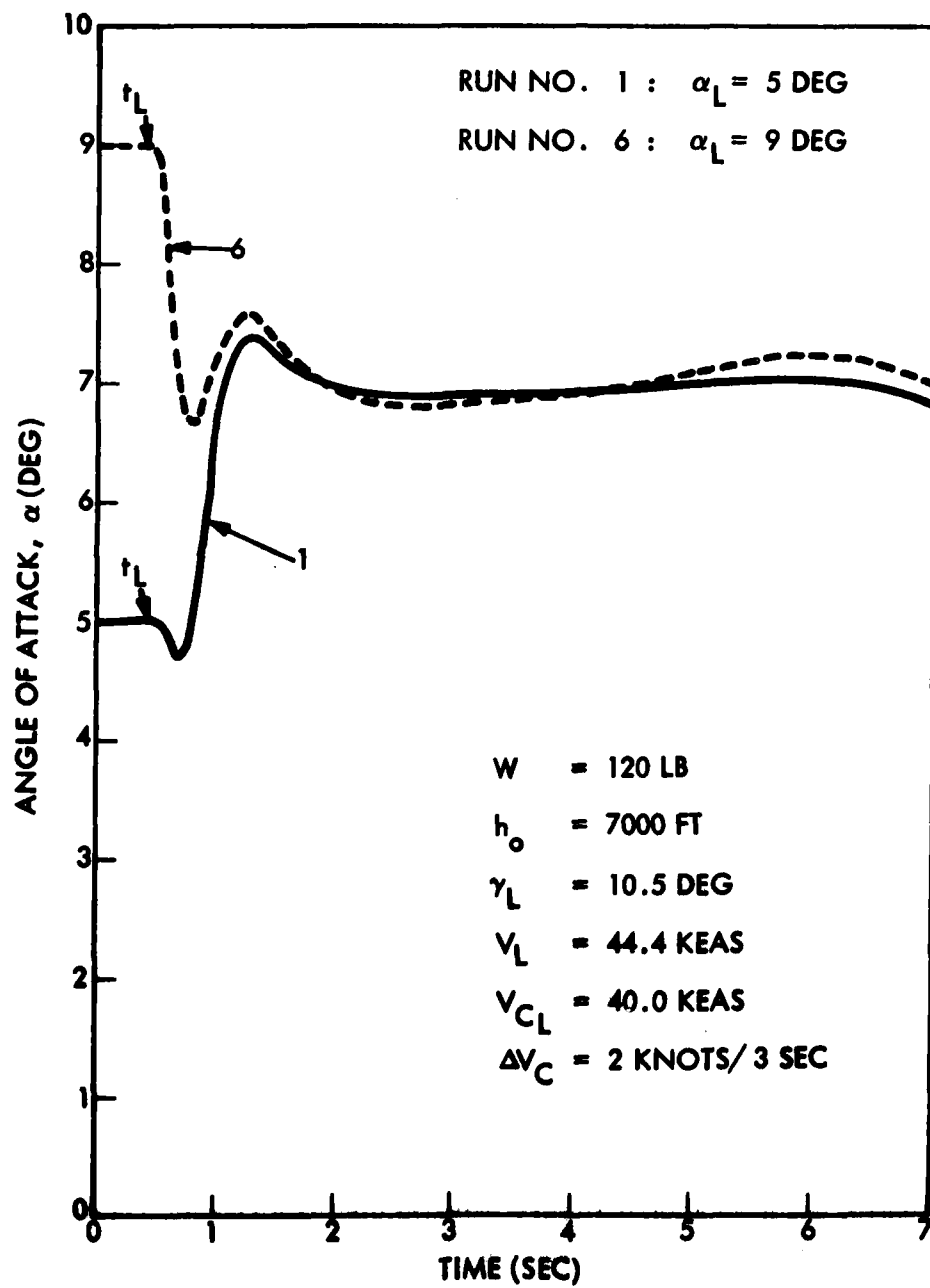


Figure 61. Aquila Launch Dynamics Angle-of-Attack Transients

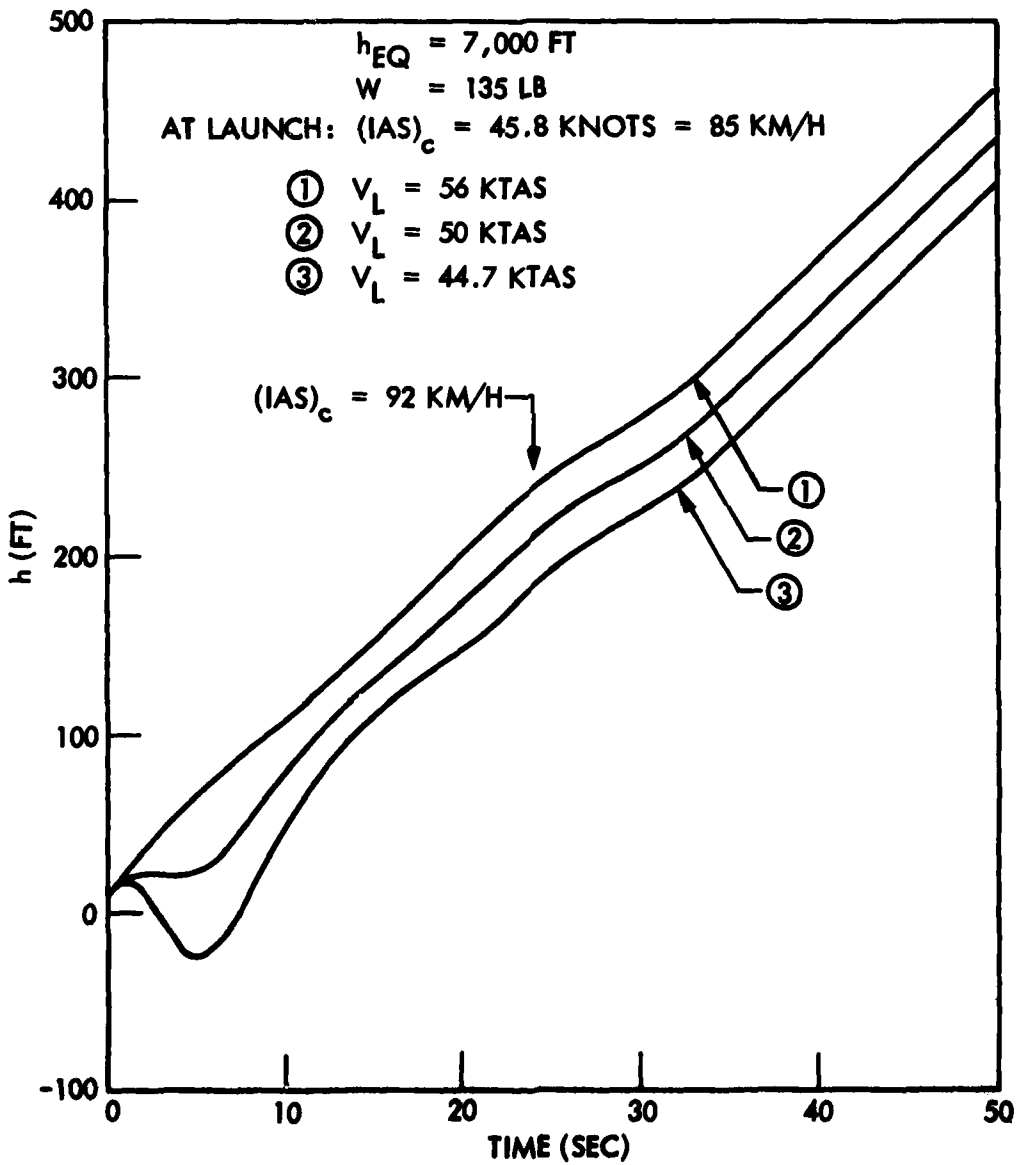


Figure 62. Aquila Altitude Profile - Automatic Launch

ornia, on 29 June 1974, in the "Tuboomer" research test vehicle RTV-2. The second-generation flight control system was used in the Aequare RPV.

Flight Control Electronic Package (FCEP). Although based in many ways upon the previous generation hardware, the Aquila FCEP included several new features as well. The prelaunch checkout, launch, recovery, and dead reckoning imposed several new operating modes in the FCEP electronics. Each of these modes required switching of analog signals to initialize, complete, or modify the pitch, altitude, and heading control electronics. The Aquila flight control system uses nine operating modes and six test modes, and has four spare modes compared to the two operating modes and one test mode used in the previous generation.

Experience gained in the previous generation of equipment indicated that the switching requirements of these modes were highly subject to change during the system development. In order to minimize the impact of design changes on the hardware, programmable read only memories (PROMs) were used to store the switch closure patterns. The address to the PROMs is derived from the signals that determine the mode, i. e., the telemetry commands, the link loss detector, the low voltage detector, and the link loss timer. Using this approach had made it possible to modify, add, and delete modes by replacing not more than four PROMs on the mode control printed circuit card.

The introduction of the approach mode used during recovery introduces two major control loop revisions. The altitude loop is disabled in this mode and the throttle is controlled by airspeed. The pitch loop, which normally controls the airspeed, is revised in this mode to control the z-axis velocity. This new mode introduces new control circuits not used in previous generation designs.

The dead reckoning mode also introduces a control loop not previously used. The earlier generations had all carried magnetometers for instrumentation

purposes, but in the Aquila the RPV heading loop is closed on the magnetometer during the dead reckoning mode. The remaining control loop electronics (i. e., the pitch, altitude, and heading) are similar in design to the previous generators.

The dead reckoning mode also introduces the requirement for storing information received via the telemetry for use as commands during the dead reckoning mode. This is accomplished by storing selected pulse-code modulation (PCM) telemetry commands in three separate digital circulating registers, each representing the RPV commands for a separate leg of the dead reckoning mission. During the dead reckoning mode the data from the circulating registers is fed to the PCM decommutator for decoding in the same manner as in the normal real-time operation. This method of storage required fewer components than would have been required by other techniques considered, makes use of the decoding and analog-to-digital features of the PCM decommutator, and eliminates the requirement to switch several digital and analog command signals between the PCM decommutator and dead reckoning signal source.

Both analog and digital circuits have been used in the implementation of the FCEP. The control loop electronics are implemented using analog techniques, while the mode control and dead reckoning storage use digital techniques. Signal conditioning functions for telemetry or aircraft power control use both techniques.

Electronic components (resistors, capacitors, integrated circuits, etc.) were selected prior to starting the design and were standardized as much as possible throughout the design in order to minimize the stocking and spares requirements. This was more successful in the analog design than in the digital design. The flight control loops are implemented using five integrated circuit types. The digital design uses approximately twenty different integrated circuit types.

The design of the electronics assumed a maximum ambient temperature within the FCEP of 85°C. Discrete power dissipating devices are limited to 50 percent of their rating at this temperature. Capacitors are derated to 50 percent of their voltage rating. All analog integrated circuits are used at less than 70 percent of their voltage rating. The digital circuits combined CMOS and TTL technology. The CMOS integrated circuits were used at 33 percent of their maximum voltage rating. Voltage derating of the TTL devices is not possible; however, these devices were very lightly loaded. The FCEP also contains the PCM telemetry encoding and decoding electronics built by AACOM Incorporated. These electronics were incorporated in the FCEP to eliminate the weight of an additional housing and the cabling that would be required to connect the FCEP to a separate PCM encoder/decoder assembly. The proximity of the PCM encoder/decoder functions to the flight control electronics also minimizes the ground loop and noise problems on the command and status signal lines.

The FCEP electronics are packaged on conventional two layer printed circuit boards. Due to the evolving design requirements it was necessary to update (B change) the printed circuit boards during the program. These updates were included on RPV S/N 6, 14, and up.

A matrix assembly contains both the card connectors, the package I/O connectors, and the interconnect wiring. This is a hand wired assembly using crimp terminations at the I/O connectors and solder sleeve terminations at the card connector. Wire wrap termination techniques were considered but connector unavailability within the program schedule prevented its use. Multi-layer board interconnect was dismissed as not practical during a development phase due to the high probability of change. Several changes were made prior to the fabrication of RPV S/N 1. The matrix wiring was also revised at RPV S/N 14 to accommodate wiring changes required by circuit changes on the printed circuit boards.

The FCEP enclosure is fabricated using Lockheed LLM graphite/epoxy prepreg with a DLS 77 epoxy impregnant. This product was developed by the Lockheed Georgia Corporation for lightweight airborne electronics enclosures. The use of this material reduced the weight of the FCEP enclosure over an equivalent design using aluminum. Fabrication man-hours of the enclosure were also reduced by this construction.

The FCEP electronics is tested at two levels prior to assembly in the RPV. The printed circuit cards are individually tested and the matrix continuity is tested prior to assembly of the package. The FCEP is then assembled and retested as a unit.

Three problems occurred during the evolution of the FCEP. The first problem was the discovery of a white material that developed on the printed circuit card connector. This material exhibited high electrical resistance and resisted normal cleaning attempts. The connector (A-MP 583577-4) consisted of a blue polyurethane molded shell with blue anodized aluminum pin protector sides and gold over nickel plated brass pins. Analysis identified the material as aluminum oxide or aluminum hydroxide corrosion products, originating from the pin protectors. Aluminum exposed via pin holes or scratches in the blue anodized finish had combined with cleaning solvents used during the printed circuit card assembly. The close proximity of the pin protectors allowed the compound to migrate to the connector pins before drying. The pin protectors (optional in this connector) were removed and the problem never recurred.

Electronic component failures were the second problem in that they were extremely high for a short period of time. This was identified as improper handling and storage combined with low humidity, which resulted in damage to CMOS integrated circuits caused by static electricity. Handling procedures were modified and special grounded assembly benches were employed. These

precautions reduced the CMOS component failure rate to a normal level comparable to non-CMOS devices. These failures were occurring at the piece part and card level. No static failures were observed at the FCEP assembly level.

Heat within the FCEP created the third problem. Due to the construction of the PCM bit synchronizer, air flow around this printed circuit card was restricted. This created a localized hot spot which affected the operation of the PCM telemetry. This occurred sporadically in ground tests but not during early flights. Concern for cooling implications with the parachute installation used only in early test flights with a Sony TV camera (Reference 5) led to a thermocouple temperature survey (initial ground tests had used temptabs) during the reliability improvement program. This later survey identified the PCM bit synchronizer temperature as near limit. Cooling vents were added to the FCEP top cover to improve the air flow, and consequently the reliability of the bit synchronizer.

Rate Gyro. The flight control design requires two rate gyro signals. Previous generation design had utilized two single-axis units for this function. A two-axis unit was selected for the Aquila RPV in order to reduce the size, weight, and the additional cabling.

The unit selected is built by Hamilton Standard and uses the Hamilton Standard Supergyro as the basic sensor. This sensor has been in production for several years and has been used on both aircraft and missile programs. The assembly includes a 28 Vdc to 400 Hz inverter for motor excitation and demodulators necessary to provide a dc output. The measurement range is ± 30 deg/sec in the pitch axis and ± 50 deg/sec in the roll/yaw axis.

Zero offset error in the roll/yaw axis results in a differential in the elevon positions, an especially undesirable feature during launch. A self-zeroing circuit was designed and included in the unit by the manufacturer to reduce this offset. This feature did not prove to be reliable due to poor repeatability and long-term drift. The circuit was subsequently disabled, and the launch

(5) Lockheed Missiles & Space Company, Inc., Aquila RPV System Test Report, CDRL AOOD, Parachute System Development Tests, LMSC-L028081, Part 3, Sunnyvale, Calif., 1 Mar 1977

procedures were modified to include the operator adjusting the trim from the ground station via the heading trim control based upon information from the status telemetry.

The zero offset was also affected when the 28 Vdc power bus dropped below 24 V. Proper operation is needed over the range of 18 to 30 Vdc. A circuit modification was made to correct this problem at the same time that the self-zeroing circuit was disabled.

Servo Actuators. The servo actuator was designed and built by Simmonds Precision. The unit requires 28 and ± 15 Vdc power and weighs approximately 0.7 lb. Output shaft rotation is 80 deg full scale, the rotation being internally limited by mechanical stops. Stall torque is in excess of 20 in.-lb.

The servo actuators required considerable evolution before they performed satisfactorily. The initial units were not stable when connected to their specified load, had excess granularity in shaft rotation, inadequate strength in the output shaft material, and tended to have motor failure after a few hours of operation.

The units were extensively modified (Reference 6). The servo feedback potentiometer was found to be one source of the granularity. The design of potentiometer used a wiper wire that is pulled over the conductive material when rotated in one direction and pushed when rotated in the other direction. The wiper tended to hang up, then skip when pushed. The potentiometer was replaced with a unit of better internal design. This reduced the granularity but did not eliminate it entirely.

A new output shaft design was prepared and incorporated for added strength.

(6) Lockheed Missiles & Space Company, Inc., Aquila RPV System Test Report, CDRL ACOD, Servo-Actuator Development, LMSC-L028081, Part 7, Sunnyvale, Calif., Aug 1977

Several design attempts were made to cure the oscillation and granularity problems without a major redesign. Backlash in the gears between the motor and the feedback potentiometer allowed the servo actuator to limit cycle. The actuator gearheads were disassembled and the gears plated, then reassembled. The plating reduced the backlash and (in conjunction with minor changes in the electronics) eliminated the oscillation in some, but not all, units.

A new servo amplifier design was prepared at LMSC and substituted for the original design. The major difference was the method used to derive the rate damping signal required for stabilization. The original design derived this signal from the feedback potentiometer. In the original design the rate damping signal was lost when the gears between the motor and the feedback potentiometer were moving through the backlash region. The replacement design derived the rate damping signal from the back EMF of the motor between power pulses. Replacing the original electronics with the new design finally eliminated the oscillation and granularity problems.

Motor failures were still a problem. The servo actuators developed "dead spots" that were traced to out-of-round commutators in the motor. During operation the brushes would skip due to the out-of-round condition and cause burn spots on the commutators. These burn spots were in turn the cause of the actuator dead spots.

The motors were disassembled and rebuilt to correct this condition. A replacement motor from TRW Globe was evaluated and found to be an acceptable replacement. New Globe motors were purchased and included in all servo actuators built for RPV 14 and up.

Accelerometers. The accelerometer used in the original Aquila flight control design was a spring-mass suspension design with a potentiometer output. The unit was built by Bourns Incorporated.

In the course of flight analysis of early RPV flights, during the recovery approach, it was noted that certain accelerometers had a tendency to stick or hang up and not respond properly. Further investigation of flight records indicated that this condition had been building up and was a function of accumulated time on the accelerometers.

Several units were disassembled for investigation. The problem was identified as wear on the potentiometer element due to the vibration produced by the RPV engine. Additional units were sent to the vendor for analysis. The vendor agreed with the LMSC analysis and suggested that another type of accelerometer be considered as very little could be done to correct the problem in the existing design.

A second (and more rugged) accelerometer was selected and evaluated in flight on RPV S/N 12. This unit is built by Systron Donner and is a closed-loop servo accelerometer. The evaluation flights were successful and the new device has been included in RPV S/N 14 and up.

The replacement accelerometers are powered by ± 15 Vdc, weighs 8 oz and has a range of -4 to +6 g.

Altitude Transducer. The altitude transducer is a lightweight (6 oz) unit that operates over the barometric altitude range of -1,000 to +10,000 ft. The unit requires 750 mW of power at ± 15 Vdc.

This transducer is a catalog item from Rosemount Incorporated and had been used previously on the Aequare RPV. This unit has performed successfully on both the Aquila and the Aequare programs with no design or manufacturing problems.

Airspeed Transducer. The airspeed transducer provides a dc output signal proportional to indicated airspeed over the airspeed range of 30 to 130 knots. The transducer weighs 6 oz and requires 750 mW of power at ± 15 Vdc.

This transducer is similar in construction to the altitude transducer and is also a catalog item built by Rosemount Incorporated. This transducer has been used on the Aequare and Aquila RPVs with no apparent problems.

Magnetometer. The magnetometer is used to resolve the earth's magnetic field in three orthogonal axes. The two axes in the aircraft horizontal plane are used for heading control during the dead reckoning flight mode. All three axis measurements are used by the ground station computer for targeting calculations.

The magnetometer was built by Superconducting Technology Incorporated. This unit operates from the 28 V power bus and requires 980 mW of power. The output signals are proportional dc levels indicating both the magnitude and polarity of the sensed field. The unit weighs 3.5 oz.

This transducer has unfortunately gone out of production during the time span of the Aquila program. Due to a low volume of magnetometer sales, the manufacturers have dropped the magnetometer from their product line and dismantled their test and repair facility.

A second source for this device which is electrically identical has been located. Although not identical dimensionally, this unit will mount in the RPV with no modifications to the mounting hardware. This potential second source device is manufactured by Develco Incorporated.

3.5 SENSORS

The sensor packages for the Aquila RPV included the following equipment for the designated sensor phases:

Phase I: unstabilized gimballed TV camera, sensor electronics,
 and ballast kit

Phase II: unstabilized gimballed TV camera, panoramic film camera,
 sensor electronics, and ballast kit

- Phase III:** stabilized gimballed TV camera, sensor electronics, and ballast kit
- Phase IV:** stabilized gimballed TV camera plus laser locator/designator, sensor electronics, and ballast kit
- Phase V:** stabilized gimballed TV camera plus laser locator/designator, sensor electronics, and ballast kit

These elements are described in Volume I of this report. This section describes the evolution and ground testing of the various sensor units.

3.5.1 Background

At the point of procurement initiation for the Aquila program, all of the specified sensor functions had been flight demonstrated in RPVs or aircraft. Candidate TV/laser sensor prototypes existed in the Praetire, Poise, and Blue Spot configurations developed by Philco-Ford, Honeywell, and General Electric respectively. Existing panoramic film cameras included the Actron 70-mm and Perkin Elmer 34-mm units. What remained for the Aquila program was to select the film camera, and to develop a family of EO sensors and designators within a proven geometric and mechanical frame compatible with interchangeable installation and operation within the Aquila airframe.

3.5.2 Requirements

The Aquila procurement documentation identified specific requirements for the sensors and for system accuracy using the sensors. These requirements are summarized in Tables 8, 9, 10, 11, and 12, for the Phase I, II, III, IV, and V sensor operations respectively. Other requirements included:

- Interchangeable installations (phase to phase) in the RPV
- Compatibility with the RPV data link and command telemetry

TABLE 8. INITIAL PHASE I, REAL-TIME TV SURVEILLANCE SENSOR SPECIFICATIONS

FUNCTION	SPECIFICATIONS	BASELINE CONFIGURATION DESIGN
Target Detection	50% Probability	50% Probability
• Tank on road	3000 meters slant range	> 3000 meters slant range at 15° FOV
• Tank in field environment	1500 meters slant range	> 1500 meters slant range at 15° FOV
Target Recognition	50% Probability	50% Probability
• Tank on road	1000 meters slant range	> 1000 meters slant range at 15° FOV
• Tank in field environment	1000 meters slant range	> 1000 meters slant range at 15° FOV
TV Sensor Characteristics		
• Field of view	Single; 15° to 20° (20° preferred); aspect ratio of 3 to 4, vertical to horizontal	Interchangeable 15° FOV and 20° FOV lenses; aspect ratio of 3 to 4, vertical to horizontal
• Video rate	525 lines per frame	525 lines per frame
• Dynamic resolution	> 200 TV l/ph as determined on the ground monitor for a 20% modulation bar pattern observed in flight at cruise air-speed with a constant down-look angle of 30°	> 200 TV l/ph as determined on the ground monitor for a 20% modulation bar pattern observed in flight at cruise air-speed with a constant down-look angle of 30°
• Brightness adjustment	Automatic for ambient over a range of 10-10,000 footlamberts average brightness	Automatic for ambient over a range of 10-10,000 footlamberts average brightness
• Camera positive detent	During navigation and ground checkout	Cage mode provides positive detent during navigation and ground checkout
• Pm tilt capability	Pan: ±60°; Tilt: +10°, -90°; (-90° desirable)	Pan: ±180°, Tilt: +15° to -60°

TABLE 9. INITIAL PHASE II, PHOTOGRAPHIC RECONNAISSANCE SENSORS SPECIFICATIONS

FUNCTION	SPECIFICATIONS	BASELINE CONFIGURATION DESIGN
Target Detection	50% Probability	50% Probability
• Track on road	3000 meters slant range	> 3000 meters slant range at 12° FOV
• Track in field environment	1500 meters slant range	> 1500 meters slant range at 12° FOV
Target Recognition	50% Probability	50% Probability
• Track on road	1000 meters slant range	> 1000 meters slant range at 12° FOV
• Track in field environment	1000 meters slant range	> 1000 meters slant range at 12° FOV
TV Sensor Characteristics	Single: 12° to 20° (20° preferred); aspect ratio of 3 to 4, vertical to horizontal 525 lines per frame > 200 TV l/ph as determined on the ground monitor for a 20% modulation bar pattern observed in flight at cruise airspeed with a constant down-look angle of 30° Automatic for ambient over a range of 10-10,000 footlamberts average brightness During navigation and ground checkout Pan: ±90°; Tilt: +10°; -60°; (-90° desirable)	Interchangeable 12° FOV and 20° FOV lenses; aspect ratio of 3 to 4, vertical to horizontal 525 lines per frame > 200 TV l/ph as determined on the ground monitor for a 20% modulation bar pattern observed in flight at cruise airspeed with a constant down-look angle of 30° Automatic for ambient over a range of 10-10,000 footlamberts average brightness Cage mode provides positive detent during navigation and ground checkout Pan: ±180°; Tilt: +15° to -60°
Aerial Camera Characteristics	70 mm (desired); 35 mm acceptable 235 f/8 Maximum flexibility Maximum flexibility	70 mm 235 feet of 2.5 MIL thin base daylight load Remote: on pad off, single frame or 4 frames preset manually; shutter speed and exposure control Single or multiple frame selection
• Film size	70 mm (desired); 35 mm acceptable	70 mm
• Film capacity	235 f/8	235 feet of 2.5 MIL thin base daylight load
• Control capability	Maximum flexibility	Remote: on pad off, single frame or 4 frames preset manually; shutter speed and exposure control
• Selection capability	Maximum flexibility	Single or multiple frame selection

TABLE 10. INITIAL PHASE III, TARGET ACQUISITION SENSOR SPECIFICATIONS

FUNCTION	SPECIFICATIONS	BASELINE CONFIGURATION DESIGN
Target Detection	50% Probability	50% Probability
• Tank on road	5000 meters slant range with WFOV	> 5000 meters slant range at 13° FOV
• Tank in field environment	2000 meters slant range with WFOV	> 2500 meters slant range at 13° FOV
Target Recognition	50% Probability	50% Probability
• Tank on road	2500 meters slant range	> 2500 meters slant range at 5° FOV
• Tank in field environment	2000 meters slant range	> 2500 meters slant range at 5° FOV
TV Sensor Characteristics		
• Field of view	Dual; adjustable in flight; WFOV-13° minimum, 20° desired; NFOV-3° to 5°; aspect ratio of 3 to 4, vertical to horizontal	Dual; adjustable in flight; WFOV 13° and 20° minimum inter-changeable, NFOV-5°; aspect ratio of 3 to 4, vertical to horizontal
• Video rate	525 lines per frame	> 525 lines per frame
• Dynamic resolution	> 300 TV l/ph as determined on the ground monitor for a 20% modulation bar pattern observed in flight at cruise air-speed with a constant down-look angle of 30°	> 300 TV l/ph as determined on the ground monitor for a 20% modulation bar pattern observed in flight at cruise air-speed with a constant down-look angle of 30°
• Brightness adjustment	Automatic for ambient over a range of 10-10,000 footlamberts average brightness	Automatic for ambient over a range of 10-10,000 footlamberts average brightness
• Camera positive detect	During navigation and ground checkout	Cage mode provides positive detect during navigation and ground checkout
• Sensor stabilization	50 μ r per axis (maximum) during normal cruise conditions in light turbulence	< 50 μ r per axis (maximum) during normal cruise conditions in light turbulence
• Camera coverage	Lower hemisphere while orbiting around or to side of target; image display oriented to pilot view	300 AZ; +15° to -100° elevation; image display completely de-rotated to keep display oriented to pilot view
• Automatic tracking	LOS within 2.3 x 2.3 meter target at 2,500 meters slant range for 95% of tracking time at normal cruise conditions	LOS within 2.3 x 2.3 meter target at 2,500 meters slant range for 95% of tracking time at normal cruise conditions
• Camera focus	Remote capability during flight	Remote capability during flight

TABLE 11. INITIAL PHASE IV, TARGET LOCATION AND ARTILLERY ADJUSTMENT SPECIFICATIONS

FUNCTION	SPECIFICATIONS	BASELINE CONFIGURATION DESIGN
Target Detection		
• Tank on road	5000 meters slant range with WFOV	50% Probability > 5000 meters slant range at 12° FOV
• Tank in field environment	2500 meters slant range with WFOV	> 2500 meters slant range at 12° FOV
Target Recognition		
• Tank on road	2500 meters slant range	50% Probability > 2200 meters slant range at 5° FOV
• Tank in field environment	2500 meters slant range	> 2200 meters slant range at 5° FOV
TV Sensor Characteristics		
• Field of view	Dual; adjustable in flight; WFOV-12° minimum, 20° desired; NFOV-3° to 5°; aspect ratio of 3 to 4, vertical to horizontal	Dual; adjustable in flight WFOV-12° and 20° minimum interchangeable NFOV; aspect ratio of 3 to 4, vertical to horizontal
• Video rate	525 lines per frame	525 lines per frame
• Dynamic resolution	> 300 TV l/ph as determined on the ground monitor for a 20% modulation bar pattern observed in flight at cruise air-speed with a constant down-look angle of 30°	> 300 TV l/ph as determined on the ground monitor for a 20% modulation bar pattern observed in flight at cruise air-speed with a constant down-look angle of 30°
• Brightness adjustment	Automatic for ambient over a range of 10-10,000 foot lambert; average brightness	Automatic for ambient over a range of 10-10,000 foot lambert's average brightness
• Camera positive detect	During navigation and ground checkout	Gage mode provides positive detect during navigation and ground checkout
• Sensor stabilization	50 μ r per axis (maximum) during normal cruise conditions in light turbulence	> 50 μ r per axis (maximum) during normal cruise conditions in light turbulence
• Camera coverage	Lower hemisphere while orbiting ground or to side of target; image display oriented to pilot view	360 AZ; +10° to 105° elevation; image display completely de-rotated to keep display oriented to pilot view
• Automatic tracking	LOS within 2.3 x 2.3 meter target at 2500 meters slant range for 95% of tracking time at normal cruise conditions	LOS within 2.3 x 2.3 meter target at 2500 meters slant range for 95% of tracking time at normal cruise conditions
• Camera focus	Remote capability during flight	Remote capability during flight
Laser Rangefinder		
• Rangesight	Aligned with TV sensor line of sight	Laser bore-sights to the RV reticle within 100 μ radians
• Accuracy (50% probability)	\pm 5 meters at target-to-RPV altitude of 2,000 feet AGL	\pm 5 meters at target-to-RPV slant range of 3,000 meters at RPV altitude of 2,000 feet AGL
Attitude Reference		
• Target location	100 meters CEP and 75 meters in altitude at RPV-to-ground station range of 20,000 meters and target-to-RPV range of 2,000 meters	100 meter CEP and 75 meters in altitude at RPV-to-ground station range of 20,000 meters and target-to-RPV range of 2,000 meters

TABLE 13. INITIAL PHASE V, TARGET DESIGNATION SENSOR SPECIFICATIONS

Parameter	Specifications	Baseline Configuration Design
Image Subsystem		
• Push on road	5000 meters slant range with WFOV	50% Probability > 5000 meters slant range at 12° FOV
• Push on field environment	2500 meters slant range with WFOV	> 2500 meters slant range at 12° FOV
Image Resolutions		
• Push on road	2300 meters slant range	50% Probability > 2200 meters slant range at 5° FOV
• Push on field environment	2200 meters slant range	> 2200 meters slant range at 5° FOV
TV Sensor Characteristics		
• Field of view	Dual, adjustable in flight; WFOV-12° minimum, 20° desired; NFOV-3° to 5° aspect ratio of 3 to 4, vertical to horizontal	Dual; adjustable in flight WFOV 12° or 20° minimum inter-changeable NFOV; aspect ratio of 3 to 4, vertical to horizontal
• Video rate	525 lines per frame	525 lines per frame
• Dynamic resolution	> 300 TV l/ph as determined on the ground monitor for a 20% modulation bar pattern observed in flight at cruise air-speed with a constant down-look angle of 30°	> 300 TV l/ph as determined on the ground monitor for a 20% modulation bar pattern observed in flight at cruise air-speed with a constant down-look angle of 30°
• Brightness adjustment	Automatic for ambient over a range of 10-10,000 footlamberts average bright-brightness	Automatic for ambient over a range of 10-10,000 footlamberts average brightness
• Camera positive detent	During navigation and ground checkout	Cage mode provides positive detent during navigation and ground checkout
• Sensor stabilization	50 #/r per axis (maximum) during normal cruise conditions in light turbulence	< 50 #/r per axis (maximum) during normal cruise conditions in light turbulence
• Camera coverage	Lower hemisphere while orbiting around or to side of target; image display oriented to pilot view	360 AZ; +15° to -105° elevation; image display completely de-rotated to keep display oriented to pilot view
• Automatic tracking	LOS within 2.3 x 2.3 meter target at 2500 meters slant range for 95% of tracking time at normal cruise conditions	LOS within 2.3 x 2.3 meter target at 2500 meters slant range for 95% of tracking time at normal cruise conditions
• Camera focus	Remote capability during flight	Remote capability during flight
Laser Designator Characteristics		
• Energy	75 millijoules (minimum)	> 75 mJ to atmosphere
• Beam divergence	0.2 mrad (maximum)	< 0.5 mrad
• Pulse rates	One, ten, or twenty pulses per second, selectable from ground station	One, ten, or twenty pulses per second, selectable from ground station
• Wave length	1.06 micrometers	1.06 micrometers
• Duty cycle	≥ 20 seconds on, ≤ 120 seconds off during normal cruise at 95° F outside air temperature at 4000 ft pressure altitude	≥ 20 seconds on, ≤ 120 seconds off during normal cruise at 95° outside air temperature at 4000 ft pressure altitude
• Tracking and stabilization	Automatic; 90% of laser beam spot on 2.3 x 2.3 meter target 95% of time at a slant range of 2500 meters at normal cruise air-speed and vibration conditions	Automatic; 90% of laser beam spot on 2.3 x 2.3 meter target 95% of time at a slant range of 2500 meters at normal cruise air-speed and vibration conditions.

- **Compatibility with the RPV electrical power system**
- **Compatibility with the RPV ground and operational environment**
 - Acceleration
 - Vibration
 - Temperature
 - Pressure

These requirements were incorporated in the sensor subcontractor specifications.

3.5.3 Approach

The approach to evolution of the Aquila sensors included the following:

- **Definition of sensor interfaces**
- **Specification of sensor requirements**
- **Procurement of sensors from an electro-optical and a photographic sensor subcontractor**
- **Qualification testing at the subcontractor facility**
- **System functional verification at LMSC**
- **Flight validation testing**

Some of the major considerations were to use currently developed and flight-tested payloads, compact, lightweight sensors with minimum technical risk, the same TV and line-of-sight pointing mechanism in all phases to reduce training, complete derotation in azimuth and elevation to reduce operator error, modular design to permit transition between phases, and a laser range finder-designator that is compatible with all laser guided ordinances. The initially proposed arrangements are shown in Figure 63. Sensor testing and trouble shooting were closely coordinated with Army technical personnel.

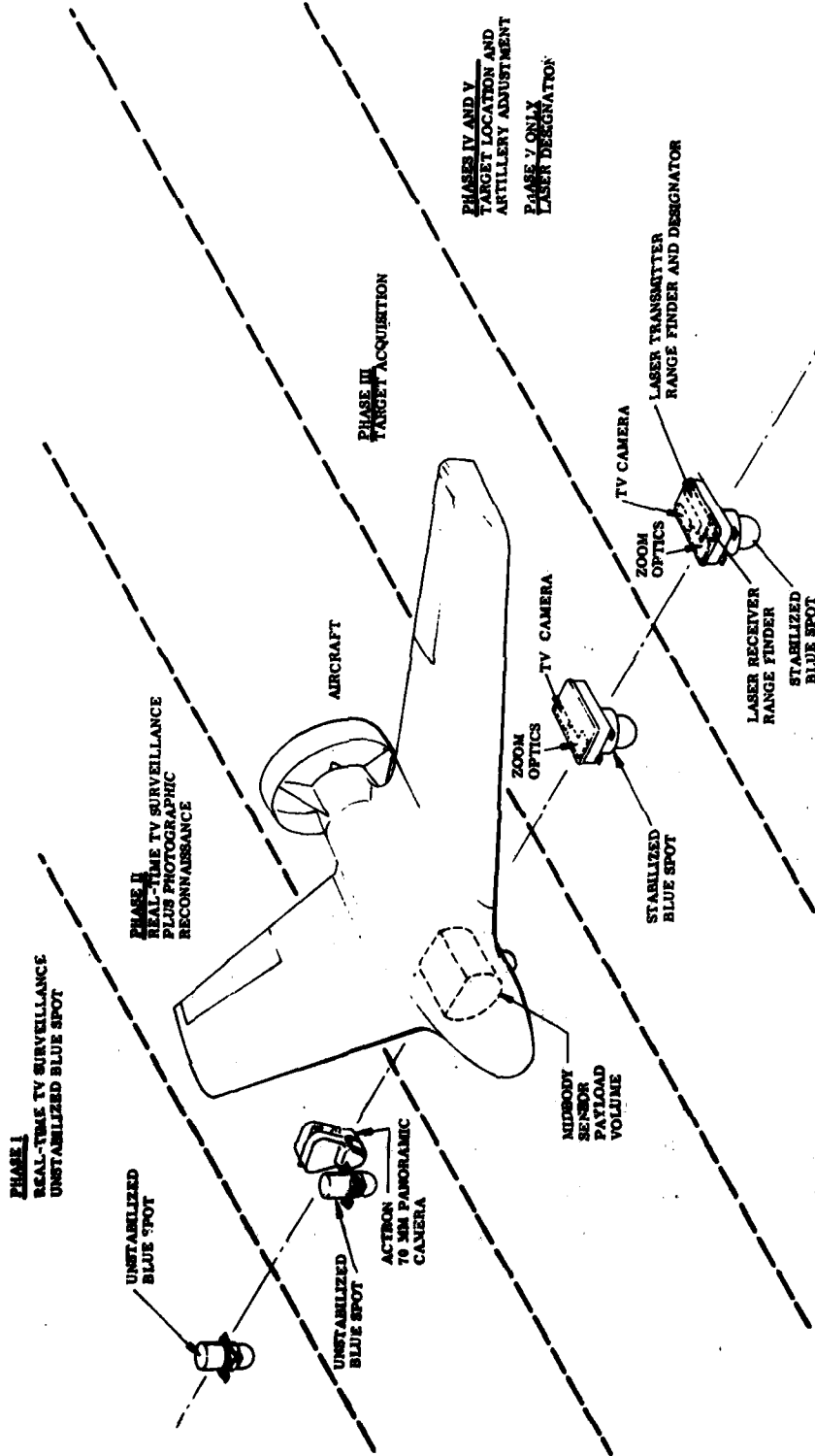


Figure 63. Development Baseline Configurations, Phases I Through V

3.5.4 Sensor Evolution

The Westinghouse-developed Blue Spot and the Actron KA-84 camera were used as the payload baseline in the proposal stages. The selection process was done with strict attention to the requirements. Performance synthesis studies were completed as an integral part of the selection process. An existing methodology was employed to predict the performance of the proposed electro-optical elements of the system. The study methodology included the analysis of the Army Night Vision Laboratory RPV flight test data and psychophysical experiments in the prediction process. Studies were done in the areas of system resolution, field-of-view requirements, effects of linear motion, effects of RPV motion, effects of contrast losses on system shades of gray, lens losses, and vidicon losses. The proposed subsystem met all requirements with the exception of the 0.2-mradian laser beam divergence. The system was still able to meet the operational requirements with the 0.5-mradian beam divergence.

Additional technical and cost analysis was done in response to questions from the Eustis Directorate. The questions were in the area of variable laser pulse rates, laser beam divergence, remote focus, automatic light control, Phase I sensor configuration, and aerial panoramic camera. As a result of this further study, the baseline for the Phase II camera was changed from a 70-mm Actron camera to a 35-mm Perkin Elmer camera. The specifications affected were weight reduction, increased number of frames, lower power consumption, and reduced cost. Another baseline change was made when a cost effective and technical risk study was done between the Westinghouse Blue Spot and Honeywell Poise sensors. The results of these studies were reviewed by the Army at a meeting with LMSC and the decision to change to the Honeywell Poise sensor was made. The relatively minor change in form factor and arrangement is reflected in Figure 64. Note the separate payload electronics package. Key capabilities for each sensor phase is also reflected in this figure.

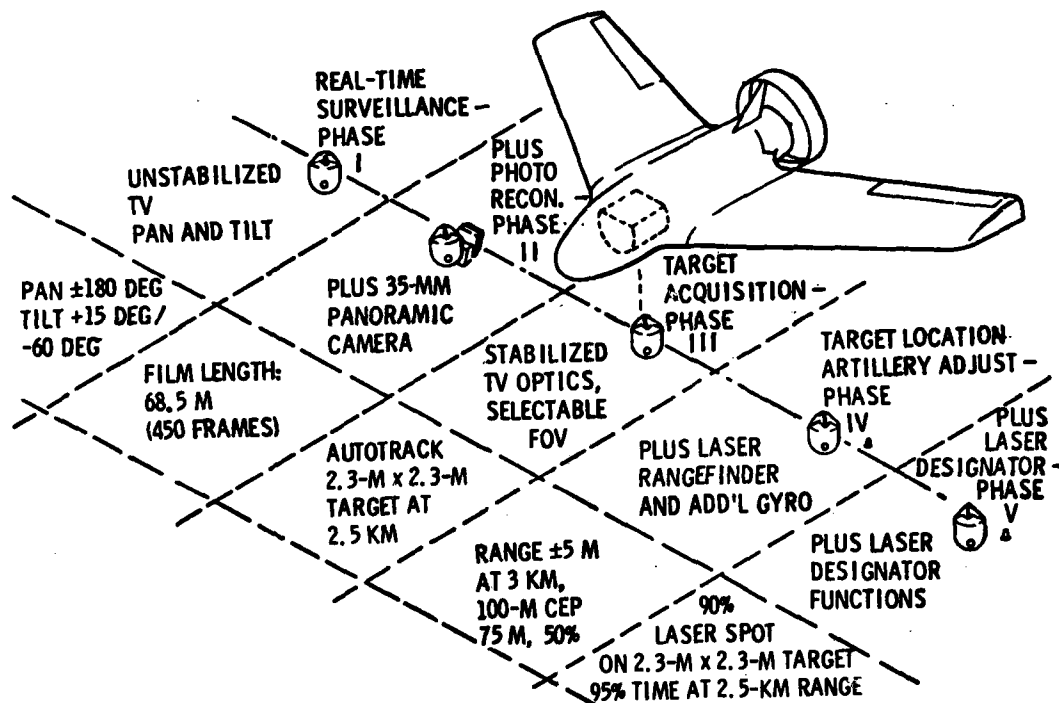


Figure 64. Aquila Payload Sensors

Requirement Evolution. Sensor system requirements have evolved from the Army specification set forth in the request for proposal. These requirements were analyzed using a combination of theoretical study and performance evaluation. The analysis considers some of the following points.

The detection of typical tactical vehicles occurs when the minimum image dimension subtends 1 ± 0.25 TV line pairs; recognition occurs when 3 ± 0.5 TV line pairs are subtended for targets on road and off road. These values correspond closely to the detection and recognition criteria for the detection and recognition of general targets by raster-scanned imaging sensors. The overall sensor resolution is a product of the optics modulation transfer function and that of the camera. Using this type of analysis, resolution and field-of-view requirements were set at 450 lines per TV picture height static and 230 lines dynamic at

12 deg field-of-view. This resolution will allow detection of a tank at 3,000 m on-road and 1,500 m off-road for an unstabilized system. Recognition at 1,000 m is possible. The shades of gray requirement takes into consideration contrast between target and background, contrast losses due to the atmospheric path, lens system, and vidicon tube. Seven shades of gray were needed with one additional shade for losses incurred because of vehicle dynamics, data link, ground display, data storage, and human observer. Field-of-view specifications evolved by the Army included a 12- to 20-deg WFOV (with 20 deg preferred) of a target. This specification was analyzed and it was determined that a 12-deg field-of-view would give a higher percentage of probability of detection.

The Phase II aerial camera is used in conjunction with an unstabilized TV sensor and provides photosurveillance. The primary requirements were determined to be film capacity, flexibility for selection and control of operating conditions, low cost and simplicity. The 70-mm camera was initially selected for image detail, standardization for photo processing and image interpretation. Cost became a primary factor, and a trade-off study revealed that the lighter weight 35-mm camera with 1.72-ft resolution satisfied the requirements. Camera operation at low altitudes and at low or high speeds dictated the variable frame rate capability. The ability to select a camera that was flight tested and lightweight limited the field considerably.

Sensor suppliers were visited and data collected to make sure that the requirements did not exceed the state-of-the-art capabilities. An analytical model was employed to predict detection and recognition capabilities of several different camera tubes. Included in the analytical model are the optics, sensor, and scene parameters. The primary reason for the better performance of silicon is the increased target background contrast provided by the extended red spectral response. Although the silicon camera tube and S-18 vidicon show essentially the same resolution for high contrast patterns, tactical target background spectral reflectivity when convolved with the solar spectrum favors the silicon spectral region. The EBS tube, which employs an S-30 photocathode ahead of a

silicon-intensified target, provides higher gain and hence better performance at lower light levels. The spectral response is not quite as "red" as the silicon vidicon, but it is better than the S-18. An intensified EBS tube has the highest gain, and hence will provide the best low light level performance. The modulation transfer function of the intensifier and coupling is such that the high light resolution limits its performance more than the others. Because the initial concern is with performance during daylight, clear weather conditions, the silicon vidicon was selected.

Static resolution requirements remained the same as for the Phase I sensor, but dynamic resolution changed to meet the added detection and recognition requirements. The stabilization of line-of-sight motion to 3 mradians/sec for aircraft motion was determined to allow 300 TVL/ph. The detection requirements were increased to 5,000 m on road at wide field of view and 2,500 m off road. The recognition requirement is 2,200 m (with 50 percent probability). The ambient light range of 10 to 10,000 ft L must be automatically adjusted. In the automatic tracking mode, the sensor video signals are gated and processed to derive angular error signals in azimuth and elevation. These signals drive the gyroscope torquers to produce line-of-sight angular rates which minimize the tracking errors. The results of analysis show that line-of-sight tracking accuracy is mainly determined by the degree of stabilization. The contributions of line-of-sight rate and acceleration are small compared to the air-frame motion induced line-of-sight motion and effects of video tracker noise. Overall sensor stabilization was required to be 50 μ radians per axis.

The Phase IV and Phase V performance requirements include the TV sensor used in Phase III and incorporate a laser range finder/designator that is bore-sighted with the TV sensor line of sight. The tracker is used as an integral part in an automatic mode. The primary requirements of the laser are range accuracy for target location and laser energy for laser guided ordnance. Target location is specified to an accuracy of 100 m circular error of probability (CEP) and 75 m (50 percent probability) in altitude. The laser range accuracy corresponding to this specification is 5 m out to a range of 3 km.

To satisfy the laser designation requirements to designate a 2.3 m by 2.3 m target with 90 percent energy at 95 percent of the time, a radial error of 188 μ radians and a beam divergence of 200 μ radians is needed. If the tracking error approaches 50 μ radians then the beam divergence may be 500 μ mradians. The requirements of variable pulse rates around the 10- and 20-pulse/sec rates are governed by the requirements of the laser-guided ordnance that is presently available. A 75 mJ, Q switched Nd:YAG laser meets these requirements.

Phase I/Phase II Unstabilized TV Sensor Evolution. Phase I and Phase II both require a TV surveillance type sensor. The original Army requirement in the request for proposal used the same TV sensor for both phases of the demonstration. The sensor was to be unstabilized and to have two interchangeable lenses of 12- and 20-deg field of view. The requirements were reviewed at the Preliminary Design Review. The selectable lens requirement was changed to a 6 to 1 zoom lens to be controlled by the operator. At a later date, lenses on all phases were changed to a 10 to 1 zoom lens. This increased zoom range was provided at the same cost by using a standard off-the-shelf zoom lens. This allowed commonality and reduced operator training.

Honeywell subcontracted the whole of the Phase I/II TV sensor to the Systems Research Laboratory except that they provided the gimbal housing, 10 to 1 zoom lens, and acrylic plastic dome. The common gimbal housing provided for identical mounting requirements and would allow interchangeability of sensors in the RPV. The dome and lens satisfied the commonality condition. The System Research Laboratory requested a change in the silicon vidicon size to give the ability to meet the 450-line resolution specification. The vidicon size was changed from 2/3-in. to 1-in. diameter. Further design change was required in the camera circuitry to obtain the required resolution. The magnetic deflection yoke and optical alignment mirror were changed. The resolution specifications were also more precisely defined. Resolution was defined with a specific degradation for each corner in both horizontal and vertical directions. The original specification required 450 TV L/ph. The specification was changed to 450 TVL/ph in the horizontal direction and 350 TV lines in the vertical direction

with a degradation to 340 TV lines horizontal and 260 TV lines vertical in three corners and the fourth corner to be greater than 300 TV lines horizontal and 230 TV lines vertical.

During the initial flight tests of the Phase I sensor a dome breakage problem was encountered. The problem was traced to the type of epoxy that was being used to attach the acrylic plastic dome to the metal extender ring. An adequate bond was not being maintained and the dome was slipping free and catching in the wind, which shattered it during flight. This was corrected by selection of a different epoxy. Weight reduction was a continual problem. Progress in this area was usually inhibited by increased performance requirements. The simplicity of the sensor configuration changed as the program developed. The weight specifications were increased after all possible weight reductions were accomplished.

Phase II Minipan Camera Evolution. The panoramic photo reconnaissance camera was required to demonstrate a Phase II type mission. The baseline design was changed from a 70 mm camera to the lighter, less costly 35 mm Minipan camera manufactured by Perkin Elmer. The original off-the-shelf design was changed in three areas. The lens assembly needed to be covered by a three-piece glass window assembly. The intervalometer was originally mounted externally and was moved to an internal position. Along with the intervalometer a frame rate control was added to allow frame rate selection and frame count from ground control. All other interfaces were compatible, and the mounting was adapted to the RPV as originally designed.

Phase III Stabilized TV Sensor Evolution. The Honeywell-developed Phase III sensor was designed to accomplish target acquisition. The same TV camera and lens were used on a stabilized gimbal, which enabled better dynamic resolution. An autotracker was developed by Honeywell and underwent several design changes. The initial tests of the video tracker were performed at Honeywell and it was determined that the slew rate commands during autotrack were too

high. When track lock was lost, the gimbal slewed off target too severely. The test was a laboratory type and proved that real target tracking was required to adequately evaluate performance. The next test was conducted from a tower at LMSC. These tests revealed that additional reduction in the loss track time period was required to maintain a 4-deg field-of-view shift limit. The contrast sensitivity was also changed. The nadir area at -87 deg required additional controls, since spinning would occur as the sensor line of sight (LOS) entered this position. Autorotation of 180 deg when in autotrack in a sector of ± 75 deg azimuth was added to allow tracking while flying over a target. The manual mode did not require this provision but control was to be maintained in this area. Also at this time the azimuth dead spot position in the azimuth encoder was moved from 225 to 270 deg.

The development of Phases III, IV, and V was undertaken in separate design projects. The requirement of commonality dictated the combination of design and interchangeability of common parts. The cage position of 0-deg azimuth and -6-deg elevation required a mechanical lock for launch and retrieval. A friction brake was used on the Phases I and II sensor but the additional weight of the Phase III, IV, and V sensors prohibited this method. Flight tests later proved that the Phase I and II sensors also needed a physical lock position. The mechanical cage mechanism on the Phase III, IV, and V sensors could not withstand the 6 g acceleration force that was applied by the launcher. Two problems were encountered in this area. The engagement of the cage pin was not great enough, and movement of the elevation gimbal bound the cage motor, which prevented the uncaging of the sensor after launch. Another cage problem was encountered during launch that resulted in the azimuth encoder gears slipping out of position. This gave a false alignment command to the gimbal drive motors to put side loading on the cage motor and also prevented uncaging of the sensor after launch. After redesign of the cage mechanism to allow greater cage pin engagement, and adding extra set screws to the azimuth encoder gears the uncaging of the sensor after launch was no longer a problem.

During evaluation tests of the sensor, which involved the Otter manned aircraft, a command link dropout problem was discovered. Because of wing and landing gear interference, ground control link was lost occasionally during flight tests. During loss link intervals the sensor would accept random commands and malfunction. After evaluation of the data, a buffer module was designed and inserted in the command cable to latch the commands present at the time of link dropout. Continued Otter flight tests proved this a successful change and allowed further test and evaluation of the sensor before actual Aquila flights. Earlier flight worthiness vibration tests were conducted at Honeywell. Honeywell document APP-166-0027 (Reference 7) contains a full report of these tests and their findings. The main areas of consideration were temperature and vibration.

Phase IV/Phase V Laser Ranger/Designator Sensor Evolution. This sensor development was primarily laser oriented. Weight reduction continued during this phase of the sensor program. In an attempt to meet the original weight requirements, alternate types of material were used for gimbal fabrication. PRD-49, a Dupont-developed Kevlar material, was used but proved to have insufficient stiffness. Resulting deflections caused excessive boresight errors. The Kevlar material was disqualified on this basis. Two types of magnesium material were tried before a suitable gimbal design was established. Later tests showed that additional ribs were needed to eliminate mechanical resonance. The resulting sensor design exceeded the weight specification. RPV weight and balance requirements were reevaluated to accommodate the increase of sensor weights.

The 12-in.-diameter transparent acrylic plastic dome produced additional development efforts because of its effect on laser boresight. The specification of 0.25-mradian change in boresight over an azimuth change of 360 deg and an elevation change of +10 and -30 deg demanded a more critical selection of dome material. Optical screening was employed, which required hand testing and careful evaluation of material before the forming process was begun. An additional electronic compensation circuit was added to eliminate the effects of the

(7) M. G. Secord and J. R. Tuominen, Report of Flight Worthiness Tests on the YG1185A01 "r", Phases I and II, Avionics Division, Honeywell, Oct 1976

small imperfections that remained after forming. Domes that did not meet the optical specification of the laser qualified domes were used on other phase sensors. Another dome-related problem was discovered during Aquila flight tests and was corrected by a modification to the RPV. The problem was that a combined movement of the air frame structure, sensor shock mounts and gimbal deflection allowed the dome to impact the skin line aft of the sensor opening during launch. This required the removal of minor aircraft skin and structure to enlarge the sensor opening in the bottom of the fuselage.

The Nd:YAG laser developed by International Laser System had some laser output power problems during development. These problems were traced to the polarizer. A replacement for this part by one from another vendor eliminated this characteristic. The laser tests with an integrated system revealed a requirement for magnetic shielding. Mumetal was used to encase the laser components, which included the laser battery. The dome guard and filter wheel acted as antennas and picked up the magnetic field of the power supply. These metal parts were removed and replaced by nonmetallic parts. The interference was observed in the video during laser fire. The original beam divergence was specified as 0.5 mradian. The laser that was developed was able to maintain a beam divergence of less than 0.3 mradian. An additional laser-related problem was discovered during laser range accuracy tests. Range readings of twice the proper value were continually observed. Analysis showed the cause to be a shift enable pulse that was being applied one-half count early. The shifted data then carried an extra count in the most significant bit position.

The integration and system tests of all phases of sensors were conducted at Fort Huachuca, Arizona, with a fully operating Aquila system. These tests are described in Section IV of Volume III of this report.

Section IV
DATA-LINK SYSTEM EVOLUTION

The Aquila data-link system consists principally of the following:

- **Ground-Based Equipment**
 - Ground command transmitter
 - Ground telemetry receiver
 - Ground encoder/decoder
 - Tracking antenna system
- **Airborne Equipment**
 - Command antenna
 - Command receiver
 - Encoder/decoder
 - Video-telemetry transmitter
 - Telemetry antenna

The final system is described in Volume I of this report. This section describes the evolution of the data-link system.

4.1 BACKGROUND

As RPV hardware has grown in complexity, data-link requirements have become more comprehensive. The selection and adaptation of existing light-weight satellite, missile, and aircraft data-link hardware has been the primary approach to the acquisition RPV data-link elements. This approach was employed successfully on the Tuboomer, Aesquare, and other RPV programs. Consequently, the Aquila data link was generated in the same manner.

4.2 REQUIREMENTS

A summary of the requirements recognized for the data link at the onset of the Aquila program included the following:

- **Data Link**
 - Range: 20 km
 - Altitude: 2,000 ft AGL and above
- **Command-Control (including telemetry)**
 - Range: 20 km
 - Altitude: 1,000 ft AGL and above
- **Fall-safe response to link loss**
- **Telemetry of RPV status data**
- **RF compatibility with test range**
- **Protection against inadvertent RF interference**

4.3 DATA-LINK SYSTEM APPROACH

The evolution approach for the Aquila data link included the following:

- **Analyze the link requirements and specify components.**
- **Procure and/or adapt existing proven hardware.**
- **Acceptance test the system elements at the vendor facilities.**
- **Integrate the data-link system elements into the GCS and RPV systems.**
- **Validate system operation in anechoic chamber, range, ground, and flight tests.**

4.4 DATA-LINK SYSTEM REQUIREMENTS EVOLUTION

Evolution of the data-link system was based on meeting the primary requirement of providing a reliable link over the RPV operating envelope of 20 km and 10 kft AGL. Another requirement was to provide precision real-time RPV location data for navigation and payload target locating.

It was also desirable to minimize development risk. This was accomplished through mechanizing the data-link system with vendor off-the-shelf hardware. Quality and performance tests were performed at the subcontractors on a package level with LMSC witnessing such tests. The system test was performed at LMSC to verify conformance with the data-link requirements.

The data-link system requirement did not change from the start of the program to its completion. However, the data-link configuration went through two cycles of design changes to arrive at the present configuration. The first major design changes were the "A" changes resulting from the Aquila Phase I testing at Crows Landing. The "A" changes involved data-link system compatibility-type changes and identification of critical interface specifications for each data-link element. These specifications resulted in extensive testing of each data-link component and an analysis of system requirements. The next set of changes resulted from the Aquila Phase II testing at Fort Huachuca, resulting in the "B" changes. These "B" changes were based on a desire to increase the link margin of the data-link system.

Summaries of the data-link margins for each of the three data-link configurations are given in Tables 13, 14, and 15. As indicated by the tables, the changes resulted in significant improvements. The link closure range was increased by a factor of 150 for the command link, a factor of 45 for the telemetry link, and a factor of 5 for the video link.

Frequency selection was based on hardware availability, required bandwidth, range and pointing accuracy, physical constraints (size and weight), and frequency allocation availability (licensing). Production flight and ground hardware in the D (1 to 2 GHz), E (2 to 3 GHz), and G (4 to 6 GHz) bands is available. Of the three, G-band was the most attractive for the following reasons: (1) high-gain capability (tracking accuracy) of the ground antenna, (2) physical constraints (portable) on the ground antenna, and (3) frequency allocation availability. Furthermore, a portion of G-band (4.4 to 5 GHz) has been

TABLE 13. LINK ANALYSIS - ORIGINAL DATA LINK

Uplink

Command Transmitter Power (10 W)	+40 dBm
Transmit Antenna Gain	+12 dBi
Space Loss (20 km)	-133 dB
Polarization Loss	-3 dB
Airborne Receive Antenna Gain	-10 dBi
Receiver Sensitivity	<u>-(-65) dBm</u>
Fade Margin:	<u>-29 dB</u>

Downlink

	<u>TM</u>	<u>Video</u>
Video Transmitter Power (10 W)	+40 dBm	+40 dBm
Transmit Antenna Gain	-15 dBi	-15 dBi
Space Loss (20 km)	-133 dB	-133 dB
Polarization Loss	-3 dB	-3 dB
Ground Receive Antenna Gain	+24 dBi	+24 dBi
Receiver Sensitivity	<u>-(-76) dBm</u>	<u>-(-82) dBm</u>
Fade Margin:	<u>-11 dB</u>	<u>-5 dB</u>

TABLE 14. LINK ANALYSIS - "A" CHANGE

Uplink

Command Transmitter Power (10 W)	+40 dBm
Transmit Antenna Gain	+12 dBi
Space Loss (20 km)	-133 dB
Polarization Loss	-3 dB
Airborne Receive Antenna Gain	-7 dBi
Receiver Sensitivity	<u>-(-94) dBm</u>
Fade Margin:	<u>+3 dB</u>

Downlink

	<u>TM</u>	<u>Video</u>
Video Transmitter Power (10 W)	+40 dBm	+40 dBm
Transmit Antenna Gain	-7 dBi	-7 dBi
Space Loss (20 km)	-133 dB	-133 dB
Polarization Loss	0 dB	0 dB
Ground Receive Antenna Gain	+24 dBi	+24 dBi
Receiver Sensitivity	<u>-(-85) dBm</u>	<u>-(-83) dBm</u>
Fade Margin:	<u>+9 dB</u>	<u>+6 dB</u>

TABLE 15. LINK ANALYSIS - "B" CHANGE, FINAL CONFIGURATION

Uplink

Command Transmitter Power (10 W)	+40 dBm
Transmit Antenna Gain	+24 dBi
Space Loss (20 km)	-133 dB
Polarization Loss	0 dB
Airborne Receive Antenna Gain	-10 dBi
Receiver Sensitivity	<u>-(-94) dBm</u>
Fade Margin:	+15 dB

Downlink

	<u>TM</u>	<u>Video</u>
Video Transmitter Power (10 W)	+40 dBm	+40 dBm
Transmit Antenna Gain	-7 dBi	-7 dBi
Space Loss (20 km)	-133 dB	-133 dB
Polarization Loss	0 dB	0 dB
Ground Receive Antenna Gain	+24 dBi	+24 dBi
Receiver Sensitivity	<u>-(-88) dBm</u>	<u>-(-85) dBm</u>
Fade Margin:	<u>+12 dB</u>	<u>+9 dB</u>

designated by the military services for drone and RPV use. Finally, experience has shown that obtaining allocations in the D- and E-bands is a long and difficult process because of already overcrowded conditions. Preliminary study indicated G-band availability at all Army test sites envisioned for the demonstration program.

Frequency allocation requests for the primary frequencies of 4.530 GHz (video/TM link) and 4.861 GHz (command link) were approved for use at Sunnyvale, Bicycle Lake, Fort Huachuca, and Fort Sill. Sets of alternate frequencies of 4851/4520 and 4841/4510 GHz were approved for backup (command/video).

4.5 AIRBORNE DATA-LINK COMPONENT EVOLUTION

4.5.1 Antennas

The initial RPV antenna development involved selection of antenna location to provide the best radiation coverage over the RPV operation envelope. Since

the development of the vehicle occurred in parallel with antenna development, testing was initially performed with the half-scale model. A number of locations compatible with the aerodynamic and structural requirements were investigated (Reference 8). The locations and patterns were traded off against gain coverage, hardware complexity, and operational reliability. After the analysis, the forward nose and aft shroud locations were selected as optimum. These locations are depicted in Figure 65.

Another consideration was use of a common antenna for both uplink and downlink. This would involve the addition of a diplexer. A tradeoff on the size, cost, and weight penalty of one antenna and a diplexer versus two antennas revealed a significant advantage with two antennas.

The original antenna selection was a biconvex blade antenna manufactured by Tecom. However, radiation patterns of this antenna revealed that a deep null existed in the azimuth plane, which should have approached omnidirectional characteristics. A substitute antenna was designed by LMSC to provide an omni-coverage independent of ground planes. This antenna was a sleeve dipole configuration that was subcontracted to Tecom for fabrication.

During the Phase I Aquila testing, a full-scale Aquila RPV was available for verifying antenna patterns. These patterns revealed two large -15 dB null areas on the bottom-mounted antenna. This discrepancy was caused by an added hook assembly that was to be used for recovery of the RPV, which was not fully defined at the time of half-scale model tests. Therefore, for the "A" change, another location was selected after a series of measurements was performed on several alternate locations. The selected location was a top, forward area with the antenna mounted on a 12-in. mast. This location is shown in Figure 66.

(8) Lockheed Missiles & Space Company, Inc., Aquila RPV System Test Report, CDRL AOOD, RPV Antenna Patterns, LMSC-L028081, Part 5, Sunnyvale, Calif., 31 May 1977

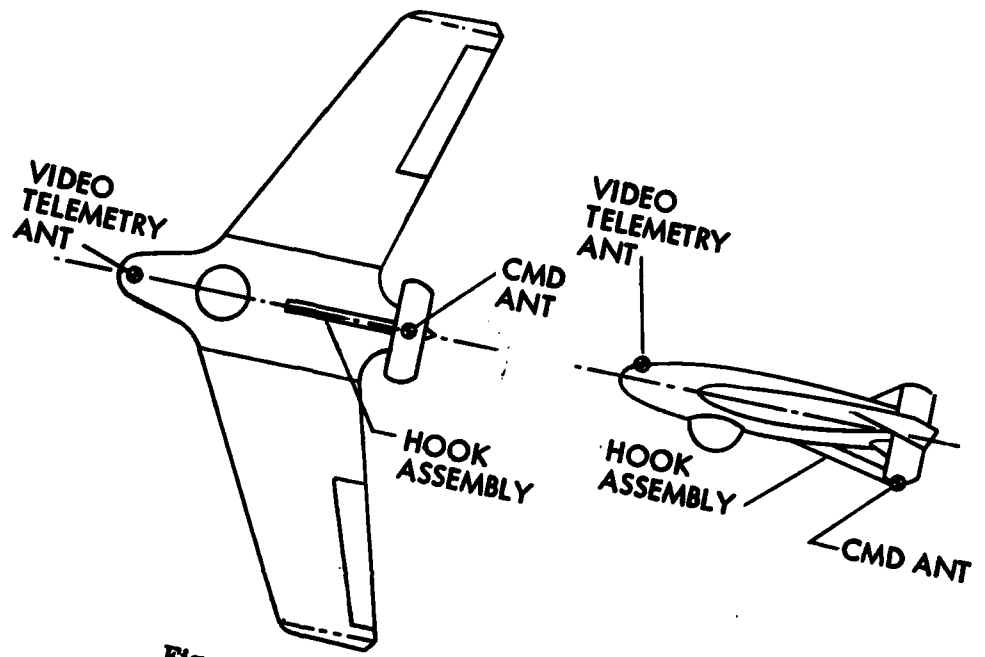


Figure 65. Original Antenna Location

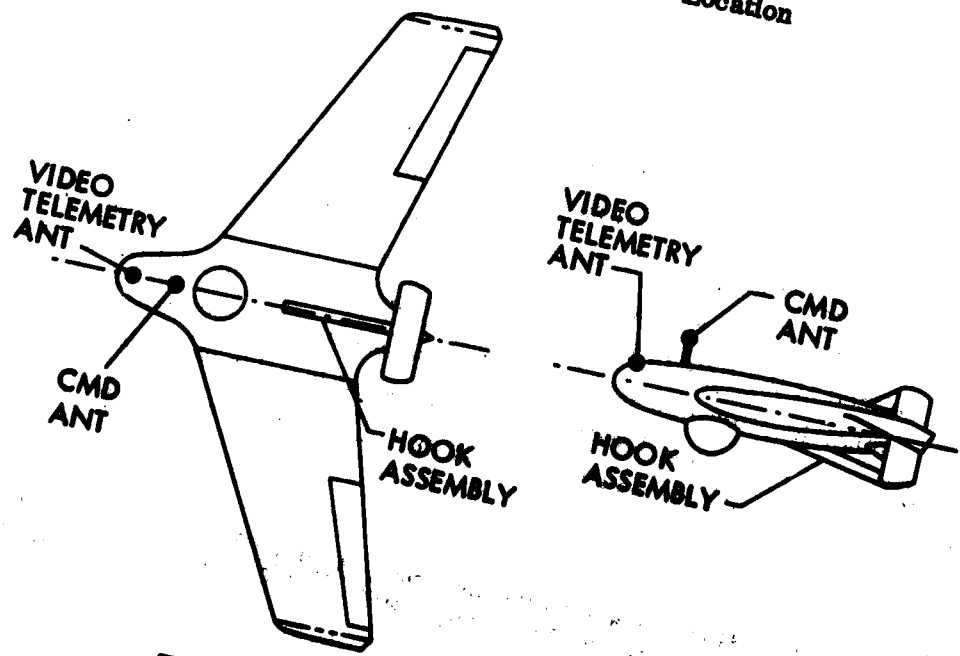


Figure 66. Antenna Location Mod A

During the Phase II Aquila testing, it was determined that the mast-mounted antenna was vulnerable to physical damage during RPV recovery operations. At the same time the recovery method was changed to a net recovery, eliminating the requirement for the hook assembly. Therefore, on the "B" change, the command antenna was moved back to the aft shroud location.

4.5.2 Command Receiver

The command receiver was a standard off-the-shelf airborne receiver that was used at various frequency bands; it was developed and manufactured by AACOM. The design was modified to operate at the command link frequency of 4.861 GHz. During Aquila Phase I testing, extensive problems were encountered in closing the command link even at relatively short ranges. After link loss in the first Crows Landing flight, laboratory tests revealed that the receiver was very susceptible to interference, particularly on the downlink frequency. This interference was entering the receiver through the antenna port and also through the wiring harness.

During the "A" change, the receiver was modified in three areas: (1) the local oscillator frequency was changed, (2) EMI filtering was increased within the receiver, and (3) additional acceptance testing procedures were incorporated. The receiver local oscillator frequency was changed from 4.691 to 5.031 GHz such that the local oscillator is operating above the command frequency. In the original condition the receiver was especially susceptible to video transmitter interference since the image frequency of the receiver was 4.511 GHz, which was only 19 MHz off the video transmitter frequency of 4.530 GHz. The added EMI filtering eliminated the possibility of interference leaking into the receiver, bypassing the preselector.

The added acceptance tests included a receiver sensitivity test tied in with the bit synchronizer to verify a lock condition. Also, an EMI test was performed to demonstrate immunity of the receiver to the video transmitter signal.

These added tests ensured the proper performance of the command receiver when operating in the RPV environment.

During Phase II testing, several command link problems occurred and no data were available other than theoretical calculation of the margin actually available for the command link. Therefore, on the "B" change, all the command receivers were retrofitted with a received signal strength output to the telemetry status. This signal was then available to aid in the evaluation of the command link. All analysis indicated that the theoretical analysis agreed with the TM data.

4.5.3 Video Transmitter

The transmitter is a modification of an existing G-band transmitter design developed by AACOM. The modification involved increasing the power output from 5 to 10 W. The transmitter is a solid-state design utilizing power amplification at one-third the output frequency and then is used to drive a power Varactor tripler to obtain the required 10 W at 4.530 GHz.

In the Mod "A" change, the subcarrier level was increased from -28 to -20 dB below the video power output. This provided an 8-dB improvement in the telemetry status link with negligible change in the video link.

4.5.4 Encoder/Decoder

The encoder/decoder design is essentially a standard AACOM unit that has been used on other RPV programs. The unit is repackaged onto three printed-circuit cards for integration into the Aquila FCEP.

During Phase I, testing problems were encountered on decoding the command signals out of the receiver. The decoder had problems locking on the command signal initially, and reacquiring lock after link loss. This was traced to a problem in the bit synchronizer phase-lock circuitry. The bit synchronizer was locking up on noise, and when a command was received the phase-lock

loop would not break out of the lock with the noise. A problem was also encountered in the phase-lock loop locking on quadrature phase which injects a step error of approximately 640 m or multiples thereof into the ranging of the RPV. Two modifications were made in the decoder bit synchronizer to remedy these problems: (1) the phase-lock loop was inhibited when the signal-to-noise ratio of the input signal from the command receiver was less than unity, and (2) the phase-lock loop was changed to prevent the loop from locking on the quadrature component of the input signal.

4.6 GCS DATA LINK ELEMENTS EVOLUTION

4.6.1 Tracking Antenna

The tracking antenna system (Reference 9), consisting of the radome, antenna pedestal, antenna dish, feed network, and antenna control unit, is a version of the tracking antenna system initially developed for the Patuxent River Naval Air Test Facility by EMP, Inc., Chatsworth, California.

On the initial interfacing of the tracking antenna to the GCS it was discovered that inadequate isolation existed between the transmit and receive antenna system. This caused saturation of the preamplifier, degrading the receiver system. This was remedied by the addition of a bandpass filter in front of the preamplifier.

After the Phase I testing, comprehensive tests of the tracking antenna system were performed. These tests revealed the following deficiencies in the antenna system: (1) excessive boresight shifts were measured as a function of transmitter antenna polarization and (2) there was inadequate antenna beam coverage in the elevation plane, leaving large areas in the RPV operation envelope where the video/TM link would not close.

(9) Lockheed Missiles & Space Company, Inc., Aquila RPV System Test Report, CDRL AOOD, GCS Tracking Antenna Development, LMSC-L028081, Part 9 Sunnyvale, Calif., Sept 1977

The "A" changes involved changing the feed on the parabolic dish from a pair of crossed dipoles to a pair of vertical dipoles. This change reduced the bore-sight shift versus polarization from ± 1.2 to ± 0.5 deg and versus elevation angle from ± 0.3 to ± 0.05 deg. A low-gain antenna system was added to provide coverage in the elevation plane. The low-gain antenna system consisted of a pair of helical antennas mounted in front of the dipole feeds. The high-gain and low-gain antenna system selection was controlled by the GCS computer via a set of coaxial switches. In addition to these changes, a prelaunch data-link confidence test was incorporated by adding a calibration network on the antenna pedestal. The network consisted of 50-dB attenuators that are switched into the uplink and downlink signal paths.

For the "B" change, it was desired to increase the margins for both uplinks and downlinks. This was accomplished by changing the low-gain antenna system from a two-element to a four-element array. The receiver feed network was reconfigured to reduce losses and improve the receiver noise figure. To increase the uplink margin, the command transmitter output was diplexed into the receiver antenna system, thereby increasing the effective radiated power by 12 dB. A summary of antenna changes is shown in Figure 67.

During the "B" changes the tracking servo loop on the antenna system was tested and analyzed. As a result of this study, the following modifications were incorporated into the antenna control unit: (1) stabilization of the bias circuit in the servo loop, (2) balancing the demodulator circuit, (3) addition of a null gate operated by the received rf level, and (4) increasing the servo gain for the low-gain antenna.

4.6.2 Command Transmitter

The command transmitter is a crystal-controlled, solid-state transmitter that is adapted from a standard model developed and manufactured by AACOM. The transmitter meets all advertised specifications and was compatible with all other data-link elements. No changes were instituted during the program.

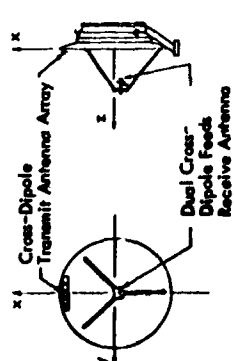
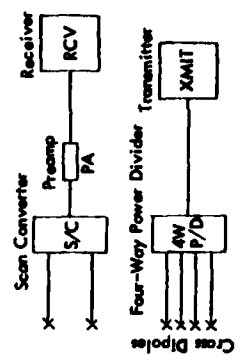
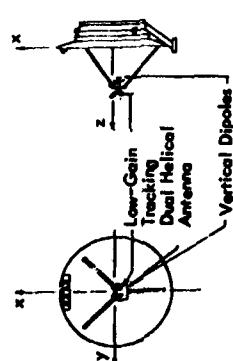
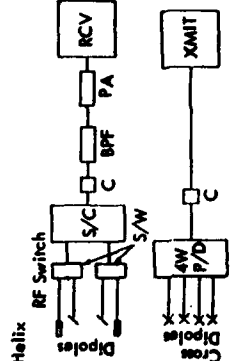
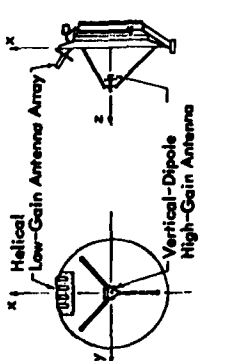
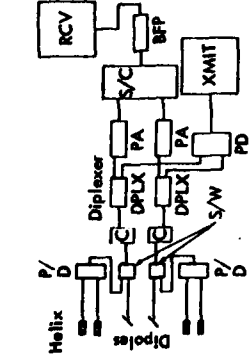
System Configuration	Antenna System Description	Antenna Configuration	RF Block Diagram
Original	<p>Tracking Antenna</p> <ul style="list-style-type: none"> 2-ft parabolic dish with offset cross-dipole array Scan converter (S/C) and preamp (PA) <p>Transmit Antenna</p> <ul style="list-style-type: none"> Four-cross-dipole array tilted 15 deg up Four-way power divider (P/D) 	 <p>Cross-Dipole Transmit Antenna Array Dual Cross-Dipole Feeds Receive Antenna</p>	
A Mod	<p>Tracking Antenna</p> <ul style="list-style-type: none"> High gain: 2-ft parabolic dish with offset vertical dipole array Low gain: Dual helical array tilted 30-deg up Each is common to calibration network, bandpass filter (BPF), and scan converter through rf switches. <p>Transmit Antenna</p> <ul style="list-style-type: none"> Four-way power divider and a calibration (C) network 	 <p>Low-Gain Tracking Dual Helical Antenna Vertical Dipole Feed Receive Antenna</p>	
B Mod	<p>Tracking and Transmit Antenna</p> <ul style="list-style-type: none"> High gain: 2-ft parabolic dish with focal-fed vertical dipole array Low-gain: four-helical array tilted 30 deg up Each is common to calibration network, bandpass filter, and scan converter through rf switches (S/W). The transmit section contains four-way power divider. The tracking section contains additional preamps, scan converter, and bandpass filter. 	 <p>Helical Low-Gain Antenna Array Vertical-Dipole High-Gain Antenna</p>	

Figure 67. Summary of the GCS Antenna Changes

4.6.3 Video-TM Receiver

The video-TM receiver is a standard, fixed-frequency, ground-based receiver developed and manufactured by AACOM, Inc. The receiver performed per vendor specifications and no modifications were made during the program.

4.6.4 Encoder/Decoder

The encoder/decoder design was adapted from previously developed AACOM PCM encoder/decoder units. The encoder/decoder was repackaged into the 9- by 7-in. printed circuit card for installation into the EIU package. The encoder/decoder performed per vendor specification and no changes were made during the program.

4.7 SYSTEM EVOLUTION

Since the data link was envisioned to be minor modifications of off-the-shelf operating data-link hardware, the data-link development was assigned to data-link subcontractors: (1) AACOM for the transmitters, receivers, and encoder/decoder; (2) EMP for the GCS tracking antenna; and (3) Tecom for the airborne antennas. The subcontractor's advertised component performance parameters were used in determining the ability of the data link to meet Aquila data-link requirements. Because of the tight development schedule, minimal system tests were performed prior to Phase A testing; however, during Phase A Aquila testing, it was evident that the data link was not meeting the requirements. Engineering actions were initiated to isolate the deficiencies and recommend solutions.

A comprehensive test program was conducted on each data-link component. The outcome of these test programs was an expanded set of performance specifications for each component to ensure compatibility among the parts of

the RPV data-link system. Deficient areas were negotiated with the subcontractors to obtain a tradeoff for the optimum point of partitioning the specifications.

Extensive antenna measurements were performed on the tracking antenna revealing the major changes required. A tradeoff was made as to whether these changes should be contracted to EMP (the vendor for the tracking antenna) or whether LMSC should institute the changes. Several factors were considered in reaching this decision. The major factor was scheduling. These changes were to be made between Phase A and Phase B testing. Also, the changes to all the data-link components were to be performed simultaneously. Therefore, various performance parameters were likely to change depending on whether the other components were successful in meeting their new specifications. Finally, the test data measured on EMP's antenna test range did not agree with LMSC's measured data. Since all data and specifications were based on LMSC measurements, it was imperative that a uniform set of performance data be available for analysis.

In view of the schedule and interface definition problems, it was decided that LMSC should make the changes on the tracking antenna system. This provided the flexibility of delaying the freeze on the antenna performance requirements until after the negotiated changes with the other data-link contractors had been verified.

After the completion of the "A" change, each component was again evaluated and the total link measured. Analyses were performed on the initial Phase B flights to verify the bench measurements and theoretical link calculations.

Analysis of the Phase B flight data indicated that two areas of data-link improvement were needed: (1) more link margin was desirable and (2) the low-gain antenna tracking loop gain was low, providing poor tracking performance.

Tradeoff studies were made in areas of the data link where improvement could be made without impacting the schedule or the configuration of the RPV, which would negate the Phase B testing. A study and measurement program was also initiated to determine whether a single antenna could provide adequate elevation coverage on the GCS. This would solve the poor low-gain tracking problem and eliminate the complexity of a dual antenna system. This study yielded an unacceptable compromise of marginally providing elevation coverage at the expense of degrading the "A" configuration high-gain antenna performance. Therefore, the "B" changes were instituted to provide the required improvement with minimal risk to schedule and to achieve desired performance.

Section V GROUND SUPPORT SYSTEM

The Aquila Ground Support System (GSS) consists of:

- Ground Control Station
- Launcher
- Retrieval System
- Electrical Generators
- Ground Support, Test, and Checkout Equipment

These elements are arranged within specified guidelines to ensure harmonious and reliable operation. The GSS and its elements, as delivered to the Army, are described in Volume I of this report. This section describes the significant analyses, design, development, and testing involved in the evolution of the Ground Support System and its elements.

5.1 GSS EVOLUTION

The integrated ground support system evolved through operational requirements and considerations, and changes necessitated by design changes in the various system elements. The evolution is characterized by an increase in mobility through truck and trailer mounting of components, and variations in arrangement to improve operational reliability. The evolution of the GSS is described in the following paragraphs.

5.1.1 Background-Situation

In previous mini-RPV programs, such as Praeire and RPAODS, the ground support systems were improvised with existing equipment with little or no consideration for mobility, operational reliability, or Army hands-on operation.

The short life and scope of these programs did not warrant such considerations. Army experience with mobile systems such as the Hawk Missile System provided a basis for establishing the mobility requirements for an Army Mini-RPV system. However, the scope of the Aquila system technology demonstrator program required some cost and schedule compromise from the effort required to provide full mobility. Consequently, the initial approach was selected to provide truck transportable, ground-based system elements. This approach was to be modified considerably as operational considerations eventually led to increased truck and trailer mounting of the primary system elements.

Ground layout of the system elements was determined primarily with considerations for clear launch and recovery flight paths and logical arrangement for system operation. Because of the unique nature of the Aquila system, no other precedents were available. The criteria for GSS layout and operation were initially derived from the Army procurement documentation. Refinements were derived from actual field operations. The initial requirements for the GSS are described in the following paragraph.

5.1.2 GSS Requirements

A summary of the initiating contract requirements for the ground support system follows:

- **Commonality with all five sensor/mission phases**
- **Up to four sorties per day - 4 days per week, 1 hour per flight**
- **Launch and recovery in unprepared areas**
- **Minimum crew for total system operation**
- **Minimum time and skill required for assembly and disassembly for launch and recovery operations**
- **Minimal detectability by enemy of launch and recovery operations**
- **Ground transportability requirements compatible with existing conventional Army ground vehicles**

- Maximum compatibility with and utilization of current and near future standard military equipment
- Navigation and control systems suitable to program objectives
- Ground control elements contained in a suitable air-conditioned/heated mobile shelter, including:
 - Navigation system
 - Control console
 - Displays
 - Recorders (video)
 - Ground data link
 - Computer
- Minimum length launch and retrieval systems, fully portable, and transportable on standard Army ground vehicle; minimum observables; no more than two people required to set up, tear down, and operate to launch or recover one aircraft; minimum time/skill to operate
- Insofar as possible, standard ground support equipment available through SB 700-20, "Army adopted and other items of material selected for authorization"
- Systematic checkout prelaunch procedure, adequate to ascertain adequate subsystems performance prior to launch; all necessary checkout of equipment transportable and compatible with the GCS and launch and retrieval systems; minimum time and skill for checkout

5.1.3 GSS Evolution Approach

The approach to meeting the Army requirements included the following:

- Commonality. The Ground Control Station console was designed to be compatible with any RPV-payload-mission options by proper switch positioning on the control panels.

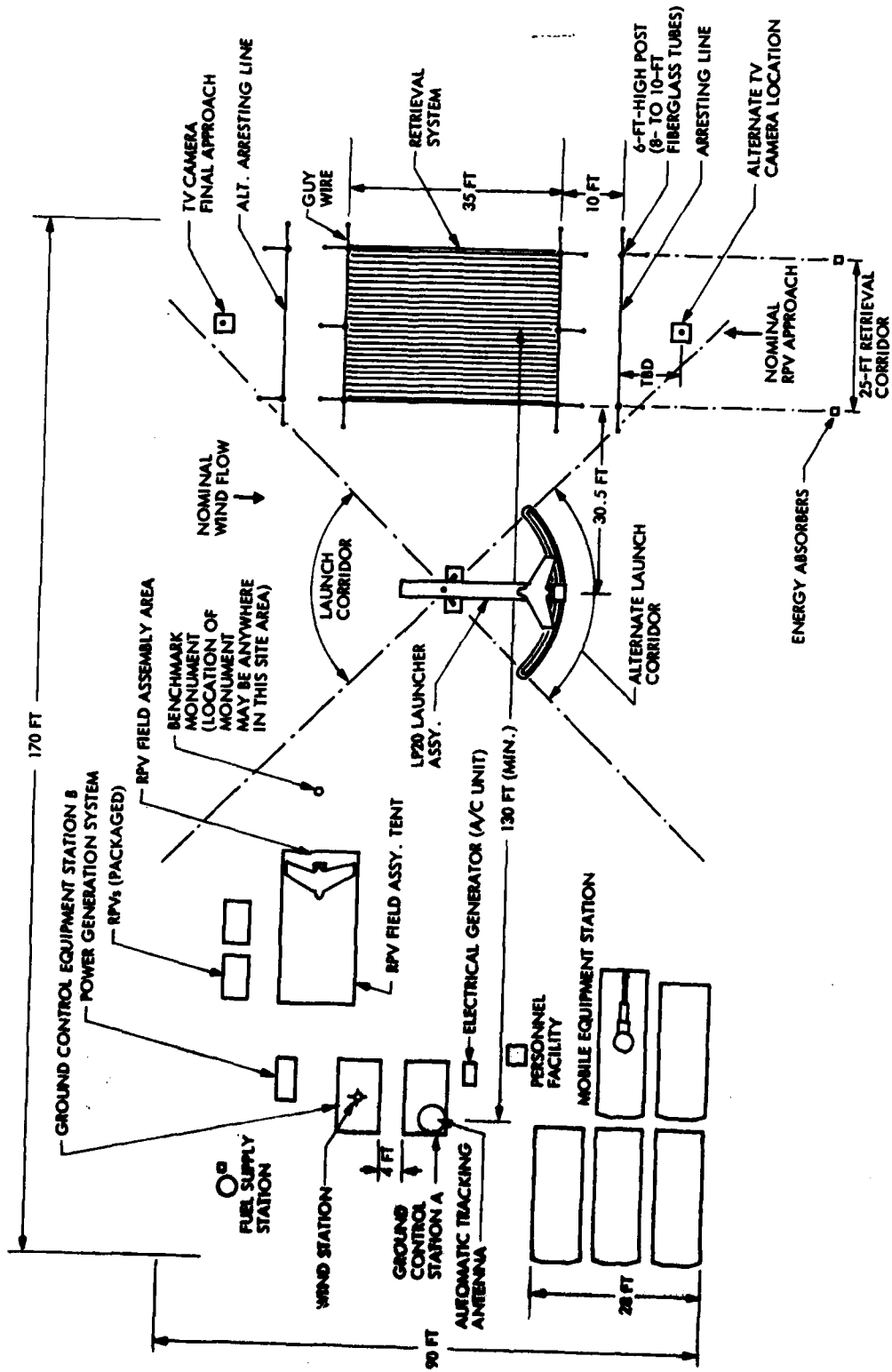
- Operational rate. Checkout procedures and equipment were generated to support the specified mission rates, subject to logistic support and crew rotation.
- Operation in unprepared areas. Truck access, clear launch-recovery paths, clear rf paths, and reasonable cable paths between system elements were the only constraints to be observed.
- Minimum crew/time/skill for total system operation. Emphasis on automated computer operations and simple mechanical systems and interfaces minimized personnel requirements.
- Minimal detectability. Use of standard Army elements (where possible - trucks, shelters, trailers) subject to camouflage techniques, and use of minimum size elements such as launcher and retrieval systems - compromised only for reliability - were employed to minimize detectability. No smoke-generating elements (such as launch rockets or starting cartridges) or high-level noise generators were selected.
- Transportability-compatibility. No special vehicles were required, and no major modifications of existing vehicles were allowed. Only conventional Army equipment was required as GFE.
- Navigation-control. The computer in conjunction with the ground data-link elements was used extensively to ensure the required navigational and control accuracies.
- Ground control elements. A soft mockup was used to establish proper man-machine interfaces and input-output displays, equipment, and techniques. Digital and analog simulations were used to update and refine the design.
- Minimum length launch-retrieval. These were established primarily by the RPV load capability - 6 g fore, aft, and vertical. Recovery length was left flexible to establish requirements for reliable clearance of frame elements by the RPV during field tests.
- Systematic checkout. The RPV suitcase tester and GCS computer were employed in step-by-step procedures to ensure reliable checkout.

5.1.4 GSS Evolution

The details of the GSS evolution to meet system requirements are contained primarily in the discussions of the GSS elements that follow this section. However, it is appropriate to discuss the evolution of the GSS site layout at this point, to "frame" the overall evolution of the GSS.

Figure 68 shows the initial site layout concept. Initially it was anticipated that two shelters would be required to house the required ground control elements. All elements, including the shelters, launcher, and retrieval system were truck transportable and ground-based during operation. A truck-mounted crane was required for loading and placement of system elements. A suitable distance was provided between the launcher and retrieval systems and the tracking antenna to ensure that the RPV speed did not tax the antenna slew rate. Launch and recovery corridors were parallel insofar as practical with a swivel and switchable capability for the launcher and switchable capability for the retrieval system to accommodate wind direction for launch and recovery operations. Launch and recovery paths were kept clear of other system elements. An RPV assembly area (tent) was located close to the launcher. Other elements were located to be compatible with reliable safe operation.

Figure 69 reflects the site arrangement envisioned at the preliminary design review. All elements remained ground based for operation, but truck transportable. Through careful design and interface review, the need for the second shelter was eliminated. The assembly area was repositioned to minimize the possibility of truck traffic over the interconnecting cables. During the preliminary design review, site set-up and tear-down time appeared to be excessive because of insufficient mobility of the major system elements. Consequently, the decision was made to operate the GCS and launcher from truck-mounted positions and to trailer mount the generators to enhance mobility and flexibility and to eliminate the need for a crane. The resulting GSS arrangement is shown in Figure 70. This site concept was selected for field testing. During field



20
14

Figure 68. Initial Aquila Site Layout

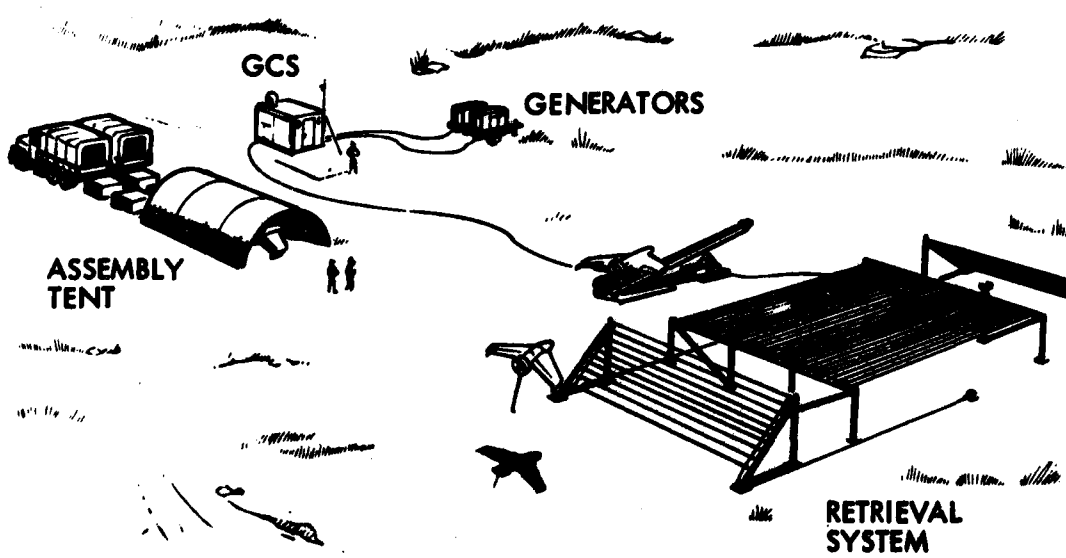
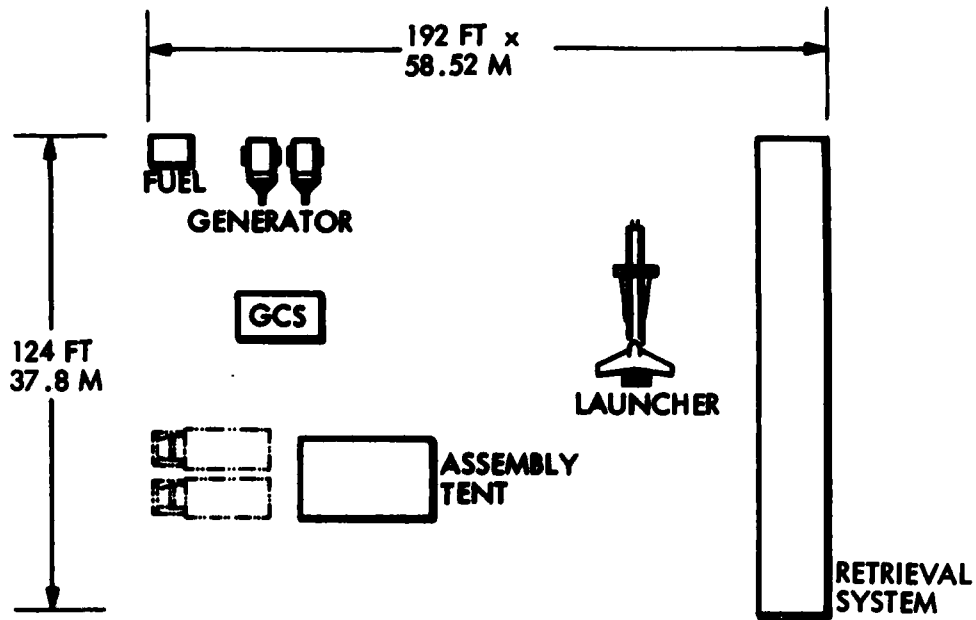


Figure 69. Preliminary Aquila Site Layout



Figure 70. Aquila Site Layout With Truck-Mounted GCS and Launcher

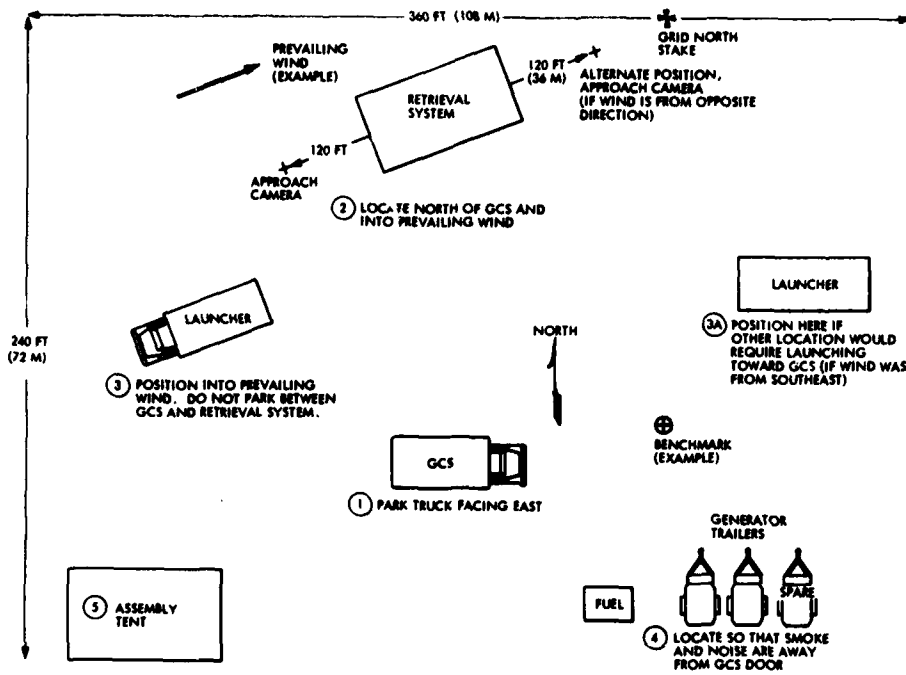
testing; the arrangement was refined to eliminate multipath problems under certain circumstances and to improve operational reliability and efficiency. The procedural refinements are reflected in Reference 10. In addition to the procedural evolution, adaptation of the vertical barrier recovery system (trailer mounted) completed GSS evolution. Figure 71 shows the final site concept, which is described in Volume I of this report.

5.2 GROUND CONTROL STATION (GCS) EVOLUTION

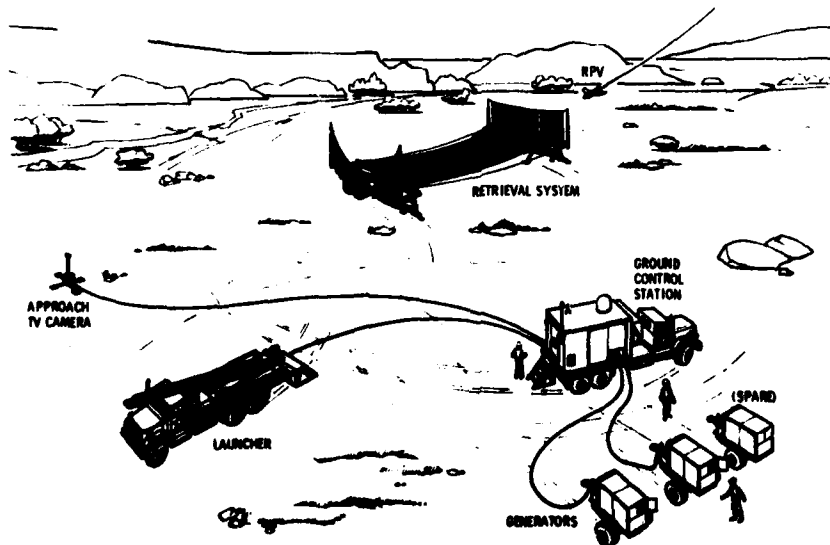
The Aquila Ground Control Station evolved from an S-280 standard Army shelter. The shelter is fitted with a heater/air-conditioner for personnel comfort and equipment air conditioning. The station contains all system controls (except launcher control box and electrical generator controls), displays, and recorders, including:

- Ground Control Console:
 - RPV controls-displays
 - Sensor controls-displays
 - Tracking antenna controls-displays
 - Plotting boards
 - Weather data display
 - Intercommunication controls
 - Electronic interface unit
 - Computer processing unit
 - Ground data link
- Teletype
- Digital Tape Recorder
- Auxiliary Electronics Cabinet
- Video Recorders
- Paper Tape Input Unit
- Air-Conditioner Controls

(10) Lockheed Missiles & Space Company, Inc., Technical Manual for Aquila RPV System Technology Demonstrator, System Description, LMSC-D056906, Volumes I, II, and III, Sunnyvale, Calif., 10 Aug 1977



a. Site Layout (Typical)



b. Deployed Aquila System

Figure 71. Final Aquila Site Layout

This section describes the evolution of the GCS; the final system is described in Volume I of this report.

5.2.1 Background

In prior Mini-RPV programs - i. e. , Aequare, Praeire, and RPAODS - no integrated ground control station that controls all system operations and is suitable for Army hands-on operation had been developed. However, experience with these programs provided insight to the Army as to the desired characteristics for a technology demonstration system. As a result of this experience and experience with such field systems as the Hawk missile system, the Army formulated requirements for a system that would provide Army hands-on experience with an RPV control station with capabilities representative of those envisioned for tactical RPV systems.

5.2.2 Approach

The approach to ground control station evolution was driven primarily by Army requirements. These included the use of a standard Army shelter and inclusion of specified displays, controls, and recording capabilities. Component selection was directed primarily at low-cost components with adequate performance to represent the performance capabilities of a tactical system, while lacking its ruggedness and (to a lesser extent) its reliability (and at a small fraction of its cost).

Insofar as practical, within the scope of the program, routine tasks and decisions were programmed for performance by the computer processor unit.

A soft mockup was used to evaluate the display-controls arrangement through the performance of mock missions.

5.2.3 Requirements

The requirements for the Ground Control Station are essentially described in the GSS requirements list, subsection 5.1.2.

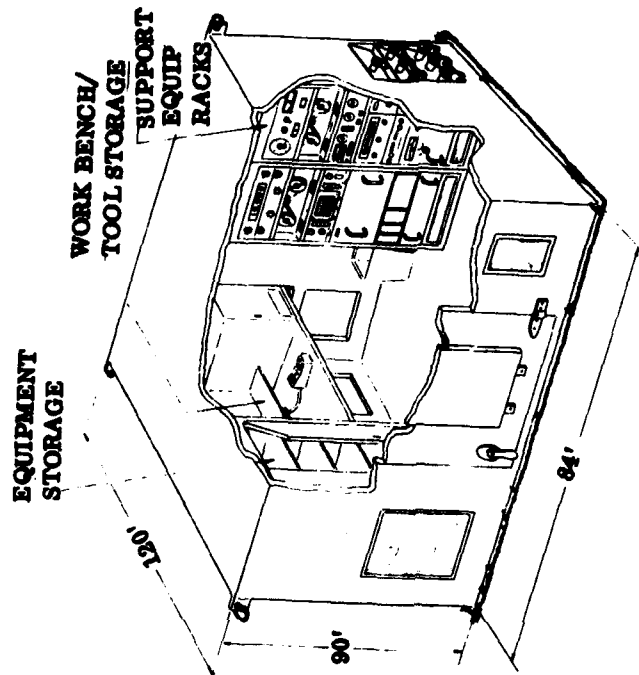
5.2.4 Ground Control Station (GCS) Evolution

As originally proposed, the Ground Control Station was to consist of two S-280 shelters: one containing mission control electronics and operator's positions and the other containing support and test equipment, noncritical mission hardware, and a maintenance area. This configuration is shown in Figure 72.

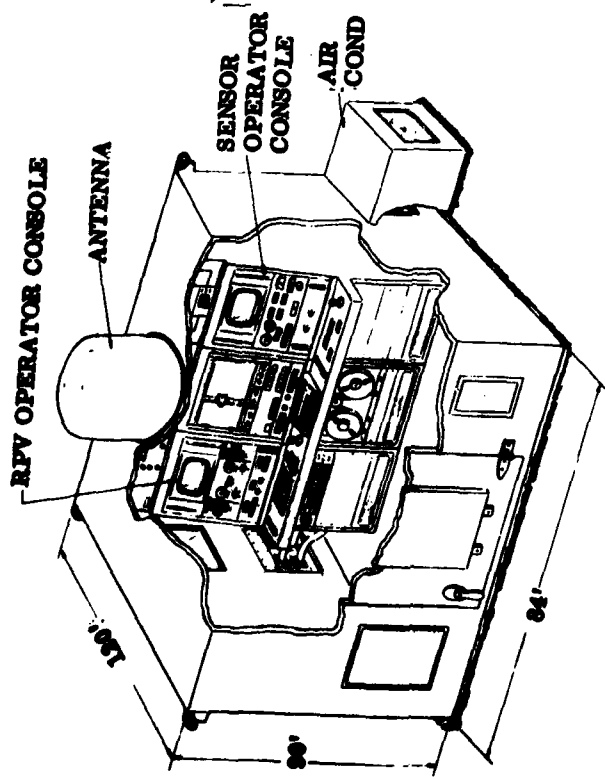
Cost and schedule constraints led to the final, single-shelter arrangement. The mission hardware from the second shelter was accommodated in the single shelter through addition of another equipment rack to the left of the RPV operator position and some wall-mounted bracketry to the right of the sensor operator. The additional, or auxiliary, equipment rack came as top and bottom halves, with the bottom containing electronics and the top used initially for miscellaneous storage. The location initially chosen for the digital tape recorder proved undesirable because of that unit's tendency to pull dirt from the floor into its vacuum tape positioning chambers. This led to its being relocated in the top half of the auxiliary rack. The final GCS component arrangement is shown in Figure 73.

The Figure 72 Shelter Number 1 console location proved undesirable with the addition of the auxiliary console. The control console was moved to a long wall, the wall to the left as the door is entered. The air conditioner and its input and output ducts were relocated on the wall opposite the door.

Console installation was a problem with the existing shelter entry dimensions, so a large panel was cut into the wall behind the control console. This panel



SHELTER NO. 2



SHELTER NO. 1

Figure 72. Initial Ground Station Shelter Configuration

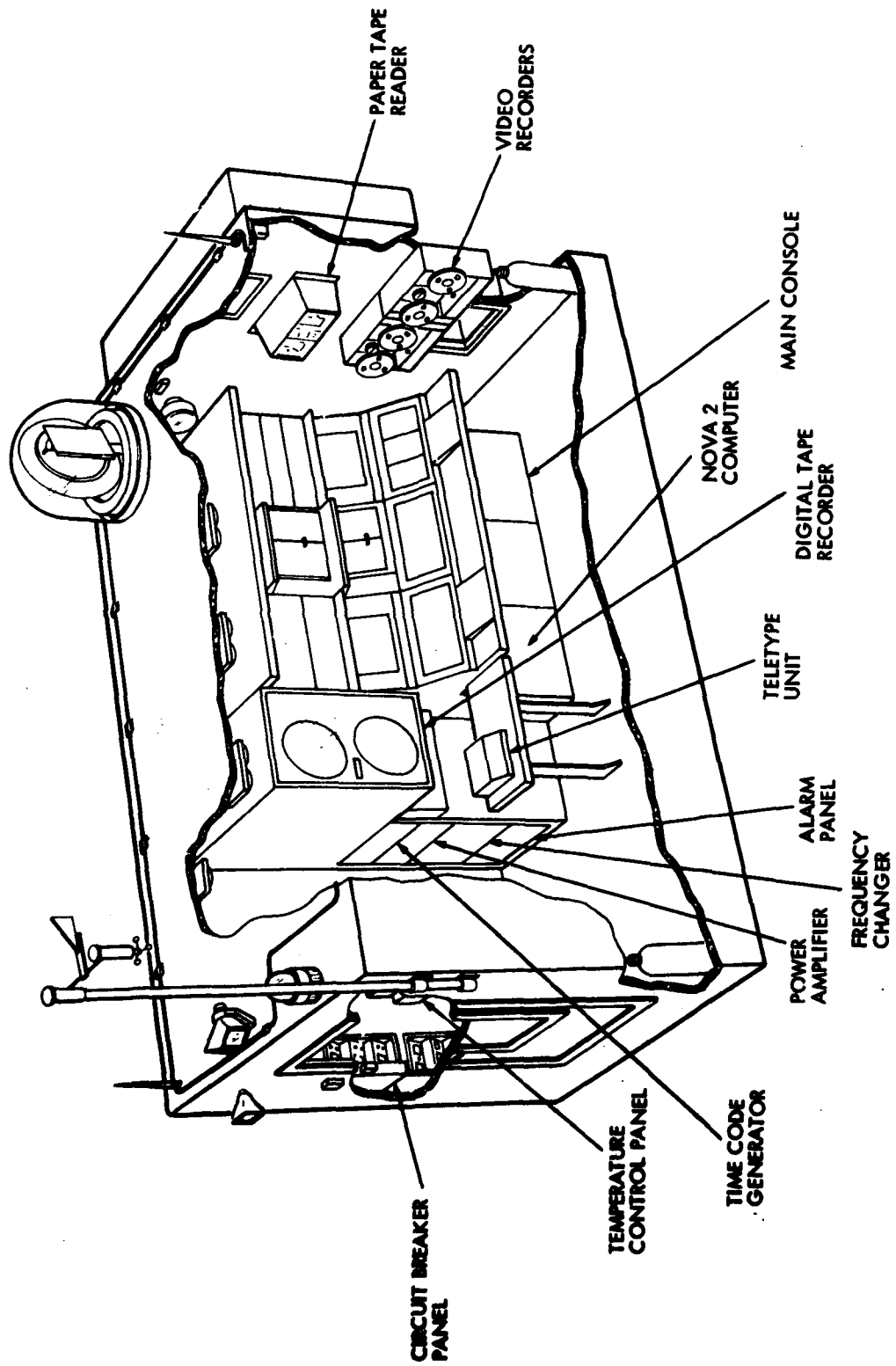


Figure 73. Ground Control Station - Final Equipment Layout

is large enough to enable installation of the console in one piece. Being that large, it contributes a significant part of the shelter's structural strength and must be installed during movement of the shelter. The panel is secured by a number of screws around its periphery.

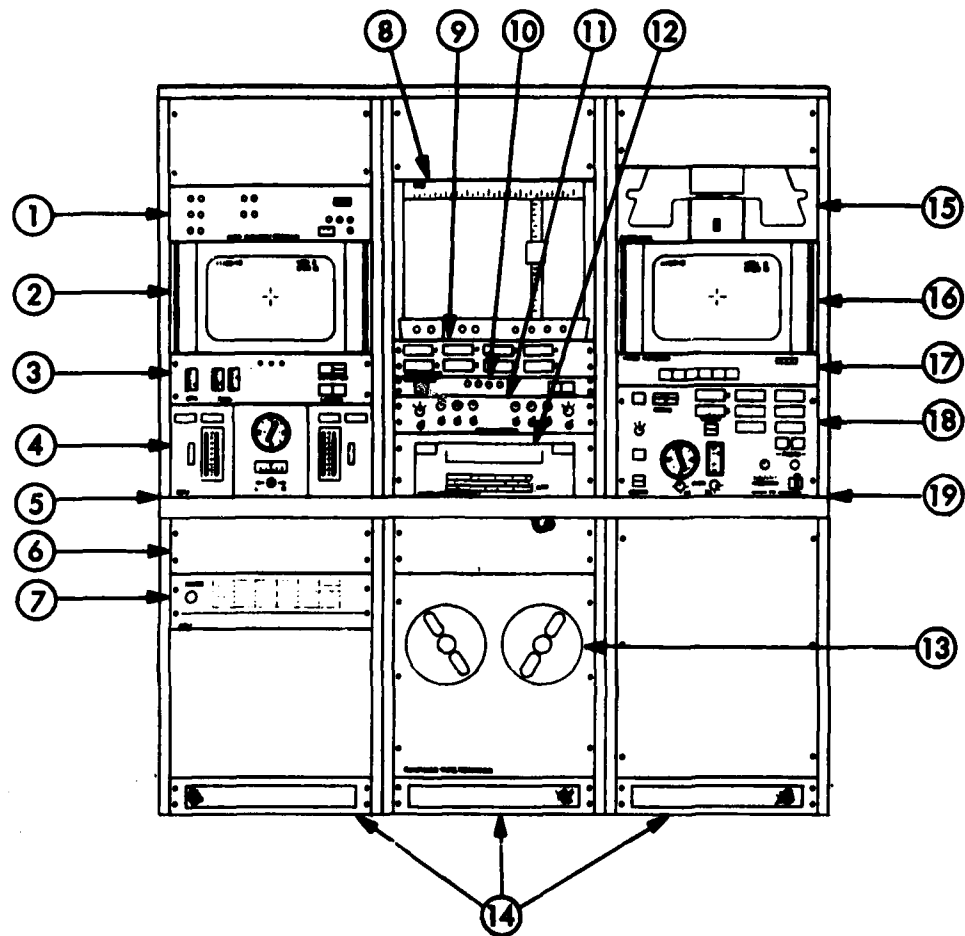
Additionally, a hole was cut for the antenna assembly in the shelter ceiling above and within the outline of the right console section. This was framed for strength and ducted to provide cooling air to the transmitter, and a molding was added to attach the radome. Three leveling screws and two bubble levels were installed for leveling the antenna during site setup.

Two holes and an external support framework were required to mount the air-conditioning unit on the outside of the shelter. The thermostat control was installed to the right of the door, inside the shelter.

Further shelter modifications included adding interior lighting, an AC power distribution panel, two cable entry panels, an external weather station on an extendable mast, lightning arresting gear, an external public address speaker, two warning sirens, and a beacon.

In normal operation the shelter is strapped onto the bed of an M-36 truck. To lift the shelter, a strongback (single point) lifting structure capable of an 8,000-lb working load was fabricated.

5.2.4.1 Console Structure. The initial console concept is shown in Figure 74. Much rearrangement and refinement of components occurred before the final item, but the basic two-man control concept remained relatively unchanged. Figure 75 shows the design mockup that was used in human factors evaluation studies to determine panel location in the console and switch-function location on the panels. Figure 75 illustrates an interim configuration during evaluation of the use of two X-Y plotters for navigation display of RPV position.



- | | |
|---|--|
| ① Antenna Control Unit | ⑪ Communication Control Panel |
| ② Pilot's Video Monitor | ⑫ Computer Terminal Keyboard and Printer |
| ③ Launch Control Panel | ⑬ Computer Magnetic Tape Recorder |
| ④ Flight Control Panel | ⑭ Blower |
| ⑤ Flight Control Joystick and
Waypoint Entry Controls (Desk Top) | ⑮ Computer Paper Tape Reader |
| ⑥ Console Power Supply | ⑯ Sensor Operator's Video Monitor |
| ⑦ Computer | ⑰ Remote Video Recorder Control Panel |
| ⑧ X-Y Navigation Plotter | ⑱ Sensor Control Panel |
| ⑨ Navigation Data Panel | ⑲ Sensor Joystick and Miscellaneous
Sensor Control Functions (Desk Top) |
| ⑩ Data-Link Control Panel | |

Figure 74. Initial Ground-Control Console Equipment Layout

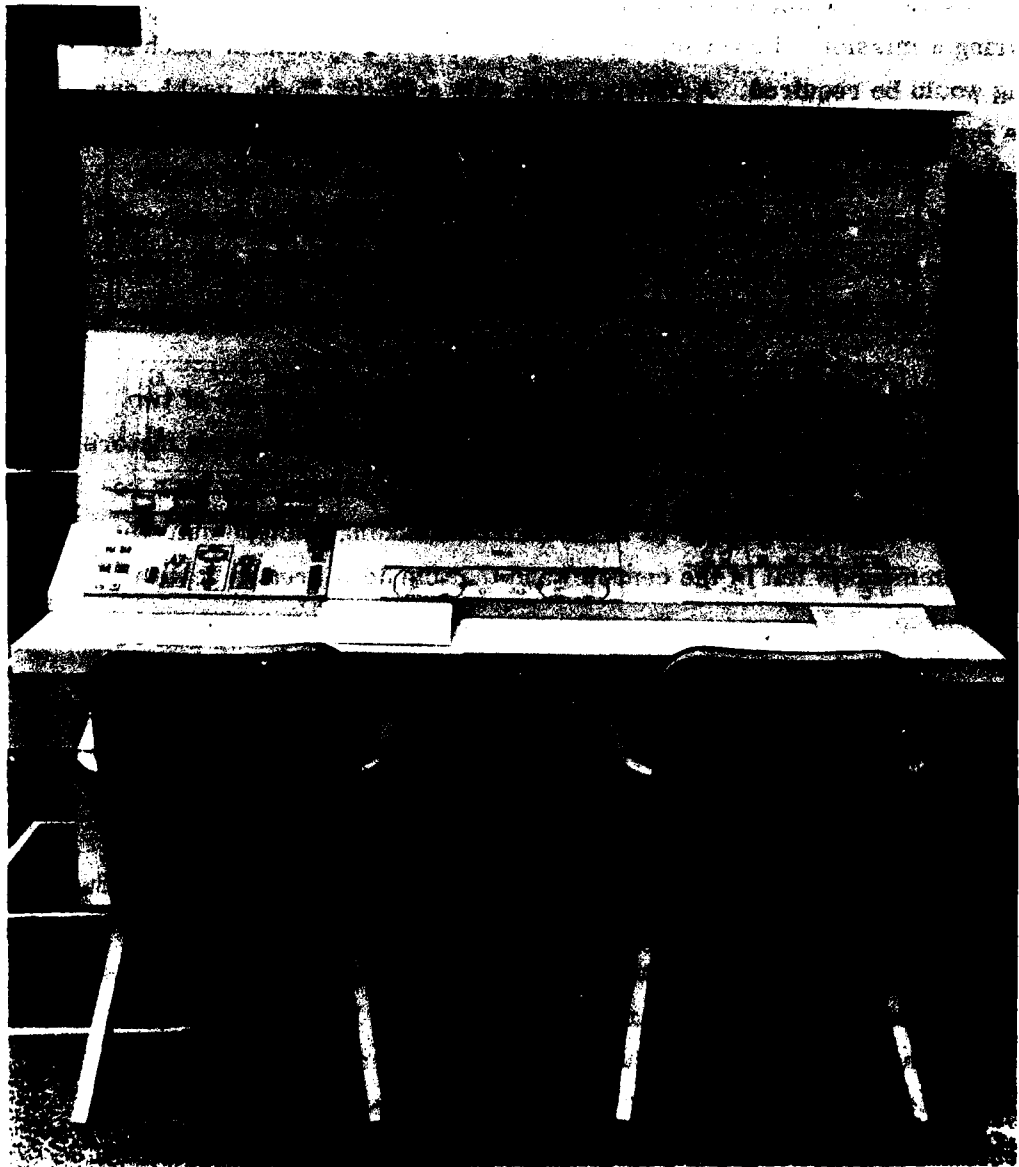
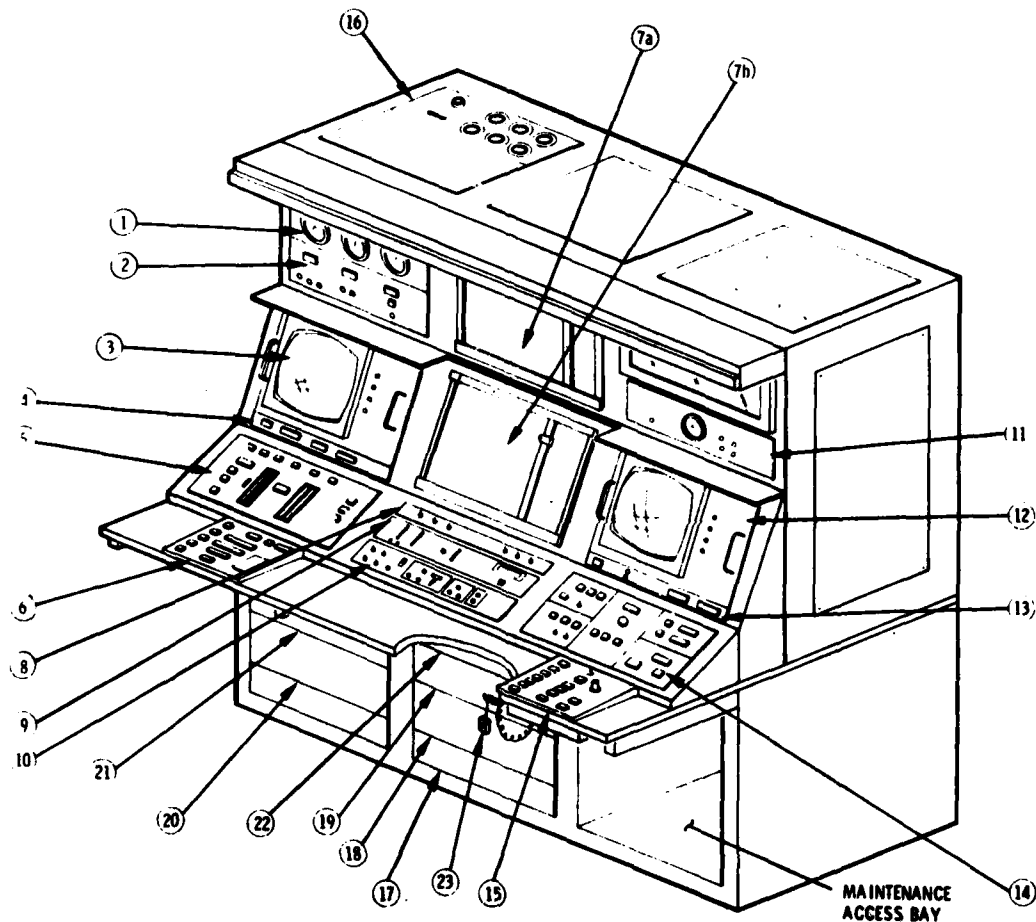


Figure 75. Ground Control Console Soft Mockup

Contract obligation was to provide a real-time navigation display compatible with 1:50,000 and 1:100,000 tactical maps covering an area of 25 by 25 km. A single 11- by 17-in. plotting surface was originally proposed as a cost-effective solution by using a switching technique to allow use of both scale maps during a mission. However, the Army preferred a system in which no switching would be required. A plotting table with a 25- by 25-in. usable surface was investigated but rejected because of high initial cost (approximately 15 times that of the single, smaller, plotter). In addition, that unit would have required customizing the console - i. e. , not using standard 19-in. -wide modules. The final solution was to use two 11- by 17-in. plotters and to configure the system such that any scale map could be used on either plotter.

Figure 76 illustrates the final console configuration. Notice the use of two sections of sloped panels - a result of the previously mentioned human factors evaluations. Also, note that the computer keyboard and printer has been removed from the center desk area (it is now a free-standing teletype unit located to the immediate left of the console) and that the desk area in general has been cleared.

5.2.4.2 Provisions for Console Equipment Cooling. In mid 1975 during field-test operations at Fort Huachuca, various console components and subassemblies were monitored for excessive temperature rise under various ambient conditions. These tests uncovered some local hot spots within the console. As a result, the following critical area cooling modifications were added to the console: (1) another blower was added above the power supply to draw air through that unit and around the computer; (2) the existing lower center console blower was reducted to direct air through the Electronic Interface Unit (EIU) in the area of the range counter module, the telemetry encoder, and the bit-synchronizer board; and (3) the console was better sealed to maintain a predictable cooling air flow. After these modifications, the console electronics was operated successfully without air conditioning for 45 min. The shelter ambient temperature increased from 90° to 105° F during this test.



- | | | | |
|----|---|----|---|
| 1 | METEOROLOGICAL PANEL (6577552) | 12 | VIDEO MONITOR (EVM-14R) |
| 2 | ANTENNA CONTROL PANEL (272003) | 13 | DATA LINK STATUS PANEL (6577344) |
| 3 | VIDEO MONITOR (EVM-14R) | 14 | SENSOR CONTROL PANEL (6577469) |
| 4 | WAYPOINT COMMAND STATUS PANEL (6577321) | 15 | SENSOR HAND CONTROL PANEL (6577465) |
| 5 | MANUAL FLIGHT CONTROL PANEL (6577317) | 16 | TEST AND I/O PANEL (6577325) |
| 6 | WAYPOINT GUIDANCE PANEL (6577313) | 17 | BLOWER (6577300-9) |
| 7 | X-Y PLOTTER (6577498) | 18 | ELECTRONICS INTERFACE UNIT (6577350) |
| 8 | X-Y PLOTTER CONTROL PANEL (6577461) | 19 | POWER INTERFACE UNIT (6577524) |
| 9 | IN-FLIGHT DIAGNOSTIC PANEL (9542488) | 20 | COMPUTER PROCESSOR UNIT (6577312) |
| 10 | INTERCOM PANEL (6577509) | 21 | POWER SUPPLY (169967) |
| 11 | TELEMETRY RECEIVER PANEL (AR-400C-V) | 22 | IN-FLIGHT DIAGNOSTIC ELECTRONICS ASSEMBLY (9542479) |
| | | 23 | LASER SAFETY SWITCH (9542524) |

Figure 76. Final Ground-Control Console Component Location

5.2.4.3 Console Control Panels. The panels visible in Figure 74 are the result of a first-cut design based on previous experience with other RPV systems. As the overall console layout evolved so did the groupings of controls that eventually became individual control panels. The goal was to group similar functions on a panel and locate panels by mission function. Thus, all sensor-oriented controls and displays moved to the right, pilot controls to the left, and common functions to the center.

Sensor Control Panel. The initial panel concept is shown in Figure 77; it hardly resembles the final one. Sensor attitude and target location displays were moved to the video monitor to ease the operator's task. Also, all the function switches associated with the stabilized platform and auto tracking system have been added. In response to range-safety requirements, a safety switch was added in series with the laser arm panel switch. This safety assembly connects to the rear chassis of this panel and extends, by retractable cable, to the front of the console.

Data-Link Status Panel. This panel, indicated in Figure 76, was included with the thought that it would be very useful during system development testing and continue to be useful during the remainder of the program. This has proven true even though some of the data are now also displayed on the in-flight diagnostic panel.

When the switchable attenuators were installed in the antenna assembly to check data-link health before launch, the switch that controls the switching relays was installed on this data-link status panel.

Sensor Hand Control Panel. This has been the most extensively modified panel in the GCS. This was the result of various iterations gone through in finally selecting a joystick. The panel rests in a cutout in the desk area in front of the sensor operator, and the first joystick used was a pistol-grip device that was pivoted below the panel surface, spring loaded to return to

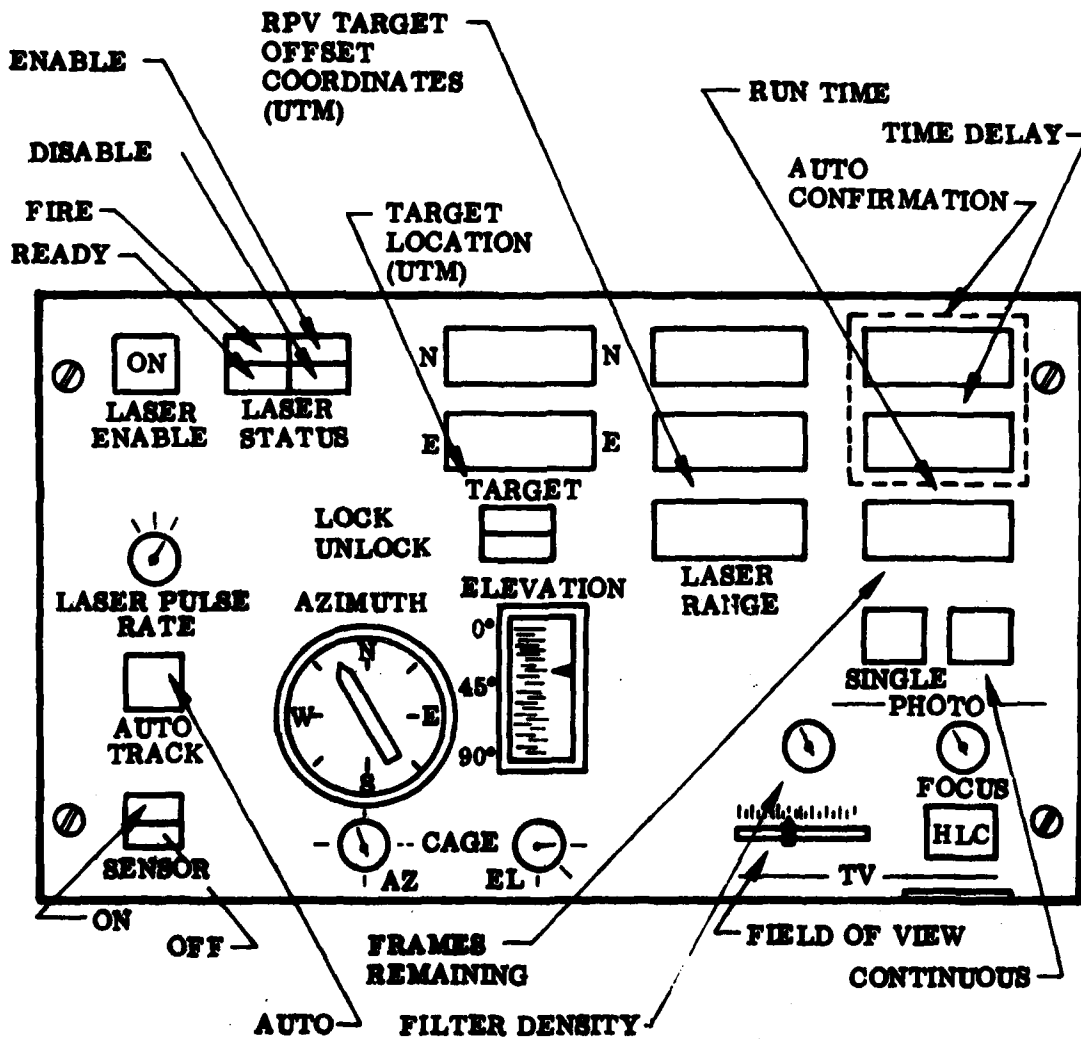


Figure 77. Sensor Control Panel - GCS

center, and acting on potentiometers in its base. The top of the stick contained three switches used for payload autotrack and slew rate control; the front trigger was the laser fire command.

Problems immediately apparent with this unit were its size and sluggish response (due mainly to it being a wrist-driven mechanism). Operator fatigue was a problem because of the elevated hand position and inadequate provisions for the operator to rest his elbow.

During field testing this joystick proved adequate in controlling payload line of sight, but the response seemed unsuitable for control of the RPV during recovery. Recovery simulations were performed, the spring loading for the two axes was verified, and a decision was made to evaluate some different control units.

From the standpoint of minimizing hardware changes it was desirable to keep the same joystick outline, so trials were made with a fixed pistol-grip assembly with a thumb-controlled strain-gage-type control at the top of the stick. This was better from a response viewpoint but was still an operator fatigue problem. Since one of the more critical operations - recovery - must be performed at the end of a mission, fatigue is a significant problem.

The final solution was to use the strain gage control but eliminate the pistol grip entirely and mount the control with a short handle protruding above the panel surface. This meant that the previously stick-mounted controls had to be moved onto the control panel. So the panel was redesigned and at the same time trimming potentiometers for the two-axis outputs were added. The potentiometers in the first joystick had a center deadband; the strain gage did not, and drifts tended to develop.

During the time the RPV was being flown with a hook recovery system aboard, the switch that manually deployed the hook was located on this panel. When

the hook was removed, that switch evolved into one that manually releases the payload shield.

Flight tests with the stabilized payload led to making the command that turns on the payload gyro a computer-generated command based on RPV roll angle. Its source initially was a switch on this panel - now an unlabeled switch.

In-Flight Diagnostic Panel. This hardware was a relatively late development coming in response to a noted need for a "quick-look" source of RPV flight control data. A panel was first built as a piece of test equipment and installed above the console in GCS 2. After several months of field usage the present panel was designed with the added capabilities of displaying pertinent data from the new subcommutated telemetry channels and also displaying the commanded antenna gain.

Communication Control Panel. The search for a quick-delivery field-usable intercom system led to one normally used in sound-stage work. Modifications of the off-the-shelf model were necessary to add another headset jack plus switches to control the external beacon, siren, and public address system. Inadequacies were noticed in the audio drive level to the video recorders and the public address system; in mid-1976 a modification was made which added an extra 20 dB of gain to those outputs.

Manual Flight Control Panel. This panel was designed to contain most of the aircraft-related functions that would be of use to the RPV pilot. It was to be the pilot's primary source of flight data, with the video monitor usable as a secondary aid during manual autopilot operations. When the RPV was modified to carry a parachute, this panel was modified to add the manual parachute deploy command switch when the parachute was installed. With deletion of the parachute from the system, that switch was disabled.

Waypoint Guidance Panel. This panel is the primary means of entering and monitoring mission waypoint information. It is hardwired to a circuitboard in the computer. During the earlier field testing operations, this subsystem was plagued with intermittent noise problems (which would occasionally clear data or enter erroneous data). The problem was associated with cable harness routing, and each ground station exhibited its own variety of the problem. Several iterations of installing different filters to solve one fault and uncover the next were required to clean up the electronics.

At one time the data entry pushbuttons on the panel extended above the panel surface. This allowed clipboards, notebooks, elbows, etc., to perform unauthorized waypoint modifications. As a solution, a plastic guard was devised to surround and protect critical switches.

5.2.4.4 Console Computer. The central processor (CPU) is an off-the-shelf Data General Nova. The CPU has capacity for ten 15-in.-square circuitboards; the data processing system uses seven such boards. One of the three remaining card slots is occupied by a board containing the hardware for the waypoint data entry and display electronics. As mentioned in the waypoint guidance panel discussion, these electronics suffered from serious noise problems - a mix of CPU clock and strobe pulse interference plus the driving of long signal lines to the waypoint guidance panel. A large amount of effort in the area of switch debouncing and pulse edge filtering was devoted to clearing up the problem. When the ground station was configured to accept the trainer-simulator (TS) it was decided to locate part of the electronics for this on the remaining space of this circuitboard. Trainer-simulator cabling is routed around the CPU from the board and terminates at an added bracket at the rear of the unit where the remainder of the TS electronics connect. This added subsystem suffered from interference similar to that of the waypoint electronics.

5.2.4.5 Console Electronics Interface Unit (EIU). This is the switching and meeting place for most of the console data and dc power paths. It was originally envisioned as a circuit-card cage and connector panel with enough spare card slots and connector space to handle future system needs. All the card slots and most of the spare areas were filled well before the first Crows Landing tests took place. The chassis is modified to mount the telemetry ground encoder-bit synchronizer bolted along one side. It was located here to minimize lengths of critical signal paths: ranging pulses, for example. Further information on that unit can be found in the section on the data link.

Another smaller circuit is bolted to the chassis; it mixes command telemetry with a gated tone used for dead-reckoning recovery in the RPV. The tone was originally supposed to go through a slip ring to the antenna where the mixing would be done in the command transmitter. However, the transmitter inputs were not compatible with that approach, and the mixing was moved into the console. As part of the trainer-simulator addition, a relay assembly was fixed to the rear of the chassis to switch video to the simulator control box.

RPV Range Counter. During field testing, there appeared to be an intermittent problem with the circuitry that accumulates counts from a crystal clock and thus determined RPV range from the GCS. Investigation showed that the counting elements were operating near their design limits at the then 60-MHz crystal frequency. That frequency was halved and the circuitboard modified accordingly. Use of the 30-MHz clock meant that the weight of the least significant bit of the accumulated round trip range increased from 5 to 10 m.

X-Y Plotter Drive. Noise in the data used to locate the RPV would cause the plotters to jitter, smearing the pen track. Filters were added in both plotter drive circuits to smooth the plotter response.

Auto/Manual Command Select. This circuitboard selects the source of three main aircraft attitude control commands. Present selection is between the computer and the manual panel controls. During system development flight testing a third source, the radio control (RC) pilot control box, existed. Problems were encountered with the RC mode of operation, which led to the loss of an RPV. It was decided to give the RC pilot another selectable mode that would make use of some of the aircraft autopilot's gyro stabilized control loops. This board was modified to implement that change.

Sensor Slew Command. This is a miscellaneous board built around the circuitry which generates slew commands for the different payloads and the GCS video monitor cursor from the same joystick. The only problems encountered involved slew control command polarities. It began with misinterpretation of the sensor specifications and continued through evolution of the joystick with the inevitable "which way is up" discussion relative to joystick elevation commands.

Analog-to-Digital (A-D) Converter. This board, like most of the others in the EIU, went from design to fabrication without benefit of an intermediate, bread-board stage. Difficulty was encountered in getting the A-D converter device (relatively new and with a preliminary data sheet) to operate properly. Once in the system, a part of the onboard data multiplexing circuitry (a recirculating counter) was prone to multiple count the ringing edges of its clock.

Telemetry Decoder. After this board was built it was discovered that the status data it was to decode had a 20-bit delay relative to command data. This exceeded the previously assumed number and required some circuitry changes.

Flight tests revealed the need for a means of trimming out bias in the computer controlled heading rate command. Those circuits were added here.

Since the RC pilot could not always hear the RPV, a circuit was added to feed a tone with a frequency proportional to rpm into his headset. The tone was reconstructed from the telemetered rpm data.

Telemetry to CPU. This circuit generates interrupt requests to the computer at the telemetry word rate. It turned out to be not always desirable to interrupt the computer. For example, the computer diagnostic test programs do not know how to handle an undefined (to them) interrupt request. The solution was to add circuitry to disable the interrupt function until the flight program calls for them.

CPU to Telemetry. This board was originally designed as a port through which the computer could transfer data into the command telemetry bit stream. One of the trainer-simulator additions was to create a way for the computer to generate pseudo-status telemetry data, simulating a closed link to an RPV. That task was accomplished by creating a new circuitboard. More recently a modification to ease computer processing was made by tying together input and output of the 32-bit shift register on this board.

Early in the test program a design weakness became evident - loss of down-link telemetry while in the manual flight control mode caused the link loss mode to be commanded. This caused unnecessary loss of hardware in a situation where the command link was still active. The logic on this board was revised to force the link loss mode off whenever manual flight control was selected.

Data-Link Status. This board has lamp drivers for indicators located on various console panels. With random status data these lamps would randomly flicker and the filament turn-on current would induce random noise spikes into other system displays. Surge-limiting resistors in the drive lines cured the problem.

Switch Interrupt Processing. Several mission-oriented panel switches reach the computer through this card. On two occasions during prelaunch activities none of those switches were operative. The reason was a failure in the control box at the launcher, which put a 15-V level on one of the other lines going to this card. The circuitry was dc coupled and the voltage was enough to disrupt the entire circuitboard. To prevent that happening, the line from the launcher has been ac-coupled into the circuitry.

Lapsed-Time Counter and Camera Frame-Rate Control. Among the circuits here are two frequency generators. One was initially required for use as a telemetry command to bring the RPV out of the dead reckoning mode; the other was a spare. Addition of the low-gain antenna added the need for a signal to drive the gain select relays on the antenna. The spare tone generator and a spare computer output from another board were used and mixed with the existing tone since there was only one available wire (slip ring) to the antenna. As mentioned in subsection 5.2.4.5 the dead reckoning tone and the transmitter were not compatible. A board change was made to remove that tone from the slip ring. At that time another command was required at the antenna to control the relays that switched the rf attenuators. The board circuitry was again changed to add a gated tone signal (same frequency as the dead reckoning tone) back onto the slip ring.

Video Interconnect. This is the console video subsystem and includes several circuitboards. Most of this circuitry had been breadboarded previously and consequently most problems occurred in the areas of board layout and noise interference. The computer input-output bus runs and is terminated in the EIU. It consists of around 20 signal lines with different phases of a 1-MHz clock on them. This induced herringbones on the video monitor presentations and also interfered with the video sync separators, causing the alphanumeric characters to jitter. Added filtering, both digital devices and video signals, decreased the noise to usable levels. A separate on-board voltage regulator was added to stabilize the outputs of several monostables which determined character positions.

This circuitry also generates the video cursor, positions it in response to the console joystick, and inputs that position to the computer. Noise was disturbing the end of the video field horizontal sync pattern and causing errors in the counter that generates horizontal cursor position data to the computer. Another circuit modification solved that problem.

5.2.5 Digital Tape Recorder

This tape recorder was included in the GCS to provide another, more convenient means of computer data entry. It has become the only method used to load flight programs. All program versions are stored on magnetic tape; all mission telemetry is recorded on magnetic tape. Recently an extensive hardware test program for console calibration and failure location has been included as another system tape. A comprehensive set of diagnostic programs for checking the computer and its peripherals is available on one of the system tapes.

Initial console location of the tape recorder was under the console desk — the only open area at that time. This proved not only awkward from an operator point of view (bending under the desk to load tape, recorder door interfering with leg room) but it was undesirable from a reliability viewpoint since the recorder's vacuum-operated tape positioning chambers would suck up dirt from the floor, contaminating the tape and causing excessive tape head wear. Addition of the auxiliary equipment rack afforded a convenient, usable place to relocate the recorder.

5.2.6 Air-Conditioner Heater

The air-conditioning system, which is fixed to the outside of the shelter, initially exhausted air directly into the shelter and onto the sensor operator. As a result of elevated component temperature problems discovered during field testing the system had deflectors added to both the inlet and exhaust to provide

more uniform cooling of the entire shelter, a greater volume of air into the radome for transmitter cooling, and an air flow directed behind the console for cooling its electronics. The deflectors also reduced the noise contributed by the air conditioner inside the shelter. In an attempt to force the operators to maintain a benign climate for the missile hardware, the system power switch was bypassed, ensuring that at least the ventilating fan is operating whenever the shelter is being used.

5.2.7 Paper Tape Reader

The paper tape reader (PTR) was initially considered to be one of the prime mechanisms for loading programs into the computer. Early in the program it was used as such to enter development-debug programs and computer diagnostic tapes. As the system matured, the digital magnetic tape unit took over as the main means of program entry, and the PTR fell into a backup position and then into disuse.

The PTR's original location in the console was occupied earlier by the telemetry receiver; the PTR now is wall hung by a bracket slightly below the air-conditioner outlet duct.

5.2.8 Video Recorders

As mentioned earlier, the two video tape recorders (VTRs) were to be located in the second shelter. With deletion of that shelter another location was found on the shelter wall opposite the door and immediately above the air-conditioner intake.

VTR selection was made on the basis of low-cost, stop-slow motion playback capability, size compatibility for shelter installation, and up to 1 hour recording time. The selected units are industrial-commercial type recorders and have not proved to be as rugged and maintenance free as desired. To solve

the remote playback synchronization problem caused by frequency drift of the diesel generator power source, a precision 60-Hz inverter was installed in the GCS as a buffer.

5.2.9 Miscellaneous

Remote Manual Control System. Figure 78 depicts the control elements of the remote control, or radio control (RC), system. The pilot's control unit was a modified hobbyist-type RC box. The other unit was located in the GCS and contained a switch and coding to select various control mode words which acted to enable different aircraft autopilot control loops. Not shown is the test circuit-board which substituted for the auto-manual command select board in the EIU and allowed selection of a hybrid arrangement of flight control commands. That board was used in any development test flights where computer control was not used.

During flight testing the shared control of mode selection between RC pilot and GCS pilot proved to be awkward, so the system was modified to eliminate the box in the GCS. The new control scheme gave the RC pilot the capability of selecting the regular RC or a new "augmented RC" mode. Augmented RC allowed control from the RC box with all RPV autopilot loops active except altitude. One of the EIU circuitboards had to be modified to allow that arrangement of commands. At the same time the RC box was completely rebuilt internally, replacing the original handwired board with a printed-circuit variety and, in general, ruggedizing the box. A tone indicative of engine rpm was added to the RC pilot's headset; some box controls were relocated for convenience and some were guarded for safety.

DC Power Supply. The most desirable location for the power supply assembly required a small, therefore efficient, unit. Fortunately, the one meeting these requirements also happened to be one of the lower cost units evaluated. Although no specific problems have occurred due to overheating, a console blower has been added to ensure adequate air circulation through the assembly.

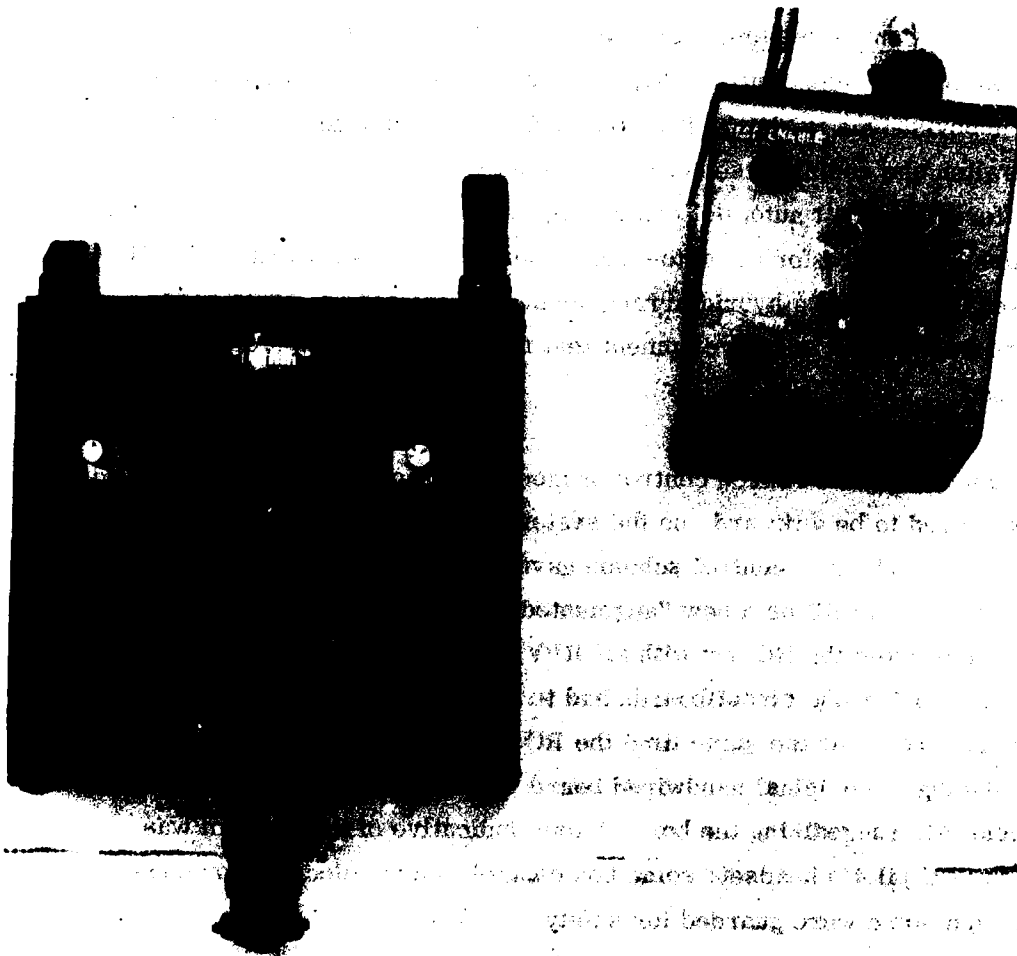


Figure 78. Radio Control Unit and Autopilot Mode Test Box

Time Code Generator. The time code generator was selected to provide timing data to the computer for tagging magnetic and video tape records and for timing pulses in the EIU.

5.3 LAUNCHER SYSTEM EVOLUTION

This section describes the evolution of the Aquila pneumatic launcher system (Reference 11) from the early preproposal conceptual studies through the design, fabrication, developmental testing, and finally system validation testing. These efforts culminated in the final launcher system configuration whose detailed description and summation of demonstrated capabilities are documented in Volume I of this report.

5.3.1 Background

During the 2 years prior to submittal of the Aquila RPV-STD proposal (30 August 1974) Lockheed studied and evaluated various launch systems based on pneumatic, mechanical, linear electromagnetic, gas generator, and rocket-powered catapult principles. The rocket system was not considered a viable candidate but could be worthy of future consideration if proper emphasis is placed on resolution of concerns regarding crew safety, fire hazard, and smoke-generation characteristics. The gas generator system, although it controls the fire hazard and essentially eliminates smoke generation, required specialized solid or liquid fuels. Furthermore, these fuels must be provided with an independently generated ignition source, or they must be hypergolic. Electromagnetic systems proved to be very heavy and also unsuited to remote site operation. LMSC and All American Engineering Company, the launch system subcontractor, therefore concentrated their conceptual evaluation on pneumatic and mechanical acceleration catapults.

Two operational, scaled systems were used to obtain confirmation of theoretical design analyses and operational experience. One system was pneumatic,

(11) Lockheed Missiles & Space Company, Inc., Aquila RPV System Test Report, CDRL AOOD, Launcher Development, LMSC-L028081, Part 10, Sunnyvale, Calif., Sept 1977

and the other was mechanical, using a bungee cord accelerator. Both systems were tested and have proved to be capable of meeting the program's objectives and requirements. The capability of remotely charging the accelerator chamber appears to favor the pneumatic system for unprepared field operations when compared to the operations and subsystems required for resetting the bungee cord mechanical system. The pneumatic system is also very easily deactivated right up to the last moment before RPV launch in the event a launch postponement is desired.

Finally, selection of the pneumatic catapult avoided a costly development phase and made use of existing launcher technology. The pneumatic system as built by All American Engineering Company (AAE), Wilmington, Delaware, was selected as the Aquila proposal baseline because it was basically an off-the-shelf system expressly designed for launching small aircraft on the 200-lb category at speeds to 70 knots.

5.3.2 Approach

The basic tenets of the Aquila launcher system approach were as follows:

- Maximum utilization of existing off-the-shelf hardware
- Maintain initial concept providing modifications only if basic requirements could not be achieved or if cost-effective improvements in service life, maintainability, mobility, reliability, and operability can be achieved within contractual limitations

The basic approach consisted of the following steps:

- Approval of baseline design with interfaces defined and controlled
- Detailed design, fabrication, and extensive developmental testing conducted by the subcontractor, AAE, at his special facilities with Lockheed monitoring the effort
- Mobility implementation and GSE interfacing provided by Lockheed with design and fabrication at Sunnyvale and checkout at Fort Huachuca

- Launcher-involved flight testing conducted by Lockheed at Fort Huachuca; troubleshooting of anomalies resulting from field operations provided as joint Lockheed-AAE effort
- Design deficiencies negotiated with and resolved by AAE
- System improvements negotiated with the Army

5.3.3 System Requirements

The initial basic launcher system operational requirements were as follows:

- No more than two people shall be required to set up, tear down, and operate this system and launch one RPV.
- Minimum time and skill shall be required for assembly, disassembly, and launch operations.
- There shall be minimum observables during launch operations.
- Launch shall be possible from unprepared sites.
- The launch subsystem shall be common to all phases of the program.

Lockheed mobility studies in May 1976 showed the feasibility of truck mounting (M36, 2-1/2 ton, 6x 6 truck) the baseline launcher system. As a direct result of these studies, launcher-system mobility became a launcher-system operational requirement.

To meet these operational requirements, the launcher-system design must have the following characteristics:

- Lightweight components, none of which separately exceeds 200 lb, which is the normal maximum weight that two men can readily lift and carry short distances (This goal was eventually waived in favor of using existing components.)
- Small-size components that separately do not have any packaged dimensions exceeding 20 ft, which is the normal maximum length that two men can handle effectively in rough field conditions (Eventually waived to use existing hardware.)

- **Simplicity of design to facilitate and speed assembly, disassembly, operation, and maintenance at remote, unprepared field sites**
- **Adaptability of installation to accommodate a wide variety of field conditions such as desert, brush, forest, glens, mountains, and snow cover**
- **System reliability to maximize operational successes and thereby reduce costs**
- **Little or no emission of noise, smoke, fumes, light, or other observable features**

The critical launcher-to-RPV interfaces were identified as follows:

- **RPV-to-shuttle mount. Five points consisting of the two midwing support rest pads, the two aft wing thrust fittings, and the skeg keeper**
- **RPV umbilical interface. Established on the RPV starboard side along BL 9, 22.**
- **RPV ground cooling. Duct to opening in port side forward wing root area; the ground mating interface is contoured to provide easy hand removal prior to launch**

5.3.4 Evolution

Design. The Aquila launcher system has evolved from the original basic concept of a ground-mounted, rotatable launcher into the current mobile truck-mounted system. The significant areas of modification and improvement are given in this section.

System Mobility. The Army's desire for mobility gave added impetus to the study of truck mounting for the launcher and RPV launch support equipment. Candidate Army vehicles were studied and mobility concepts reviewed.

The M36, 2-1/2 ton, 6 x 6 truck with the installation concept shown in Figure 79 was selected. Most components have been through-bolted with locking hardware; notable exceptions are the ground-cooling system, which rests on a rubber pad, and the control box, which has a 30-ft cable for remote (for safety of launch) operations.

Shuttle Evolution. The launcher concept is based on equipment in existence prior to August of 1974. The interface between the Aquila RPV and the launcher required development of an interfacing shuttle assembly. The baseline shuttle design of 1974 is shown in Figure 80. The interfaces shown are the five points on the aircraft - two wing support pads that provide midwing support, two trailing-edge supports that also restrict rotation about the center of gravity, and finally a skeg keeper that holds the RPV until launch release is achieved at the end of the launcher piston stroke.

System performance tests conducted at the AAE facility in 1975 showed no evidence of shuttle structural failure. Subsequent flight testing was conducted at Fort Huachuca and resulted in a launch failure (Flight 14A) on 25 August 1976. Motion pictures taken at the time of the attempted launch show the RPV reacting to the applied launch acceleration. The "settling" of the RPV into the aft wing supports and the resultant spring return caused the RPV skeg keeper to disengage prior to achievement of launch speed. The RPV pitched up and over the launch rail, completing two reverse turns before impacting the ground in a nearly horizontal attitude.

The skeg-keeper fingers were designed to compensate for some RPV movement, and no immediate reason could be found for a premature release. Subsequent investigation of the launcher shuttle showed a buckling of the flat-plate design, which created an excessive misalignment between skeg and keeper. The crash of the RPV is attributed to this failure of the shuttle. The buckling is a direct result of the method of decelerating the shuttle that is allowed to

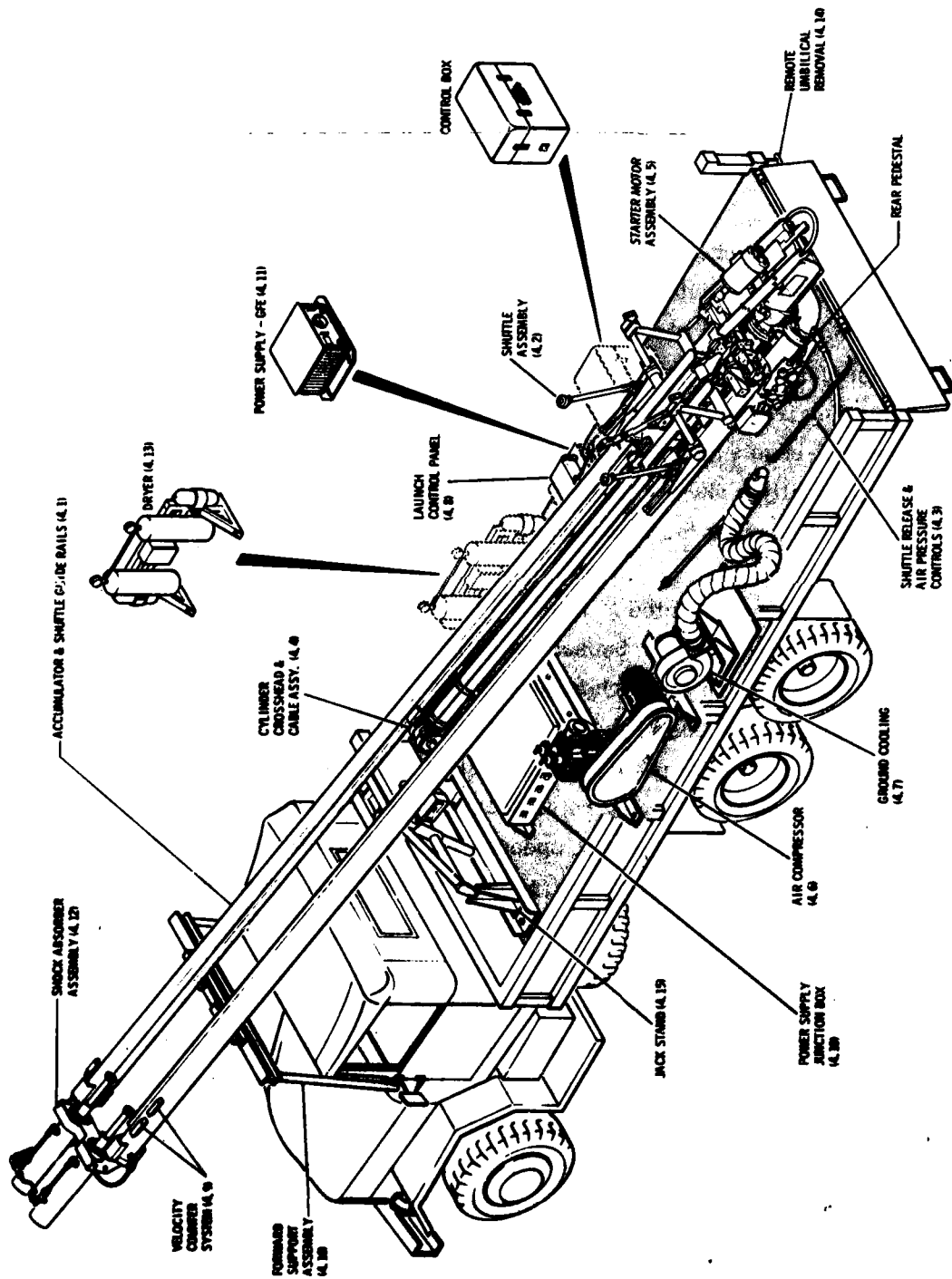
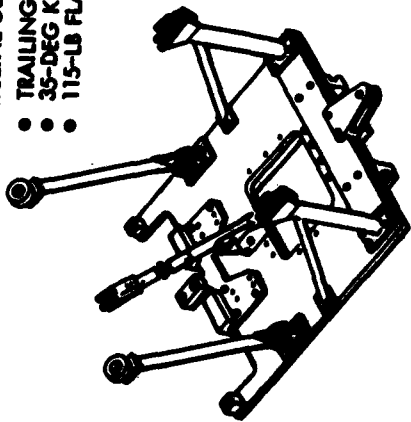


Figure 79. Launcher Assembly

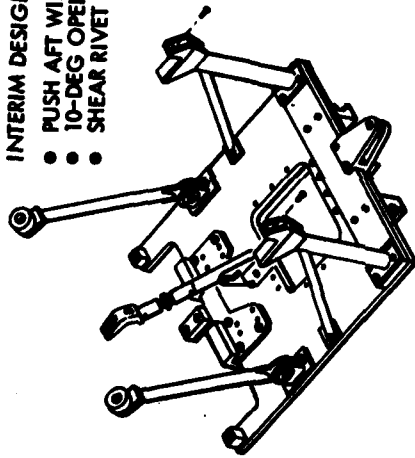
BASELINE DESIGN - 1974

- TRAILING-EDGE WING SUPPORT
- 35-DEG KEEPER WITH SPRING
- 115-LB FLAT PLATE



INTERIM DESIGN

- PUSH AFT WING SUPPORT
- 10-DEG OPEN KEEPER
- SHEAR RIVET RELEASE



**FINAL RPV-STD DESIGN -
INTERIM DESIGN PLUS**

- I-BEAM CONSTRUCTION
- 85-LB WEIGHT
- DAGGER HOLDBACK

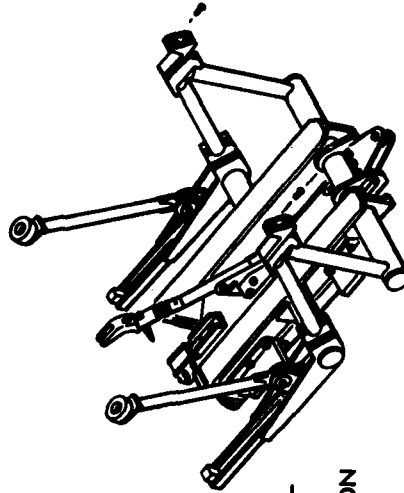


Figure 80. Evolution of RPV Launcher Shuttle Design

impact on two hydraulic shock absorbers, stopping the 115-lb shuttle in 10 in. The resulting deceleration is in excess of 130 g and resulted in a gradual failure of the shuttle plate.

Since the buckling failure mode is a relatively slow process requiring many shuttle operations, it was decided to retain the flat plate as an interim design with modifications to minimize launch acceleration effects between RPV and shuttle.

The interim shuttle (Figure 80) was redesigned at two fundamental interface areas. The aft wing loads were transferred into the wing roots by addition of external channels on top and bottom of the wing and bolted at the wing-to-fuselage attach points. The channels terminate in a push block which interfaces with a redesigned shuttle thrust fitting. An expendable soft shear rivet restrains the RPV in the launch position. At the end of the launch stroke, when the shuttle has begun deceleration, RPV momentum shears the soft rivet and the RPV becomes airborne.

The second change was in the design of the skeg keeper. The restraining spring was discarded and the angle of the keeper fingers was decreased from 35 to 10 deg. This provided a better holddown to the RPV skeg and maintained easy exit for the Aquila at launch.

The final shuttle design (Figure 80) is expressly designed to survive the high deceleration loads by rugged I-beams in the longitudinal directions. Torque loads in the wing supports (forward and aft) are reacted through stiff hollow tubes into the I-beams. A significant feature of the design is the reduction of shuttle weight from 115 to 85 lb. The design includes a dagger assembly and neoprene catcher, which prevents the skeg-keeper arm assembly from rebounding and possible launch interference. The forward arms are restrained from rebound by friction pads about the arm pivot points.

Launcher Electronics. The launcher electrical/electronic system controls, operates, and interlocks launch sequencing. Functionally, the system can be separated as follows:

- Visual status indicators
- Compressor on-off and pressure limits
- Safety interlocks
- Launch velocity counter
- Manual launch control with safety key
- Emergency alarm interconnect
- Remote interface for GCS launch command
- Intercom

The electrical/electronic system has worked reliably throughout the demonstration program, with the exception of the velocity counter system. As originally designed, the counter was a noise susceptible single-ended circuit that did not provide sufficient noise immunity for the GCS computer. An improved circuit with differential inputs was later installed. The velocity counter sensors presented another problem area insofar as their proximity to the decelerating shuttle. This is a high shock load environment that has caused transistor failure and has caused the operating points of the magnetic pickup to shift from the normal. The magnet to trip the velocity counter sensors rides on the crosshead of the piston assembly. Shock transients at this location cause demagnetization of the magnet. This is being alleviated by installation of magnets made of Alinco VIII material, which is only slightly affected by the shock load encountered during the deceleration process.

The majority of the velocity counter electronics have been transferred from the sensor location near the shock absorbers to the control box, which is located remotely from the launcher.

Another improvement is the addition of a counter on the control box, which provides an improved accuracy determination of velocity over that obtainable

through the GCS computer. The GCS can determine time only in plus or minus 0.5 ms increments, which is equivalent to plus or minus 2 knots. The velocity counter can resolve the time to 20 μ s, which is equivalent to 0.08 knot.

Accumulator Evolution. The accumulator and surrounding structure are subjected to shock load when the shuttle assembly impacts the front-end hydraulic shock absorbers. In July of 1976, AAE experienced a weld failure in the accumulator structure at the head of the launcher where the shock absorbers interface with the accumulators. The weld failures were first experienced by AAE on another program and, as a result, the company performed a field retrofit by welding reinforcing material to the accumulator structure and then hydrostatically verifying accumulator integrity.

A second weld failure point was detected at the accumulator base pedestal mount. This structure was modified slightly by AAE. A launcher similar to the Army LP20-209 model was procured by LMSC for RPV testing. During design of this LMSC unit, a new heavy-duty pedestal was designed and procured for use on the truck-mounted launchers. The new pedestal will no longer permit rotation of the launcher about the pedestal base. Since the launcher is not required to be ground mounted, this loss of flexibility is acceptable.

Dryer Evolution. Field experience has shown the basic launcher to be a reliable, functional item. There have, however, been periods of downtime that are directly attributable to excessive moisture in accumulator, pistons, control valves, and seals. The compressor has no means of moisture removal prior to delivery of air to the accumulator. The air temperature is often over 180° F when the delivered air exceeds pressures of 100 psig. Under even moderate humidity conditions, as much as a litre of water has been drained from the system. The liquid precipitates out of the air when cooled in the accumulator and the air pressure control panel at ambient temperature, and causes deterioration and rusting of seals, valves, and control regulator. To provide increased time between required maintenance, a regenerative dryer has been added to the system.

Test Results. The summary of results from launcher tests is presented in Table 16. These tests include the first developmental test at AAE on 18 August 1975, the preflight developmental testing at Fort Huachuca, actual RPV flight test demonstrations at Fort Huachuca, and the new shuttle developmental testing at AAE and subsequent completion of RPV flight-test demonstrations on 10 July 1977. During this period 190 launcher tests were made.

These tests equate to a launcher reliability of 0.98 for all launchings, and to a launcher reliability of 1.00 for all launchings with the current lighter, improved shuttle.

During the period of the 190 launchings, the RPV weight varied from 126 lb to over 145 lb. Developmental testing with inert weights or dummy projectiles up to 165 lb occurred on several occasions. Launch velocities for Aquila RPV varied from 45.6 to 52 knots. Test data for other than RPVs approached 60 knots launch velocity.

On the basis of these results showing high reliability under widely varying conditions, the concepts of launch and launch support have been shown to be valid and repeatable in day-to-day use.

Performance. Launcher performance capability has been confirmed by test for launch velocities to 60 knots and for vehicle weights up to 200 lb. The accumulator pressure required to launch the RPV can be closely approximated by an expression where pressure is linearly proportional to the weight and to an exponential power of the velocity. For the current shuttle (weight 85 lb), the experimental test data was used to derive the following:

$$P = 8.716 \times 10^{-4} V^{1.866} (W) \quad (8)$$

where

- P = initial launch pressure (psig)
- V = RPV launch velocity (knots)
- W = total weight; RPV weight plus 85 lb for shuttle (lb)

TABLE 16. LAUNCHER TEST SUMMARY

<u>Test Type</u>	Total	Launcher	
		Success	Failure
Demonstration Flight			
Airborne	59	59	0
Launch	1	0	1 ^(a)
Developmental			
RPV-003	11	11	0
ITV	49	46	3 ^(b)
Blivit	31	31	0
Shuttle	<u>39</u>	<u>39</u>	<u>0</u>
TOTAL	190	186	4
Launcher Type			
Serial Number			
9753	95	91	4
9754	70	70	0
10755	<u>25</u>	<u>25</u>	<u>0</u>
TOTAL	190	186	4
Shuttle Type			
Original - Flat Plate - 115 lb	131	127	4
Current - I Beam - 85 lb	<u>59</u>	<u>59</u>	<u>0</u>
TOTAL	190	186	4

(a) RPV-003 launch incident.

(b) All three failures due to improper test setup - i. e., failure to watch installation tolerances.

Based on this equation, the performance plot (Figure 81), showing initial pressure as a function of launch velocity and RPV weight, was generated and used during Aquila testing.

RPV acceleration loads can be found theoretically, but a more direct method is found when experimentally determined g values for various shuttle weights and launch velocities are plotted versus the kinematic values for linear acceleration. Figure 82 is such a plot of data from Aquila and from other programs that use pneumatic catapults. The straight line is the theoretical linear acceleration; the data points are experimental data. As can be seen, the linear acceleration approximation holds very closely for a wide range of data. Thus, the g values of Figure 81 are those for an ideal linearly accelerated RPV. When using the chart, the 6-g restriction for acceleration should be maintained; thus the launch velocity selected should not exceed 52 knots.

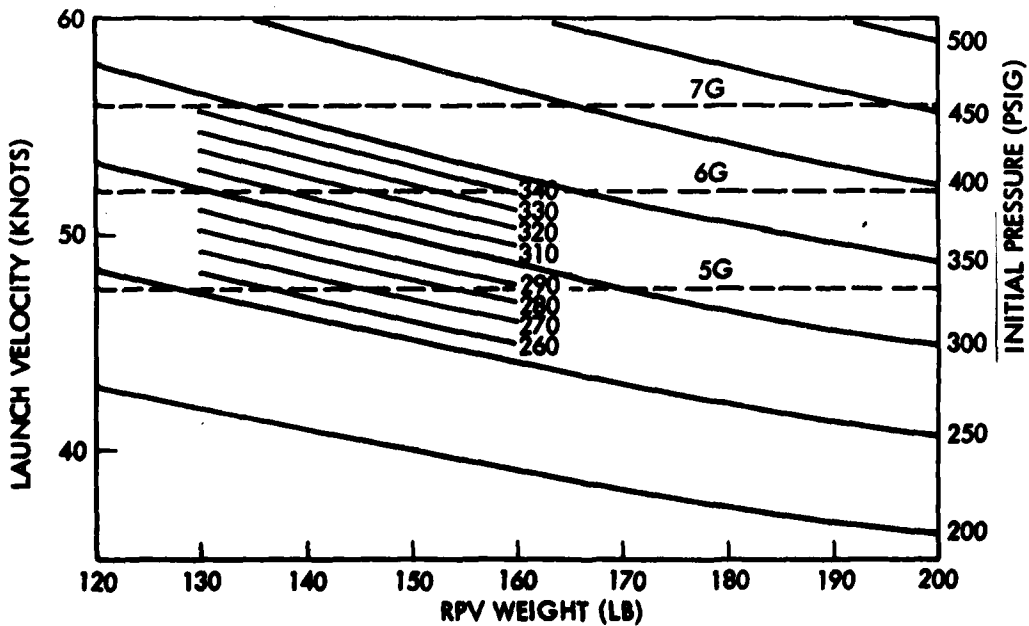


Figure 81. RPV Launch Velocity Versus Weight, Pressure

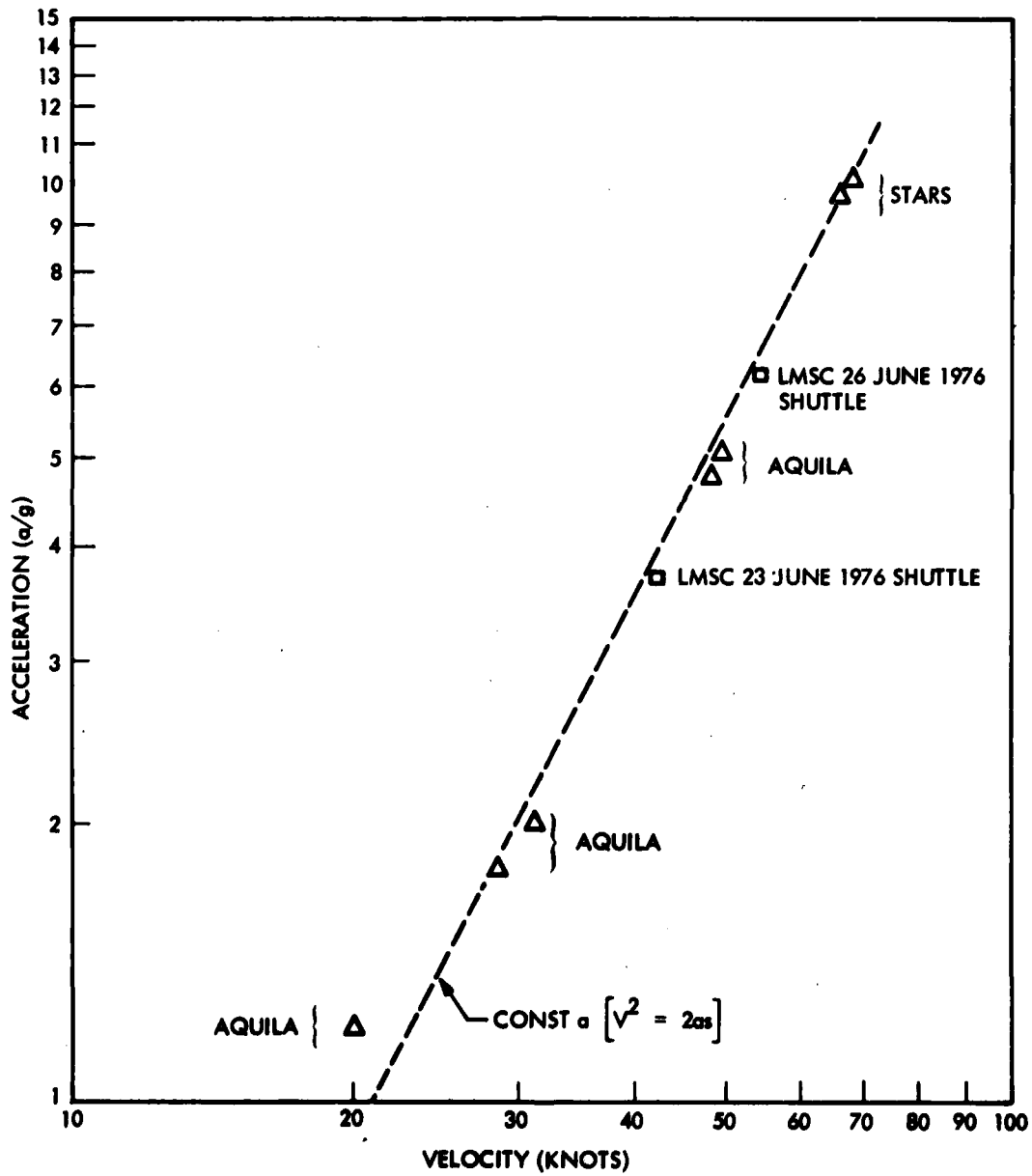


Figure 82. RPV Acceleration Versus Velocity

Conclusions. The prime objective for the Aquila RPV-STD launcher development program was to produce a reliable launch system which could be used repeatedly for developmental flight testing and which would offer the potential for further development into the highly mobile, low observable launch system which would support any RPV mission in any field environment. The linear pneumatic system developed for Aquila has shown proven reliability in excess of 98 percent under widely varying conditions. The system provides prelaunch conditioning to the RPV and the proper inclination and attitude during launch. The system is truck-mounted (2-1/2-ton long bed M36), and has demonstrated mobility in limited field usage. The design of the basic system has been augmented by RPV support systems which also provide mission mobility.

During development, problems relating to shuttle redesign, addition of dryers, and modification of velocity sensors were successfully resolved. The current system has shown mobility, flexibility, and high reliability during flight tests, and the original objectives have been met.

5.4 RETRIEVAL SYSTEM EVOLUTION

This subsection describes the evolution of the Aquila retrieval system (Reference 12) from the early preproposal conceptual studies (which led to selection of a parallel strap system) through design, fabrication, development testing, and early system validation flight testing. Problems occurring during early system validation flight testing led to introduction of the vertical barrier system. The detailed description of the current vertical barrier retrieval system and its demonstrated capabilities are documented in Volume I of this report.

5.4.1

During the 2 years prior to the submittal of the Aquila RPV-STD proposal on 30 August 1974, Lockheed and All American Engineering (AAE) - the subcontractor - studied, evaluated, and tested various retrieval systems. Table 17

(12) Lockheed Missiles & Space Company, Inc., Aquila RPV System Test Report, CDRL AOOD, Retrieval System Development, LMSC-L028081, Part 6, Sunnyvale, Calif.

TABLE 17. COMPARATIVE CHARACTERISTICS OF VARIOUS RETRIEVAL SYSTEMS

System Type	Ease of RPV Recovery	RPV Slide Length	Initial RPV Impact	RPV Engagement Height	Ease of Field Installation	Reliability and Maintainability	Payload Vulnerability	Development Status
Arrow-100 and parallel strap retrieval assembly*	Easy	Short	High	High	Easy	High	Low	Demonstrated
Arrow-100 and str-100 retrieval	Easy	Short	High	High	Easy	Acceptable	High	Well-advanced designs
Water-100	Easy	Long	Low	Low	Easy	Low	High	Major design data
Shaw-100/1000 str-100 retrieval	Moderately difficult	Short	High	High	Complex	Low	High	Conceptual designs
Shaw-100/1000 str-1000 retrieval	Difficult	Long	Low	Medium	Complex	Low	Low	Conceptual designs
Shaw-100/1000 str-10000 retrieval	Difficult	Long	Low	Medium	Complex	Low	High	Conceptual designs

*This retrieval system was chosen by LMSC and AAS for the RPV Systems Technology Demonstrator Program.

summarizes the evaluation of the various systems considered, versus desired system characteristics. The arrester line/parallel strap system was selected as the proposal baseline primarily because it was the only system whose capabilities were demonstrated and because no other system offered significant potential for improved site operations and minimal potential for RPV losses due to near misses. To further support this selection, Lockheed, AAE, and Development Sciences, Incorporated (DSI), completed a series of full-scale aerial tests to demonstrate the operational feasibility of the parallel strap system. A dummy DSI "Sky Eye" RPV airframe, properly ballasted, was used in these tests. Figure 83 shows photographs of some of the significant pieces of equipment used during the tests. Dynamic dead-load tests simulating the energy, inertia, mass, and other physical characteristics of an in-flight RPV were conducted. Force, distances, deceleration rates, and deflection data were obtained for analytical evaluations of the system design and retrieval dynamics theory. Figure 84 presents photographs of the dummy RPV in various stages of the successful retrieval process. Arrester line engagement, RPV deceleration, RPV throw-distance, parallel strap maximum deflection under RPV load, and g-load levels were all within the desired design limits. The operational success potential of the parallel strap system was demonstrated, and the system concept was judged to be developable for effective, safe RPV retrieval.

5.4.2 Approach

The basic approach for the Aquila retrieval system was similar to the Aquila launcher system, i.e.:

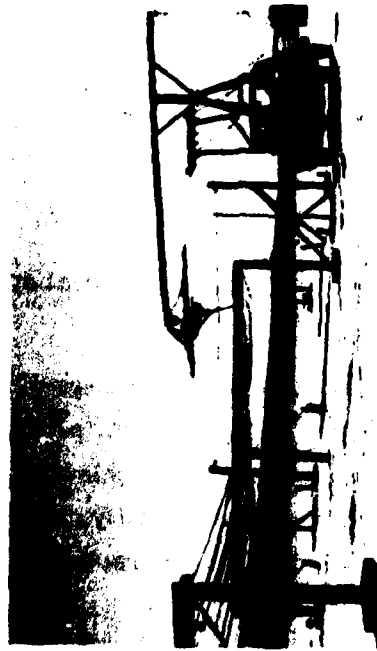
- Maximum utilization of off-the-shelf hardware
- Maintenance of initial concept, providing modifications only if basic requirements could not be achieved, or if cost-effective improvements in service life, maintainability, mobility, reliability, and operability can be achieved within contractual limitations



(a) General layout of the retrieval subsystem along the direction of flight



(b) Arrester line energy dissipator anchored in place



(c) Dummy RPV, launch truck, arrester line, and retrieval assembly

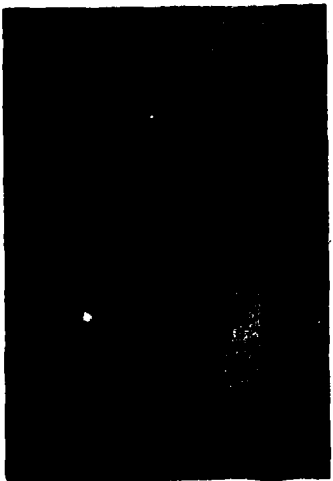


(d) Dummy RPV resting in the retrieval assembly

Figure 83. Photographs of Sky Eye Flight Retrieval Site



(a) Launch truck and dummy RPV approaching arrester line at 60 mph



(b) Dummy RPV at 60 mph about to hook arrester line



(c) Dummy RPV hook engaging arrester line



(d) Dummy RPV at point of maximum deflection in retrieval assembly



(e) Retrieval RPV at rest



(f) Parallel strap retrieval assembly allows easy RPV removal

Figure 84. Photographs of Sky Eye Flight Retrieval

The following steps were carried out in the implementation of this basic approach:

1. Baseline design was approved with interfaces defined and controlled.
2. Detailed design, fabrication, and extensive development testing were conducted by AAE at their special facilities with Lockheed monitoring the effort.
3. Early involvement in Lockheed-conducted flight testing at Fort Huachuca; troubleshooting of anomalies resulting from field operations and system modifications to improve reliability provided by joint LMSC-AAE efforts. (Early problems relating to complexity, reliability, and maintainability of parallel strap system as well as adverse impact of trailing hook assembly on RPV performance led to the decision to change the baseline system to the vertical barrier retrieval system. The vertical barrier system was selected for development after an exhaustive study of more than 40 mini-RPV retrieval systems.)
4. New baseline system was originally conceived as a mobile system and was designed, developed, and tested at AAE.
5. Minor design deficiencies in the new baseline system would be resolved and negotiated with AAE.
6. System improvements would be negotiated with the U.S. Army.

5.4.3 System Requirements

The basic retrieval system operational requirements are identical to those of the launcher system and are as follows:

- No more than two people shall be required to set up, tear down, and operate the system and retrieve one RPV.
- Minimum time and skill shall be required for assembly, disassembly, and retrieval operations.
- There shall be minimum observables during retrieval operations.

- Retrieval shall be possible from unprepared sites.
- Retrieval subsystem shall be common to phases of the program.

The same Lockheed studies that showed the feasibility of truck mounting the launcher also showed the feasibility of trailer mounting the parallel strap system.

To meet the requirements of practicality, low cost, reliability, and field maintainability, the system must have the following characteristics:

- Lightweight components, none of which separately exceeds 200 lb
- Small size components that separately have no package dimension exceeding 20 ft
- Design simplicity to facilitate speed of assembly, disassembly, operation, and maintenance at remote unprepared field sites
- Ability to accommodate a wide variety of field conditions such as desert, brush, forest, glens, mountains, and snow cover
- System reliability to maximize operational successes
- Little or no production of noise, smoke, fumes, lights, or other observable features

Other specific design characteristics which evolved are as follows:

- Environments for retrieval- test demonstrations Fort Huachuca, Arizona; Fort Sill, Oklahoma; and/or other similar places
- RPV descriptions:
 - Weight (including fuel) 140 lb nominal
 - Length 6 ft nominal
 - Wing span 11.9 ft nominal
 - Body diameter 12 in. nominal
 - Propeller shroud diameter 22 in. nominal
- Engagement ground velocity 38 to 58 knots, low-approach angle
- Capture loads 6 g in the three major RPV axes

● Retrieval crew	Two persons
● Retrieval crew skills	Minimum
● Duty cycle (RPV-STD aircraft)	4 sorties per day; 4 days per week; 1-hour flight time per sortie (minimum)
● Recycling time	10 min maximum
● Life	250 retrievals between overhauls, minimum (not including consumables, i. e., fluids, straps, and lines)
● Safety	Remotely activated system
● Ambient winds during operation	20 knots, gusts to 35 knots, 4,000-ft altitude at 95° F
● Design altitude	4,000 ft (MSL) at 95° F (hot day)
● Installation and disassembly times	Maximum 1 hour each (2 men)
● Reorientation of retrieval direction time	Maximum 10 min (2 men)
● Retrieval direction	Bidirectional retrieval capability
● Mobility	Mounted, transportable, and operational on two Army M345 trailers, each capable of being drawn by one Army M35 or M36 truck

5.4.4 Evolution of Parallel Strap System

System Description. During the initial phases of the RPV-STD Program, a system employing an RPV trailing engagement hook and called the Parallel Strap Retrieval System was used.

Figure 85 is a sketch of the Aquila RPV in a final approach to the Parallel Strap Retrieval System. The RPV is shown with a deployed trailing engagement hook prior to engagement with one of an array of 10 horizontal arresting lines. The arresting lines are arranged on a 45-deg inclined array ahead of

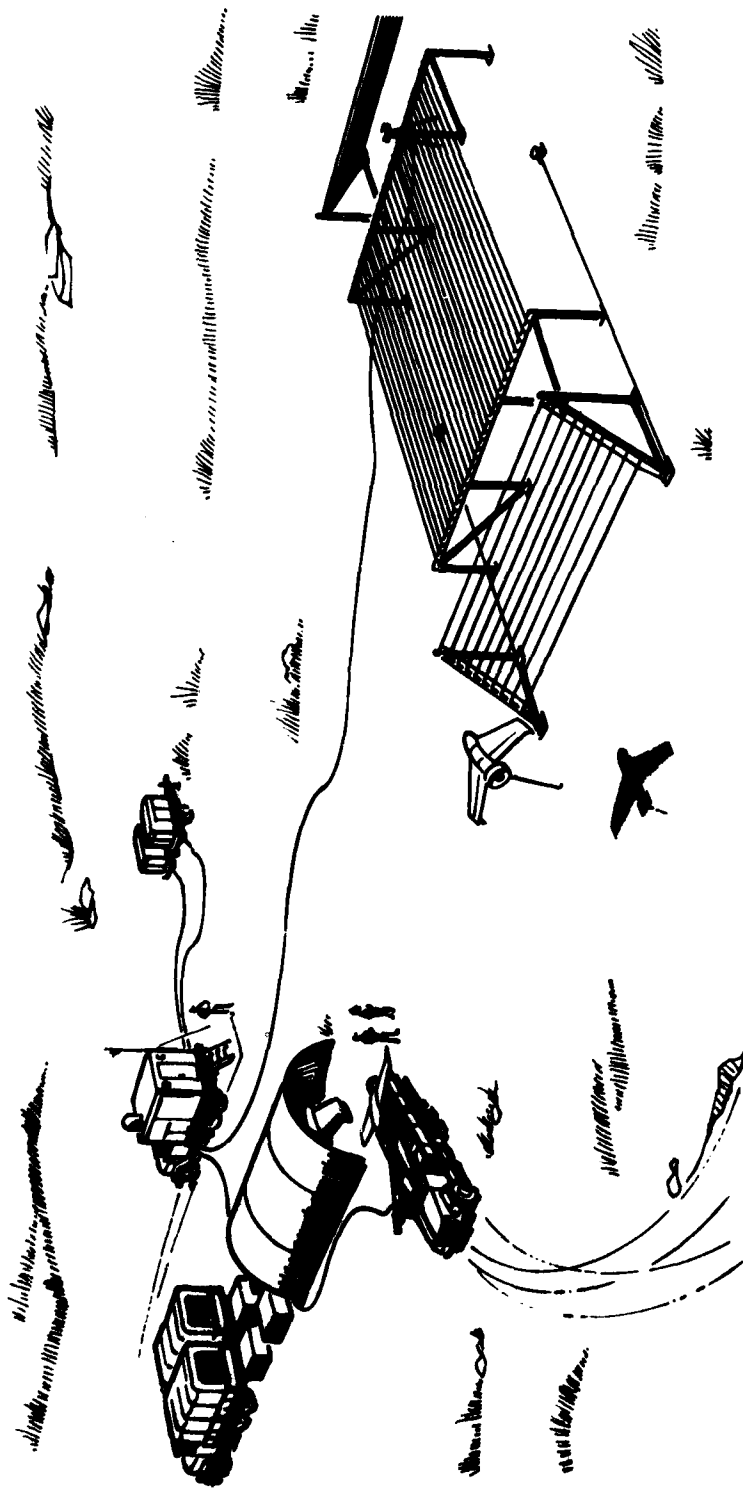


Figure 85. Sketch of Aquila RPV in Final Approach to Parallel Strap Retrieval System

the landing net. Upon engagement of the hook with any one or more of the lines, the vehicle will be decelerated to zero forward velocity and then pancake-landed into the landing net. Deceleration forces are generated by two rotary hydraulic energy absorbers to which the arresting lines are attached through a system of pulleys and sheaves.

Figure 86 shows an Aquila in final approach just before a successful retrieval. Figure 87 shows the RPV being decelerated after hook engagement and just before its successful pancake landing in the net.

Development Testing. Flight test activity, which employed this horizontal parallel strap system, was preceded by an intensive design and simulated flight test program to develop and qualify the system. LMSC as the prime contractor was supported by All American Engineering Company as the subcontractor.

Figure 88 shows photographs of an Aquila inert test vehicle (ITV) in the process of retrieval during a simulated flight test. The ITV had the external contours of the Aquila airframe and was ballasted to the appropriate gross weight (120 lb) and center-of-gravity location. It was also instrumented to record axial, transverse, and vertical loads as a function of time during retrieval.

Note, in Figure 88, the action of the deployed payload protector shielding the payload from adverse effects of impacting the horizontal landing net straps.

These tests were conducted on an aircraft taxiway at the Wilmington, DE, airport. The Parallel Strap Retrieval System was installed alongside the runway ramp. The ITV was suspended from a structure mounted on a 2-ton truck. With the hook already deployed, the truck was accelerated along the aircraft taxiway to the desired ground speed. At the appropriate moment before trailing hook engagement with the horizontal arresting lines array, the ITV was released automatically into a free-flight, unpowered glide. High-speed motion picture photography recorded the ITV retrieval trajectory, hook



Figure 86. Aquilla RPV in Final Approach Before Retrieval



Figure 87. Aquilla RPV Decelerating After Hook Engagement, Before Landing in Net

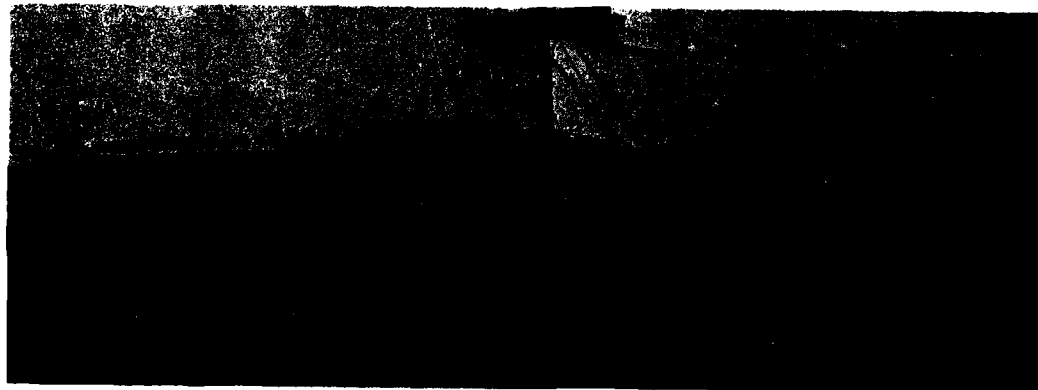
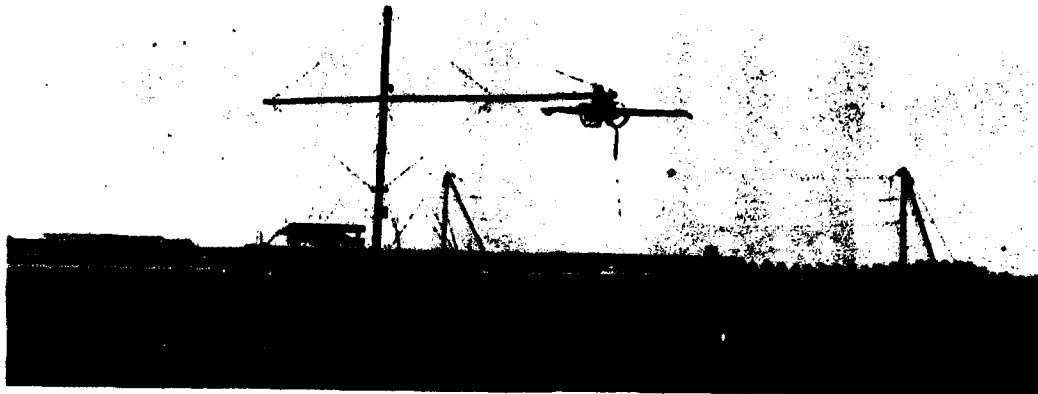


Figure 88. Aquila Inert Test Vehicle (ITV) in Process of Retrieval During Simulated Flight Test. (Top Photo) Approach at 45 knots immediately before ITV release and free-flight-glide hook engagement; (Center) ITV decelerating after hook engagement and before landing in net; (Bottom) Retrieved ITV at rest in landing net

and arresting line dynamics, and subsequent ITV and landing net impact motions. Thirty-five simulated flight retrieval system development tests were conducted before the system was committed to actual flight retrieval of the Aquila.

Three types of tests were conducted during the retrieval system simulation test program:

- Static (ITV Drop) Tests. These tests were conducted to obtain qualitative data of ITV vertical deceleration loads on the landing net from various pendant engagement altitudes.
- Dynamic (ITV Engagement) Tests. These tests were conducted at a maximum velocity of 48 knots. The tests were conducted by accelerating the test truck and releasing the ITV at the proper time to perform a dynamic engagement of the ITV tailhook system into the recovery system pendant network.
- Dynamic (No ITV Drop) Hook Engagement Tests. The tests were to study the action of ITV pole and hook assembly with the engagement pendant network without jeopardizing the ITV.

Three types of data were obtained - instrumentation, photo, and visual observation.

For the static (ITV drop) tests, the results are shown in Tables 18 and 19.

Typical accelerometer traces are presented in Figures 89 and 90. Maximum vertical deceleration was measured at 5.2 g from a drop height of 12 ft with 20 ft-lb tape tension (Figure 89).

For the dynamic (ITV engagement) tests, instrumentation traces were obtained of:

- Water twister tape tension
- Water twister rpm
- ITV engagement and landing accelerations

TABLE 18. RESULTS OF STATIC (ITV DROP) TESTS OF 9-4-75

Drop No.	Drop Ht. (ft-in.)	Landing Net Position		Net Tape Tension (lb-ft)	Acceleration, Vertical (g)	Visual Observations-Remarks
		Horiz.	Lateral (ft)			
1	3-6	Center	12	20	2.7	No photo coverage; small transmitter installed in tail of ITV, no damage
2	4-0	Center	12	20	4.1	No problems apparent
3	8-0	Center	12	20	3.7	Repairs required to four net turnbuckles
4	8-0	Center	12	20	5.0	Repeat of test 3
5	12-0	Center	12	20	5.0	No problems apparent
6	4-0	Center	12	20	4.0	No problems apparent
7	12-0	Center	6 ^(a)	20	5.2	No problems apparent

(a) Off center.

TABLE 19. RESULTS OF STATIC (ITV DROP) TESTS OF 9-19-75

Drop No.	Drop Ht. (ft.-in.)	Landing Net Position		Net Tape Tension (lb-ft)	Acceleration, Vertical (g)	Visual Observations-Remarks
		Horiz.	Lateral (ft)			
1	12-0	Center	12	20	4.2	ITV appears to bounce on landing
2	12-0	Center	12	20	3.5	Same
3	12-0	Center	12	10	3.2	Reduced net tension; slightly less bounce
4	12-0	Center	12	10	4.0	Same
5	12-0	Center	12	5	2.8	Reduced net tension

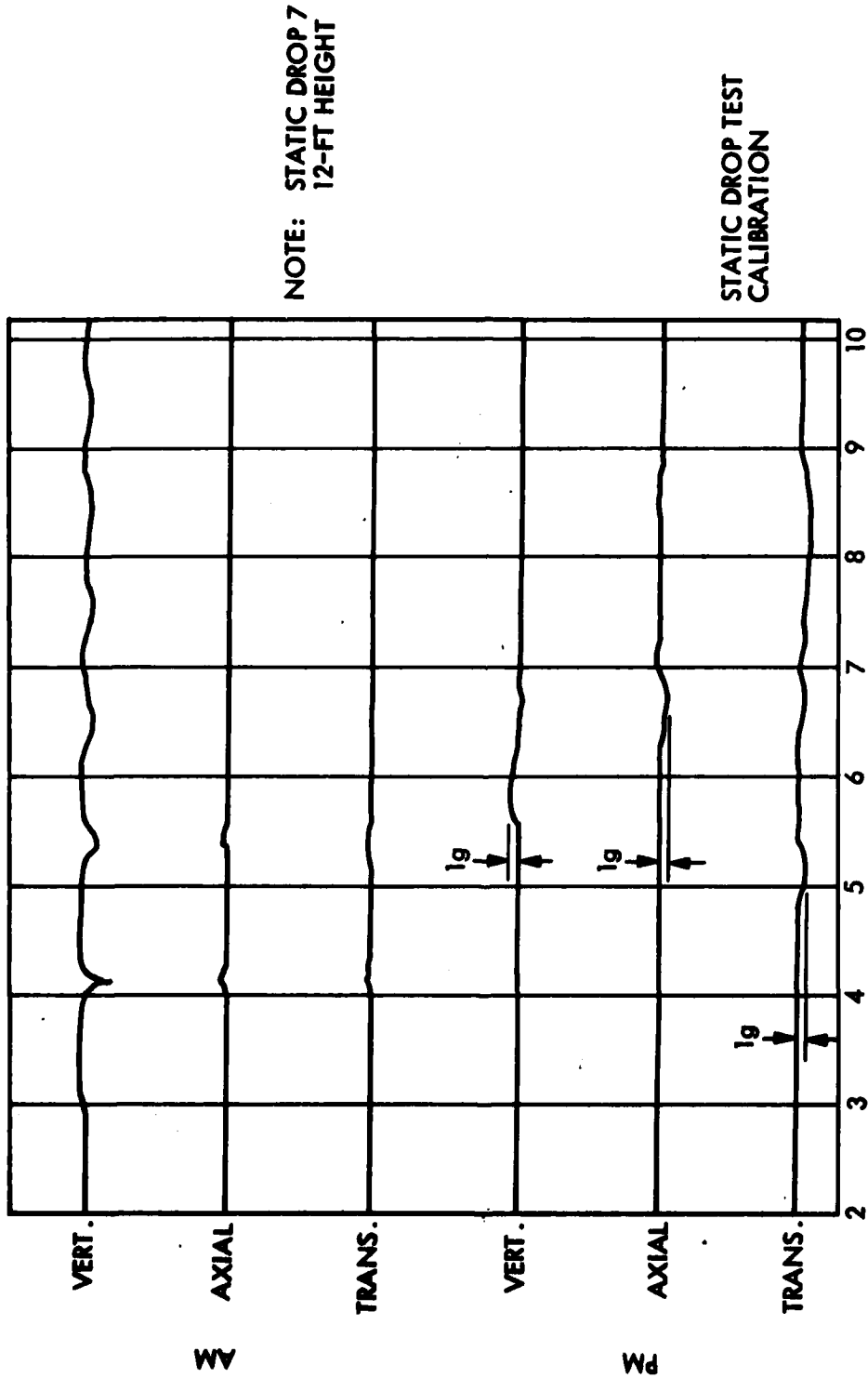


Figure 89. Acceleration Data From 9-4-75 Static Drop Tests

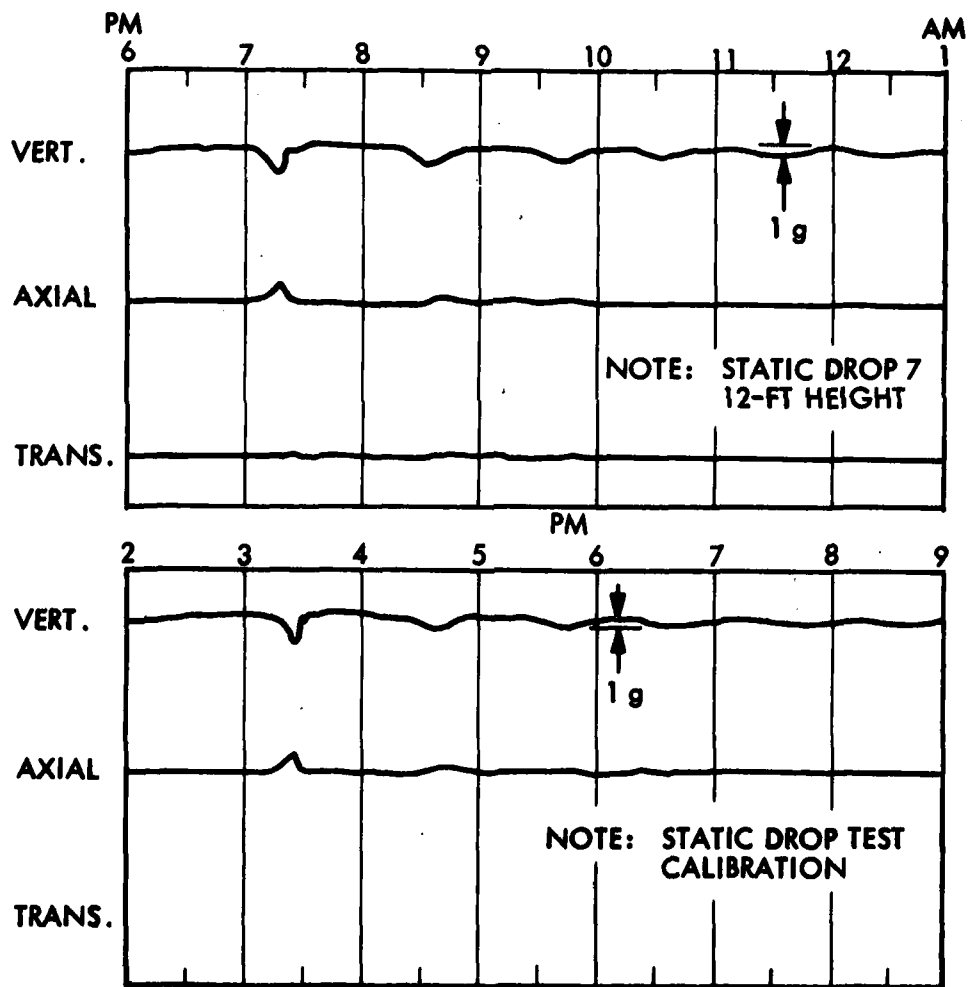


Figure 90. Acceleration Data from 9-19-75 Static Drop Tests

Data from these tests are furnished in Table 20.

The recovery system was shown to be satisfactory for the recovery of the Aquila vehicle. During normal arrestments and landings up to 48 knots, the recovery system did not impose accelerations in excess of 6 g. Engaging velocities to 58 knots were not accomplished because of test truck limitations.

Theoretical test data and actual test data indicate that the axial acceleration values will remain below 6 g up to 58 knots (Figure 91).

The development testing also included an intensive engagement hook development program involving proper design of the hook and hook system, its stowage aboard the RPV, its proper in-flight deployment, and estimates of its drag and aerodynamic control moment effects on the flight characteristics of the vehicle.

Figure 92 shows a typical hook engagement of the arresting line array, and Figure 93 shows closeup views of the hook and hook assembly. Note the keeper that permits an arresting line to enter the throat of the hook but prevents its expulsion. Figure 94 is a sketch showing the relationship of the Aquila RPV, deployed hook assembly, and arresting line array immediately before hook engagement.

Several undesirable features of the arresting-hook/parallel-strap system became clear in the course of its development and use and contributed directly to the loss of RPVs.

- The deployed RPV trailing hook induced undesirable drag and control-moment effects on the RPV during its final approach to the retrieval site.
- The extremely lightweight structure required for the engagement hook assembly (approximately 1.7 lb) provided very limited durability when subjected to retrieval engagement loads (from one to not more than three retrievals before major repair).

TABLE 20. RESULTS OF DYNAMIC (ITV ENGAGEMENT) TESTS

Test Date 1975	AAE Test No.	LUBC Test No.	Recovery OK Yes No	Eng. Vel. (ft./s.)	ITV Type	Hook Type	Shank Type	ITV Drop Position & Alignment				Acceleration (g)		Max. Tester Type (lbs.)	Max. Tester Vel. (rpm)	Ldg. Net Torque (lb)ft				
								12' On-Ctr	6' Off-Ctr	Hi Lo	Hi Lo	Vert	Anal				Hi	Lo	705	NR
8-31	1	3	X	1	45	DSI	DSI	X	HI	18'	HI	18'	Not Recorded	Not Recorded	Not Recorded	20				
8-28	2	3	-	X	None	Same	Same	X	HI	18'	HI	18'	15+ (offscale)	No Runout	No Runout	20				
9-4	1A	1	-	X	None	Same	Same	X	HI	18'	HI	18'	15+ (off scale)	No Runout	No Runout	20				
9-18	A	-	X	-	1	AAE P/N 19SK188-5	AAE P/N 19SK188-5	X	HI	18'	HI	18'	Not recorded	Not Recorded	Not Recorded	20				
9-18	B	-	X	-	1	Same	Same	X	HI	18'	HI	18'	Not Recorded	Not Recorded	Not Recorded	20				
9-18	C	-	X	-	1 & 2	Same	Same	X	HI	18'	HI	18'	Not Recorded	Not Recorded	Not Recorded	20				
9-19	C	-	X	-	1	Same	Same	X	HI	18'	HI	18'	Not Recorded	Not Recorded	Not Recorded	20				
9-22	1B	1	X	-	1	DSI	DSI	X	HI	18'	HI	18'	3.0	2.2	0.7	205	140	540	NR	10
9-22	2B	3	X	-	1	Same	Same	X	HI	18'	HI	18'	4.0	2.9	0.3	207	155	600	NA	10
9-26	3B	4	X	-	1	Same	Same	X	HI	18'	HI	18'	5.8	3.0	0.7	150	135	625	NR	10
9-26	4B	-	-	X	None	Forbidden Hook 19SK188-6	Forbidden Hook 19SK188-6	X	HI	18'	HI	18'	15	Off-scale	4.0	No Runout	No Runout	NR	10	
10-1	E	-	X	-	1	AAE Wood	AAE P/N 19SK188-7	X	HI	18'	HI	18'	Not Recorded	Not Recorded	Not Recorded	Not Recorded	Not Recorded	Not Recorded	Not Recorded	10
10-2	5B	3	X	-	2	DSI	DSI	X	HI	18'	HI	18'	Not Recorded	Not Recorded	Not Recorded	115	150	610	NR	10

Products numbered 1 through 6 - Top to Bottom
 Hook failed to engage

TABLE 20. (Cont.)

Test Date 1975	AAE Test No.	LADC Test No.	Essary CK Yes No	Eng. Prod. No.	Eng. Vel. (kts.)	ITV Type	Hook Type	Shank Type	ITV Drop Position & Alignment				Acceleration (g) Vert	Max. Twister Tens (Lbs.) Rt.	Max. Twister Vel. (rpm) Lt.	Ldg. Net Torque (lb) Lt.
									12' On-Ctr	6' Off-Ctr	Hi Lo	Hi Lo				
10-2	6B	-	-	X	39	Same	Same	Same	X	Hi 18'	24°	∞	15+ Offscale	No Runout	No	10
10-3	F	6	-	X	2	AAE Wood	AAE P/N ISSK188-8	Same	X	-	24°	-	Not Recorded	Not Recorded	Not Recorded	10
10-3	G	8	-	X	1 & 2	Same	Same	Same	X	-	24°	-	Not Recorded	Not Recorded	Not Recorded	10
10-7	H	9	-	X	5	Same	Same	Same	X	Lo 13'	-	-	Not Recorded	Not Recorded	Not Recorded	10
10-7	I	10	-	X	5	Same	Same	Same	-	Lo 13'	-	-	Not Recorded	Not Recorded	Not Recorded	10
10-8	J	10	-	X	5	Same	Same	Same	-	Lo 13'	-	-	Not Recorded	Not Recorded	Not Recorded	10
10-8	K	11	-	X	None	Same	Same	Same	X	-	24°	Lo 13'	Not Recorded	Not Recorded	Not Recorded	10
10-8	-	-	-	-	-	-	Same	AAE Wood	-	-	-	-	-	-	-	-
10-9	-	-	-	-	-	-	Same	Same	-	-	-	-	-	-	-	-
10-10	L	11	-	X	2 & 4	AAE Wood	Same	Same	X	-	24°	Lo 13'	Not recorded	Not Recorded	Not Recorded	10
10-10	M	11	-	X	2 & 3	Same	Same	Same	-	X	-	24°	Not Recorded	Not Recorded	Not Recorded	10
10-10	N	8	-	X	4	Same	Same	Same	X	-	Lo 13'	-	Not Recorded	Not Recorded	Not Recorded	10

TABLE 20. (Cont.)

REMARKS: (By AAE Test No.)

- 1 ITV recovered OK. Hit far net post on runouts. Slight damage to ITV. 1 gal Prestone in each twister.
- 2 No recovery. Overshot top pendant. ITV hit far net posts. ITV damaged. Landing net poles and guy wires damaged. Hook and pole flew horizontally prior to engagement due to stretch of shank restraint bungees. (Shank originally set for 10° down angle.)
- 1A No recovery. Hook struck No. 2 pendant. Hook spring broke. Hook released. ITV damaged. 6 qt fluid in twisters - 4 Prestone, 2 water.
- A Good recovery with AAE wood ITV & AAE hook. ITV pole sheath broke at fuselage. Pole broke at sheath.
- B Good recovery. Sheath and pole again broke same places as prev. test.
- C Good recovery. Sheath and pole again broke same places as prev. test.
- D Good recovery. Sheath and pole again broke same places as prev. test.
- 1B Good recovery. No damage to any member, except black coating on Kevlar loop worn through.
- 2B Good recovery. No damage. However, ITV accidentally dropped during rigging for next run. Down for repair.
- 3B Good recovery. However, ITV bounced on landing and flipped over backwards. Broke sheath & pole. Also pulled hook retainer off pole. First off-center test.
- 4B Hook contacted No. 1 pendant but did not engage. ITV overflow landing net. Landed in soft ground, slid about 70 ft. Damaged bottom fuselage. Down for repairs. Forked hook used. Possible cause, design discarded.
- E Good recovery, but broke pole. Used AAE aluminum sheath. Used new AAE -7 hook.
- 5B Good recovery. Kevlar worn. Hook shank OK. Twisters filled to capacity with transmission fluid (2 gal each).
- 6B No recovery. Hook did not engage. Severe lateral oscillations of pole assy due to high winds. ITV damaged. Down for repairs. (Note 24° skew.)

TABLE 20. (Cont.)

- F** No release of ITV. Cable cutters did not fire. Hook engaged OK. Broke Kevlar loop. No other damage.
- G** Good recovery. However, new method of holding sheath at 10° angle did not work, but caused no problems. (Note 24° skew.) End of Hi Pos. Tests.
- H** Good recovery, but hook shank unstable. First Lo level tests.
- I** Good engagement but Kevlar line broke and slipped through plastic coating. ITV over end of net. No damage. Removed 2 ft plastic coating at hook. Coated Kevlar with Bees Wax.
- K** No engagement. Hook hit pendant but bounced off. Hook shank unstable. ITV flipped off net. No damage. (Note 24° skew.)
- 4 good hook-only tests with AAE hook and wood pole. (No ITV release.)
- 10 good hook-only tests with AAE and LMSC poles.
- L** Good recovery. Good landing. AAE wood pole held to 20° down angle till hook engagement. Pendant tension 15-20 lb. (Note 24° skew.)
- M** Good recovery - Same setup. (24° skew). No problems of any kind.
- N** Good recovery - Same setup as previous two tests except not skewed. No problems - last test.

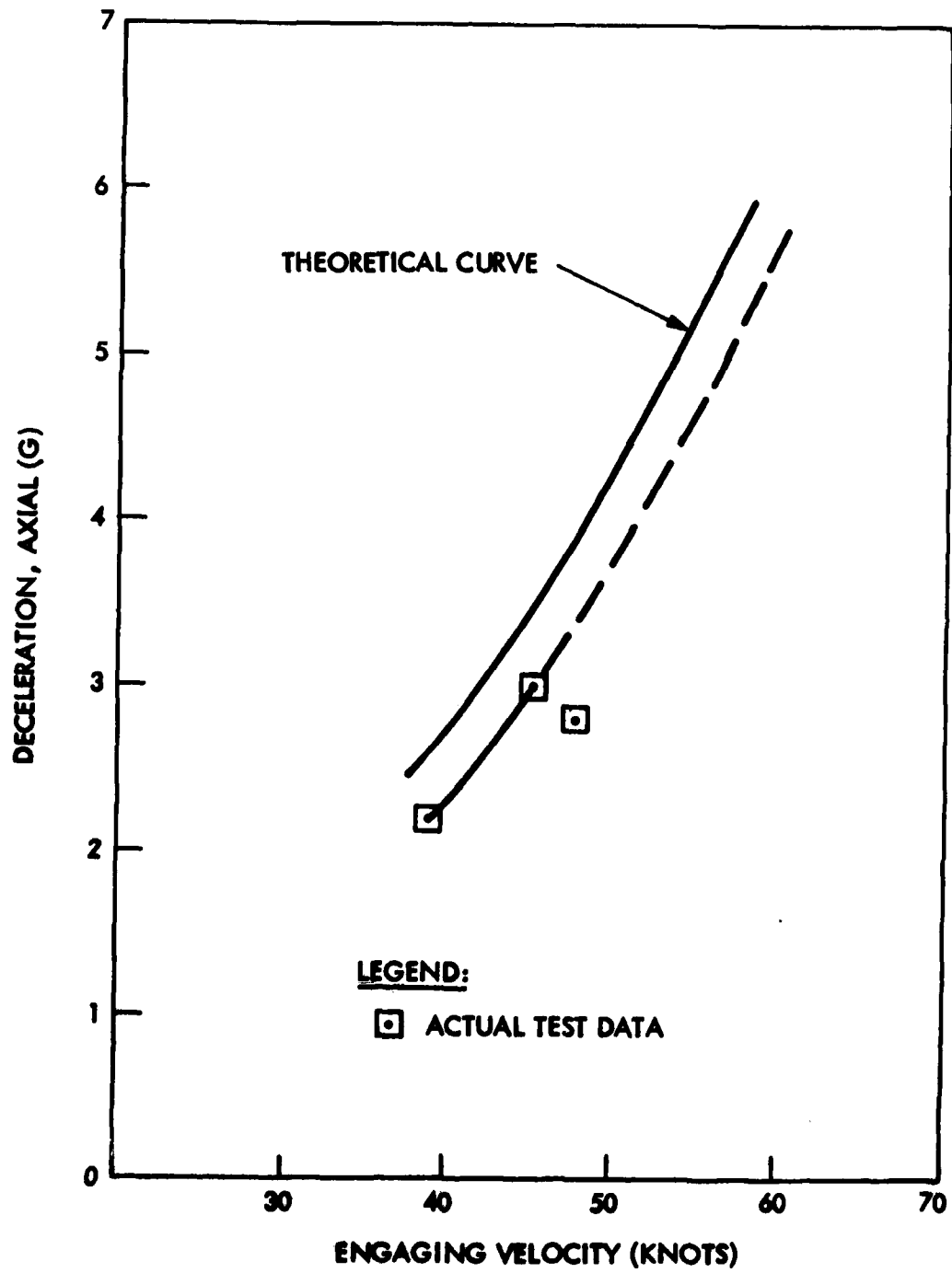


Figure 91. Axial Deceleration Data (ITV)

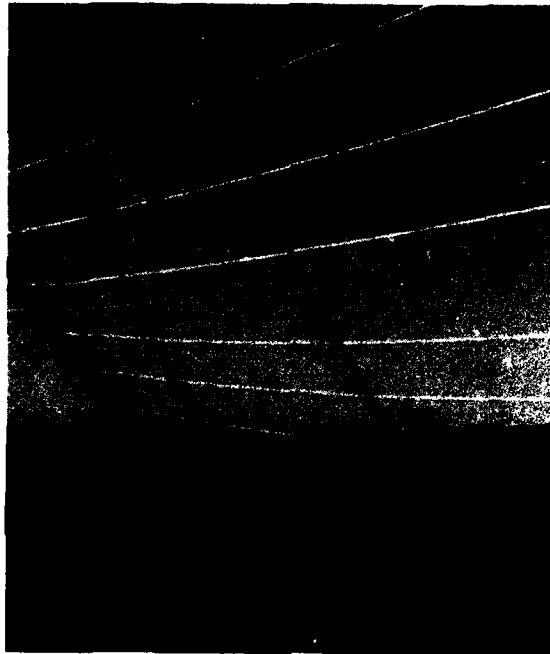


Figure 92. Typical Hook Engagement of Arresting-Line Array

- Proper stowage of the engagement hook assembly on the RPV required special personnel training and skills to ensure readiness in flight for remote deployment of the hook assembly on command.
- The intricate nature, extremely light weight, and low-drag requirements of the hook assembly – combined with its limited life before repair – made the engagement hook assembly a costly item.

In parallel with the Aquila flight test program involving the arresting hook/parallel strap retrieval system, highly successful development tests were being conducted on the vertical barrier retrieval system, which eliminated ~~engineers~~ lack of mobility and high damage potential – with tall pole frames ~~or other vertical net systems~~. As a result of these successes, the vertical

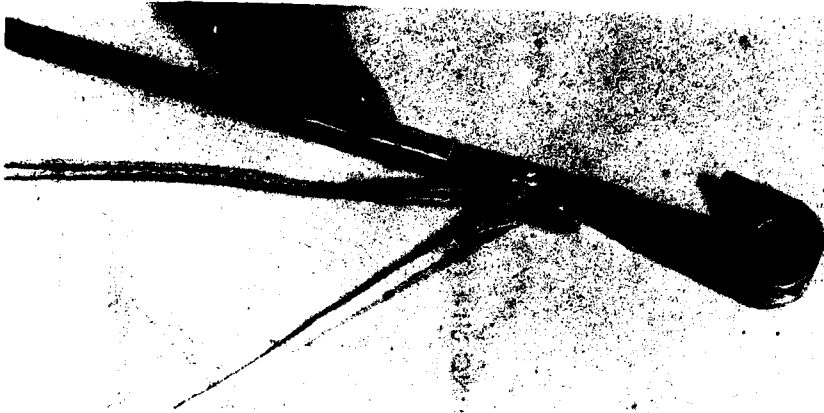


Figure 93. Engagement Hook Assembly. (Top Photo) Hook; (Center) Hook assembly folded and ready for insertion into sheath; (Bottom) Hook assembly sheathed and ready for attachment to RPV

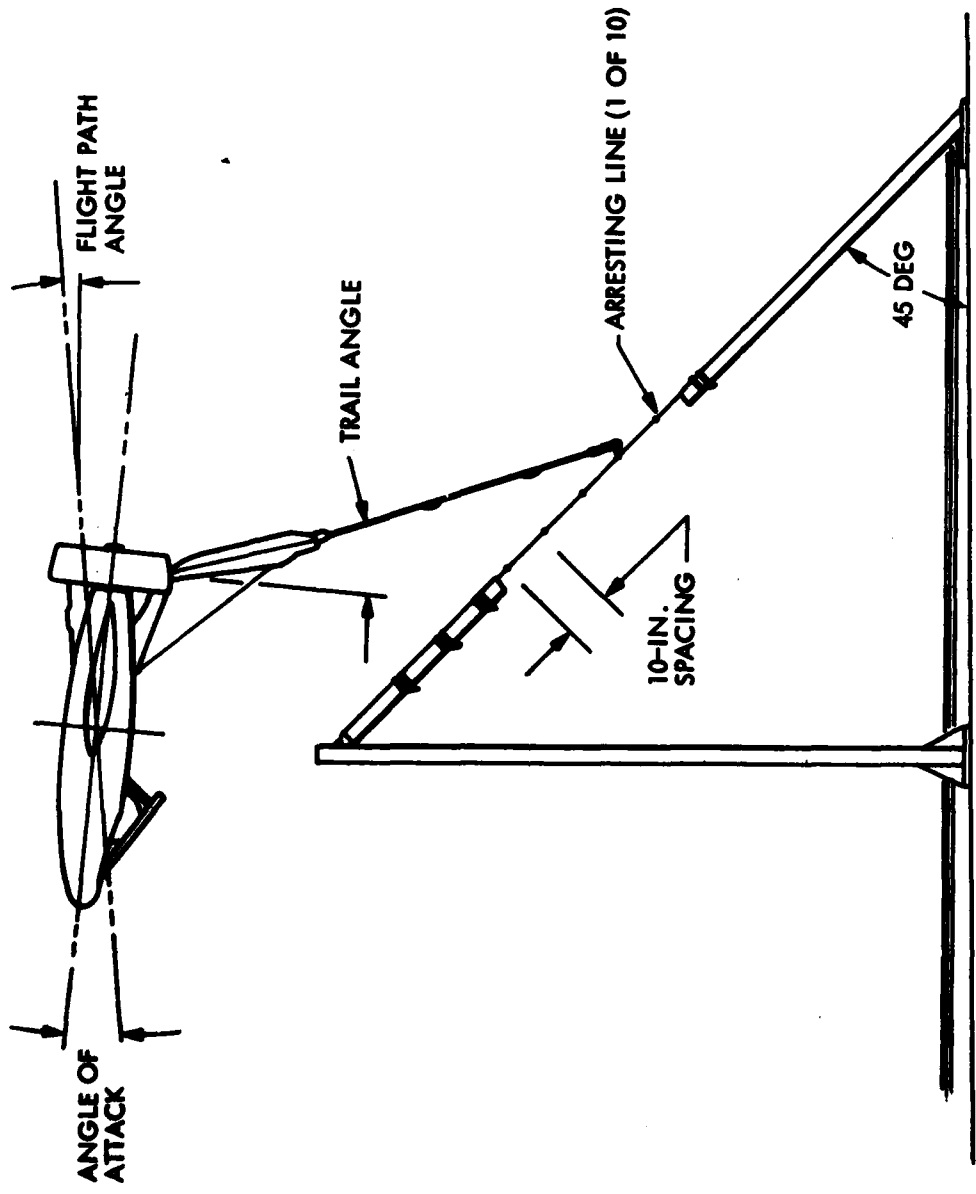


Figure 94. Sketch of Aquila, Showing Deployed Hook Assembly Before Arresting Line Engagement

barrier system was adopted for subsequent Aquila flight tests, thereby eliminating the problems of the hook assembly and hook engagement. As an added advantage, the vertical barrier retrieval system was developed as a mobile item, on standard Army transport equipment, that would not require any ground-staking and would be deployable at unprepared sites with very little or no site clearing.

The vertical barrier system was selected for development after an exhaustive study of more than 40 different mini-RPV retrieval system concepts, all of which were identified as adaptable to tactical Army multimission RPVs. Through various combinations and permutations of these individual systems, the list is easily expanded to well over 100.

5.4.5 Evolution of Vertical Barrier System

5.4.5.1 System Description. Figure 95 shows the concept of the vertical barrier system and Figure 96 its method of RPV flight retrieval. Basically, the system consists of two vertical barriers placed at either end of one horizontal RPV landing net. Two vertical barriers are employed to permit RPV retrieval without reorienting the retrieval system relative to wind direction. Operationally, the vertical barrier serves to absorb and dissipate the flight kinetic energy of the RPV, and the horizontal landing net serves to absorb the potential energy of the RPV resulting from its arrested height above the landing net.

The flying and structural characteristics of the Army multimission RPV and its final approach guidance system indicated that a vertical barrier having a vertical dimension of 15 ft and a horizontal span of 35 ft would be appropriate. This overall size would provide an effective retrieval window of 12 ft (vertical) by 21 ft (horizontal). This size is based on the location of the RPV center of gravity at impact and provides ample safe margins for the wing span and propeller shroud outside the retrieval window itself.

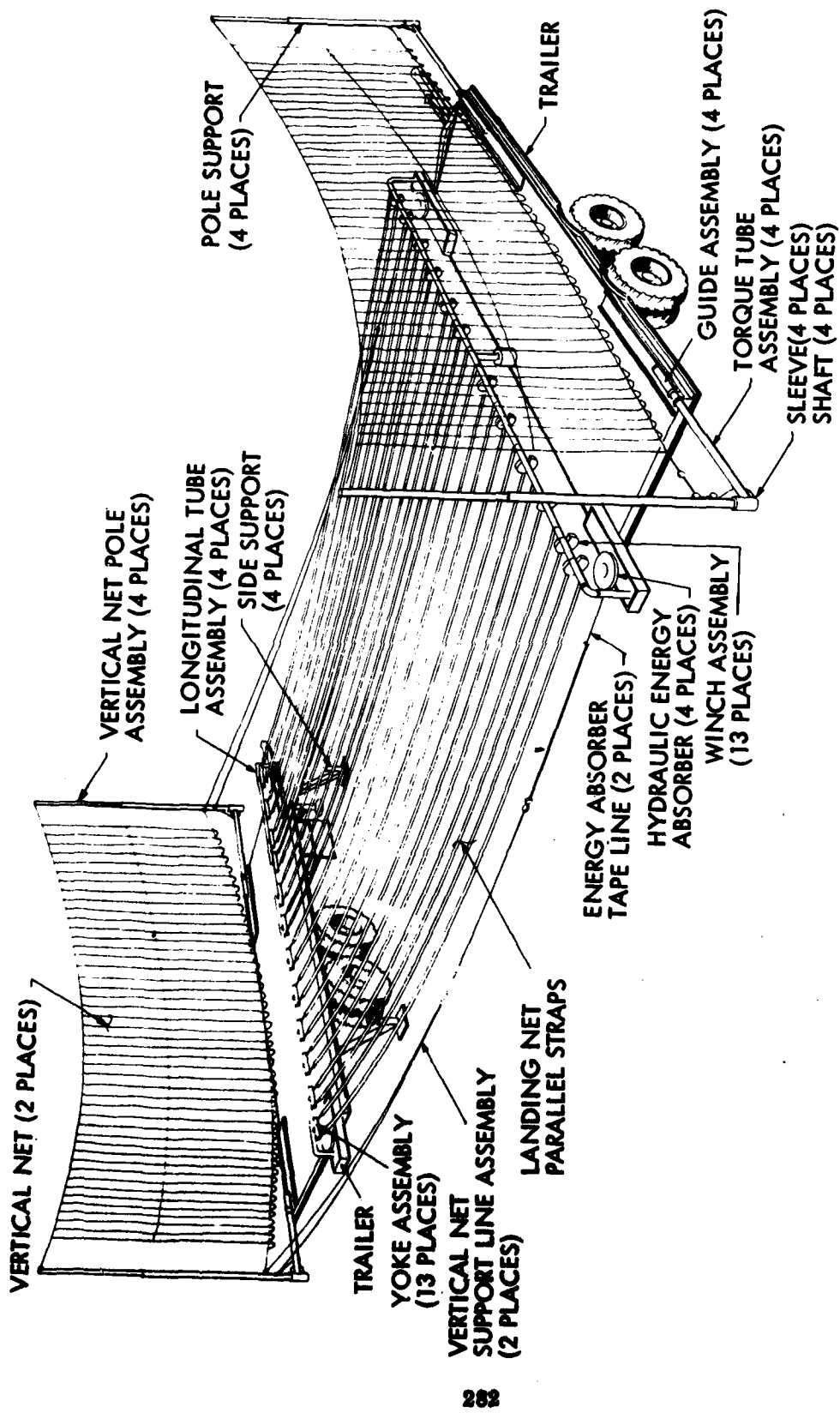
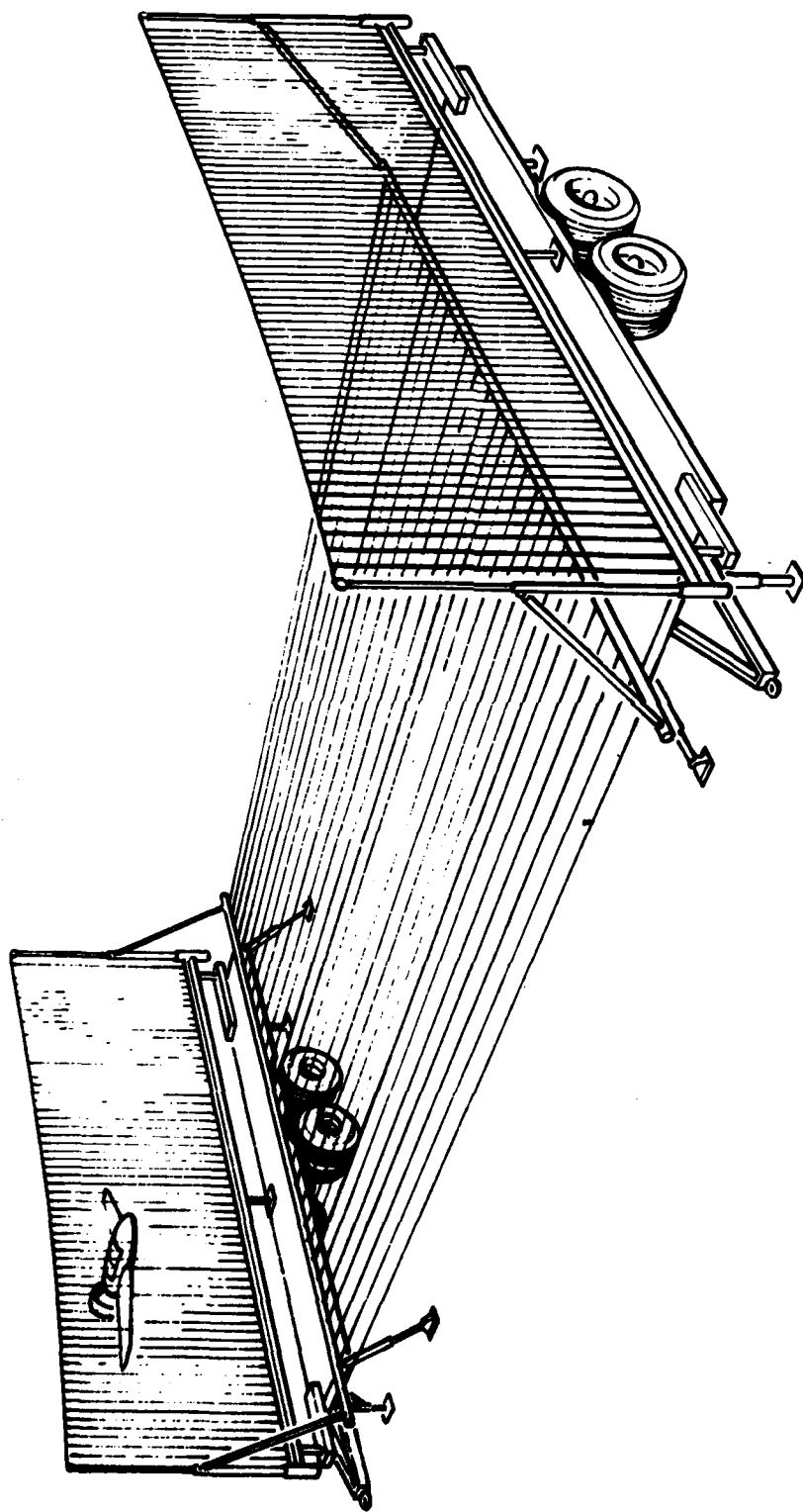
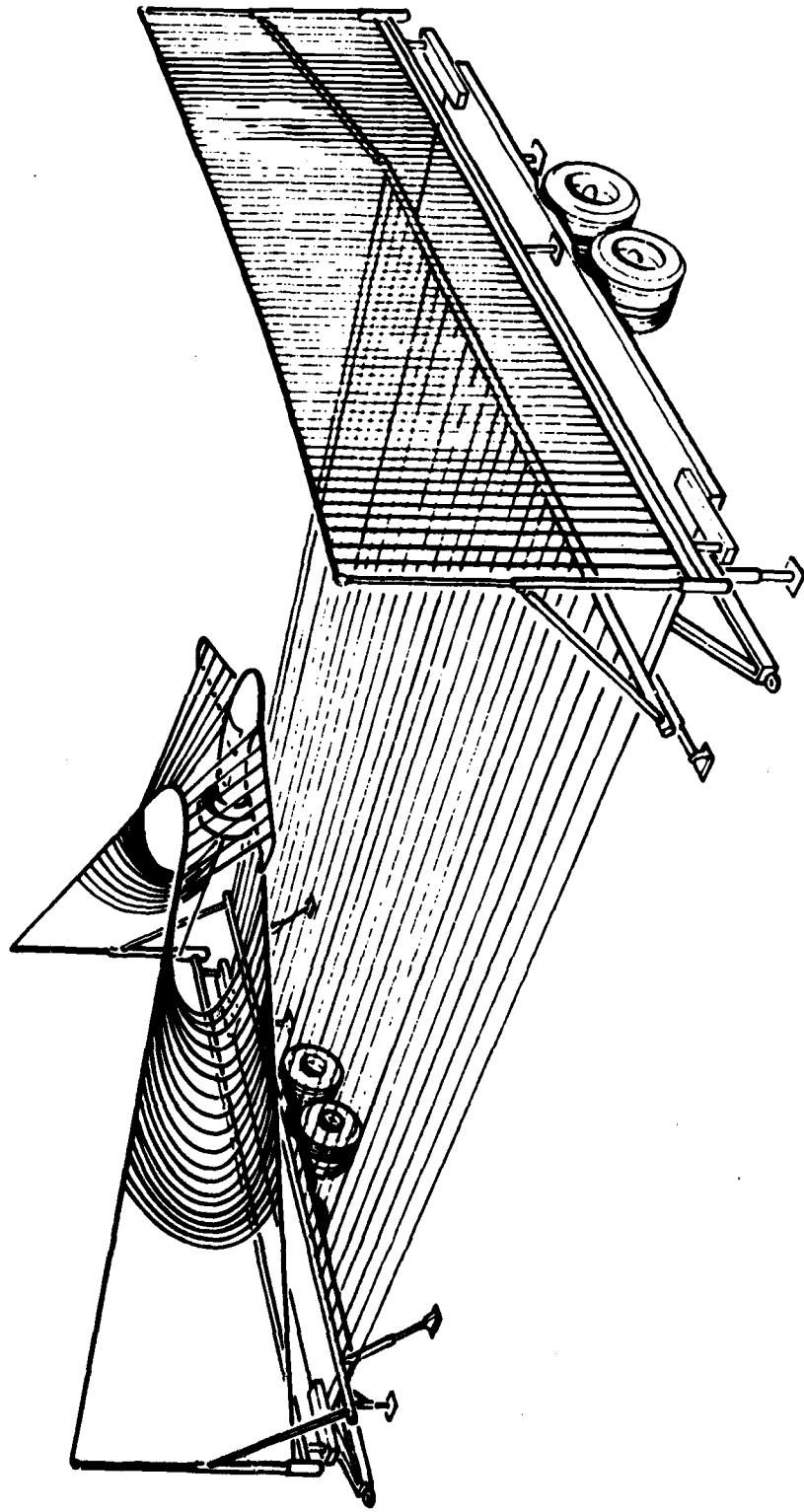


Figure 95. Vertical Barrier System Concept



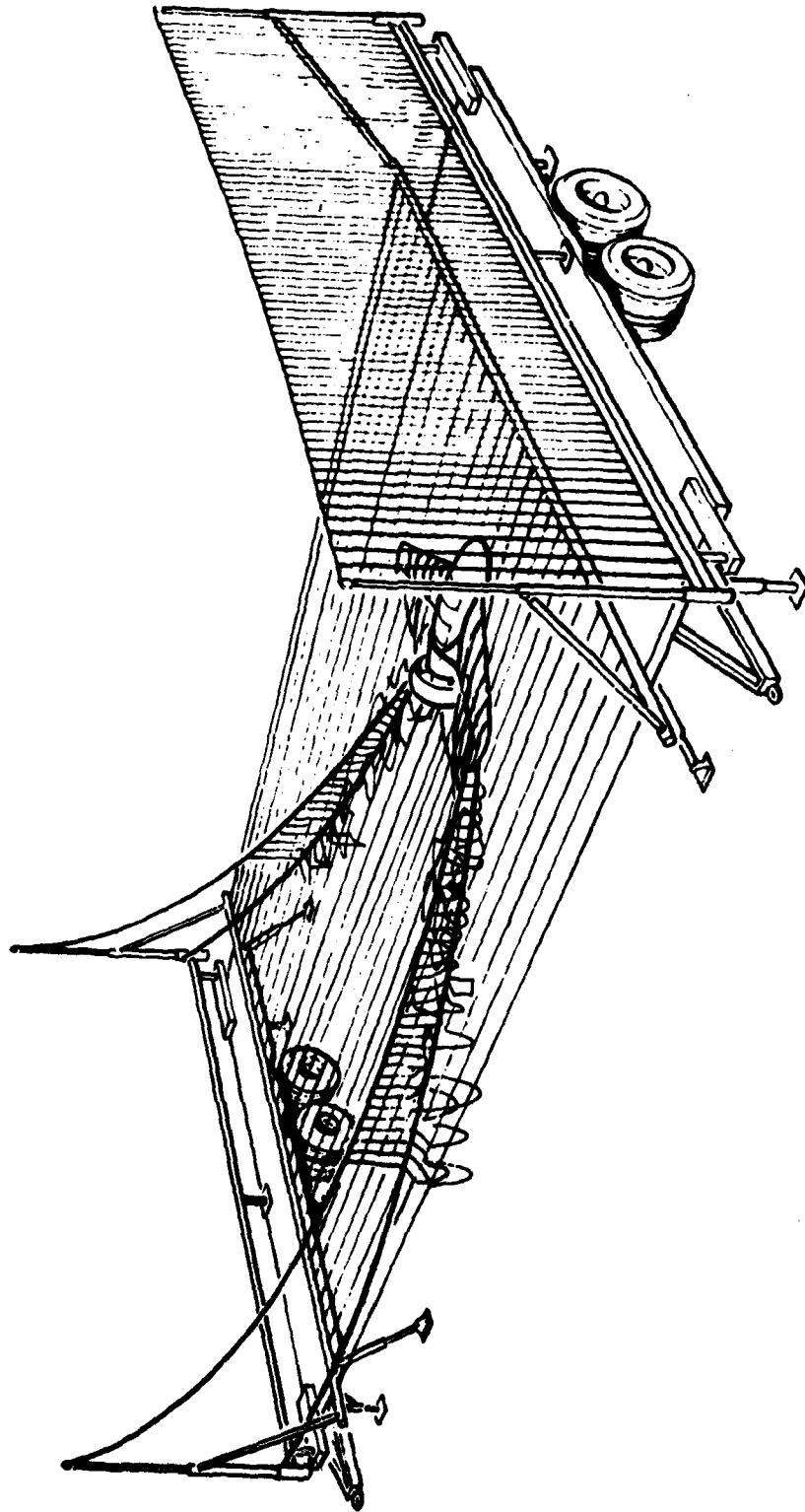
a. Approach of RPV

Figure 96. Operational Concept of Vertical Barrier System



b. Engagement With Net and Deceleration

Figure 96. (Cont.)



c. RPV at Rest in Landing Net

Figure 96. (Concl.)

Each vertical barrier net, supported between two vertical poles, is connected at its four corners by lines through pulleys to two rotary hydraulic energy absorbers. The energy absorber assembly consists of a hydraulic-fluid-filled housing with two sets of eight stator vanes fixed to the top and bottom of the housing. Nine rotary vanes attached to the rotor shaft are located in the space between the upper and lower sets of stator vanes. The rotor shaft is driven by a tape reel on which a roll of high-strength nylon tape is stored. When the in-flight RPV engages the vertical barrier net, the nylon tape connected to the vertical barrier pays out and the desired arresting force is provided by the hydraulic fluid in vortex motion induced by the rotor. The rotor and tape reel have a common shaft, so that rotation of the tape reel during RPV retrieval deceleration spins the rotor vanes at a high speed. To make the system ready for another RPV retrieval, the nylon tape is rewound on the reel, thereby also reerecting the vertical barrier in its proper place. A hold-back brake mounted on the energy absorber housing provides the force needed to maintain the vertical barrier erect in winds to 20 knots and gusting to 35 knots.

The horizontal RPV landing net has a width of 25 ft and a length of 60 ft. These dimensions are an appropriate match for the 15- by 35-ft vertical barrier and provide the desired RPV deceleration characteristics within the structural load limits of the Army multimission RPV.

The landing net consists of 1-3/4-in.-wide, high-strength dacron straps spaced 1 ft apart over its entire 25-ft span. The straps are stored on reels for easy field setup and strikedown. The reels are equipped with a ratchet drive so that the straps can be tensioned properly to 10 ft-lb of torque with a torque wrench.

The entire retrieval assembly is mounted on two standard Army M345 trailers, each of which can be drawn by a standard Army M35 or M36 truck.

5.4.5.2 Development Testing.

Test Facilities. The mobile vertical barrier system was constructed and a development program was conducted consisting of 21 inert RPV vehicle retrieval system development tests and 11 RPV structural retrieval tests.

The retrieval system was mounted on two M345 trailers obtained from Army inventory. A full-scale inert RPV test vehicle was constructed of wood and metal. It was instrumented with three-axis accelerometers to measure axial, vertical, and transverse retrieval loads. Ballast was added to bring the vehicle gross weight to 140 lb and was balanced to properly locate the center of gravity.

A pneumatic launcher was used to accelerate this inert test vehicle to velocities ranging from 33.5 to 51.5 knots. Figure 97 shows this inert test vehicle mounted on the pneumatic launcher in preparation for a retrieval system test. The vehicle was launched for impact into various points on the vertical barrier net and at various vehicle attitudes.

During retrieval, instrumentation in addition to the accelerometers measured the initial impact velocity, gathered force-time-distance data from the energy absorber, and located the point of impact. High-speed motion pictures were taken to evaluate the trajectories and motions of the vehicle during retrieval.

Following these retrieval system development tests, 11 additional development tests were conducted to evaluate the effects of retrieval on the RPV structure and skin. An actual RPV airframe was used for this series of tests. Six of these tests were conducted in the same manner and over the same general range of conditions as the retrieval system development tests, using the wood and metal inert test vehicle.



Figure 97. Inert Test Vehicle Mounted on Pneumatic Launcher for Retrieval Test

The remaining five tests were conducted with the RPV pneumatic launcher mounted on a standard Army M36 truck. Figure 98 shows the RPV airframe vehicle in battery position on the launcher before being launched into the retrieval system. In both portions of the complete test series, the same RPV instrumentation was provided and data were obtained.

Development Test Results. Development tests were run in August 1976 at Wilmington, Delaware, and in September 1976 at Fort Huachuca.

Summaries of the data obtained in the 32 development tests conducted on this program prior to actual RPV flight retrieval demonstrations are presented in Tables 21 and 22. Table 21 presents the data on all 21 tests obtained with the inert test vehicle (ITV) shown in Figure 97; it also presents the data obtained in the first six tests using the RPV structural test vehicle (AQ-003) shown in Figure 98. (The five shuttle-only tests are not included in these totals.)

Table 22 presents the data obtained in the last five tests using the RPV structural test vehicle.

Figure 99 shows a series of photographs of the ITV after launch and in various stages of retrieval. Because only one such photograph was taken in any single test, the series is necessarily composed of photographs of the ITV from different tests. The test during which each photograph was taken is indicated in the caption; the corresponding test data are in Table 21.

Figure 99(a) shows the ITV in free flight just as it leaves the pneumatic launcher but before it impacts the vertical barrier net. This photograph was taken during test event 18; a summary of data obtained is shown in Table 21. The following specific facts can be noted: the velocity of the vehicle at the instant of the photograph was 33.5 knots; the vehicle impacted the center of the vertical barrier net; it approached the net in a horizontal flight path; the yaw or skew angle was 0 deg; the maximum vertical load upon impacting the landing net was 1.8 g; the transverse loads were negligible; and the retrieval was 100-percent successful, with no damage either to the ITV or to any portion of the retrieval system itself.

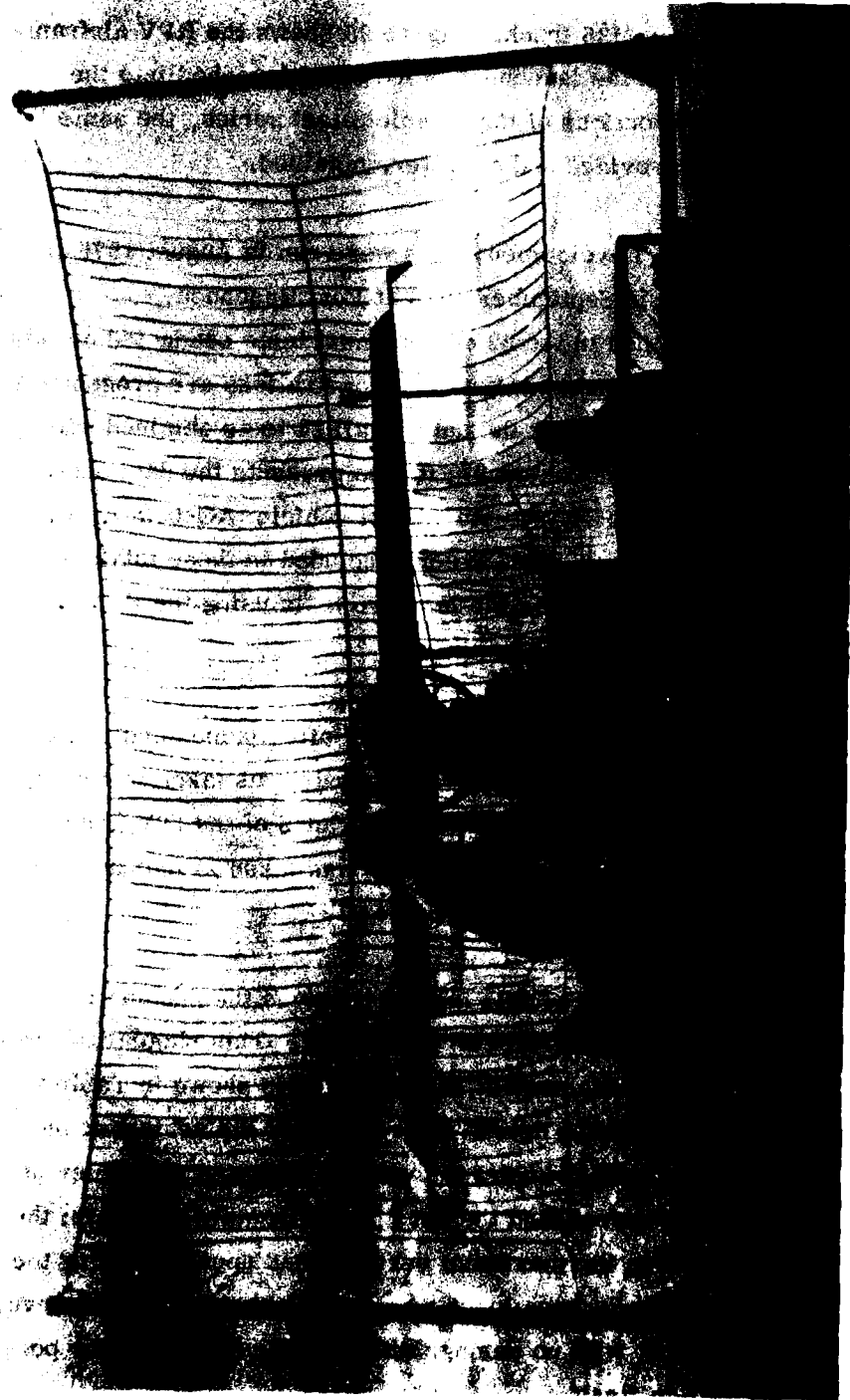


Figure 98. RPV Airframe Test Vehicle in Battery Position Before Launch Into Vertical Barrier Retrieval System

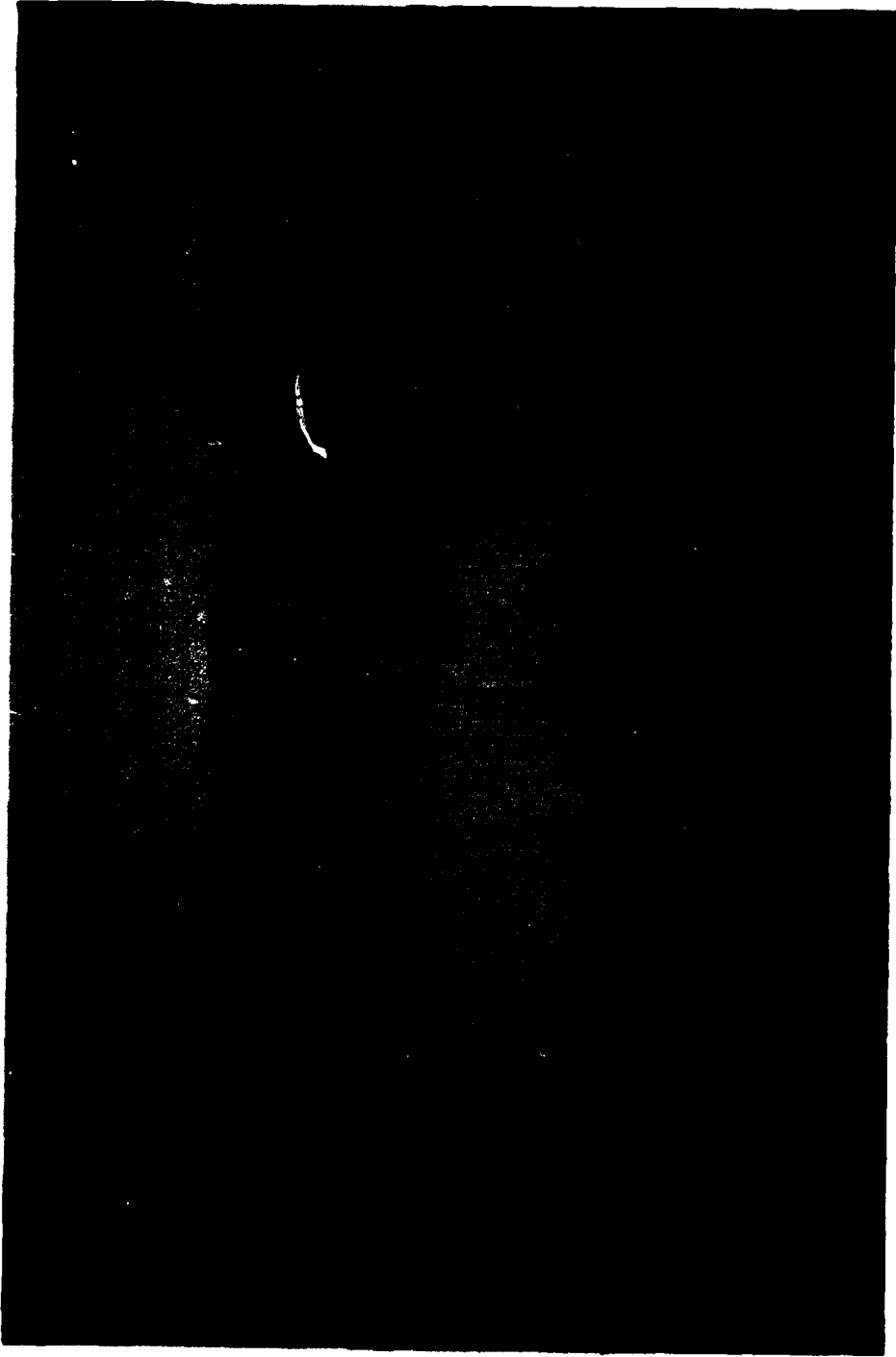
TABLE 21. TEST DATA SUMMARY (DEVELOPMENT TESTS CONDUCTED AT FACILITIES IN WILMINGTON, DE)

EVENT NUMBER	DATE	VEHICLE TYPE	LAUNCH PRESSURE (PSIG)	VELOCITY (KNOTS)	INCLINATION ANGLE (DEG.)	VERTICAL NET IMPACT	VEHICLE ALIGNMENT SKED ANGLE (DEG.)	MAXIMUM IMPACTOGRAPH LOADS G's				MAXIMUM TAPE TENSION (LBS)		DATE PAYOUT (HR.)		REMARKS
								HYDRAULIC	AXIAL	END LOAD	VERTICAL	TRANS.	LEFT	RIGHT	LEFT	
12	8/4	SHUTTLE ONLY	90	44.0	5	H-C	-	-	-	-	280	260	-	320	SUCCESS	
13	8/4	ITV	160	37.2	5	H-C	0	-	-	-	210	300	-	360	SUCCESS	
14	8/4	ITV	200	43.5	5	H-C	0	1.9	3.1	~0	275	350	-	360	SUCCESS	
15	8/4	ITV	270	51.3	5	H-C	0	2.6	4.2	1.2	-	-	-	-	NO RETRIEVAL TEST. PRE-MATURE LAUNCH ITV RELEASE	
16	8/4	ITV	270	51.3	5	H-C	0	-	-	-	-	-	-	-	SUCCESS	
17	8/5	SHUTTLE ONLY	90	44.5	0	C-C	0	1.5	1.8	~0	225	278	-	336	SUCCESS	
18	8/5	ITV	120	33.5	0	C-C	0	2.0	2.0	~0	200	290	-	336	SUCCESS	
19	8/5	ITV	150	49.5	0	C-C	0	1.8	2.0	~0	200	290	-	336	SUCCESS	
20	8/6	SHUTTLE ONLY	90	45.0	0	C-C	0	2.2	2.9	~0	240	230	-	336	SUCCESS	
21	8/6	AG-003	200	44.1	0	C-C	0	2.4	2.9	~0	240	230	-	336	FIRST AQUILA 003 STRUCTURE TEST - SUCCESS/TOP ANT. LOST	
22	8/6	AG-003	270	51.5	0	C-C	0	2.2	2.4	~0	340	400	-	336	NO DAMAGE - SUCCESS	
23	8/6	ITV	200	44.4	0	C-C	24 LEFT	-	-	-	310	250	-	336	SUCCESS	
24	8/6	ITV	270	50.8	0	C-C	24 LEFT	-	-	-	300	290	-	336	SUCCESS	
25	8/6	ITV	200	42.6	5	H-C	24 LEFT	2.5	2.8	-	260	250	-	336	SUCCESS	
26	8/6	ITV	270	49.6	5	H-C	24 LEFT	2.3	3.3	-	300	275	-	336	SUCCESS	
27	8/9	SHUTTLE ONLY	90	43.5	0	C-C	0	-	-	-	-	-	-	-	NO DAMAGE - SUCCESS	
28	8/9	AG-003	160	42.0	0	C-C	0	2.1	2.2	~0	350	325	-	336	NO DAMAGE - SUCCESS	
29	8/9	AG-003	270	50.0	0	C-C	0	2.2	3.0	~0	300	275	-	336	NO DAMAGE - SUCCESS	
30	8/9	AG-003	200	41.0	5	H-C	0	2.7	4.2	~0	360	360	-	336	LAST AQUILA 003 STRUCTURE TEST - NO DAMAGE/SUCCESS	
31	8/9	AG-003	270	51.2	5	H-C	0	2.7	4.2	~0	360	360	-	336	TRAILERS MOVED 7' LEFT	
32	8/9	ITV	180	41.0	0	C-R	0	2.3	1.7	1.0	200	300	-	276	SUCCESS	
33	8/9	ITV	270	51.0	0	C-R	0	-	-	-	300	400	-	276	SUCCESS	
34	8/9	ITV	180	43.3	5	H-R	0	2.4	3.0	-	250	300	-	336	LEFT WING FELL BETWEEN LRDC NET STRAPS - QUAL. SUCCESS	
35	8/9	ITV	270	51.0	5	H-R	0	-	-	-	300	300	-	336	LEFT WING FELL BETWEEN LRDC NET STRAPS - QUAL. SUCCESS	
36	8/9	ITV	270	50.9	5	H-R	0	-	-	-	-	-	-	-	SUCCESS	
37	8/10	SHUTTLE ONLY	90	41.2	5	H-R	0	-	-	-	-	-	-	-	ADDED TWO TRANSVERSE STRAPS TO LRDC NET - SUCCESS	
38	8/10	ITV	285	48.6	5	H-R	0	2.7	1.3	1.0	300	350	-	276	SUCCESS	
39	8/10	ITV	270	50.5	5	H-R	0	2.8	1.3	1.0	280	360	-	276	SUCCESS	
40	8/10	ITV	180	41.2	5	H-R	0	-	-	-	200	275	-	276	SUCCESS	
41	8/10	ITV	180	40.7	5	H-R	0	-	-	-	250	300	-	276	SUCCESS	
42	8/10	ITV	270	51.0	5	H-R	0	-	-	-	250	350	-	276	SUCCESS	
43	8/10	ITV	270	50.2	7 1/2	H-R	0	2.7	1.9	1.0	280	310	-	276	HIGHEST SHOT ELEVATION ITV IMPACTED 33" BELOW NET TOP SUCCESS	

NOTE: FIRST 11 EVENTS WERE USED TO SELECT THE PROPER ROTOR DIAMETER FOR THE ENERGY ABSORBERS AND FOR LAUNCHER CHECK RUNS. RESULTS OF THESE TESTS INDICATED THAT AN 11 3/4-INCH DIAMETER ROTOR WOULD BE BEST.

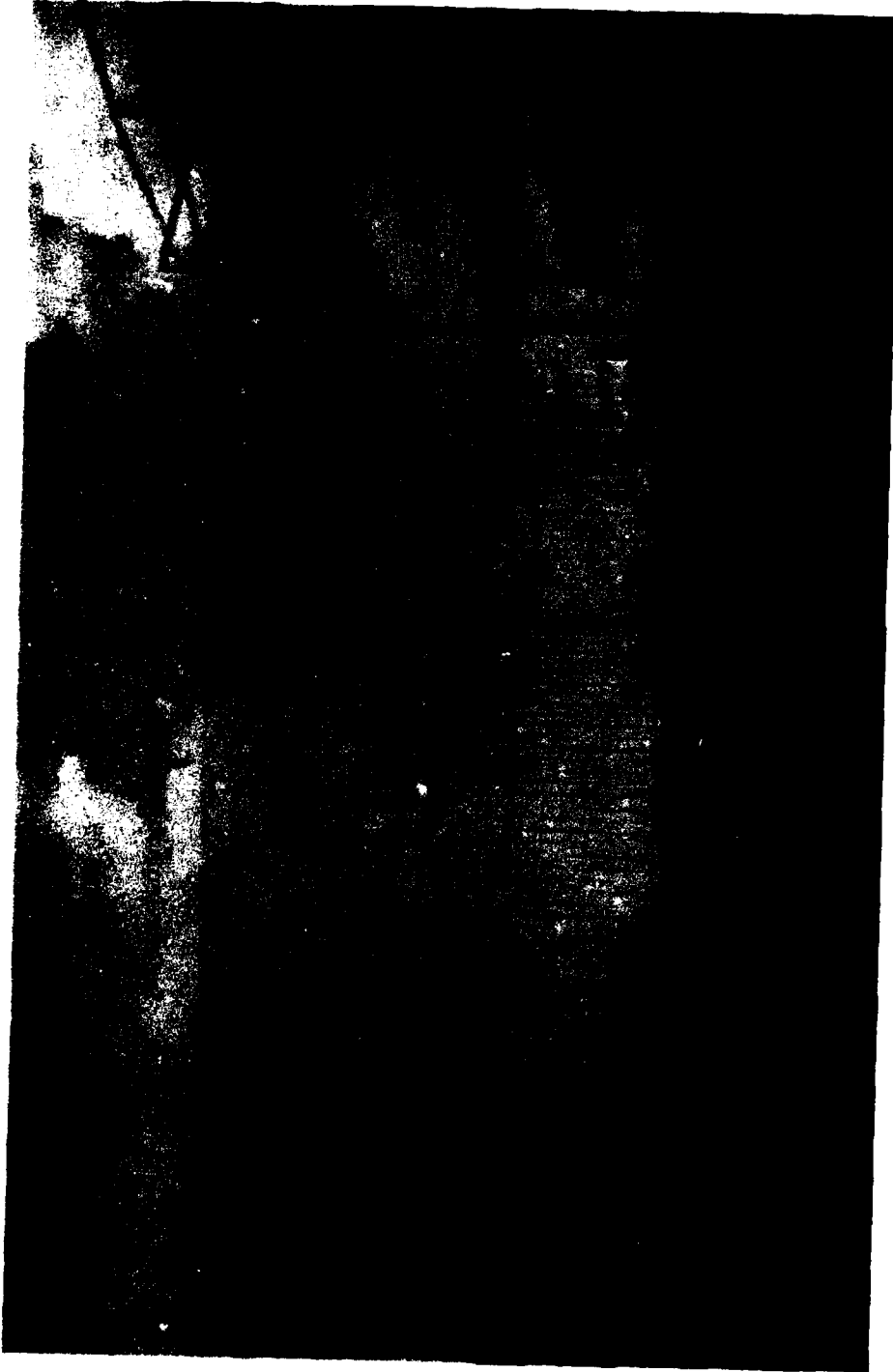
TABLE 23. TEST DATA SUMMARY (DEVELOPMENT TESTS CONDUCTED AT FACILITIES IN FORT HUACHUCA, AZ)

TEST NO.	VEHICLE	VEHICLE WEIGHT (LBS)	LAUNCH PRESSURE (PSIG)	VELOCITY (KNOTS)	INCLINATION ANGLE (DEG.)	VERTICAL HIT	VEHICLE ALIGNMENT SEEN ANGLE (DEG.)	MAXIMUM SEISMOGRAPH LOADS G's				REMARKS
								AXIAL		VERTICAL	TRANS.	
								HYDRAULIC	END LOAD			
1	244 AQ 003	136	270	N/A (49.0)	6.0	C-C	0	2.9	2.1	3.8	~0	SUCCESS
2	245 AQ 003	136	240	N/A (46.0)	6.0	C-C	0	2.2	2.5	3.7	~0	SUCCESS
3	246 AQ 003	136	240	N/A (46.0)	6.0	C-C	0	2.1	2.2	4.2	~0	SUCCESS
4	246 AQ 003	136	240	N/A (46.0)	10.5	H-C	0	2.5	3.0	6.5	0.7	LEFT WING TOP CRACKED UPON LANC. HIT IMPACT
5	247 AQ 003	136	270	N/A (49.0)	10.5	H-C	0	2.3	2.0	4.4	0.7	BOTH WINGS CRACKED UPON LANDING HIT IMPACT



a. Before Impact With Vertical Barrier (Test Event 18)

Figure 99. Retrieval of Inert Test Vehicle



b. At Impact With Vertical Barrier (Test Event 15)

Figure 99. (Cont.)



c. Engagement With Vertical Barrier and Deceleration (Test Event 14)

Figure 99. (Cont.)



d. At Rest in Landing Net (Test Event 14)

Figure 99. (Concl.)

Figure 99(b) shows the ITV just as it impacted the vertical barrier net. This photograph was taken during test event 15. The velocity of the ITV was 51.3 knots, and the vehicle impacted the vertical barrier net in a high-center location. This impact location was obtained by increasing the elevation of the launcher to a 5-deg incidence angle. Thus, the ITV is rising into the vertical barrier net along a 5-deg incidence angle. The maximum axial loads experienced were 2.6 g; the maximum vertical loads experienced on impact with the landing net were 4.2 g. A small transverse load of 1.2 g was also measured in this test. This test was also 100-percent successful.

Figure 99(c) shows the ITV being decelerated after impact into the vertical barrier net. This photograph was taken during test event 14. Table 21 shows that the velocity of the ITV at retrieval was 49.5 knots. Other data obtained for this test can be found in Table 21. This test was also successful.

Figure 99(d) shows the ITV as it appeared after successful retrieval and at rest in the parallel-strap, horizontal landing net. The vertical barrier straps are spaced along the entire wing leading edge, thereby distributing the retrieval deceleration loads over the entire wing span in a desirable manner.

Structural Loads Experienced By RPV. Figure 100 presents a typical set of three-axis force traces of the loads experienced by the RPV structural test vehicle during launch and retrieval. This set of traces was obtained during test event 31. Table 21 shows that the RPV vehicle was launched at a velocity of 51.2 knots, impacting the vertical barrier in the high-center portion, traveling on a +5-deg flight-path incidence angle. The maximum impactograph loads listed are those obtained from force traces like those shown in Figure 100. The accelerometers in the impactograph instrument were oriented so as to measure axial, transverse, and vertical loads relative to the RPV fuselage axis.

In Figure 100, point A marks the initiation of the launch acceleration of the RPV. This load increases very rapidly to a peak value of about 6.3 g. A

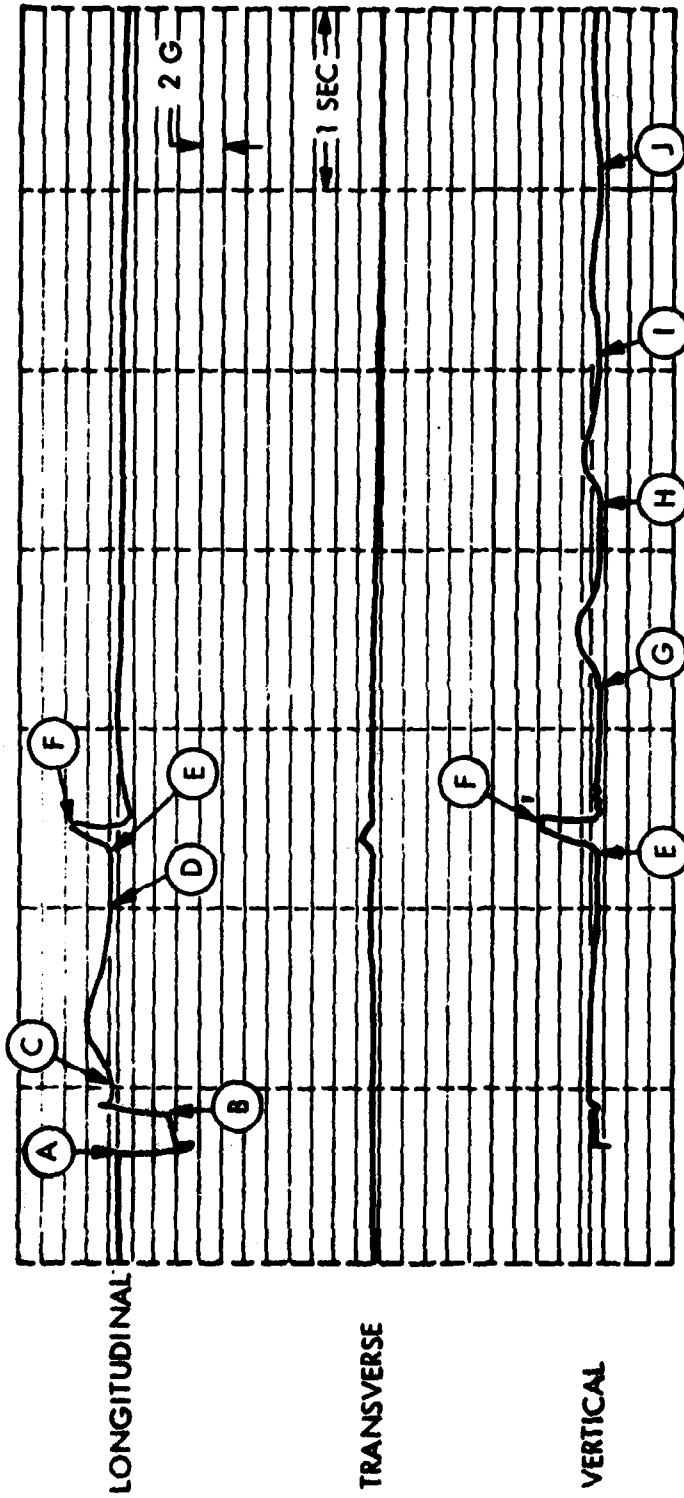


Figure 100. Three-Axis Force Traces of Loads Experienced by RPV Structural Test Vehicle During Launch and Retrieval

small vertical load on the vehicle was also recorded at this time and is due in part to the 5-deg angle of attack of the RPV and in part to mechanical takeup in launcher shuttle clearances in the vertical direction. At point B, the launch acceleration has been completed and the RPV released into free flight. The recorded RPV velocity at this point is 51.2 knots.

After a short free-flight glide of about 10 ft, initial contact with the vertical barrier starts with an increase (point C) in the longitudinal forces measured by the vehicle. The deceleration loads increase to a maximum value of about 2.7 g and then decrease until the RPV has been stopped in its forward flight (point D). The RPV then drops into the horizontal landing net, making an initial contact at point E. At this time a sharp rise in the vertical as well as the longitudinal loads occurs up to point F.

The rise in the longitudinal loads accompanying the rise in the vertical loads results from cross-coupling due to the small nose-down impact of the RPV upon engaging the landing net. A small transverse load was also recorded. After the initial landing impact, four additional oscillations of rapidly decreasing load amplitude were recorded. Table 21 shows that the structural RPV was retrieved during this test event without damage to the vehicle or to the retrieval system.

Figure 101 presents the retrieval force, tape-reel and -rotor revolutions, and time traces of both the right- and left-hand hydraulic energy absorbers recorded during RPV retrieval. The energy absorbers, connected to each side of the vertical barrier net, provide the RPV deceleration forces. A revolution counter was mounted on the tape reel, and a force transducer was mounted within the connection between the tape and purchase rope connected to the corners of the vertical barrier net. In general, the two energy absorbers provided about equal retrieval loads and energy absorptions.

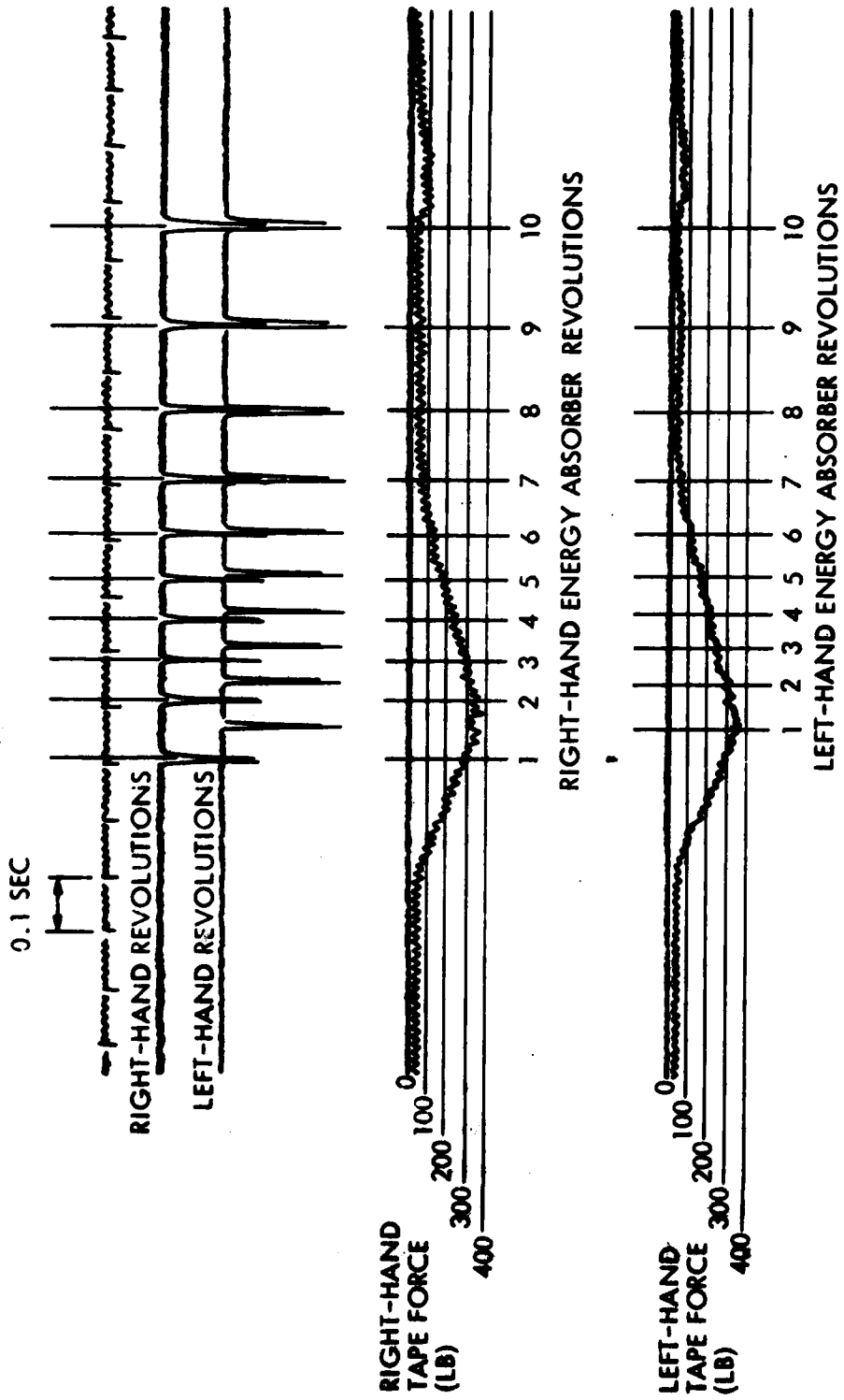


Figure 101. Forces, Revolutions, and Time Traces of Hydraulic Energy Absorbers During RPV Retrieval

However, the right-hand absorber was initiated about 40 ms before the left-hand unit. This was due to a small difference in right- and left-hand retrieval loading and to the hold-back brake force, which for this series of tests was set at about 40 lb on each energy absorber. The expected similarity of the shape of these load curves to the shape of the longitudinal deceleration force curves measured on the RPV, as shown in Figure 100, is evident by comparison.

Figure 102 presents the measured maximum axial deceleration loads imposed on the RPV by the vertical barrier net during retrieval as a function of RPV retrieval velocity. These loads do not exceed 3 g at velocities up to 51.5 knots. All but one data point are those developed in tests where maximum retrieval loads are generated only by the hydraulic action of the energy absorbers. As would be expected, the maximum hydraulic load gradually increases with increasing values of initial RPV impact velocity. However, if the RPV has not been fully stopped by the hydraulic action of the energy absorbers before the energy-absorber tape has been fully payed out, the RPV will be arrested in a final phase by elastic loading of the vertical net system and the payed-out tape. The theoretical elastic loading curve for this system is seen to rise very rapidly with initial RPV impact velocity. In fact, it crosses the hydraulic load curve at about 53 knots and reaches a 6-g RPV axial load value at about 58 knots.

One test point was obtained at which elastic loading was encountered as shown in Figure 102. The shape of the RPV axial load curve with elastic loading present as measured with the accelerometer impactograph is shown in Figure 103. For the conditions of this RPV retrieval test, the elastic load developed was lower than the maximum hydraulic load developed. It is estimated, however, that the elastic load will always exceed the hydraulic load at all RPV velocities greater than about 53 knots. The elastic loading curve can be shifted to higher RPV impact velocities by increasing the payout distance of the energy-absorber tape. When this is done, of course, the RPV deceleration distance will also be increased.

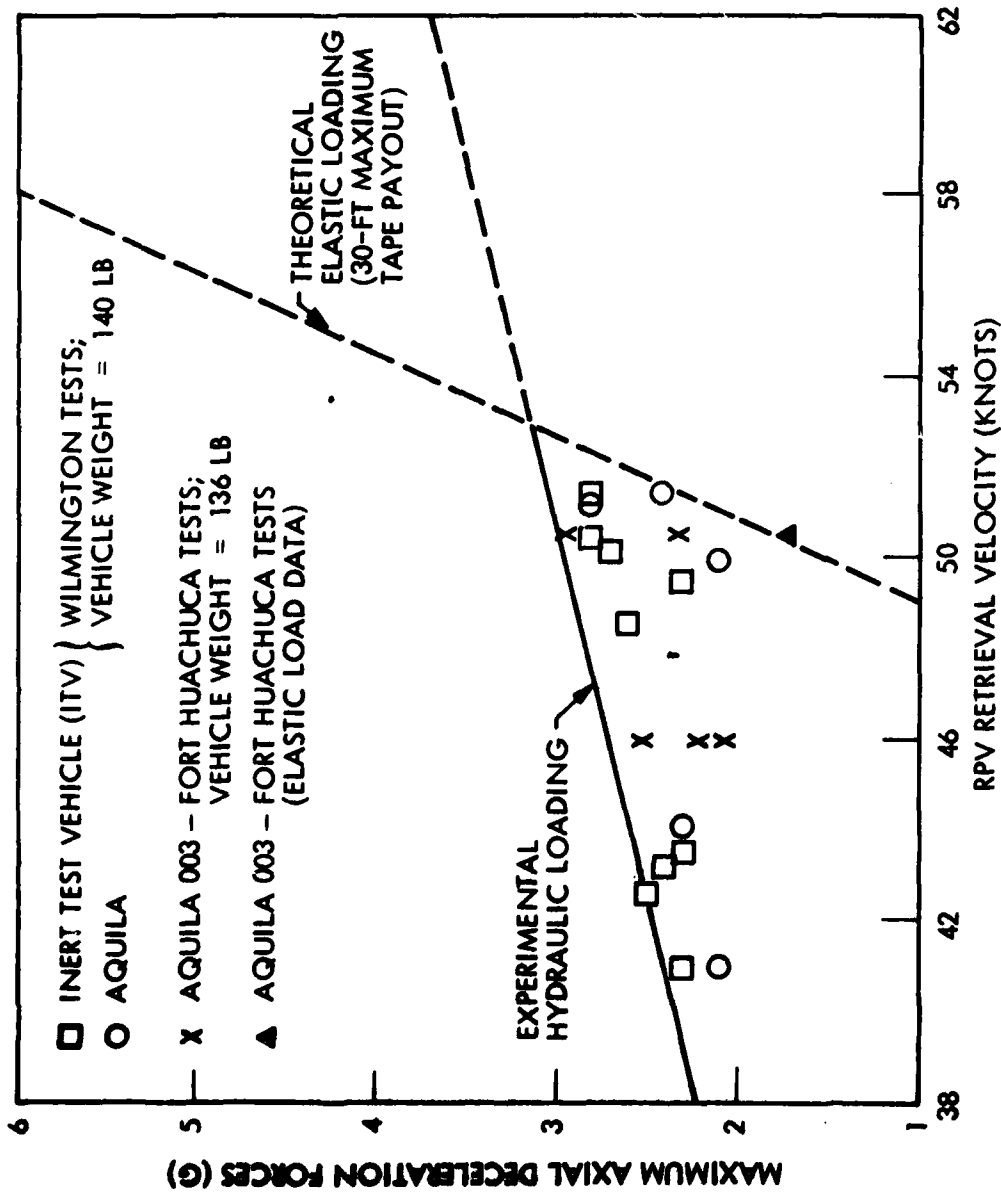


Figure 102. Maximum Axial Deceleration Loads Imposed on RPV by Vertical Barrier

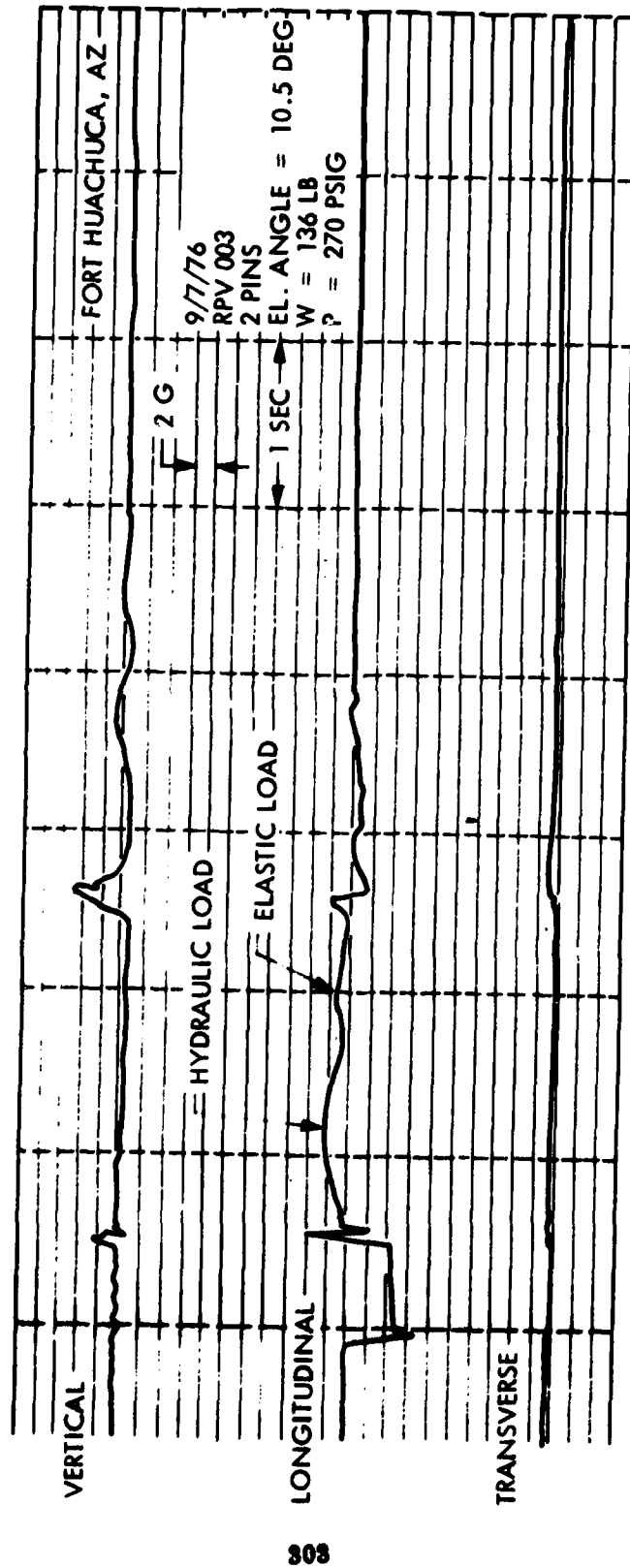


Figure 103. Longitudinal Force Trace as Affected by Application of Elastic Line Load to RPV

Figure 104 presents the maximum vertical deceleration forces experienced by the RPV ITV as a function of vehicle retrieval height above the landing net. At a maximum RPV retrieval height of 15 ft above the landing net, a measured vertical impact load on the RPV of 6.5 g was measured. This force rapidly decreases to about 3 g when the RPV impacts the vertical barrier at about 6.5 ft above the landing net.

A 6-g vertical load is induced into the RPV structure after a 14-ft drop into the horizontal landing net. A 14-ft drop is the maximum fall that the RPV will experience when it enters the top boundary of the vertical barrier retrieval window from a horizontal or 0-deg flight-path approach angle. The test data for the 15-ft drop were acquired by increasing the incidence angle to a +10.5 deg (or rising) trajectory into the vertical barrier net. Such a flight trajectory is not normally to be expected, and Table 22 shows that structural damage to the wing did occur in these two test events. In fact, the usual flight-path approach angle is slightly negative (approximately -4 deg); so the actual drop into the landing net will be slightly less than 14 ft when the vehicle enters the vertical barrier net at the uppermost boundary of the retrieval window.

Sufficient data were not obtained to resolve the spread of the data in Figure 102 or 104. All the data obtained to date have been plotted on these figures. In addition to the effects of RPV vertical impact height and RPV impact velocity, the data include the effects of RPV skew angles to 24 deg and flight-path inclination angles from 0 to +10.5 deg.

Transverse loads never exceed approximately 2 g in either direction and have not been plotted.

The hydraulic fluid used in the energy absorbers was standard automotive transmission fluid. Figure 105 presents the viscosity of the fluid used as a function of temperature. The development tests reported herein were conducted over a temperature range from about 50° to 100° F. No change in performance with temperature was noted.

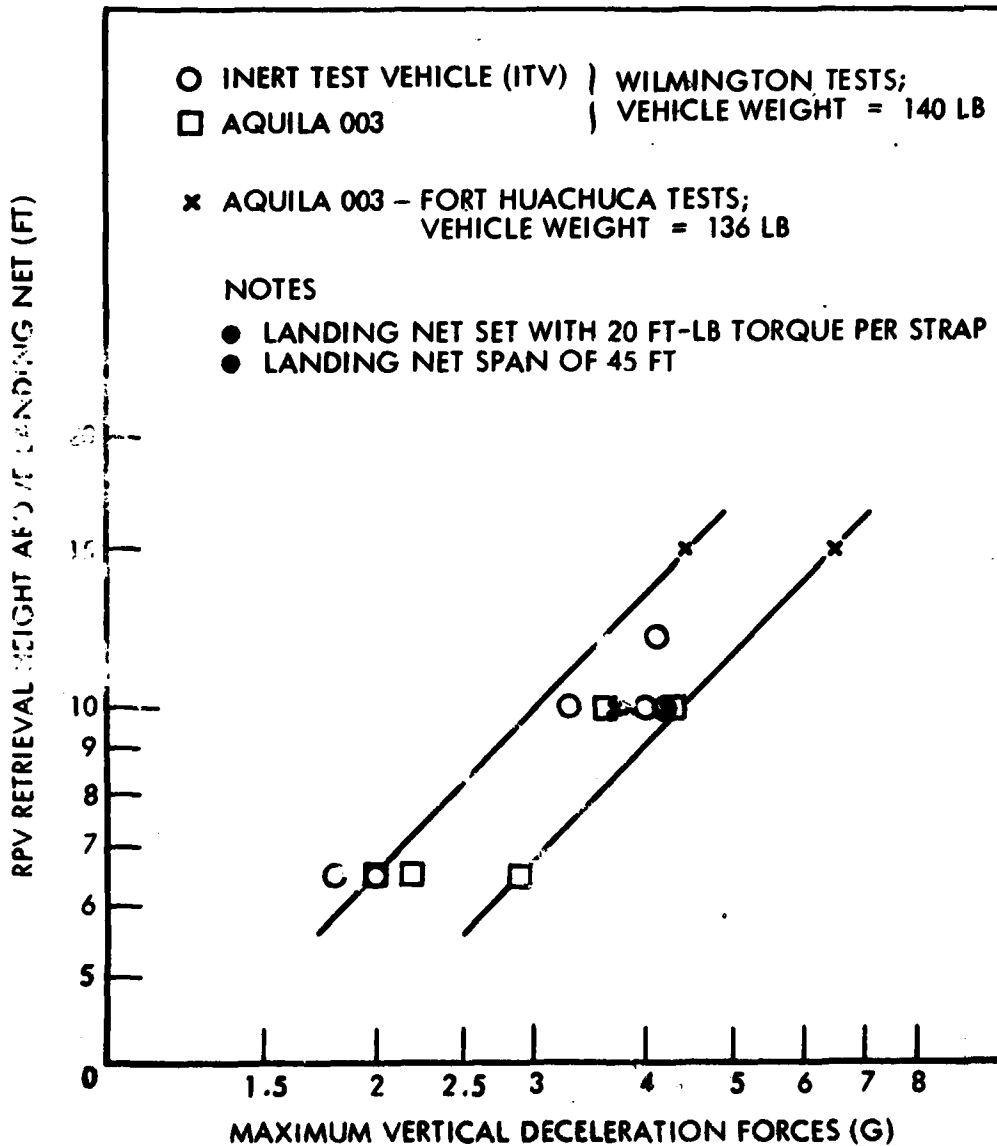


Figure 104. Maximum Vertical Deceleration Loads Imposed on RPV by Horizontal Landing Net

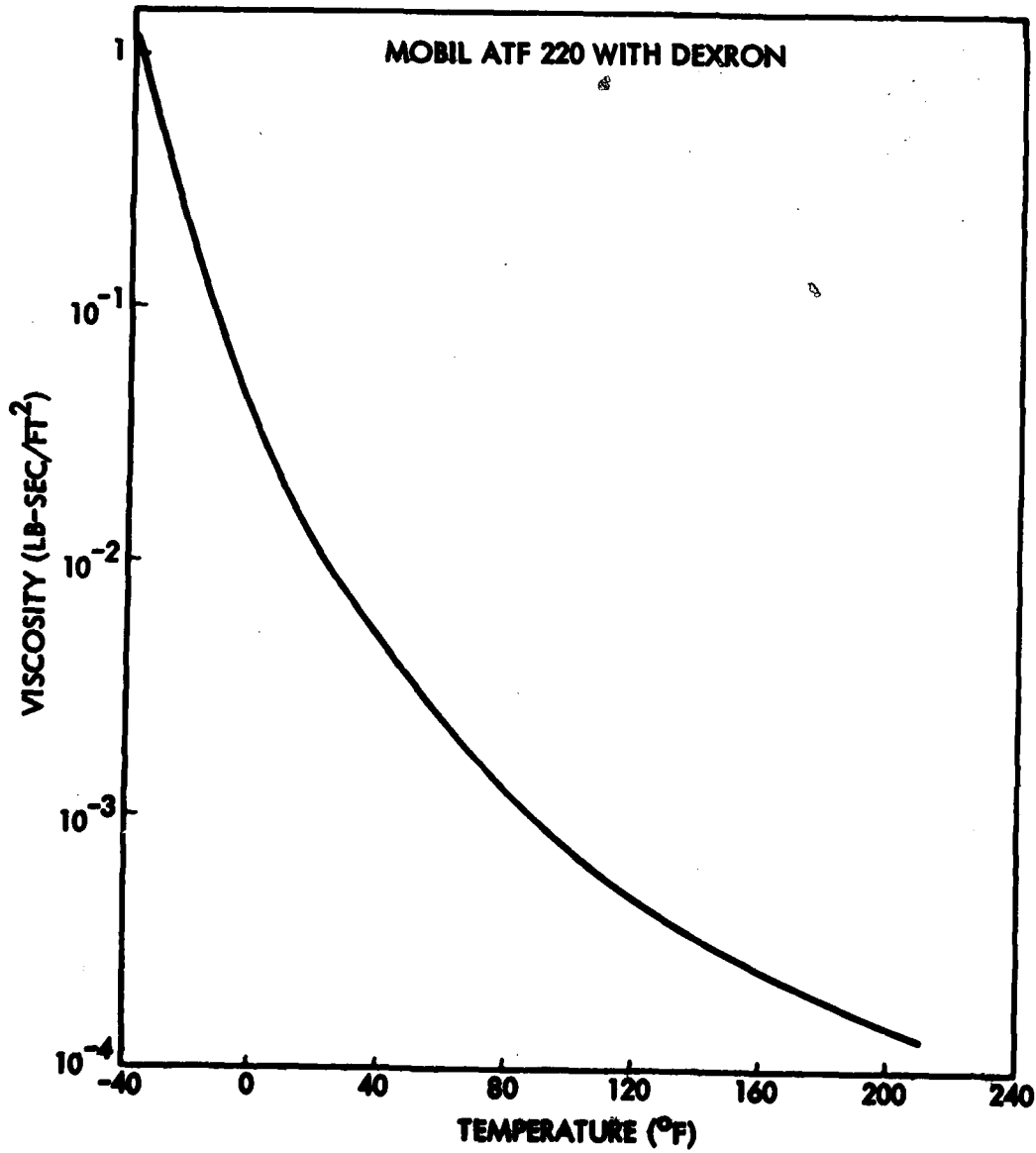


Figure 105. Viscosity of Hydraulic Fluid Used in Energy Absorbers

In this temperature range, the theoretical contribution of fluid viscosity to peak retardation forces generated by the energy absorbers is not greater than about 3 percent. Thus, no measurable effects with temperature would be expected over the temperature range of these tests. However, the viscosity of the fluid does increase very rapidly as temperature is significantly lowered. For example, if the fluid temperature is decreased to -15°F , the viscosity contribution to energy-absorber retardation-force generation will be about 30 percent of the total force. Since the viscous contribution is principally additive, the hydraulic deceleration loads will be increased significantly over those shown in Figure 102. Furthermore, at about -40°F , the viscous contribution will be about five times the total hydraulic force generated in these development tests. Thus, for extreme cold weather operation, the hydraulic fluid used in the energy absorbers must be changed to a fluid of lower viscosity, but of approximately the same fluid density.

Flight Test Results. Following these tests, over 40 successful consecutive Aquila RPV flight retrievals were achieved by late June 1977. The first four flight retrievals were made using the "Sky Eye" RPV. It was guided into the retrieval window by an operator using visual-guidance radio control of the RPV. Following these tests, the Army Aquila RPV was used in the next 36 flight retrievals, of which the last 30 were made with a closed-loop RPV control system using a semiautomatic retrieval guidance system and the RPV autopilot system. Figure 106 shows the Aquila in the process of deceleration just after engagement with the vertical barrier net; Figure 107 shows the RPV nearly fully arrested by the vertical barrier net; and Figure 108 shows the vehicle at rest in the horizontal landing net at the conclusion of a successful flight retrieval.

Based on the data and results of the development test program, however, the field installation of the Vertical Barrier Retrieval System was modified in two respects. First, the length of the landing net was increased from 45 to 60 ft, to increase the distance between the point of RPV impact on the landing net and

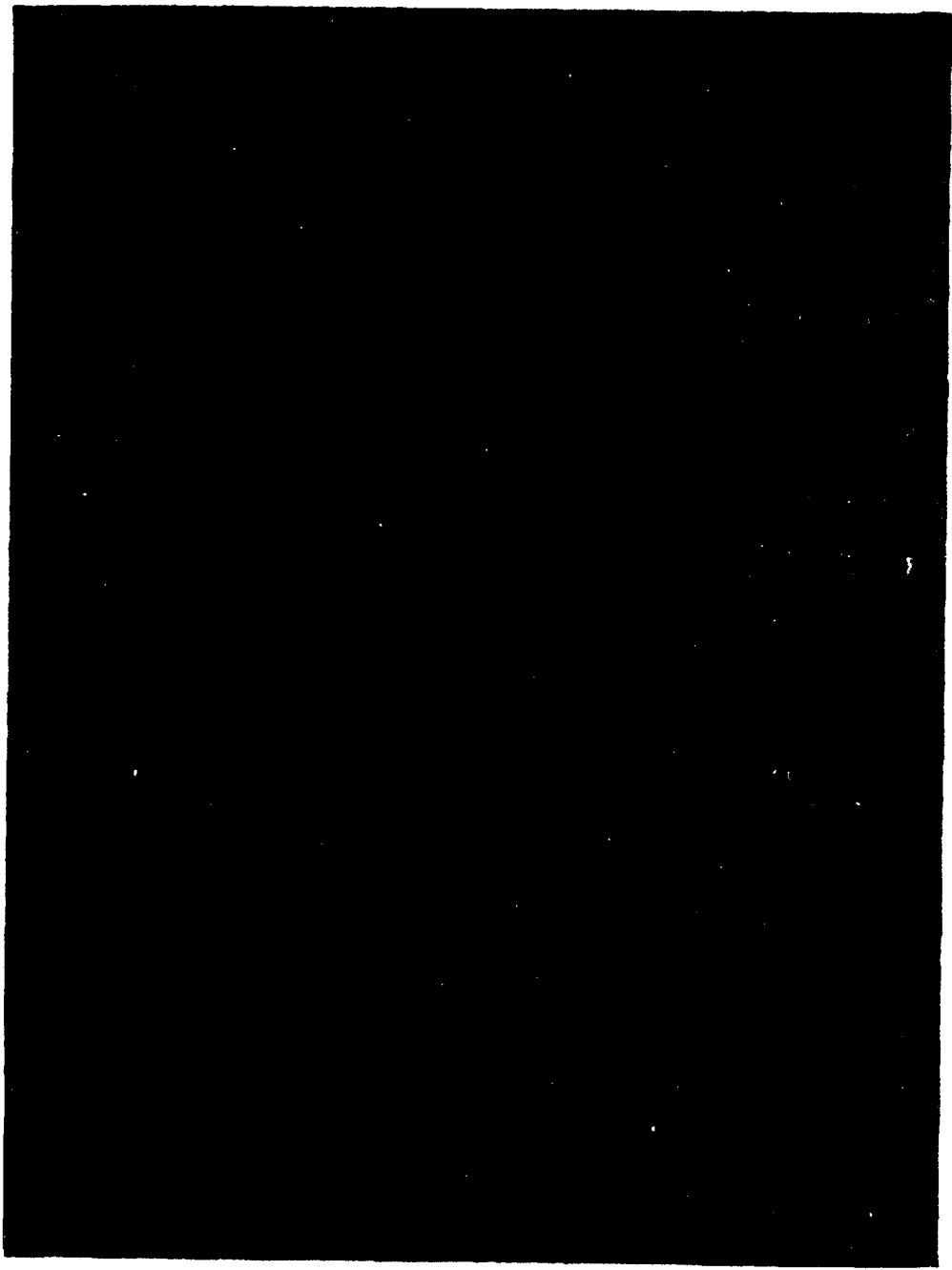


Figure 106. Aquila RPV Being Decelerated by Engagement With Vertical Barrier



Figure 107. Aquila RPV at Nearly Full Arrest by Vertical Barrier

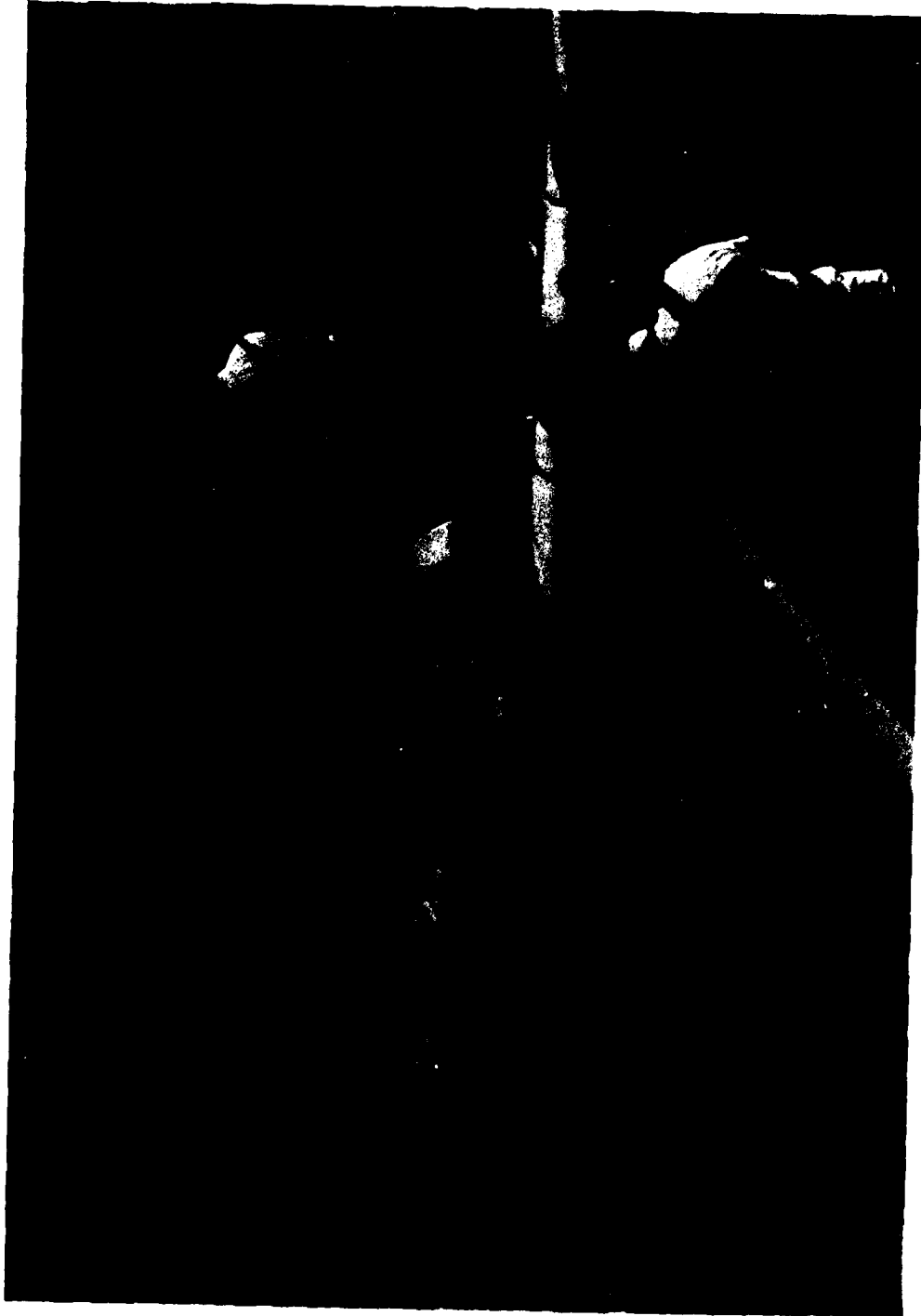


Figure 108. Aquila RPV at Rest in Horizontal Landing Net After Successful Retrieval

the end of the horizontal landing net. A desirable secondary effect of this change is to reduce slightly the maximum vertical deceleration forces induced into the vehicle from those shown in Figure 104.

Second, the hold-back force on the energy absorbers was increased from 40 to 97 lb. This change was made to increase the capability of the system to maintain the vertical barrier net in an erected retrieval position against winds.

In the course of the flight test program, wind effects on the vertical barrier net indicated that the currently deployed system with the 97-lb holdback force was sufficient to maintain the vertical barrier net in place in winds up to 13.5 knots at a 4,500-ft altitude on a standard day.

From a military operational standpoint, the Aquila RPV is capable of flight in winds to 20 knots gusting to 35 knots at a 4,000-ft altitude on a 95° F day. Figure 109 shows the estimated capability of a 160-lb hold-back force to maintain the vertical barrier net in position against winds at various altitudes for hot, cold, and standard days. It can be seen that the 160-lb hold-back force will meet the Aquila RPV flight criteria at the design altitude. This force is recommended for future field test operation in accordance with Aquila RPV design flight criteria. An examination of maximum tape tension force developed on the energy absorbers shows that the lowest value developed was 200 lb at an RPV inert test vehicle velocity of about 41 knots. The margin of 40 lb appears adequate for a proper release of the hold-back on the energy absorber during RPV retrievals. This also requires that the RPV have a ground speed of not less than about 41 knots.

It should be noted from Figure 109 that, at sea level on a standard cold day, winds exceeding an estimated 28.5 knots will cause the net to fail to remain erected even with the 160-lb hold-back force on each energy absorber. This

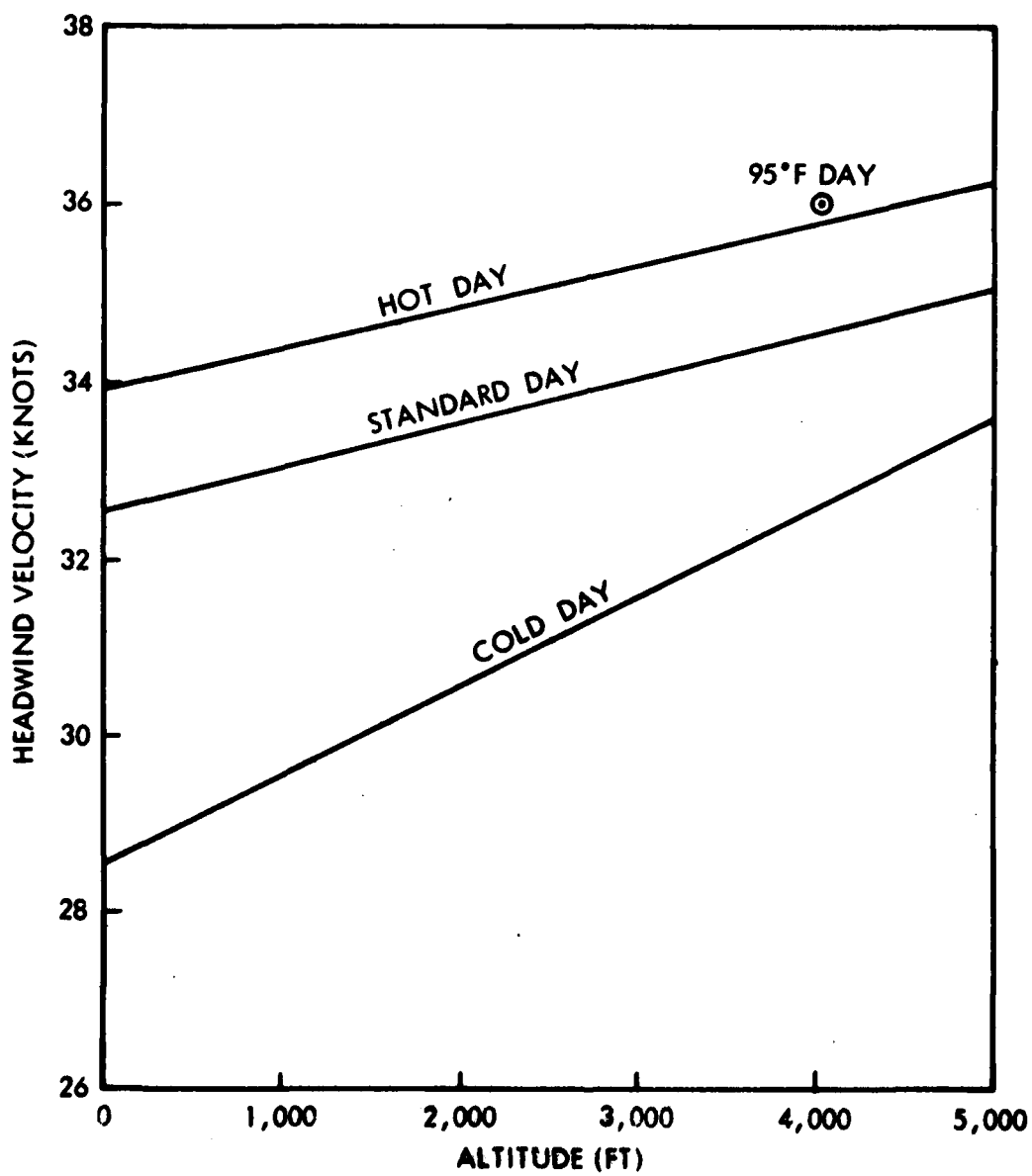


Figure 109. Maximum Velocity of Headwind Against Which Vertical Barrier Will Remain Erected (Hold-Back Brake Release Load of 100 lb on Each Energy Absorber)

occurs because of the increased air density at sea-level cold-day conditions compared with the design conditions - a 95° F day at 4,000-ft altitude.

Conclusions. A Vertical Barrier RPV Retrieval System that has been successfully developed and demonstrated is far superior to RPV retrieval systems requiring an RPV airborne deployable engagement hook. The Vertical Barrier Retrieval System design emphasizes and has demonstrated the following:

- RPV adaptability (Sky Eye and Aquila successful retrievals)
- No requirement for RPV airborne retrieval equipment
- Selection of retrieval system orientation to accommodate change in wind direction
- Retrieval at unprepared sites (Fort Huachuca, environments)
- System mobility (trailer-mounted for RPV retrieval and transportation to new sites)

Section VI
SITE SETUP AND SYSTEM OPERATION

The guidelines used for developing the site setup and system operation of the Aquila Program were as follows:

- Operation from unprepared site
- Minimum personnel required
- Minimum skill level
- Simplicity of operation
- Minimum setup-operation time

Since the requirements of the RPV-STD program addressed operation in a field environment using a mini-RPV system with greater payload, performance, and navigation capabilities than previously demonstrated, a semiautomatic operating system, which placed the complex operating burdens within the computer, was proposed. Thus, the man/machine interface could be greatly simplified if the difficult operator tasks could be identified and automated.

To identify the tasks required for completion of the basic Aquila missions, a functional flow analysis was performed that covered every aspect of system operation. Since this study preceded many of the hardware design functions, it drove, rather than reflected, many of the Aquila operating system parameters. This study also highlighted the significant man/machine interface requirements.

- GCS initialization
- Waypoint programming
- Search/loiter programming
- Prelaunch RPV checkout
- Inflight RPV command-status
- Recovery

An individual study of how each of these interfaces was developed is presented in section 6.2.

The site setup and site geometry evolved from the performance capabilities-limitations of the RPV, launcher, and retrieval system. The RPV performance specifications (i.e., weight, velocity, rate of climb) were the driving factors in the launcher and retrieval system design. A detailed discussion of site geometry evolution is contained in the following section.

6.1 SITE SELECTION AND GEOMETRY

The driving factors for site selection and geometry were launch, recovery, and RPV control. Launch and recovery constraints are similar in nature and will be discussed together.

6.1.1 Launch and Recovery Constraints

Because of limitations in the RPV longitudinal acceleration forces of ± 6 g, both launch and recovery velocities were minimized. Since the stall speed of the Aquila baseline vehicle was ≈ 36 knots, launch and recovery operations with a 20-knot tailwind would have required prohibitively long launch rails and retrieval net runouts to ensure acceptable acceleration-deceleration forces. Therefore, the dual-direction launcher-retrieval concept was selected. Launch and retrieval analyses were run on a 6 degrees-of-freedom computer model of the RPV using wind velocities up to 20 knots (steady state), with gusts up to 35 knots. The wind directions were varied from direct headwind through crosswind to direct tailwind. As expected, the model displayed system failure with strong tailwinds, but verified safe operation under all wind conditions that contained no tailwind components, even up to the 35-knot crosswind gusts. Placing the launcher on a M36 truck allowed full mobility and choice of launch direction. For retrieval, the net system was designed to accept recovery from two opposite directions, with only minor adjustments required to switch direction. (Thus, one placement of the recovery system to recover upwind and downwind with respect to the prevailing wind would then allow retrieval under all specified wind conditions.)

The next concern was recovery (or glide slope) angle. A steep recovery angle minimized the requirement for clearing ground obstacles and eased the criteria for site selection. However, the steeper recovery angles required addition of larger drag brakes to maintain acceptable recovery velocities. Because of weight-complexity constraints on the RPV, the drag brake chosen was a one-shot system. Activated by springs, and deployed by a solenoid, the drag brake was deployed prior to recovery and could not be retracted in flight. Since the area in front of and behind the net had to be equally free of obstructions to allow bidirectional recovery, the "balanced field concept" was adopted. This concept states "there is no utility in designing a flight vehicle which can take off from a short field but requires a longer one to land upon or vice-versa." As applied to the Aquila RPV, increasing the recovery angle necessitated a larger drag brake area, which in turn decreased the recovery "abort" rate-of-climb. Thus an increase in the recovery angle causes a decrease in the abort climb angle, resulting in no net reduction in terrain preparation since operation in both recovery directions must be anticipated. After analysis of several recovery angles - 2, 4, 6, and 8 deg - the 4-deg recovery angle was selected because the RPV with a drag brake sized for this angle was capable of a 4-deg abort climb angle. Therefore, maximum terrain clearance during recovery was provided with the 4-deg glide slope.

To allow sufficient terrain clearance for this configuration, both approach paths should be cleared of obstacles which are higher than 2 deg above the horizon, for a distance of 1,000 m, within 45 deg of each side of the projected retrieval centerline.

Since the RPV has the drag brake stowed during launch, the launch rate of climb exceeds 4 deg and no additional terrain clearance constraints are imposed during launch.

6.1.2 RPV Control Requirements

Control of the RPV was the other significant constraint in site selection. Considering the maximum slew rate of the tracking antenna, RPV flight perpendicular to the antenna at distances closer than 15 m would cause the antenna to lose track of the vehicle. Thus 15 m is the minimum acceptable spacing between the tracking antenna and the launcher or the retrieval system. For similar reasons the GCS van was placed perpendicular to the directions of retrieval to prevent loss of track during recovery or abort operations.

At the frequencies used for command control of the Aquila RPV, the range is essentially line of sight. The GCS van must be located in an area which provides unobstructed fields of view of the launcher retrieval system and areas of anticipated flight operations.

6.1.3 Additional Site Considerations

Although not as significant as the above constraints, the following site selection guidelines are presented:

- Access. Although all components are capable of mobile deployment, operation in areas with limited access should not normally be considered.
- Size. Total site size is partially determined by cable lengths and minimum spacing requirements. A typical site should be approximately 108 by 72 m and should vary in elevation no more than 6 m within its boundaries. Since no two sites are totally similar, it is necessary to consider safety, ease of operation, and capability of performing the mission as the main objectives during site selection.

6.2 SYSTEM OPERATION

After initial hardware was developed, the system operation further evolved during the period of field testing at Crows Landing NALF, California, and Fort Huachuca, Arizona. This was the first opportunity for the components to be operated fully

and together in a field environment, and many improvements to the overall system resulted from these field tests. Evolution of the key elements of system operation is discussed in this section.

6.2.1 GCS Initialization

Initialization of the GCS tracking antenna is required for accurate location of the RPV and targets during flight. The UTM coordinates of the antenna must be known to ± 10 m, and the antenna bearing must be referenced to within ± 1.0 mradian of grid north.

The antenna location problem was easily solved by converting the range and bearing from the benchmark to the antenna into rectangular UTM coordinates using the site computer. Using the theodolite and surveyors tape provided for this purpose, accuracy of ± 2 m was easily achieved.

Alignment of the antenna to grid north is a more difficult problem. A prism was mounted in a bracket on the back of the tracking antenna facing exactly 180 deg away from the azimuth of the tracking antenna beam. The prism acts as a retro-reflector in the vertical plane and as a mirror in the horizontal plane. To align the antenna, the radome is removed from the antenna, and the theodolite which was first initialized on the north sighting stake, is now rotated to view the antenna. The antenna is now rotated electrically, or manually, to face the prism toward the theodolite. Initially a xenon beacon was used to complete the fine adjustment; however, field operation proved easier than anticipated and a more direct method is now used. The theodolite operator moves to either side of the theodolite, while watching the prism, to see his reflection. Once his reflection is found, he "walks in" the reflection by signaling the antenna operator to move the antenna in small increments until he can see his reflection while standing behind the theodolite. At this time the theodolite is used to zero in the azimuth. When the theodolite's image can be viewed in the prism by looking through the theodolite, the system is autocollimated. The theodolite azimuth

and elevation values are recorded and entered into the computer via the site set-up program while the antenna is still in this position. This procedure has been used for all antenna initializations at Fort Huachuca and has proved capable of consistent accuracy to ± 1.0 mradian.

6.2.2 Waypoint Programming

Waypoint programming has not changed since its inception early in the Aquila program. For convenience, and to provide growth capabilities, 100 waypoint registers (00 to 99) were set aside for waypoint data storage. Each register contains all of the data required to fly to that point - waypoint coordinates, altitude, and airspeed. To allow for special waypoint modes, the registers were allocated in the following manner:

- Register 00-49 For Waypoint Navigation
- Register 50-59 For Dead Reckoning
- Register 60-69 For Search
- Register 70-79 For Loiter
- Register 80-89 For Primary Recovery Path
- Register 90-99 For Secondary Recovery Path

Registers 50 through 79 are not used in the conventional manner, but are used as storage for special parameters specifying the type of flight profile to be followed.

The waypoint system was first operated successfully at Fort Huachuca. Since that time, changes have been made in the guidance equations to optimize performance of the RPV in following the planned ground track over a wider range of airspeeds, and at extended distances from the ground site. These improvements have been implemented entirely in the software by changing gain terms, averaging data, and adding an integral term to the guidance equation to "wash out" bias errors. All waypoint modes - waypoint, dead reckoning, loiter, and search - have been demonstrated in the field, and are now performed in a routine manner.

6.2.3 Prelaunch RPV Checkout

Initial prelaunch RPV checkout was conducted in the field by an LMSC test-engineering team. A high number of redundant, detailed tests were performed during the first 20 or so flights to establish a data base for tactical RPV checkout requirements. The prelaunch checkout is now performed semiautomatically. Additions to the prelaunch software program of automatic computer "go/no-go" checks, and the deletion of nonrequired checks have both combined to ensure a thorough RPV prelaunch checkout in a fraction of the time once used. For example, the first test flights conducted at Fort Huachuca required prelaunch RPV checks of 2 days duration; current Army prelaunch checks with the semiautomatic system require 1-1/2 hours. Additionally, the computer is able to check the yaw-roll gyro and engine response more accurately than the human operator.

6.2.4 Inflight RPV Command-Status

Inflight command-status design has not changed from the initial configuration first tested at Crows Landing. The flight commands are sent to the RPV using three basic data words - altitude, airspeed, and heading rate. Additional discrete words are used for flight-control mode commands. Although no automatic flight modes were verified at Crows Landing, the three basic autopilot loop commands were all exercised. From the first flights at Crows Landing, RPV status has been calculated and displayed in the ground station by the computer. Once initial software "bugs" were eliminated, the inflight status displays have demonstrated their usefulness for monitoring the RPV and assisting in the diagnosis of system malfunctions. A set of inflight emergency procedures has been compiled for use with these displays. Recently, an inflight diagnostic panel was added to the system to provide additional information on the command flight modes and telemetry status.

6.2.5 Recovery

Recovery operations have undergone the greatest change of all Aquila system operations. Because of the limited space and time available at Crows Landing, the testing there was conducted using temporary tricycle landing gear and no testing of the landing system was possible. During the first flights at Fort Huachuca, the RPVs were recovered in a horizontal net by flying a vehicle suspended hook into an array of arresting lines. The RPV was flown in a direct remote control mode, like a conventional RC model airplane during final approach. The RC pilot was positioned behind the net. Although data were obtained at this time on the ability of the ground recovery camera to locate the RPV, no automatic recoveries were attempted. These initial recovery attempts also highlighted many problems inherent in the hook/arresting-line recovery system, forcing abandonment of that technique. Full 6 degrees of freedom non-linear, digital computer simulations of the recovery guidance equations were run, at this time, as well as "man-in-the-loop" analog computer simulations. In a similar manner as with the waypoint equations, gains were optimized and an integral term was added to the heading rate guidance equation to compensate for bias errors. The simulations demonstrated a high degree of success with these changes. When flight operations were resumed using the new vertical barrier net, a series of successful flights and recoveries were made using the RC mode for recovery. These flights demonstrated the feasibility and reliability of the new barrier net.

6.2.6 Procedures

During the total period of evolution of the system, the functions required for system operation have been reviewed and changed as necessary to reflect the current operation of the system. These functions have been compiled into a procedural guide manual, (Reference 10).

The manual covers all aspects of system operation, from site setup through RPV recovery. Current system emergency procedures are included in an appendix.

The manual defines operation of the system in a test configuration at Fort Huachuca. Many similarities exist between these procedures and tactical operating procedures; however, they must be considered as only a guide to system operation when used in operations simulating a tactical system.

Section VII
CONCLUSIONS

Evolution of the Aquila Remotely Piloted Vehicle System Technology Demonstrator Program hardware was conceived to provide the Army with representative tactical RPV field experience without the cost and time normally required for full system development. Use and adaptation of existing, proven hardware and the use of commercial grade components did, indeed, provide for early flight test (11 months from program initiation). The system initially did not perform with sufficient reliability, however, and additional development and testing was required before operations became routine. Based on the results of the program and its implications relative to modern RPV systems and their development, the conclusions are:

- Application and adaptation of existing system elements, and use of commercial components, coupled with limited system development produced an effective RPV system technology demonstrator for the Army at a fraction of the cost of a full engineering system development.
- An effective tactical RPV system can be accomplished with complete engineering development and an upgrading of component reliability to provide the reliability and effectiveness required by the Army in the tactical environment.

REFERENCES

1. AQUILA RPV SYSTEM TEST REPORT, CDRL AOOD, PART 4, AERODYNAMICS, LMSC-L028081, Lockheed Missiles and Space Company, Inc., Sunnyvale, California, May 1977.
2. Krachman, Howard E., Developmental Sciences, Inc.; AQUILA STRUCTURAL INTEGRITY REPORTS, LMSC Subcontract GS10B7130A, DSI Job No. 2846-SR, Lockheed Missiles and Space Company, Inc., Sunnyvale, California, 30 October 1975.
3. AQUILA RPV SYSTEM TEST REPORT, CDRL AOOD, PART 11, ENGINE SYSTEM DEVELOPMENT, LMSC-L028081, Lockheed Missiles and Space Company, Inc., Sunnyvale, California, 22 December 1977.
4. AQUILA RPV SYSTEM TEST REPORT, CDRL AOOD, PART 2, SYSTEM SIMULATION, LMSC-028081, Lockheed Missiles and Space Company, Inc., Sunnyvale, California, 14 February 1977.
5. AQUILA RPV SYSTEM TEST REPORT, CDRL AOOD, PART 3, PARACHUTE SYSTEM DEVELOPMENT TESTS, LMSC-028081, Lockheed Missiles and Space Company, Inc., Sunnyvale, California, 1 March 1977.
6. AQUILA RPV SYSTEM TEST REPORT, CDRL AOOD, PART 7, SERVOACTUATOR DEVELOPMENT, LMSC-028081, Lockheed Missiles and Space Company, Inc., Sunnyvale, California, August 1977.
7. Secord, M. G., and Tuominen, J. R., REPORT OF FLIGHTWORTHINESS TESTS ON THE YG1165A01"R", PHASES I AND II, Honeywell Avionics Division, Minneapolis, Minnesota, October 1976.
8. AQUILA RPV SYSTEM TEST REPORT, CDRL AOOD, PART 5, RPV ANTENNA PATTERNS, LMSC-LG28081, Lockheed Missiles and Space Company, Inc., Sunnyvale, California, 31 May 1977.
9. AQUILA RPV SYSTEM TEST REPORT, CDRL AOOD, PART 9, GCS TRACKING ANTENNA DEVELOPMENT, LMSC-L028081, Lockheed Missiles and Space Company, Inc., Sunnyvale, California, September 1977.
10. TECHNICAL MANUAL FOR AQUILA RPV SYSTEM TECHNOLOGY DEMONSTRATOR, SYSTEM DESCRIPTION, VOLUMES I, II, AND III, LMSC-D056906, Lockheed Missiles and Space Company, Inc., Sunnyvale, California, 10 August 1977.
11. AQUILA RPV SYSTEM TEST REPORT, CDRL AOOD, PART 10, LAUNCHER DEVELOPMENT, LMSC-L028081, Lockheed Missiles and Space Company, Inc., Sunnyvale, California, September 1977.

REFERENCES (CONTINUED)

12. AQUILA RPV SYSTEM TEST REPORT, CDRL AOOD, PART 6, RETRIEVAL SYSTEM DEVELOPMENT, LMSC-LO28081, Lockheed Missiles and Space Company, Inc., Sunnyvale, California, 30 June 1977.